

STATE OF CALIFORNIA DEPARTMENT OF TRANSPORTATION  
**TECHNICAL REPORT DOCUMENTATION PAGE**

TR0003 (REV. 10/98)

1. REPORT NUMBER CA18-2578		2. GOVERNMENT ASSOCIATION NUMBER		3. RECIPIENT'S CATALOG NUMBER	
4. TITLE AND SUBTITLE Calibration of LRFD Geotechnical Axial (Tension and Compression) Resistance Factors ( $\phi$ ) for California				5. REPORT DATE January, 2017	
7. AUTHOR(S) Xinbao Yu <sup>1</sup> , Murad Abu-Farsakh <sup>2</sup> , Yujie Hu <sup>1</sup> , Alicia Rae Fortier <sup>2</sup> , Mohammad Rakib Hasan <sup>1</sup>				6. PERFORMING ORGANIZATION CODE	
9. PERFORMING ORGANIZATION NAME AND ADDRESS  <sup>1</sup> Department of Civil Engineering University of Texas at Arlington 416 Yates Street Arlington, TX 76019  <sup>2</sup> Department of Civil & Environmental Engineering Louisiana State University 3255 Patrick F. Taylor Baton Rouge, LA 70803				8. PERFORMING ORGANIZATION REPORT NO.  na	
12. SPONSORING AGENCY AND ADDRESS  California Department of Transportation Division of Research, Innovation & System Information, MS-83 1120 N Street Sacramento, CA 95814				10. WORK UNIT NUMBER	
				11. CONTRACT OR GRANT NUMBER  DRISI Research Task No. 2587 DRISI Project No. P266 Contract No. 65A0526	
15. SUPPLEMENTAL NOTES  This report provides calibration results for both drilled shaft and driven pile foundations. A separate report (Shantz, 2018) provides additional analysis of the driven pile data that includes estimates of resistance factor uncertainty and consideration of a verification based reliability framework.				13. TYPE OF REPORT AND PERIOD COVERED  Final Report	
16. ABSTRACT  Driven pile load tests were collected from the existing Caltrans driven pile database, as well as from some new load tests resulting from this research effort. The final compiled driven pile database includes 110 piles, consisting of 22 concrete piles, 74 pipe piles, 12 H-piles, and 2 CRP piles, all from California. Drilled shaft load tests were collected primarily from Louisiana, Mississippi, and Caltrans. The final drilled shaft load test database includes 79 drilled shafts, 41 of which are from MS, 30 from LA, and 8 from western states (2 CA, 3 AZ, and 3 WA). The static capacity of the driven piles was based exclusively on top-down static load tests. These tests were analyzed following current Caltrans driven pile design practices. For small piles, Nordlund method was used for piles in sand and $\alpha$ -method for piles in clay. For large piles, API method was used piles in sand or clay. For drilled shafts, capacity was based on O-Cell measurements. The predictions of total, side, and tip resistance were made using both the FHWA 2010 design method (Brown et al. 2010 method) and the FHWA 1999 design method (O'Neill and Reese method).  The Monte Carlo simulation method was used to perform the LRFD calibration of resistance factors for both driven pile and drilled shaft under the strength I limit state, which is specified in the Transportation Research Circular No. E-C079, a 2005 Transportation Research Board publication. The total resistance factors obtained at different reliability indexes ( $\beta$ ), 2.33 and 3.0, were determined and compared with those available in literature. Resistance factors for driven piles and drilled shafts are recommended for California.				14. SPONSORING AGENCY CODE  913	
17. KEY WORDS  Pile, drilled shaft, CIDH, load-test, LRFD, calibration, resistance factor, O-cell		18. DISTRIBUTION STATEMENT  No restrictions. This document is available to the public through the National Technical Information Service, Springfield, VA 22161			
19. SECURITY CLASSIFICATION (of this report)  Unclassified		20. NUMBER OF PAGES  236 Pages		21. PRICE	

## **DISCLAIMER STATEMENT**

This document is disseminated in the interest of information exchange. The contents of this report reflect the views of the authors who are responsible for the facts and accuracy of the data presented herein. The contents do not necessarily reflect the official views or policies of the State of California or the Federal Highway Administration. This publication does not constitute a standard, specification or regulation. This report does not constitute an endorsement by the Department of any product described herein.

For individuals with sensory disabilities, this document is available in Braille, large print, audiocassette, or compact disk. To obtain a copy of this document in one of these alternate formats, please contact: the Division of Research and Innovation, MS-83, California Department of Transportation, P.O. Box 942873, Sacramento, CA 94273-0001.

**Calibration of LRFD Geotechnical Axial (Tension and Compression)  
Resistance Factors ( $\phi$ ) for California**

# Final Report

By

Xinbao Yu, Ph.D.

Murad Y. Abu-Farsakh, Ph.D., P.E.

Yujie Hu, Graduate Student

Alicia Rae Fortier, Graduate Student

Mohammad Rakib Hasan, Graduate Student

Department of Civil Engineering

University of Texas at Arlington

416 Yates St.

Arlington, TX 76019

State Project No. xxxx

conducted for

State of California Department of Transportation

The contents of this report reflect the views of the author(s) who is (are) responsible for the facts and the accuracy of the data presented herein. The contents do not necessarily reflect the official views or policies of the STATE OF CALIFORNIA or the FEDERAL HIGHWAY ADMINISTRATION. This report does not constitute a standard, specification, or regulation.

January 23, 2017

## ABSTRACT

Caltrans geotechnical engineers are using the California Amendments to AASHTO LRFD Specs (2008, 2011 and 2013) for LRFD design of deep foundation. However, the Caltrans Amendments using one unified resistance factor (0.7) for different foundation type, design methods, and loading conditions (compression and tension). AASHTO provides different resistance factors for different design methods and loading conditions and the resistance factors are more conservative than the one used by Caltrans. In order to calibrate resistance factors for driven piles and drilled shaft, extensive efforts were undertaken to collect driven pile and drilled shaft load test data. Driven pile load tests were collected from Caltrans existing compiled driven pile database as well as some new load tests as the result of this research effort. The final compiled driven pile database includes 110 piles which consist of 22 concrete piles, 74 of pipe piles, 12 H-piles, and 2 CRP piles, all from California. The compiled database includes project background information, soil data, pile materials and properties, and load test data. Drilled shaft load tests were collect from Louisiana and Caltrans. The Louisiana drilled shaft load tests are obtained from the results of a series of research efforts conducted at Louisiana Transportation Research Center (LTRC) over the past few years (Abu-Farsakh et al. 2010; Abu-Farsakh et al. 2013). The Mississippi drilled shaft data consists of 41 drilled shaft load tests. Efforts were made through Caltrans research office to reach out Caltrans bridge foundation engineers and FHWA office to collect drilled shaft load tests completed in bridge projects completely recently. Total 30 load tests reports of drilled shafts from LA, and 8 cases from Western states were included in the final drilled shafts. Several drilled shafts were not included because of incomplete soil data (cases) or load tests not performed to 1 inch settlement. The final drilled shaft load test database includes 79 drilled shafts among which 41 are from MS, 30 from LA, 8 from Western States (2 CA, 3 AZ, and 3 WA).

The driven pile database is compiled and analyzed using Mathematica. The measured pile capacity is determined using 1 inch settlement criteria or %5 pile diameter (whichever is larger) for both compression and tension load. The static capacity of driven piles was analyzed following current Caltrans driven pile design practice. The predictions of total, side, and tip resistance versus settlement behavior of drilled shafts were established from soil borings using both FHWA 2010 design method (Brown et al. method) and FHWA 1999 design method (O'Neill and Reese method). The measured drilled shaft axial nominal resistance was determined from either the Osterberg cell (O-cell) test or the conventional top-down static load test. For the drilled shafts that were tested using O-cells, the tip and side

resistances were deduced separately from test results. Both predicted and measured resistance was determined at two failure criterion: 1 inch and 5% B settlement. Statistical analyses were performed to compare the predicted total, tip, and side drilled shaft nominal axial resistance with the corresponding measured nominal resistance.

Caltrans method for static capacity tends to under estimate the measured pile capacity. Large uncertainty of the estimation, standard deviation of bias, is observed. For drilled shafts, both 2010 and 1999 FHWA design methods overestimate the total drilled shaft resistance. Reliability analyses are performed to calibrate resistance factors for the current design in consistent with the intent of the Specifications in designing, constructing, and accepting foundations for a consistent risk of failure quantified through a uniform reliability index. The total collected load test database are grouped according to region, pile type, soil type, construction method to develop specific calibrated resistance factors accounted for these design uncertainties. The Monte Carlo simulation method was selected to perform the LRFD calibration of resistance factors of drilled shaft under strength I limit state which is specified in the Transportation Research Circular No. E-C079, a 2005 Transportation Research Board publication. The total resistance factors obtained at different reliability index ( $\beta$ ), 2.33 and 3.0, were determined and compared with those available in literature. Resistance factors for driven piles and drilled shafts are recommended for California.

## **ACKNOWLEDGMENTS**

This research project was funded by the Caltrans, project number 65A0526. The financial support of this project is acknowledged.

## TABLE OF CONTENTS

ABSTRACT.....	iii
ACKNOWLEDGMENTS .....	v
TABLE OF CONTENTS.....	vii
LIST OF TABLES.....	ix
LIST OF FIGURES .....	xi
CHAPTER 1 INTRODUCTION .....	14
Project Background.....	14
Objective.....	15
Scope.....	15
Research Approach.....	15
CHAPTER 2 LITERATURE REVIEW .....	16
LRFD Calibration of Driven Piles.....	16
Oregon DOT .....	16
Kansas DOT.....	21
Florida DOT.....	34
Minnesota DOT .....	37
Wisconsin DOT .....	41
Illinois DOT.....	44
Washington DOT.....	49
Iowa DOT .....	51
Summary.....	54
LRFD Calibration of Drilled Shafts.....	58
Florida DOT.....	58
Iowa DOT .....	62
New Mexico DOT .....	67
Louisiana DOTD.....	73
3.    CHAPTER 3 CALTRANS DRIVEN PILE and Drilled Shaft DESIGN PRACTICE	81
Design Practice of Driven Piles.....	81
Design Process.....	81
Geomaterial sub-layer investigation .....	82
Limit states and load combination review .....	82
Trial driven pile dimension.....	82
Nominal bearing resistance calculation .....	82
Strength limit evaluation.....	104
Service limit evaluation .....	105
Measured Pile Resistance from Load Test .....	105
Design Practice of Drilled Shaft .....	106
Subsoil Investigation.....	106
Construction Method .....	108
Drilled Shaft Dimension .....	109
a) Standard Plan CIDH .....	109
b) Non-Standard Plan.....	109

Resistance of Drilled Shaft .....	109
c) Resistance in Cohesive Soil .....	110
d) Resistance in Cohesionless or Granular Soil .....	111
e) Resistance in Intermediate Geomaterial .....	113
f) Resistance in Rock .....	116
Nominal Axial Resistance .....	120
Pile Load Test .....	121
Settlement of Drilled Shaft .....	121
References .....	124
4. CHAPTER 4 deep foundation DATABASE and analyses .....	125
Driven Pile Database .....	125
Drilled Shaft Database .....	132
Database Description .....	139
Analyses of Drilled Shaft Database .....	146
Drilled Shaft Nominal Resistance .....	147
Prediction of Load-Settlement Behavior of Drilled Shaft .....	147
Measured Load-Settlement Behavior of Drilled Shafts .....	151
Measured and Predicted Resistance at Different Failure Criteria .....	153
5. CHAPTER 5 Results and analyses .....	156
Drilled Shaft Results .....	156
Predicted vs. Measured Drilled Shaft Resistance .....	156
Data quality check .....	156
Statistical Analyses of Total Resistance .....	164
Design variable analysis .....	168
Breakdown table .....	173
Separate Resistance Analysis .....	174
Reliability Theory .....	180
Calibration of Resistance Factors Using Monte Carlo Simulation .....	183
Calibrated total resistance factor .....	186
Calibrated total resistance factor for breakdown table .....	187
Calibrated side and tip resistance factors .....	193
Calibrated side and tip resistance factors for breakdown table .....	193



## LIST OF TABLES

Table 3-1. Empirical values for $\phi$ , $D_r$ , and unit weight of granular soil based on corrected $N'$ .....	93
Table 3-2. Design Table for Evaluating $K_\delta$ for Piles when $\omega = 0^\circ$ and $V = 0.0093$ to $0.0930$ $m^3/m$ (0.10 to $1.00$ $ft^3/ft$ ).....	97
Table 3-3. Design Table for Evaluating $K_\delta$ for Piles when $\omega = 0^\circ$ and $V = 0.093$ to $0.930$ $m^3/m$ (1.0 to $10.0$ $ft^3/ft$ ) .....	98
Table 3-4. Design Parameters for Cohesionless Siliceous Soil .....	103
Table 3-5. Factors $\phi$ for cohesive IGM's. (O'Neil and Reese, 1999).....	114
Table 3-6. Estimation of $\alpha_E$ (O'Neil and Reese, 1999).....	117
Table 3-7. Estimation of $E_m/E_i$ (O'Neil and Reese, 1999) .....	117
Table 3-8. Approximate relationship between rock-mass quality and material constants used in defining nonlinear strength (AASHTO LRFD Bridge Design Specifications, 6th Ed.) .....	118
Table 3-9. Geomechanics Rock Mass Classes Determined from Total Ratings (AASHTO Bridge Design Specifications, 6th Ed.).....	119
Table 3-10. Geotechnical Resistance Factors for Drilled Shafts (California Amendments to AASHTO LRFD Bridge Design Specifications).....	121
Table 4-1 Pile type distribution from database .....	126
Table 4-2 Load test distribution according to pile types.....	127
Table 4-3 Pile diameter distribution in database.....	128
Table 4-4 Pile length distribution .....	129
Table 4-5 Soil profile distribution from the database .....	130
Table 4-6 Tip soil conditions from database.....	130
Table 4-7 Location of test shaft cases in Western states .....	133
Table 4-8 Construction information of selected drilled shaft cases.....	135
Table 4-9 Shaft length distribution .....	139
Table 4-10 Shaft diameter distribution in database .....	140
Table 4-11 Side soil type summary for drilled shaft database.....	141
Table 4-12 Tip soil conditions for drilled shaft database .....	142
Table 4-13 Summary of total and separated resistance from measured data and predicted methods.....	155
Table 5-1 Original results of the analysis conducted on test shafts located in Mississippi, Louisiana, and Western states.....	157
Table 5-2 Original 8 cases and combined new shaft case .....	160
Table 5-3 Statistical summary of biases .....	164
Table 5-4 Filter criteria used for database breakdown analyses.....	174
Table 5-5 Summary of bias for drilled shaft side resistance.....	175
Table 5-6 Summary of bias for drilled shaft tip resistance.....	175
Table 5-7 Statistical characteristics and load factor .....	183
Table 5-8 Calibrated total resistance factors for the whole database.....	187
Table 5-9 Construction condition for drilled shaft database.....	187
Table 5-10 Calibrated total resistance factors according to dry construction method.....	187

Table 5-11 Calibrated total resistance factors according to wet construction method .....	188
Table 5-12 Calibrated total resistance factors according to unknown construction method	188
Table 5-13 Statistical characteristics and calibrated total resistance factors according to different classification ( $\beta=3.0$ ).....	189
Table 5-14 Statistical characteristics and calibrated total resistance factors according to different classification ( $\beta=2.33$ ).....	190
Table 5-15 Statistical characteristics and calibrated total resistance factors based on detailed soil profile ( $\beta=3.0$ ) .....	191
Table 5-16 Statistical characteristics and calibrated total resistance factors based on detailed soil profile ( $\beta=2.33$ ) .....	192
Table 5-17 Calibrated side resistance factor for the whole database with different design analysis.....	193
Table 5-18 Calibrated tip resistance factor for the whole database with different design analysis.....	193
Table 5-19 Statistical characteristics and calibrated side resistance factors according to different classification ( $\beta=3.0$ ).....	194
Table 5-20 Statistical characteristics and calibrated side resistance factors according to different classification ( $\beta=2.33$ ).....	195
Table 5-21 Statistical characteristics and calibrated side resistance factors based on detailed soil profile ( $\beta=3.0$ ) .....	196
Table 5-22 Statistical characteristics and calibrated side resistance factors based on detailed soil profile ( $\beta=2.33$ ) .....	197
Table 5-23 Statistical characteristics and calibrated tip resistance factors according to different classification ( $\beta=3.0$ ).....	198
Table 5-24 Statistical characteristics and calibrated tip resistance factors according to different classification ( $\beta=2.33$ ).....	199
Table 5-25 Statistical characteristics and calibrated tip resistance factors based on detailed soil profile ( $\beta=3.0$ ) .....	200
Table 5-26 Statistical characteristics and calibrated tip resistance factors based on detailed soil profile ( $\beta=2.33$ ) .....	201

## LIST OF FIGURES

Figure 1-1. Work flow to Calibrate Resistance Factors for LRFD Design of Driven Pile (DP) and Drilled Shaft (DS) .....	16
Figure 2-1. Standard Normal Variable to $\lambda$ Bias Fits for EOID in Scenario A. ....	20
Figure 2-2. Standard Normal Variable for 164 End-of-Drive Biases (PDA and CAPWAP), Driven by Diesel Hammers.....	24
Figure 2-3. Example of Geotechnical Data for a Driven Pile (Abu-Farsakh et al. 2009). ....	28
Figure 2-5. Histogram and Probability Density Function of Resistance Bias for 2010 FHWA Design Method (Abu-Farsakh et al. 2013). ....	32
Figure 2-6. Cumulative Distribution Function (CDF) of Bias Values (2010 FHWA Design Method) Calibration Results (Abu-Farsakh et al. 2013).....	32
Figure 2-7. Cumulative Distribution Plot for WSDOT Predictive Method showing Difference between Fit to all Data and Fit to Extremal Data (Long et al. 2009).....	43
Figure 2-8. Measured (1-in. $\Delta$ ) Vs. Estimated Side Resistance in Clay (Ng et al. 2014).....	66
Figure 3-1 Adhesion Values for Piles in Cohesive Soils (after Tomlinson, 1979).....	86
Figure 3-2 Adhesion Factors for Driven Piles in Clay- SI Unis (Tomlinson, 1980).....	88
Figure 3-3 Adhesion Factors for Driven Piles in Clay- US Unis (Tomlinson, 1980) .....	89
Figure 3-4 $\beta$ Versus OCR for Displacement Piles after Esrig and Kirby (1979) .....	90
Figure 3-5 $\lambda$ Coefficient for Driven Pipe Piles after Vijayvergiya and Focht (1972) .....	91
Figure 3-6 Relationship of $\delta/\phi$ and Pile Soil Displacement, V, for Various Types of Piles (after Nordlund, 1979) .....	93
Figure 3-7 Design Curve for Evaluating $K_\delta$ for Piles when $\phi = 25^\circ$ (after Nordlund, 1979). 95	95
Figure 3-8 Design Curve for Evaluating $K_\delta$ for Piles when $\phi = 30^\circ$ (after Nordlund, 1979). 95	95
Figure 3-9 Design Curve for Evaluating $K_\delta$ for Piles when $\phi = 35^\circ$ (after Nordlund, 1979). 96	96
Figure 3-10 Design Curve for Evaluating $K_\delta$ for Piles when $\phi = 40^\circ$ (after Nordlund, 1979)96	96
Figure 3-11 Correction Factor for $K_\delta$ when $\delta \neq \phi$ (after Nordlund, 1979).....	99
Figure 3-12 Chart for Estimating $\alpha_t$ Coefficient and Bearing Capacity Factor N'q (Chart modified from Bowles, 1977).....	100
Figure 3-13 Chart for Estimating $\alpha_t$ Coefficient and Bearing Capacity Factor N'q (Chart modified from Bowles, 1977).....	100
Figure 3-14 Relationship Between Maximum Unit Pile Toe Resistance and Friction Angle for cohesionless soil (after Meyerhof, 1976) .....	101
Figure 3-18. Factor $\alpha$ for cohesive IGM (O'Neil and Reese, 1999).....	114
Figure 4-1 Breakdown of pile type and number .....	126
Figure 4-2 Pie chart of pile type distribution .....	126
Figure 4-3 Breakdown of total database based on load direction.....	127
Figure 4-4 Diameter of piles distribution from database .....	128
Figure 4-5 Length of piles distribution .....	129
Figure 4-6 Soil profile distribution from database.....	130
Figure 4-7 Soil type at pile tip .....	131
Figure 4-8 Approximate locations of test shafts in Mississippi and Louisiana .....	133
Figure 4-9 Test shaft schematic .....	134
Figure 4-10 Investigated concrete filled length distribution.....	139

Figure 4-11 Investigated shaft diameter distribution .....	140
Figure 4-12 Construction method for drilled shaft database .....	141
Figure 4-13 Tip soil conditions for drilled shaft database (FHWA 2010).....	142
Figure 4-14 Tip soil conditions for drilled shaft database (FHWA 1999).....	143
Figure 4-15 Measured resistance contribution from tip 1 inch standard (%) .....	143
Figure 4-16 Measured resistance contribution from tip - cohesionless soil, 1 inch standard (%).....	144
Figure 4-17 Measured resistance contribution from tip - cohesive soil, 1 inch standard (%) .....	144
Figure 4-18 Measured resistance contribution from tip 5% diameter standard (%).....	145
Figure 4-19 Measured resistance contribution from tip - cohesionless soil, 5% diameter standard (%) .....	145
Figure 4-20 Measured resistance contribution from tip - cohesive soil, 5% diameter standard (%).....	146
Figure 4-21 Normalized load transfer representing the average trend value for drilled shaft (after O'Neill and Reese 1999).....	148
Figure 4-22 An example of a predicted and measured top-down load-settlement curve .....	149
Figure 4-23 2010 Normalized Trend Curves for to total load-settlement (Brown et al. 2010) .....	150
Figure 4-24 Original and adjusted O-Cell Load Displacement Curves .....	152
Figure 4-25 Equivalent top-down settlement curve.....	152
Figure 4-26 Measured Nominal Resistance at 1inch and 5%B ((LT-8786) .....	153
Figure 4-27 Extrapolation of Load-Settlement Curve .....	154
Figure 5-1 FHWA 1999 predicted total resistance vs. measured total resistance at 5% B...	161
Figure 5-2 FHWA 2010 predicted total resistance vs. measured total resistance at 5% B...	161
Figure 5-3 FHWA 1999 predicted total resistance vs. measured total resistance at 1 inch..	162
Figure 5-4 FHWA 2010 predicted total resistance vs. measured total resistance at 1 inch..	162
Figure 5-5 FHWA 1999 predicted nominal resistance vs. measured resistance at 1 inch....	163
Figure 5-6 FHWA 2010 predicted nominal resistance vs. measured resistance at 1 inch....	163
Figure 5-7 PDF and histogram of bias of total resistance at 5% B via FHWA 1999 method .....	165
Figure 5-8 PDF and histogram of bias of total resistance at 5% B via FHWA 2010 method .....	165
Figure 5-9 PDF and histogram of bias of total resistance at 1 inch via FHWA 1999 method .....	166
Figure 5-10 PDF and histogram of bias of total resistance at 1 inch via FHWA 2010 method .....	166
Figure 5-11 PDF and histogram of bias of measured resistance at 1 inch and nominal resistance via FHWA 1999 method .....	167
Figure 5-12 PDF and histogram of bias of measured resistance at 1 inch and nominal resistance via FHWA 2010 method .....	167
Figure 5-13 Ln-residual at 5% B via FHWA 1999 method vs measured total resistance .....	168
Figure 5-14 Ln-residual at 5% B via FHWA 1999 method vs diameter of shaft .....	169
Figure 5-15 Ln-residual at 5% B via FHWA 1999 method vs length of shaft .....	169

Figure 5-16 Ln-residual via FHWA 1999 method vs measured side resistance at 5% B.....	170
Figure 5-17 Ln-residual via FHWA 1999 method vs measured side resistance in clay at 5% B .....	170
Figure 5-18 Ln-residual via FHWA 1999 method vs measured tip resistance at 5% B.....	171
Figure 5-19 Ln-residual via FHWA 1999 method vs measured tip resistance in sand at 5% B .....	171
Figure 5-20 Ln-residual via FHWA 1999 method vs measured tip resistance in clay at 5% B .....	172
Figure 5-21 Ln-residual via FHWA 1999 method vs measured tip resistance in IGM at 5% B .....	172
Figure 5-22 Ln-residual via 1999 method at 5% B vs construction method .....	173
Figure 5-23 PDF and histogram of bias of side resistance at 5% B via FHWA 1999 method .....	176
Figure 5-24 PDF and histogram of bias of side resistance at 5% B via FHWA 2010 method .....	176
Figure 5-25 PDF and histogram of bias of side resistance at 1 inch via FHWA 1999 method .....	177
Figure 5-26 PDF and histogram of bias of side resistance at 1 inch via FHWA 2010 method .....	177
Figure 5-27 PDF and histogram of bias of tip resistance at 5% B via FHWA 1999 method	178
Figure 5-28 PDF and histogram of bias of tip resistance at 5% B via FHWA 2010 method	178
Figure 5-29 PDF and histogram of bias of tip resistance at 1 inch via FHWA 1999 method .....	179
Figure 5-30 PDF and histogram of bias of tip resistance at 1 inch via FHWA 2010 method .....	179
Figure 5-31 Probability density functions for load and resistance .....	181
Figure 5-32 Distribution of limit state equation .....	181
Figure 5-33 Probability of Failure corresponding to varies $\beta$ values (after Allen et al., 2005) .....	182

# CHAPTER 1 INTRODUCTION

## Project Background

The AASHTO LRFD Bridge Design Specifications (AASHTO LRFD Specs, 2012) uses an assortment of geotechnical resistance factors for deep foundations. Distinction is made between driven piles and drilled shafts, mode of failure, the method used to predict or measure resistance, and type of the soil. The California Amendments to AASHTO LRFD Specs (2008, 2011, and 2013) have condensed the tables using the values that are generally less conservative than those provided by AASHTO, albeit conforming to current and past successful Caltrans practices, policies, and procedures. Although acceptable for a temporary transition period, such calibration needs improvement to be consistent with the intent of the specifications in designing, constructing, and accepting foundations for a consistent risk of failure quantified through a uniform reliability index.

The AASHTO LRFD Specs have in general been calibrated to a target reliability of 3.5 for individual superstructure members. This level of safety may or may not be appropriate for some or all deep foundation components, depending on prediction method, type and frequency of investigation, mode of failure, geological information, and redundancy of the foundation system.

According to current practice of Caltrans, communication between the Structural and Geotechnical Designers begins with the Structural Designer providing the tabularized dimensions and loads outlined in Caltrans' MTD 3-1. The Geotechnical Designer then provides the tip elevations for tension, compression, and settlement under the controlling load combinations for the LRFD Service, Strength and Extreme Event limit states. The pile is tipped to develop adequate Factored Nominal Resistance to support Factored Loads reported by Structure Designer. Details are to be published in the Geotechnical Manual chapter on Deep Foundations: [[http://www.dot.ca.gov/hq/esc/geotech/geo\\_manual/manual.html](http://www.dot.ca.gov/hq/esc/geotech/geo_manual/manual.html) (pending)].

Since LRFD implementation to foundations in 2008, constant resistance factors of 0.7 and 1.0 (both tension and compression) have been used for Strength and Extreme Event limit states, respectively. LRFD resistance factor of 0.7 was obtained from the Working Stress Design (WSD) factor of safety of 2.0, load factors of LRFD, and the ratio of LRFD permanent loads to live load. Although the AASHTO Standard Highway Specifications began going away from WSD and providing tables of performance factors similar to LRFD in 1993, Caltrans reverted to the practice described above for Load Factor design (LFD) as well as LRFD calibration.

Considering construction costs of deep foundations, calibration of the resistance factors to provide an accurate design is crucial and may result in significant cost savings. Still, the cost

and time required for QC/QA measures such as frequency and type of pile load test will need to be balanced with the benefits of consistent reliability and potential cost savings.

The recommendations are to consider the level of geotechnical information available during design (such as Log of Test Borings); provide practical direction on the frequency and type of the tests performed during the design phase or for verification during construction; and suggest assumptions to be used by geotechnical engineers in design of driven piles and drilled shafts. Furthermore, analysis of existing records available from testing of deep foundations for Caltrans projects must be considered for developing resistance factors. When possible and appropriate, the proposed values for resistance factors should be derived using calibration techniques similar to those used by the AASHTO LRFD Specs.

### **Objective**

The objective of this research project is to recommend revisions to the California Amendments to the AASHTO LRFD Specifications and Caltrans technical documents pertaining to resistance factors used in design and evaluation of deep foundations.

### **Scope**

To reach the objectives of this study, geotechnical information, design reports of deep foundation, and load test data, pile driving records and PDA etc. were collected by working with the Caltrans Foundation Testing Branch (FTB). The collected data was digitized and compiled into excel files using a standard template for design capacity analysis using design analysis methods specified in AASHTO. The measured nominal resistance can be determined using static load test data or PDA analysis depending on the available load test data. The obtained load test database is grouped into several subgroups in according to their pile type, soil type, bearing type (axial compression or tension). Resistance factors for each classification group were calibrated. The predicted and measured resistances are determined according to the methods provided in the California Amendments. Statistical analyses are performed to evaluate the performance of each design method. LRFD calibration of resistance factors will be performed using the calibration procedure outlined by the TRB transportation research circular No. E-C079. Each design method will be assessed for the safety and serviceability risks.

### **Research Approach**

Calibration of resistance factor for chosen design methods requires a high quality database of resistances. The loads acting on the pile foundations are transferred from the superstructure to substructure and then to the foundation level. The probabilistic characteristics of the loads are

generally taken from AASHTO specifications. The actual transferred loads are not studied in most calibrations of geotechnical resistance factors. The research effort in this project is focused on collecting pile and drilled shaft test data to develop a database of high quality pile load tests. Figure 1 illustrates the framework of the calibration process. The calibration methodology and data analyses follow TR Circular No. E-C079 and NCHRP Report 507 by Paikowsky et al. with modification according to the Caltrans design practice (Paikowsky et al. 2004; Allen et al. 2005).

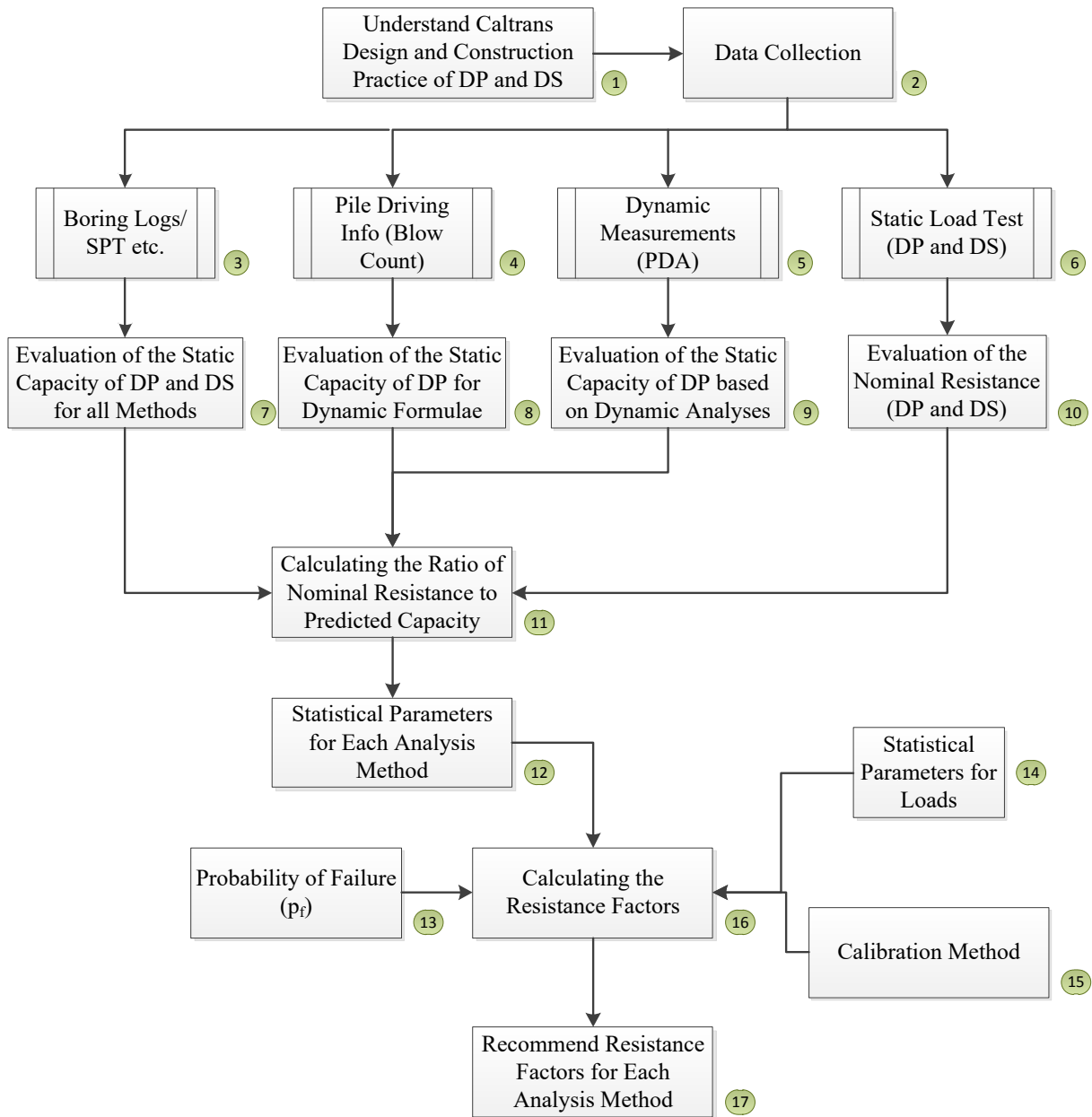


Figure 1-1. Work flow to Calibrate Resistance Factors for LRFD Design of Driven Pile (DP) and Drilled Shaft (DS)



Driven pile load tests were collected from Caltrans existing compiled driven pile database as well as some new load tests as the result of this research effort. The final compiled driven pile database includes 110 piles which consist of 22 concrete piles, 74 of pipe piles, 12 H-piles, and 2 CRP piles, all from California. The compiled database includes project background information, soil data, pile materials and properties, and load test data. Drilled shaft load tests were collect from Louisiana and Caltrans. The Louisiana drilled shaft load tests are obtained from the results of a series of research efforts conducted at Louisiana Transportation Research Center (LTRC) over the past few years (Abu-Farsakh et al. 2010; Abu-Farsakh et al. 2013). The Mississippi drilled shaft data consists of 41 drilled shaft load tests. Efforts were made through Caltrans research office to reach out Caltrans bridge foundation engineers and FHWA office to collect drilled shaft load tests completed in bridge projects completely recently. Total 30 load tests reports of drilled shafts from LA, and 8 cases from Western states were included in the final drilled shafts. Several drilled shafts were not included because of incomplete soil data (cases) or load tests not performed to 1 inch settlement. The final drilled shaft load test database includes 79 drilled shafts among which 41 are from MS, 30 from LA, 8 from Western States (2 CA, 3 AZ, and 3 WA).

The driven pile database is compiled and analyzed using Mathematica. The measured pile capacity is determined using 1 inch settlement criteria for both compression and tension load. The static capacity of driven piles was analyzed following current Caltrans driven pile design practice. The predictions of total, side, and tip resistance versus settlement behavior of drilled shafts were established from soil borings using both FHWA 2010 design method (Brown et al. method) and FHWA 1999 design method (O'Neill and Reese method). The measured drilled shaft axial nominal resistance was determined from either the Osterberg cell (O-cell) test or the conventional top-down static load test. For the drilled shafts that were tested using O-cells, the tip and side resistances were deduced separately from test results. Both predicted and measured resistance was determined at two failure criterion: 1 inch and 5% B settlement. Statistical analyses were performed to compare the predicted total, tip, and side drilled shaft nominal axial resistance with the corresponding measured nominal resistance.

Based on the analysis results, bias (the ratio of measured nominal resistance to predicted capacity) was calculated for defined failure criteria and the statistical parameters for each analysis method can also be determined. Resistance factors for each analysis method are calibrated using the recommended calibration approach in TR Circular No. E - C079.

## CHAPTER 2 LITERATURE REVIEW

This literature review focuses on recent state DOT research on the calibration of load resistance factor design (LRFD) resistance factors for deep foundations, including both driven piles and drilled shafts, which were reviewed separately. TRID, an integrated database from TRB, was the main search engine used for the literature review. The review results are grouped by state, with an overview each state's completed/ongoing research efforts. Special focus was on the database and its quality. The calibrated pile capacity prediction method and brief results were presented. For each calibration method, the calibration approach, data quality check, and statistical processing of the database were reviewed to provide references for the current Caltrans calibration study.

### LRFD Calibration of Driven Piles

#### Oregon DOT (Thompson et al. 2009; Smith et al. 2011)

Portland State University (PSU) completed two phases of LRFD calibration research on the implementation of LRFD principles for driven-pile design for the Oregon DOT (Smith and Dusicka 2009; Smith et al. 2011). ODOT currently uses the dynamic method to evaluate nominal axial static capacity for each driven pile in the field, with resistance factors specified by AASHTO. ODOT typically applies the wave equation software (WEAP) at the end of the initial driving (EOID), and occasionally at the beginning of pile restrike (BOR), to capture increases in capacity from the set-up. However, the AASHTO resistance factor,  $\phi$ , for WEAP at EOID, is too low for the efficient design of piles to match the likely probabilities of pile failure. The Phase I research evaluated the National Cooperative Highway Research Program's (NCHRP) recommended resistance factor of 0.4 for a recently completed pile-supported bridge. The case study showed that the number of piles at the bent would be doubled under new AASHTO requirements. This suggests that the standard will add considerable pile foundation costs to all new bridges. This cost increase was a strong incentive to complete a statistical recalibration of GRLWEAP dynamic capacity resistance value in a phase 2 of this study.

The goal of the Phase II research was to determine the appropriate resistance factors for the GRLWEAP method, using an extended high-quality pile load test database, including data from the NCHRP 507 study, the FHWA DFLTD (Raghavendra, et al., 2001) database, and other sources. The recalibration effort utilized the ratio between Davisson's criteria of measured load test capacity and the corresponding GRLWEAP capacity prediction at both EOID and BOR conditions.

## Database

The driven pile data was compiled from previous databases, including PDLT2000, the Deep Foundation Load Test Database (DFLTD), FL Database, FHWA database, and other data sources found in research papers and reports. The compiled database created by the research project is called Full PSU Master database. Over 150 new cases were added to the ODOT-supplied PDLT2000 and DFLTD databases to establish a new Full PSU Master database with 322 piles. The research group created two Microsoft Excel© spreadsheets, containing separate tabs for the DRIVEN input, GRLWEAP input, summary, output, and notes and references. Each of the fully-qualified case histories was analyzed using DRIVEN and GRLWEAP, and the results were summarized for the purpose of statistical calibration of the resistance factor for EOID and BOR. The two spreadsheets were the PSU PDLT2000 Master database and the Full PSU Master database. The PSU PDLT2000 Master database contained 156 driven pile case histories extracted from the PDLT2000 database and supplemented by additional details from the DFLTD. The Full PSU Master database reached a total of 322 driven piles from a number of the various sources identified above and included all the PSU PDLT2000 Master cases. PDLT2000 and DFLTD cases contributed over 50% of the total number of case histories finally entered into the master database. A breakdown of all of the sources included in the Full PSU Master database is shown in Table 2-1. There was considerable overlap between the numbers of pile case histories because some data was tracked to more than one source; i.e., the total sum of the case histories in Table 2-1 is greater than the total number of case histories in the Full PSU Master.

Table 2- 1. Source of Data for Pile Case Histories for Resolution of Errors and Anomalies

Source of Pile Case History	Pile Case Histories in Full PSU Master
PDLT 2000	156
DFLTD	102
Prof. James Long	28
Data sent by state DOT	18
Data for state DOT project, but not sent by DOT	61
Scholarly articles	60
TOTAL represents overlap between sources	425

The breakdown of the databases, by pile and soil type, is shown in Table 2-2. The largest state contributors were Florida at 53, South Carolina at 23, Louisiana at 22, and Wisconsin at 14, with 24 more states contributing less than 10 cases each. The resistance of each soil layer was examined, and a general soil-type category was assigned for ease of organization. Cohesive soils contributing more than 80 percent of a pile's capacity were designated as clay;

cohesionless soils contributing more than 80 percent of a pile’s capacity were designated sand; and soils that were layered, and comprised of both clay and sand, were called mixed.

Table 2- 2. Breakdown of all 322 piles in the Full PSU Master Database by Pile and Soil Type (Smith et al., 2011)

Major Contributing Soil Type	Pile Type					Total Cases
	Concrete Pile	H-Pile	Closed End Pipe Pile	Open Ended Pipe Pile	Other	
Sand	62	19	17	4	1	103
Clay	17	5	10	1	0	33
Mix	14	9	16	5	1	45
Unknown	54	24	38	20	5	141
Total Cases	147	57	81	30	7	322

### Soil Data

The original purpose of the PDLT2000 was for the prediction of driven pile capacity by PDA dynamic methods; however, too few soil properties were provided in this database, making it necessary to rely upon the DFLTD and additional databases. Soil strength parameters for the majority of the piles in the Full PSU Master, sensitivity analyses were conducted due to the lack of subsurface soil boring logs.

### Data Anomalies and Cross Checking

The PDLT2000 and the DFLTD pile databases were examined and compared to the values recorded for the same piles in other databases and in other original source reports. The parameters found errors, including the pile blow counts, pile lengths, and penetration depths. Cross-examinations of DFLTD and PDLT2000 showed that 72 of the 156 qualified piles in the PDLT2000 had 43 anomalies, with 29 piles having no site identifier for any follow-up investigation. Twenty-eight piles had more than one anomaly, especially the BOR blow count. After resolution of errors and anomalies, 103 of the 156 PDLT2000 entries qualified for DRIVEN and WEAP final analysis. In cases where piles from the PDLT2000 were matched with piles in the DFLTD by a site identifier, soil data was obtained from the DFLTD, which was judged to be the most reliable source. Details of the cross checking can be found in the published report (Smith et al. 2011).

### Calibration Approach

In this study, statistics calculations were based on 179 cases from Tier 1 and Tier 2 in the Full PSU Master database. To help identify possible errors, a simple blow count-based BOR/EOID

set-up ratio (SR) breakdown was performed. Four cases with  $SR > 30$  were taken out, and the remaining 175 valid cases were calibrated for the resistance factor. Calibration followed the procedures outlined by AASHTO (Allen et al. 2005).

The bias for the WEAP method was calculated as the ratio between Davisson's load test criteria and the corresponding resistance predictions from WEAP at EOID and BOR. The load-related statistics were taken at the value most often selected by LRFD researchers, using AASHTO Strength I load combinations, for driven pile studies on redundant pile groups of five or more ( $\beta = 2.33$ ).

### **Database Examination and Quality Metrics**

Allen et al. (2005) makes it clear that the statistical quantity and quality of pile data must be assessed for quality LRFD calibration. In the PSU study, the data quality was evaluated by assigning each pile data a tier number, which described the level of reliance on input assumptions, to analyze the case in both DRIVEN and GRLWEAB. Similar output rank was assigned to each case history output. In the NCHRP 507 study, an arbitrary  $\pm 2$  S.D. range tail outliers filter was applied, and cases beyond this range were removed. This approach was also used to study the effect of such data removal on the calibrated resistance factors. The pile blow count-based BOR/EOID set-up ratio (SR) breakdown was examined, for piles that used the same hammer on restrike, to help identify possible reported blow-count keystroke-entry errors. Load test time filters were also applied to examine their effect on the data.

For Monte Carlo simulation, Allen pointed out that the overall "fit" to statistical distributions, particularly the extreme tail-shape fit, dictates the COV and partially controls the differences between the First Order Second Moment (FOSM) and a random number from Monte Carlo-derived  $\phi$  values (Allen et al. 2005). The most accurate Monte Carlo-based calibration fit results are driven by the lower portion of the  $\lambda$  distribution, where resistance predictions are non-conservative and the risk of failure is higher. Smith (2011) incorporated the recommendations offered by Allen et al., using lognormal "best fits" from three fitting approaches: regressed fitting all the case history data points, regressed fitting by dropping data points from the upper  $\lambda$  tail (conservative), and fitting the lower  $\lambda$  tail by visual adjustment. Figure 2-1 shows an example of using the above three mentioned fitting approaches. The much better visual tail fit raised the Monte Carlo-calibrated EOID  $\phi$  factor in Scenario A (175 piles included in Tier1 and 2) by 50 percent compared to the FOSM method results.

Table 2-3 summarizes all the calibration results for the data processed with different quality controls and filters. Scenario G represents the broadest and best inclusive ODOT category for all piles in all soils, with 94 case histories used at EOID and 114 used at BOR. Twenty low

blow count piles were removed from EOID by the  $N > 2$  BPI (blow counts per inch) requirement. Based on the results of Scenario G, the EOID Monte Carlo resistance factor of  $\phi$  for all soils and pile types was calibrated to be 0.57, which is over 40 percent higher than that recommended earlier by AASHTO codes (2, 3), and over 10 percent higher than the current AASHTO code (5). It also provided a new restrike BOR resistance factor of 0.41. Most investigators have followed AASHTO  $\phi$  step increments of 0.05 in the past, which leads to recommendations from this study of 0.55 at EOID and 0.4 at BOR.

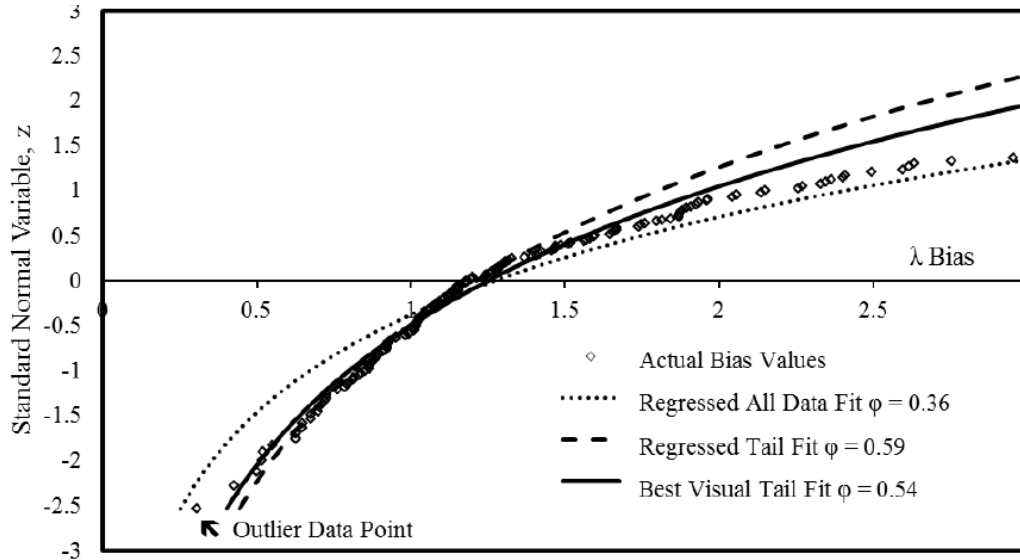


Figure 2-1. Standard Normal Variable to  $\lambda$  Bias Fits for EOID in Scenario A.

Table 2- 3. FOSM and Monte Carlo Best Visual Tail Fit Based  $\phi$  and  $\phi/\lambda$  Efficiencies for  $\beta = 2.33$  (Smith et al., 2011)

Model Filter Set			Cases	Monte Carlo (best fit)					FOSM	
				Mean $\bar{z}$	S.D.	COV	$\phi$	$\phi/\lambda$	$\phi$	$\phi/\lambda$
Scenario A	Tier 1 and Tier 2	EOID	175	1.38	0.65	0.471	0.54	0.35	0.35	0.23
		BOR	175	0.91	0.41	0.451	0.39	0.39	0.38	0.38
Scenario F	Tier 1 + 2a, BPI>2	EOID	69	1.38	0.61	0.442	0.59	0.42	0.59	0.42
		BOR	79	0.96	0.41	0.427	0.42	0.42	0.42	0.42
Scenario G	Tier 1 + 2a + 2b, Rank 1, BPI>2	EOID	94	1.28	0.55	0.43	0.57	0.43	0.56	0.42
		BOR	114	0.96	0.43	0.448	0.41	0.42	0.4	0.41
Scenario I Clay & Mixed	Tier 1 + 2a + 2b, Rank 1, BPI>2	EOID	43	1.23	0.3	0.244	0.83	0.57	0.64	0.44
		BOR	56	1.08	0.45	0.417	0.49	0.44	0.49	0.44
Scenario J Sands	Tier 1 + 2a + 2b, Rank 1, BPI>2	EOID	51	1.17	0.51	0.436	0.55	0.45	0.51	0.42
		BOR	58	0.82	0.36	0.439	0.36	0.42	0.36	0.42

Note: Rank 1 means pile cases with no key assumptions were required for analysis and no anomalies were present in output. Typically, in soft soils, GRLWEAP capacity approximately equals DRIVEN capacity, and for harder soils GRLWEAP capacity is less than DRIVEN

#### Kansas DOT (Penfield et al. 2014)

The Kansas Department of Transportation (KDOT) currently uses a variation of the Engineering News Record (ENR) formula (KDOT-ENR) to determine the driven pile capacity in the field. Past KDOT project experience strongly indicates that the KDOT-ENR formula tends to predict a much lower pile nominal resistance than the one measured by PDA, CAPWAP, or a combination of the two. The University of Kansas was contracted by the KDOT to conduct a LRFD calibration of the KDOT-ENR formula for verification of the pile capacity in the field.

The objective of this study was to compare available KDOT-ENR data to PDA and CAPWAP data in order to arrive at a revised version of the KDOT-ENR formula (Penfield et al. 2014). Originally reported ENR capacity was compared with measurements obtained by using a pile-driving analyzer (PDA) system and CAPWAP. The PDA/CAPWAP values were assumed to be the true capacity. There were 175 end-of-drive data points and 189 restrike data points available

for statistical analysis. The calibrated resistance factor was used as a multiplier coefficient and added to the existing KDOT-ENR formula. A set of resistance factors for PDA and CAPWAP at EOD and BOR were recommended for 11 pile cases driven by Delmag/APE (diesel) hammers and gravity hammers.

### **Database**

The KDOT provided pile data to researchers at the University of Kansas in May of 2012. This data had been collected by the KDOT since 1986 from 54 bridge sites around the state of Kansas. The information provided by KDOT consisted of bridge foundation geology reports, PDA reports, CAPWAP files, PDA files, and other related documentation. All relevant data was entered into the Microsoft Access database. The database included information for both end-of-drive piles and restrikes. Some piles only had end-of-drive (EOD) because restrrike is not necessary when EOD meets the required capacity.

EOD capacity was determined by the movement (set) in the last 20 blows of driving. The restrrike capacity was determined by the movement of the pile in the first five blows of driving. In some cases, the first five blows did not provide a reliable estimate, so the first 20 blows were used to determine restrrike capacity.

From all the collected piles, only piles with reported KDOT-ENR capacity and a PDA and/or CAPWAP capacity were analyzed. This screening led to 175 piles with EOD and 189 piles with beginning-of-restrrike (BOR). This resulted in 364 sets of data points, or biases, available for analysis. Of the total, 246 piles were entered into the database, among which 223 were H-piles, 13 were pipe piles, and 10 were concrete piles. Two different types of pile-driving hammers were used by KDOT in the majority of the cases: Delmag/APE (diesel) hammers and gravity hammers. KDOT utilizes a different pile-driving formula for diesel and gravity hammers. Of the 175 end-of-drive pile cases, 164 were performed with a Delmag/APE diesel hammer, and 11 were performed with a gravity hammer. There were a total of 189 restrikes driven by diesel hammers. Of these, 29 yielded a PDA-predicted capacity and 160 yielded a CAPWAP-predicted capacity. Only diesel hammers were analyzed for restrikes since there were not enough data points for the other hammer types.



### **KDOT-ENR Formula**

$$P_u = \frac{1.6WH}{\left(s + 0.1 \left(\frac{X}{W}\right)\right)}$$

Where

$P_u$  = formerly pile capacity and currently the target nominal capacity;

W = Weight of the piston, given in the hammer specifications (kips);

H = Maximum hammer drop (in feet);

s = Set per hammer blow for the last 20 blows for EOD and first five blows for restrike (inches);

X = Weight of pile + weight of pile cap and/or anvil (kips).

Note that the units of H (height of stroke) and s (set per hammer blow) are entered into the formula in different units. H is entered in feet, and s is entered in inches. A factor of safety of 7.5 is built into this formula. Since the units of the numerator are ft.-kips and the units of the denominator are inches, the factor of safety is determined as  $12/1.6 = 7.5$ .

### **Data Quality**

The researchers selected only the piles with reported KDOT-ENR and PDA and/or CAPWAP capacity. This ensured that the data best represented the DOT practice and reflected true operation uncertainty. Performing the back-calculation for the KDOT-ENR formula may have introduced an element of error. Since the KDOT-ENR was normally calculated in the field, generally by the same two or three investigators, it was decided that performing a back-calculation was not acceptable because it may not produce consistent results.

### **Calibration Approach**

The calibration was performed using the Monte Carlo method, following the method in the Transportation Research Circular E-C079 (Allen et al. 2005). The figure below shows an example of the measured bias used for the Monte Carlo calibration. The lognormal distribution of the measured bias was adopted, and statistical characteristics and load factors were also adopted from the Transportation Research Circular E-C079. Both dead and live loads were assumed to be normally distributed. A DL/LL ratio of 2.0 was chosen.

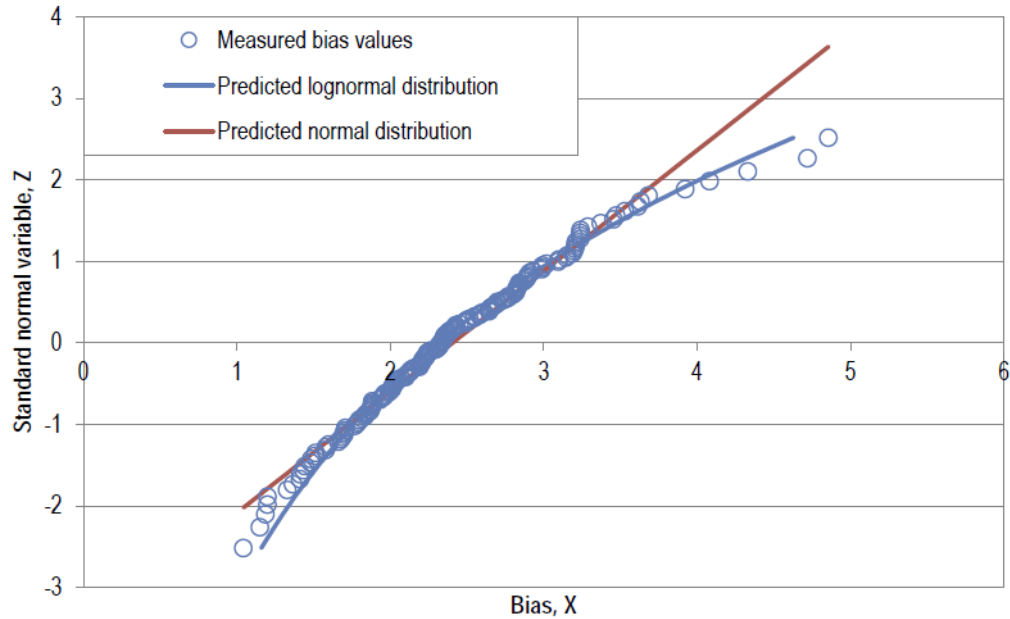


Figure 2-2. Standard Normal Variable for 164 End-of-Drive Biases (PDA and CAPWAP), Driven by Diesel Hammers.

From the database created above, biases were calculated as measured-to-predicted values, where the measured value was the pile-bearing capacity given by the PDA or CAPWAP, and the predicted pile-bearing capacity was given by the KDOT-ENR formula. Statistical analysis, following Allen et al., (2005), was performed to determine the lognormal parameters used for the Monte Carlo calibration, as shown in Tables 2-4 and 2-5.

Table 2- 4. Parameters for End-of-Drive Pile Blows Used in Monte Carlo Simulation

	No. of Cases	$3 R$	$COV_R$
PDA	48	2.49	0.328
CAPWAP	116	2.38	0.256
Combined PDA/CAPWAP	164	2.41	0.285
Gravity (PDA and CAPWAP)	11	2.57	0.133

Table 2- 5. Parameters for Restrikes Used in Monte Carlo Simulation

	No. of Cases	$3 R$	$COV_R$
PDA	29	2.74	0.254
CAPWAP	160	2.24	0.251
Combined PDA/CAPWAP	189	2.31	0.272

For calibration, statistical characteristics and load factors were adopted from the Transportation Research Circular E-C079 and are shown below. Both dead and live loads are assumed to be normally distributed.

Table 2- 6. Statistical Characteristics and Load Factors

	Bias	COV	Load factor
Live load	$\lambda_{LL}=1.15$	$COV_{LL}=0.2$	$\hat{U}_{LL}=1.75$
Dead load	$\lambda_{DL}=1.05$	$COV_{DL}=0.1$	$\hat{U}_{DL}=1.25$

NOTE: Bias is the mean value of the measured/predicted load. COV is the coefficient of variation, which is the standard deviation divided by the mean.

50,000 random cases were generated in the Monte Carlo simulation for the resistance factor calibration. Table 2-7 shows the resistance factors that were determined for various reliability indices.

Table 2- 7. KDOT-ENR Resistance Factors from Monte Carlo Simulation

	$\beta = 1.5$	$\beta = 2.0$	$\beta = 2.5$	$\beta = 3.0$	$\beta = 3.5$
End-of-Drive					
PDA	1.88	1.59	1.35	1.16	0.95
CAPWAP	2.02	1.76	1.53	1.35	1.17
Combined	1.95	1.68	1.45	1.25	1.07
Restrikes					
PDA	2.38	2.09	1.85	1.63	1.45
CAPWAP	1.91	1.68	1.47	1.28	1.13
Combined	1.90	1.65	1.43	1.24	1.09
EOD Gravity	2.64	2.43	2.25	2.07	1.94

Recommended KDOT-ENR Formula

$$P_u = \varphi_{ENR} \frac{1.6WH}{\left(s + 0.1 \left(\frac{x}{w}\right)\right)}$$

The resistance factor is given in Table 2-6. These resistance factors are greater than one, which is unusual, but is true for this case because the factors taken into account are not only the uncertainty of the KDOTENR method, but also the significant under-prediction of pile resistance that comes from using the KDOT-ENR method. (Louisiana DOTD; (Abu-Farsakh et al. 2009; Abu-Farsakh et al. 2010; Abu-Farsakh et al. 2013))

The Louisiana Department of Transportation and Development (LADOTD) sponsored a series of LRFD calibration efforts for their driven pile and drilled shaft design and construction. The first calibration was conducted on driven piles in 2009, the drilled shaft calibration for the 1999 FHWA design method was completed in 2010, and the Brown et al. method (2010 FHWA design method) was completed in 2013. A research project on the calibration of the modified Gates formula for driven piles is ongoing.

The first project, LTRC Final Report 449, focused on LRFD calibration of driven piles. Efforts were focused on the static and dynamic analysis method (CAPWAP) for driven-pile capacity estimation. The static methods calibrated were the  $\alpha$ -method, the Nordlund method, and three CPT-based methods. The LTRC Final Report 470 described the calibrated 1999 FHWA drilled shaft design method. With the publication of the new drilled shaft design method in 2010, a re-calibration of the drilled shaft design for the new method was conducted, with eight new drilled test data collected since the completion of the previous drilled shaft calibration. The ongoing research project for the modified Gates equation was intended for driven pile construction of smaller projects where dynamic measurements were not available. The databases used for all of the calibration were mostly collected in Louisiana, with some cases of drilled shafts collected from its neighboring state, Mississippi. In general, the calibrated resistance factors closely matched the AASHTO standards. Noticeable improvement of resistance factors were observed for static methods for driven piles.

### **Database**

Driven Pile Database: Driven pile load tests were collected from LADOTD project archives. The created driven pile database included a total of 53 square precast, prestressed concrete (PPC) piles, as shown in Table 2-8. The pile sizes ranged from 14 inches to 30 inches. The majority of the piles (51 of 53) were friction piles, as most of the driven piles were used in southern Louisiana, where thick soil deposits are dominant. The majority of the soil type was cohesive soil. The driven pile database was created in EXCEL's spreadsheet format. It included project information, soil stratification, and pile properties, load test data, CPT profile, dynamic test data, etc. Figure 2-3 below shows an example of the soil properties collected. The information collected for each pile allowed for the calculation of pile capacity, using static analysis, CPT-based methods, and CAPWAP (reported values). Measured pile capacity was determined from static load testing, using Davisson's failure criteria for piles with a size less than 24 inches and the modified Davisson failure criteria, used for piles exceeding a size of 24 inches.

Drilled Shaft Database: In the first drilled shaft calibration project, an extensive search was conducted to collect all available drilled shaft test data in Louisiana and Mississippi. A total of 26 drilled shaft cases, which met the FHWA 5% B settlement criterion, were collected. (B was

the diameter of the drilled shaft.) In a continuing effort to implement LRFD design methodology for deep foundations, eight new drilled shaft test data were added to the database in the second calibration. The final combined database had 34 cases, as shown in Table 2-9. The diameters of the drilled shafts included in the database ranged from 2 ft. to 6 ft., and the lengths ranged from 35.1 ft. to 138.1 ft. Fifteen of the cases collected from Mississippi and fifteen cases collected from Louisiana were O-cell tests. In addition, four cases in Louisiana were conventional top-down load tests. The soils encountered in the investigated database included silty clay, clay, sand, clayey sand, and gravel. Most of the soil strata was not homogenous and contained inter-bedded layers. Consequently, the soil type for this database was classified as mixed soils, and the total resistance factor calibrated in this study was considered for mixed soil. True drilled shaft capacity was determined from the collected O-Cell load test. In addition, separated resistance, i.e., tip and side resistance, were also determined. The detailed soil profile enabled drilled design calculation through software SHAFT 5.0. The predicted shaft resistance was interpreted from the predicted load-settlement curve, using the FHWA 5% B failure criterion.

Table 2- 8. Summary of the Characteristics of the Investigated Piles (Abu-Farsakh et al., 2009)

Square PPC Pile Size	Pile Type		Predominant Soil Type		
	Friction	End- Bearing	Cohesive	Cohesionless	Limit of Information
14"	22	0	19	3	0
16"	5	0	3	0	2
18"	2	0	1	1	0
24"	9	1	7	3	0
30"	13	1	9	5	0
Total	51	2	39	12	2

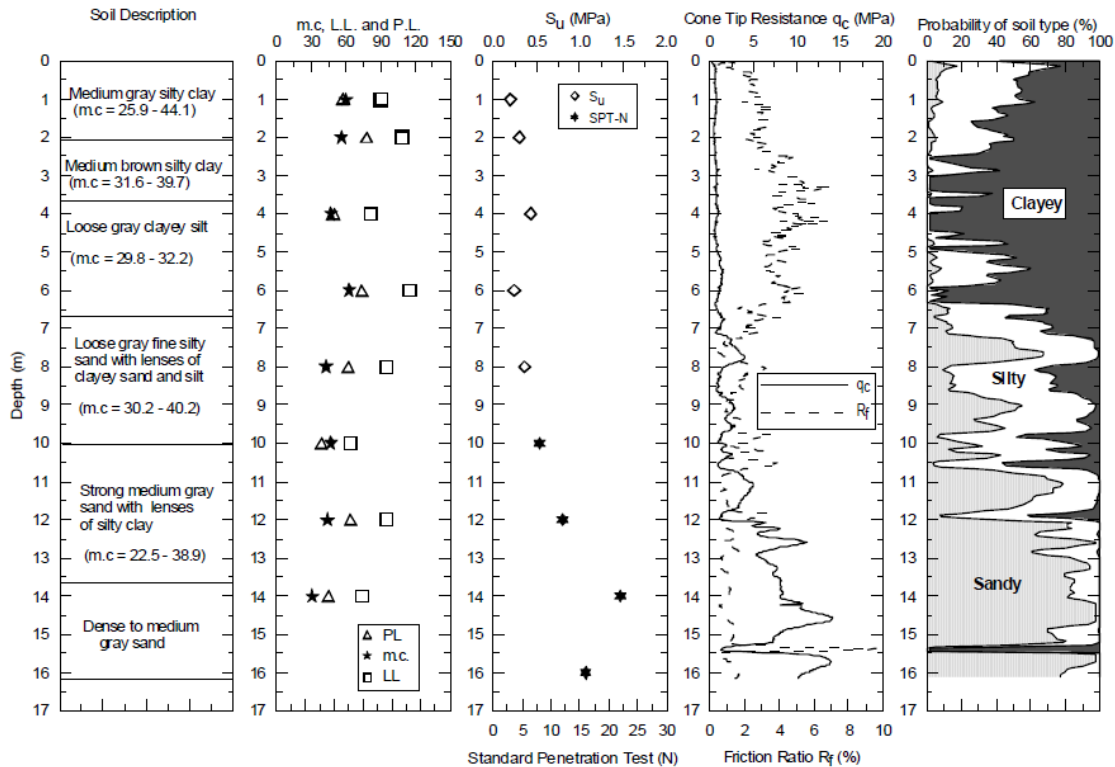


Figure 2-3. Example of Geotechnical Data for a Driven Pile (Abu-Farsakh et al. 2009).

All collected drilled shaft load test reports were compiled, along with information and data regarding the project (soil stratification and properties, drilled shaft characteristics, load test data, etc.), and were then processed and transferred from each load test report to tables, forms, and graphs. The following data and information were collected and compiled for each drilled shaft load test report. The soil data consisted of information on the soil boring location (station number), soil stratigraphy, unit weight, laboratory testing (shear strength, physical properties, etc.), and in-situ test results (e.g., Standard Penetration Test (SPT) for cohesionless soil).

### Data Anomalies and Cross Checking

The data sources were load test reports provided by the Louisiana DOTD and the Mississippi DOT. The research team was able to create a high quality database to satisfy the input requirements for selected capacity prediction methods for driven pile and drilled shafts. Only test data that met or almost met the failure criteria was selected in the databases. Only PPC piles that had been tested to failure and included adequate soil information were selected for the driven pile database. The drilled shaft cases were selected based on initial screening to identify cases with subsurface soil conditions similar to Louisiana soils and which contained mostly O-cell load tests, which allows for calculation of separated resistance.

Table 2- 9. Summary of the Characteristics of the Investigated Drilled Shafts (Abu-Farsakh et al., 2013)

I.D.	Location	Dia.	Length	Soil Type	Load Test
DS-01	Caddo, LA	2.5	53.1	Silty Clay, Sand Base	Top Down
DS-02	Caddo, LA	2.5	35.1	Clay and Sand with Sand Base	Top Down
DS-03	E. Baton Rouge, LA	3	54.1	Clayey Silt, Sand Base	O-cell
DS-04	Ouachita, LA	5.5	76.1	Silty Sand with Sand Base	O-cell
DS-05	Calcasieu, LA	6	86.9	Stiff Clay with Clay Base	O-cell
DS-06	Winn, LA	2.5	77.4	Sand Clay with Sand Base	O-cell
DS-07	Winn, LA	2.5	65	Fully Sand with Clay Base	O-cell
DS-08	E. Baton Rouge, LA	2.5	49.9	Silt, Clay with Clay Base	O-cell
DS-09	Beauregard, LA	5.5	40.7	Clay, Silt with Clay Base	O-cell
DS-10	Caddo, LA	3	44.9	Clay, Silty Clay with Clay Base	Top Down
DS-11	Caddo, LA	3	62	Clay with Sand Base	Top Down
DS-12	Union, MS	4.5	49.9	Fully SAND	O-cell
DS-13	Union, MS	4	73.1	Sand with Clay, Sand base	O-cell
DS-14	Washington, MS	4	123	CLAY/SAND-Sand Base	O-cell
DS-15	Washington, MS	4	138.1	SAND	O-cell
DS-16	Washington, MS	4	119.1	CLAY, SAND with SAND	O-cell
DS-17	Washington, MS	5.5	94.1	SAND/CLAY with SAND Base	O-cell
DS-18	Washington, MS	4	96.1	SAND with Sand Base	O-cell
DS-19	Washington, MS	4	82	SAND/GRAVEL/Sand Base	O-cell
DS-20	Washington, MS	4	97.1	Sand with Clay Interlayer and	O-cell
DS-21	Washington, MS	4	82	SAND with SAND Base	O-cell
DS-22	Lee, MS	4	89	Clay	O-cell
DS-23	Forrest, MS	6	47.9	SAND	O-cell
DS-24	Perry, MS	4.5	64	SAND/CLAY, Clay Base	O-cell
DS-25	Wayne, MS	4	64	Sand with Clay Base	O-cell
DS-26	Madison, MS	2	40	CLAY with Clay Base	O-cell
DS-27	E. Baton Rouge, LA	4	67.5	Fully Clay, Clay Base	O-cell
DS-28	E. Baton Rouge, LA	2.5	81.5	Fully Clay, Clay Base	O-cell
DS-29	E. Baton Rouge, LA	4	77.5	Fully Clay, Clay Base	O-cell
DS-30	Caddo, LA	6	43	Clay, Sand with Sand Base	O-cell
DS-31	Caddo, LA	5.5	47.5	Fully Sand with Sand Base	O-cell
DS-32	Caddo, LA	5.5	48	Sand, Clay with Sand Base	O-cell
DS-33	Caddo, LA	5.5	53.85	Clay, Sand with Sand Base	O-cell
DS-34	Caddo, LA	5.5	51.12	Clay, Sand with Sand Base	O-cell

### Calibration Approach

Based on the analysis of 53 driven piles, a statistical analysis was performed to evaluate the accuracy and performance of the various pile capacity estimation methods. Statistical parameters of the inverse of the bias ( $R_p/R_m$ ) for driven piles were calculated and are shown in Table 2-10. The mean and standard deviations of the  $R_p/R_m$  ratio for the static method were 1.12 and 0.32, respectively, indicating an average of 12 percent overestimation. Figure 2-4 shows an example of the distribution of bias for the static method. Lognormal distribution was used for the resistance factor calibration. Resistance factors were calibrated using three methods: first order second moment (FOSM), first order reliability method (FORM), and Monte Carlo Simulation method (MCS). The calibration procedure followed the standard calibration procedure proposed by Allen et al. (2005). In this case, as in the drilled shaft calibration, selected statistical parameters of dead and live loads were derived from AASHTO LRFD specifications as follows:

Table 2- 10. Statistical Characteristics and Load Factors (ref.)

	Bias	COV	Load factor
Live load	$\lambda_{LL}=1.15$	$COV_{LL}=0.18$	$\hat{U}_{LL}=1.75$ ,
Dead load	$\lambda_{DL}=1.08$	$COV_{DL}=0.13$	$\hat{U}_{DL}=1.25$ ,

Dead load to live load ratio of 3 and reliability index of 2.33 were assumed for the calibration. The bias statistics parameters were directly calculated from the bias data.

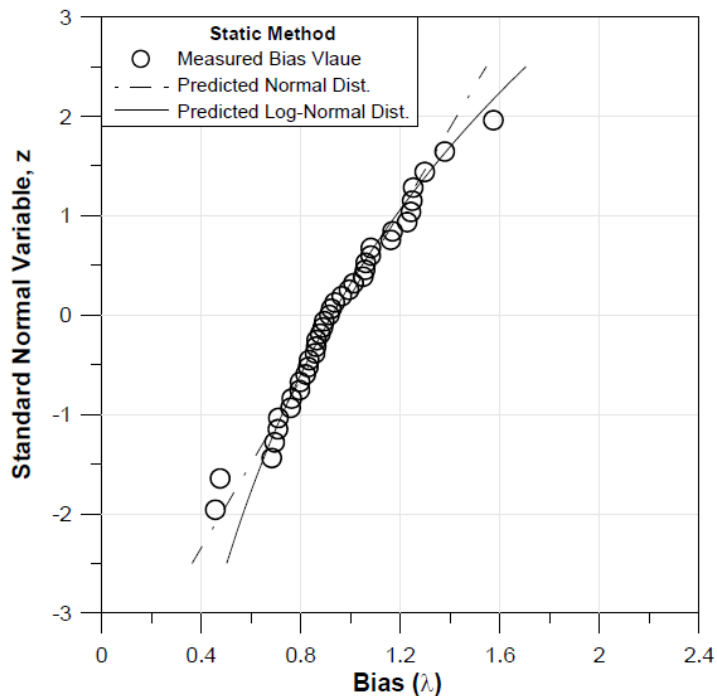


Figure 2-. Cumulative Distribution Function (CDF) of Bias Values (Static Method) (Abu-Farsakh et al. 2013)



Table 2- 11. Evaluation Summary of the Various Prediction Methods (Abu-Farsakh et al., 2013)

	$R_p/R_m^*$		Best fit calculations	
	Mean	STD	$R_{fit}/R_m^*$	$R^2$
Static $\alpha$ -method	1.12	0.32	1	0.84
Schmertmann method	1.2	0.37	1.2	0.81
LCPC method	1.05	0.38	1.11	0.78
de-Ruiter & Beringen	0.9	0.28	0.94	0.84
Average of CPT methods	1.05	0.33	1.08	0.82
CAPWAP–EOD method	0.35	0.23	0.32	0.69
CAPWAP–14 days BOR method	0.83	0.22	0.92	0.91

Statistical parameters for the 2010 FHWA drilled shaft design method are shown in Table 2-12. The slope of the best-fit line is 1.02, which indicates a two percent over-estimation of shaft resistance when using the 2010 FHWA design method for Louisiana soils. The histogram plot and CDF plot are shown in Figures 2-5 and 2-6. As shown in these figures, lognormal distribution matches the histogram and CDF curves better than normal distribution. The bias statistical parameters were determined using three methods: direct measurement, fit-to-all, and fit-to-tail. Abu-Farsakh et al. (2013) believes that the resistance factor based on measured bias is more favorable since the measured bias data can be utilized to its full extent.

Table 2- 12. Statistical Analysis of the 2010 FHWA Drilled Shaft Design Method (Abu-Farsakh et al., 2013)

Summary Statistics				Best fit calculations
$R_m/R_p$			$R_p/R_m$	
Mean ( $\lambda_R$ )	$\sigma$	COV	Mean	$R_{fit}/R_m$
0.99	0.3	0.3	1.1	1.02

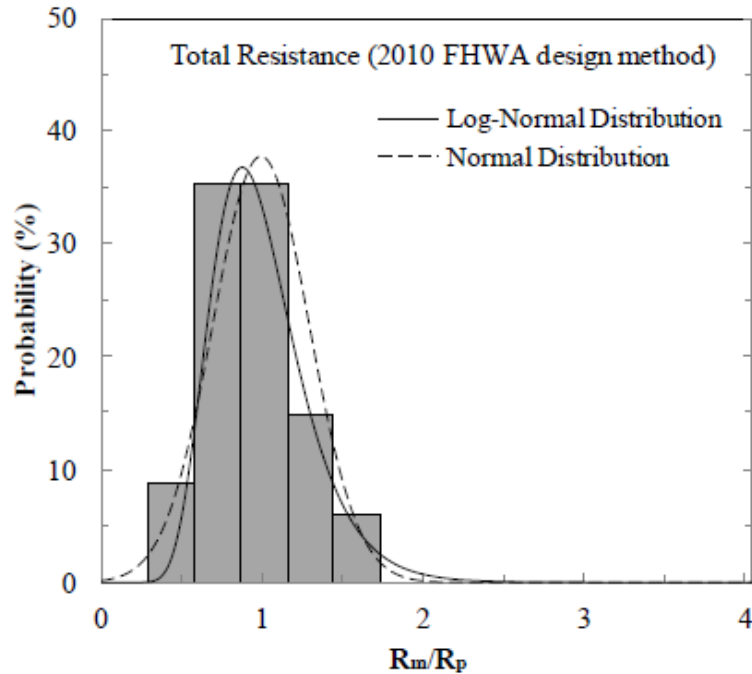


Figure 2-4. Histogram and Probability Density Function of Resistance Bias for 2010 FHWA Design Method (Abu-Farsakh et al. 2013).

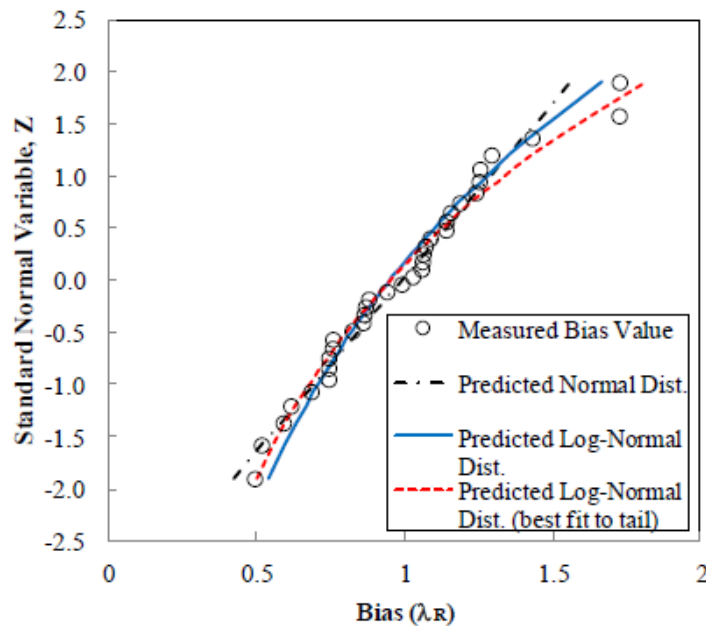


Figure 2-5. Cumulative Distribution Function (CDF) of Bias Values (2010 FHWA Design Method) Calibration Results (Abu-Farsakh et al. 2013).

The calibrated resistance factors for driven pile are shown Table 2-13. The resistance factor for the static method increased to 0.63, as compared with 0.35-0.45 from AASHTO. Based on the results of the reliability analyses for  $\beta_T = 2.33$ , the De Ruiter-Beringen method showed the

highest resistance factor ( $\phi_{De-Ruiter} = 0.66$  [FOSM], 0.74 [FORM], and 0.73 [Monte Carlo simulation method]), while the Schmertmann method showed the lowest resistance factor ( $\phi_{Schmertmann} = 0.44$  [FOSM], 0.48 [FORM], and 0.49 [Monte Carlo simulation method]), which is lower than the AASHTO recommended value of 0.5. The resistance factors obtained for the CAPWAP (EOD) were 1.31 (FOSM) and 1.41 (FORM), which were higher than the CAPWAP (14 day BOR) resistance factors of 0.55 (FOSM), 0.61 (FORM), and 0.62 (Monte Carlo simulation method). This is mainly due to the pile set-up. Although the CAPWAP (EOD) has a high resistance factor, it is not an economical and reliable approach because it significantly underestimates the resistance and has a low efficiency factor. However, the dynamic measurement is mainly used for pile drivability, rather than for design.

Table 2- 13. Resistance Factors ( $\phi$ ) for Driven Piles ( $\beta T = 2.33$ ) (Abu-Farsakh et al., 2009)

Design Method		Proposed Resistance Factor ( $\phi$ ) and Efficiency Factor ( $\phi/\lambda$ ) for Louisiana Soil						Resistance Factor, $\phi$ [AASHTO (11)]
		FOSM		FORM		Monte Carlo Simulation		
		$\phi$	$\phi/\lambda$	$\phi$	$\phi/\lambda$	$\phi$	$\phi/\lambda$	
Static method	$\alpha$ -Tomlinson method and Nordlund method	0.56	0.58	0.63	0.66	0.63	0.66	0.35-0.45
	Schmertmann	0.44	0.47	0.48	0.52	0.49	0.53	0.50
Direct CPT method	LCPC/LCP	0.54	0.51	0.60	0.56	0.59	0.56	—
	De Ruiter and Beringen	0.66	0.55	0.74	0.62	0.73	0.61	—
	CPT average	0.55	0.53	0.61	0.59	0.62	0.59	—
Dynamic measurement	CAPWAP (EOD)	1.31	0.36	1.41	0.39	—	—	—
	CAPWAP (14 days BOR)	0.55	0.44	0.61	0.52	0.62	0.47	0.65

Table 2- 14. Resistance Factors ( $\alpha$ ) and Efficiency Factors ( $\alpha/\lambda$ ) for Drilled Shaft (Abu-Farsakh et al., 2013)

$\beta_T = 3.0$	Resistance Factor, $\alpha$	Efficiency Factor,
Current study (2010 FHWA design method)	0.48 in mixed soils 0.41 in mixed soils (fit to tail)	0.48 0.41
Current study (1999 FHWA design method)	0.60 in mixed soils 0.50 in mixed soils (fit to tail)	0.47 0.38
Liang and Li	0.45 in clay 0.50 in sand 0.35 in mixed soils	
Paikowsky and AASHTO	0.45 in cohesive soils 0.55 in cohesionless soils	

**Florida DOT** (McVay et al. 2000; McVay et al. 2002; McVay et al. 2004; McVay et al. 2012)

The University of Florida began data collection of driven pile tests for the Florida Department of Transportation (FDOT) in 1988 (Sharp et al. 1988). The UF pile load test database for driven piles, entitled PILEUF, included data collected from over 72 different sites and more than 180 different tests (both end-of drive and beginning of restrike) conducted across Florida (McVay et al. 2000). Later on, data on cylinder piles, including soil properties and conventional load test data, were collected and added to the deep foundation test database in Florida (McVay et al. 2004).

This work focused on evaluating the accuracy of dynamic predictions of static pile capacity by using the LRFD framework. The dynamic prediction methods evaluated included ENR, modified ENR, PDA, Gates, FDOT method, CAPWAP, Paikowsky method, and Sakai. In the case of the older driving formulas, the database was broken into both small (i.e., less than 1779 kN for Davisson capacity) and large (greater than 1779 kN for Davisson capacity) capacity piles.

The PILEUF database was a primary source for development of the calibrated resistance factor for driven piles, provided in the AASHTO bridge design specifications. It (PILEUF) has 285 entries (247 piles), of which 218 entries (72 sites, 180 piles) are in Florida, including square concrete, round concrete, pipe, and H piles. Only data from Florida was analyzed for the calibration. For each site, the soils along the pile shaft and tip were classified into one of nine categories: plastic clay, silt-and-clay mixture (or silts and marl), clean sands, limestone (or very shelly sands), clayey sand, sandy clay, silty clay, rock, and sandy gravel or tills. The piles were subdivided based upon material and shape: square concrete, round concrete, pipe, and H pile. All information in the database (SPT, PDA, CAPWAP, driving record, load-\ settlement,  $J_c$ , etc.)

was obtained from engineering reports provided to the owner (FDOT). Measured capacities used in this study were obtained by plotting the static load-settlement response of the pile and determining its Davisson (1972) capacity. The latter was selected over Debeer's or Fuller-Hoy's approach because it resulted in tolerable settlements under service loads (Sharp et al. 1988). It should also be noted that CAPWAP and case PDA pile capacities in the database were obtained from consultant reports, along with  $J_c$  values that represented the state of practice.

The calibration process in this study was based on the reliability theory, using first-order second-moment methods (FOSM). Target indexes  $\beta_T=2$  ( $P_f=2.5\%$ ) to  $\beta_T=2.5$  ( $P_f=0.62\%$ ) were designed for single piles (both EOD and BOR). Selected statistical parameters of dead and live loads, which were used in AASHTO LRFD specifications, are shown in Table 2-10.

The ratio of dead to live load is a function of a bridge's span length. Larger span lengths result in larger dead loads, but live loads are usually insensitive to span length. A span length of 27 m was chosen for this case, and the corresponding  $Q_D/Q_L$  equaled 1.58. The results for all the dynamic methods mentioned previously for both EOD and BOR are summarized in Tables 2-15 and 2-16.

Table 2-15. Load and Resistance Factor Design (LRFD) of Driven Piles Using Dynamic Methods at EOD (McVay et al., 2002)

Prediction Method	Number Of cases	Mean, $\lambda_R$ (Dav/Pred)	Standard Deviation	COV <sub>R</sub>	$P_f=0.62\%$ ( $\beta_T=2.50$ )			$P_f=2.50\%$ ( $\beta_T=1.96$ )		
					$\phi$	FS	$\phi/\lambda_R$	$\phi$	FS	$\phi/\lambda_R$
CAPWAP	44	1.597	0.559	0.350	0.733	1.970	0.459	0.912	1.584	0.571
PDA	48	1.344	0.443	0.329	0.645	2.237	0.480	0.796	1.814	0.592
Paikowsky Energy	27	1.110	0.372	0.335	0.527	2.740	0.475	0.651	2.216	0.587
Sakai et al Energy	21	1.504	1.256	0.835	0.231	6.254	0.153	0.348	4.150	0.231
FDOT (overall)	72	2.381	1.341	0.563	0.669	2.160	0.281	0.909	1.588	0.382
FDOT (<1779 kN)	34	1.490	0.782	0.525	0.457	3.161	0.307	0.611	2.362	0.410
FDOT (>1779 kN)	38	3.158	1.248	0.395	1.307	1.104	0.414	1.658	0.871	0.525
ENR (overall)	77	0.299	0.159	0.532	0.090	16.024	0.301	0.121	11.935	0.405
ENR (<1779 kN)	34	0.250	0.129	0.515	0.078	18.395	0.314	0.105	13.801	0.419
ENR (>1779 kN)	43	0.338	0.171	0.507	0.108	13.388	0.319	0.143	10.074	0.424
Modified ENR (overall)	61	0.446	0.267	0.599	0.115	12.533	0.258	0.159	9.086	0.357
Modified ENR (<1779 kN)	25	0.325	0.222	0.683	0.069	20.818	0.214	0.099	14.604	0.305
Modified ENR (>1779 kN)	36	0.530	0.321	0.606	0.135	10.720	0.254	0.186	7.749	0.352
Gates (overall)	74	1.742	0.787	0.452	0.633	2.280	0.363	0.822	1.756	0.472
Gates (<1779 kN)	32	1.071	0.351	0.328	0.515	2.802	0.481	0.635	2.272	0.593
Gates (>1779 kN)	42	2.254	0.717	0.318	1.109	1.302	0.492	1.361	1.061	0.604

Table 2-16. Load Resistance Factor Design (LRFD) of Driven Piles Using Dynamic Methods at BOR (McVay et al., 2002)

Prediction Method	Number Of cases	Mean, $\lambda_R$ (Dav/Pred)	Standard Deviation	COV <sub>R</sub>	P <sub>f</sub> =0.62% ( $\beta_T=2.50$ )			P <sub>f</sub> =2.50% ( $\beta_T=1.96$ )		
					$\phi$	FS	$\phi/\lambda_R$	$\phi$	FS	$\phi/\lambda_R$
CAPWAP	79	1.260	0.438	0.347	0.581	2.485	0.461	0.722	1.999	0.573
PDA	42	1.036	0.322	0.311	0.518	2.787	0.500	0.634	2.277	0.612
Paikowsky Energy	72	0.836	0.301	0.360	0.374	3.857	0.448	0.468	3.086	0.560
Sakai et al Energy	52	1.457	0.784	0.538	0.433	3.334	0.297	0.583	2.477	0.400
FDOT (overall)	63	2.574	1.293	0.502	0.832	1.735	0.323	1.103	1.309	0.429
FDOT (<1779 kN)	8	1.355	0.380	0.280	0.724	1.995	0.534	0.875	1.650	0.646
FDOT (>1779 kN)	55	2.751	1.284	0.467	0.966	1.495	0.351	1.262	1.144	0.459
ENR (overall)	71	0.235	0.160	0.681	0.050	28.597	0.215	0.072	20.080	0.306
ENR (<1779 kN)	9	0.186	0.057	0.306	0.094	15.348	0.505	0.115	12.562	0.617
ENR (>1779 kN)	62	0.242	0.169	0.698	0.050	28.841	0.207	0.072	20.120	0.296
Modified ENR (overall)	63	0.363	0.246	0.676	0.079	18.314	0.217	0.112	12.881	0.308
Modified ENR (<1779 kN)	8	0.277	0.062	0.224	0.166	8.704	0.598	0.196	7.356	0.708
Modified ENR (>1779 kN)	55	0.376	0.260	0.692	0.079	18.321	0.210	0.113	12.810	0.300
Gates (overall)	71	1.886	0.715	0.379	0.810	1.783	0.429	1.020	1.416	0.541
Gates (<1779 kN)	9	1.067	0.201	0.189	0.681	2.121	0.638	0.796	1.815	0.746
Gates (>1779 kN)	62	2.005	0.684	0.341	0.938	1.540	0.468	1.162	1.242	0.580

From the two tables above, it can be seen that the absolute value of  $\phi$  does not indicate the accuracy of the dynamic predictive method. For instance, the  $\phi$  factor, by using CAPWAP method at BOR condition, is 0.581 (when  $P_f = 0.62\%$ ,  $\beta_T = 2.5$ ), which is less than 0.832 resulting from the FDOT driving formula. The latter occurs because the FDOT formula has a bias factor (measured/ predicted) of 2.754 versus 1.26 by using the CAPWAP method.

The accuracy of the dynamic method is indicated by the coefficient of variation, which is the ratio of standard deviation to mean. Based on this, the CAPWAP, PDA, and Paikowsky's energy method show the highest accuracy. The efficiency (economic) performance of these predictive methods can be evaluated by the ratio of  $\phi/\lambda_R$ , indicating that the percentage of measured capacity can be used for design to reach a predefined structure reliability. The higher the value of  $\phi/\lambda_R$ , the more cost effective this method is. It can be shown that modern methods, based on wave mechanics, such as CAPWAP, PDA and Paikowsky's energy methods, are roughly twice as economic as the ENR, modified ENR, and FDOT driving formulas when reaching the same safety level. Additionally, the  $\phi/\lambda_R$  at BOR condition demonstrated slight improvement over the EOD for a target failure probability (i.e.,  $\phi/\lambda_R = 0.459$  at EOD versus 0.461 at BOR using CAPWAP,  $\phi/\lambda_R = 0.480$  at EOD versus 0.500 at BOR by using PDA).

This study also revealed the influence of the span length. The  $\phi$  factors and the back-calculated FS (safety factor) are insensitive to span length. Given a reliability index of 2.5 for both EOD and BOR, the resistance factor only decreases 6.8%, and the safety factor decreases 1.6% when

the span length is increased from 15 to 50 m (ratio of dead load to live load is increasing). However, the  $\phi$  factors are very sensitive to target reliabilities  $\beta_T$  (i.e., failure probabilities).

### **Minnesota DOT** (Paikowsky et al. 2009; Budge 2014)

P+ASE  $\bar{\alpha}$  To comply with the LRFD design of deep foundations mandated by FHWA in 2007, the Minnesota DOT completed its first phase of LRFD calibration of resistance factors in 2009. MnDOT used its driving formula to verify driven pile capacity during construction. The driving formula uses the weight of the hammer, height of fall of the hammer, final set of pile, and different factors for timber, concrete, shell, steel, and H piles. This equation was analyzed, along with four additional dynamic formulae, using two databases of driven piles: the MNDOT LT 2008 H-Piles database and the MNDOT LT 2008 Pipe piles database. The research also proposed a new MnDOT formula that was tailored for the pile driving practices of MnDOT. The new MnDOT dynamic equation used rated hammer energy and blows per inch at the EOD condition.

### **MnDOT LT 2008**

The database PD/LT 2000, used for AASHTO specification LRFD calculation, was used as a primary source of driven pile cases in the Phase I report published in 2009. Some new relevant cases from DOTs and other sources were collected and considered second sources of the MnDOT LT 2008 database. Cases favorable to MnDOT practice were selected from the database, and the two main databases, MnDOT LT 2008 H Pile database and MnDOT LT 2008 Pipe Pile database, were created and combined to produce the MnDOT LT 2008 database. The H pile database contained 166 cases on 137 different H piles, and the pipe pile database contained 167 cases on 138 different pipe piles. Detailed information on pile types, data associated with each pile, soil type, end of driving resistance, and range of hammer-rated energies were included. The database of the H pile and pipe piles were then sorted according to the soil type at the pile's side and tip, end of driving resistance, and range of hammer-rated energy. A separate database was created called MnDOT/LT 2008 Control, and was used for evaluating the research findings.

It was found from the database analysis that the current MnDOT driving formula over-predicted pile capacity with a mean bias of 0.8 when the bias was calculated as the ratio of measured capacity to dynamically-predicted capacity. Additionally, the current MnDOT produced large scatter with coefficients of variation of 0.5 to 0.8 for H and pipe piles at EOD condition. This caused the resistance factor to be calibrated and established at 0.25 instead of 0.4 (currently used) for both redundant H and pipe piles at EOD conditions. This reflects a significant

economic loss for a consistent level of reliability. Four other dynamic formulae used for analyzing the databases were Engineers News Record (ENR), Gates, FHWA modified Gates, and WSDOT. The bias for these formulae ranged over a wide spectrum, from 1.43 to 1.58 for the Gates equation and from 0.81 to 0.89 for other equations for H and pipe piles. The coefficient of variation for these formulae varied from 0.35 to 0.4. Such results provided the researcher with the ability to develop the new MnDOT dynamic equation, which was derived by using linear regression, to gain higher efficiency and reduction in costs. The currently-used MnDOT equation and new proposed equation are shown below. With the new MnDOT dynamic formula, resistance factors of 0.6 and 0.45 were suggested for H and pipe piles, respectively, which is shown below. However, the new MnDOT dynamic formula and its associated resistance factors needed to be evaluated further with static load tests and dynamic prediction methods.

Current MnDOT equation:

$$R_u = \frac{10.5E}{S + 0.2} \times \frac{W + C \times M}{W + M}$$

Where,

- R<sub>u</sub> = ultimate carrying capacity of pile, in kips
- W = mass of the striking part of the hammer in pounds
- M = total mass of pile plus mass of the driving cap in pounds
- S = final set of pile, in inches
- E = energy per blow for each full stroke in foot-pounds
- C = 0.1 for timber, concrete and shell type piles, 0.2 for steel H piling

New MnDOT equation

$$R_u = 30\sqrt{E_h} \times \log(10 \times N)$$

Where,

- R<sub>u</sub> = ultimate carrying capacity of pile, in kips
- E<sub>h</sub> = rated hammer energy kips • ft.
- N = blows per inch (PBI) at the end of driving (EOD)

Table 2-17. Summary of Recommended Resistance Factors for the Existing and Proposed

Pile Type	Recommended $\phi$		Assumptions
	Mn/DOT	New Mn/DOT	
H Piles	0.25	0.60	Resistance Factors were calculated for a target reliability $\beta=2.33$ , probability of failure $pf=1\%$ , assuming redundant pile use
Pipe Piles	0.25	0.45	



In Phase II, the following databases were reviewed to understand practices, developments, and major findings related to driven piles in the Midwest states.

**PHASE II:** Due to the resistance factors established in the Phase I study being conservative, and with the need to re-evaluate them, a Phase II study was performed. The Phase II study extended the Phase I analysis by broadening the scope of the study into timber and pre-stressed precast concrete piles. A new formula, MPF12, (Minnesota Pile Formula 2010) was proposed for MnDOT driven pile construction practices by performing WEAP analysis. The MPF12 used weight of hammer, stroke height, and pile set, with different modification factors for different piles. Phase II of the study also expanded related issues associated with wave equation analyses and static load tests.

**MnDOT Database:** A database which contains dynamic measurements and signal analyses was provided by MnDOT. It included 126 pipe-pile cases associated with hammer type and rated energies. From the 126 cases, 95 included dynamic measurements that enabled the calculation of rates of energy transferred. As such, MnDOT made an assumption that observed energy equals 75% of nominal energy. (Nominal energy  $E_n$  was replaced by  $0.75E_n$ .)

Phase II of the study focused on the review of other practices and a comparison of equations. Dynamic analyses of the database were conducted using the following dynamic equations: Washington State DOT formula, MnDOT equation, proposed new MnDot equation developed in the Phase I study, and the Gates formula. Because the static load test information had not been carried out for these cases, measured capacities were derived from dynamic measurements: CAPWAP (Case Pile Wave Analysis Program) and Energy Approach (EA) methods.

The equation developed in Phase I adjusted for  $E=0.75 E_n$  was modified to:

$$R_u = 20 \sqrt{\frac{W \times H}{1000}} \times \log\left(\frac{10}{S}\right)$$

Where,

$R_n$  = nominal resistance (tons)

H = stroke (height of fall) (ft.)

W = weight of ram (lbs.)

S = set (pile permanent displacement per blow) (inch)

The calibration process was done by using both First Order Second Moment (FOSM) and Monte Carlo (MC), and the calculated resistance factors varied with conditions:

For pipe piles, use  $\zeta=0.5$  for EOD,  $\zeta=0.65$  for BOR, keep  $2 < BC \leq 15$ , for H piles,  $\zeta=0.6$  for both EOD and BOR when BC equal or less than 15.

**PSC Database:** The modified equation was studied for its application to precast prestressed concrete (PPC) piles by applying it to large/voided piles and comparing it with CAPWAP predictions and static load tests results. Overall, 137 cases were used in the PSC database, related to 38 EOD piles and 99 BOR piles. Recommendations based on the calibrations from both the FOSM and MC methods are shown below.

For non-voided PSC pile sizes  $\leq 24''$ , use  $\zeta = 0.5$  for both EOD and BOR when  $2 < BC \leq 15$  BPI, which is the same as previously recommended for steel pipe piles, for voided PSC sizes between 20 to 54 inch,  $\zeta = 0.8$ .

**Timber Piles Database:** An investigation was also done into the possibility of using this equation for timber piles. Appropriate resistance factor calibration was based on 25 of original 28 piles. Measured capacity was based on interpretation of the load test results, utilizing Davisson’s criterion. The MPF 12 equation was proposed to multiply by 0.5, for accurate capacity predictions, since Timber involves large damping and loss of energy. The recommended resistance factor  $\zeta = 0.6$  resulted from calibration by using the timber pile modified equation.

$$R_u = 10 \sqrt{\frac{W \times H}{1000}} \times \log\left(\frac{10}{s}\right)$$

The findings related to the dynamic pile formula in the Phase II study in Minnesota can be used as recommended below.

Table 2-18. Recommendations for using the Findings Related to Dynamic Pile Formula

Application	Format	Variables	Resistance Factor $\zeta$	Comments
<b>Pipe, Concrete and H Piles</b>	$R_u = 20 \sqrt{\frac{W \times H}{1000}} \times \log\left(\frac{10}{s}\right)$	$R_n$ =nominal resistance (tons) H= stroke (height of fall) (ft.) W=weight of ram (lbs.)	For pipe and concrete piles $\zeta=0.50$ , $2 < BC \leq 15$ BPI For H piles $\zeta = 0.60$ , $2 < BC \leq 15$ BPI	The value of the energy (W·H) used in the dynamic formula shall not exceed 85% of the manufacturer’s maximum rated energy for the hammer used considering the settings used during driving
<b>Timber Piles</b>	$R_u = 10 \sqrt{\frac{W \times H}{1000}} \times \log\left(\frac{10}{s}\right)$	S=set (pile permanent displacement per blow) (inch)	$\zeta = 0.60$	

## **Wisconsin DOT (Long et al. 2009)**

Research was performed by the University of Illinois at Urbana/Champaign for the Wisconsin Department of Transportation (WisDOT) in 2009 to evaluate the prediction of pile axial capacity of driven piles, using four different dynamic formulae: Engineering News formula (currently used by the WisDOT), FHWA-Gates formula, Pile Driving Analyzer, and Washington State Department of Transportation (WsDOT). Additional analysis was conducted to improve the performance of the FHWA-Gates equation. The research aimed at finding an appropriate prediction formula for transitioning to LRFD design applicable to WisDOT practice and limiting the resulting increase in cost.

### **Database**

The database used in the report was similar to other DOT reports. Two databases were combined, including static and dynamic load tests. The first collection of load tests was compiled of several smaller load test databases, including Flaate (1964), Olson and Flaate (1967), Fragaszy et al., (1988, 1989), FHWA, Allen (2005), and Paikowsky (NCHRP 507, 2004). A total of 156 load tests were collected for this database. The second collection was created by utilizing data provided by the WsDOT. The Wisconsin database contained results from 316 piles from several locations in Wisconsin. The soil type data classified soil as clay, sand, or a mixture of the two. Additionally, soil exhibiting drained behavior was classified as sand, and soil exhibiting undrained behavior was classified as clay. In both the first and second collections, only steel H-piles, pipe piles, and metal shell piles were investigated.

### **Calibration Approach**

Resistance factors were calibrated using the First Order Second Moment (FOSM) and the First Order Reliability Method (FORM). Both the processes are outlined in the NCHRP 507 report. The bias for FOSM was calculated as the mean value for the ratios of measured capacity to predicted capacity. Target reliability was 2.33 and 3.0, according to AASHTO guidelines for redundant and non-redundant piles. The values in Table 2-6 were used for the resistance factor design. The ratio of dead load to live load was given a value equal to 2.

### **Database Examination and Quality Metrics**

The database contained a large number of piles and pile cases, but only those with static load test results and enough information to make a simply dynamic prediction (CAPWAP) of capacities were used. Furthermore, the pile cases were limited to pile types of H piles, open and close-ended steel pipes, and concrete-filled pipes. Timber and concrete piles were excluded from the study, along with piles driven using drop hammers.

For the first database collection, major emphasis was given to those with static load test results, since that data was available for a large number of cases. A ratio of predicted capacity to measured capacity was determined, indicating how the accuracy of a prediction method performed compared to the static load test results. According to data analysis, the FHWA-Gates formula over predicted at low capacities and under predicted at capacities larger than 750 kips. The performance of pile types, pile hammers, and soil types were also investigated, which led to the development of “corrected” FHWA Gates formula. A summary of statistics associated with prediction methods is shown below.

Table 2-19. Summary of Statistics Associated with Prediction Methods

Mean	COV	Method
0.43	0.47	Wisc-EN
1.11	0.39	WSDOT
1.13	0.42	FHWA-Gates
0.73	0.4	PDA
1.2	0.4	FHWA-Gates for piles < 750 kips
1.02	0.36	“Corrected” FHWA-Gates for piles > 750

The second database provided by WisDOT contained 316 piles in Wisconsin. Measured capacity resulted from PDA and CAPWAP, due to the lack of static load tests; however, measured capacities and predicted capacities were consistent with the results from the first database.

Final resistance factors were suggested based on the FORM method, which was found to be more accurate. For the FHWA-Gates and corrected FHWA-Gates method, only piles with axial capacities less than 750 kips were used in the analysis to maintain the performance of those methods. The four dynamic formulae and the newly proposed corrected FHWA-Gates formula were evaluated based on efficiency, which was defined as the ratio of resistance factor to mean of bias. Using a target reliability index  $\beta_T = 2.33$  and FORM, summarized resistance factors for different methods are shown below:

Table 2-20. Summary of Resistance Factors Developed using FORM at a Target Reliability ( $\beta_T = 2.33$ )

Method	Resistance Factor
EN-Wisc	0.9
FHWA-Gates	0.42
PDA	0.64
WSDOT	0.46
Corrected FHWA-Gates	0.54

Similar to the Oregon DOT report, ‘fitting the tail’ of the distribution of  $Q_M/Q_P$  was performed for the smallest 50% of the  $Q_M/Q_P$  data, as shown in the figure below. The resistance factors were then re-evaluated, based on the tail fitting making the resistance factor more representative. Resistance factors were concluded for the three methods with least values of scatter. A fit to extremal data resulted in a more accurate representation for portions of the distribution and led to greater resistance factors. The target reliability index  $\beta_T = 2.33$ , resistance factors are shown below, based on the FORM method. Based on the results of the investigation, it was concluded that the new proposed “corrected” FHWA-Gates or WSDOT formulas was superior for predicting axial pile capacity.

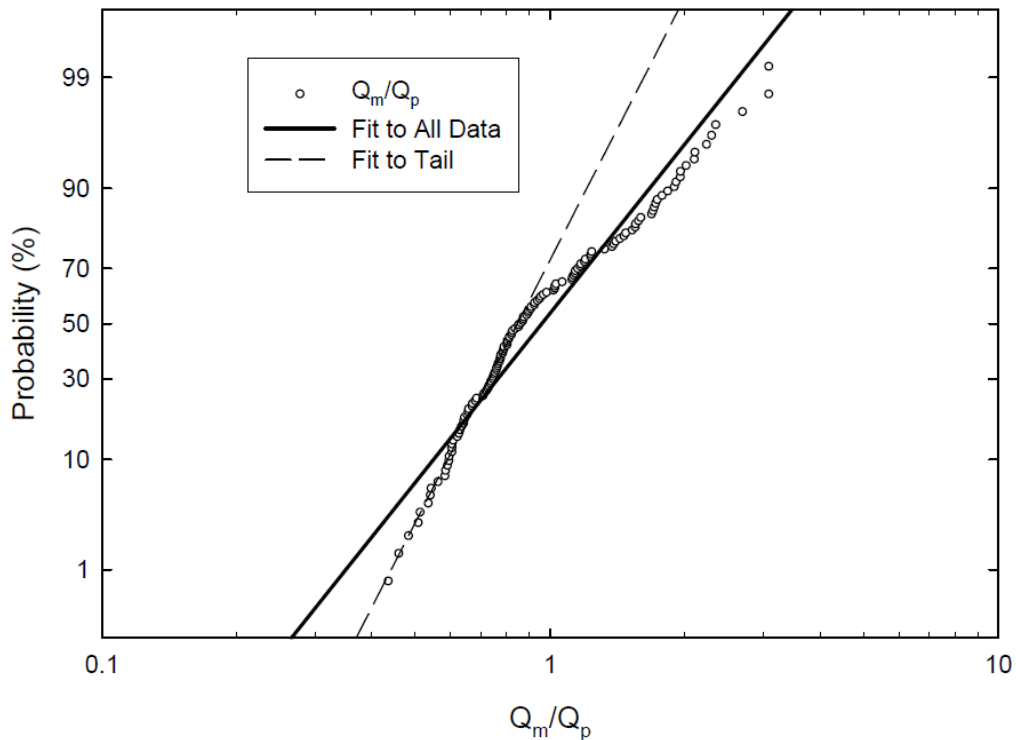


Figure 2-6. Cumulative Distribution Plot for WSDOT Predictive Method showing Difference between Fit to all Data and Fit to Extremal Data (Long et al. 2009).

Table 2-21. Summary of Resistance Factors Developed using FORM at a Target Reliability ( $\beta_T = 2.33$ ), based on Distributions Matching Extreme Cases

Method	$\phi$
Corrected-FHWA	0.61
WSDOT	0.55
FHWA	0.47

The Engineering News formula was found to be highly inefficient for use with LRFD in comparison with all other methods, requiring the capacity to be increased by 50%. The FHWA-Gates formula was further modified to increase its precision by considering hammer, pile, and soil type, and by including adjustment factors. The corrected FHWA-Gates formula was found to be the best in terms of efficiency. The suggested resistance factors for the corrected FHWA-Gates method, using FORM, was 0.54 and 0.42 for a reliability index of 2.33 and 3.0, with coefficient of variation of 0.41 for axial pile capacity of less than 750 kips. The resistance factors, using FOSM, were 0.49 and 0.37 for the same order of reliability index. The resistance factor was improved by tail fitting to achieve a value of 0.61 for coefficient of variation of 0.36 and reliability index of 2.33. With such modifications, the demand in increase of axial pile capacity was assumed to be within 1 %.

**Illinois DOT** (Long et al. 2009; Long and Anderson 2012; Long and Anderson 2014)

A report, ICT-09-037 was prepared by the University of Illinois at Urbana/Champaign on research funded by the Illinois Department of Transportation (IDOT) in 2009. At the time IDOT, was using static analysis for estimating pile lengths and dynamic analysis during construction at EOD condition. The method produced a mismatch between the estimated and actual pile lengths used in the field. The IDOT static method and the FHWA-Gates dynamic method were used. The research investigated a group of static and dynamic methods for comparison purposes. The static methods studied were the IDOT Static, Olson's method, Driven (FHWA), ICP, and K-IDOT. The dynamic methods were EN formula, FHWA-Gates, WSDOT, WEAP, and UI-FHWA. The study involved only steel piles. Finally, suitable formulae were determined based on accuracy, precision, and agreement of the results between static and dynamic predictions.

In 2012, Phase I research was performed at the university to improve pile driving in Illinois. The specific goals of the research were to increase pile capacity, based on pile driving practice and geology specific to Illinois; improve estimated pile length by including set up phenomenon; improve resistance factors; and assess stress levels during driving to avoid damage. Dynamic testing was performed on 45 piles (37 piles, excluding piles driven to rock) in 19 different sites, using Pile Driving Analyzer (PDA) at EOD and BOR conditions. Capacity of the pile was determined by using CAPWAP at the beginning of restrike (BOR) conditions. The axial capacity was calculated by using static methods (K-IDOT, DRIVEN, Olson and ICP) and dynamic equations (FHWA-Gates, WSDOT, MnDOT). The project was reported in FHWA-ICT-12-011 by the University of Illinois at Urbana/Champagne.

The Phase II study, presented in report ICT-14-021, was performed in 2014 to increase data points from 45, in a previous report, to 111, with both EOD and BOR test data. The objectives of the Phase II study were to revise driving and acceptance of criteria for piles driven to rock, reassess the resistance factors, determine time effects for piles, and further modify the prediction formula by incorporating time-dependent change in pile capacity into the WSDOT method. Predictive methods for estimating pile capacity investigated in this study included: K-IDOT (static) method, WSDOT (dynamic equation), WEAP, PDA, and CAPWAP. Since pile capacity changes with time, a 14-day capacity was chosen as a reasonable time to present a time period in which most of the set-up occurred. Consequently, the CAPWAP (BOR) was normalized to 14 days, CAPWAP (BOR\_14) to enable comparison of the pile set-up effect. In the Phase I study, the BOR capacity data did not incorporate the duration of the set-up period. The normalized 14-day capacity CAPWAP (BOR-14) was used as the measured capacity for calculating statistics.

### **Database**

The report presented in 2009 consisted of three databases: International database, Comprehensive database, and IDOT database. These databases have been described in detail in the report, as well as in several other DOT reports.

### **The International Database**

The International database was a compilation of the following databases: Flaate (1964), Olson and Flaate (1967), Fragaszy et al., (1988, 1989), FHWA, Allen (2005), and NCHRP 507. This database consisted of 132 pile load tests where static load tests had been conducted and pile driving information was available to allow the prediction of pile capacity. This database provided the information necessary to develop resistance factors for dynamic formula.

### **The Comprehensive Database**

The Comprehensive database consisted of 26 load tests on driven piles and required the piles to have static load test data to failure, hammer type and EOD condition information, and subsurface information. Additionally, the piles were required to be analyzable using static and dynamic methods. This was the only database that allowed determination of resistance factors for static methods. The resistance factors developed with this dataset were considered tentative because of the lack of load tests.

### **Illinois Database**

The Illinois database had 92 piles, H and pipe piles in clay and sand, selected from over 300 cases. There was enough information to estimate capacity using both static and dynamic formulae, but no static load tests were performed on those piles. For a pile to be included in the

database, it needed to have adequate pile driving and soil information, along with axial capacity, developed due to end bearing, of less than 80% of the total axial capacity.

In the ICT 27-69 report from 2012, the database was limited to pile testing performed within Illinois only. The database had 45 piles tested in 19 different locations in Illinois, with 19 H piles and 26 shell piles with closed end. All the piles were driven with open-ended diesel hammers. The soil types were clay, sand, and mixed. In the Phase II study report, ICT-14-021, the database from Phase 1 was extended to 111 piles, with tests in 38 different locations. H-piles and shell piles were collected, with a wide range of lengths, sizes, and capacities, and each test pile was monitored with PDA during the initial driving and restrike. The site locations were distributed throughout the state.

### **Data Anomalies and Cross Checking**

In the database from the second report from 2012, ICT 27-69, only 44 piles were used in the capacity statistics since a sensor on one of the piles malfunctioned.

### **Calibration Approach**

In the report presented in 2009, the resistance factors were calibrated using the FORM and FOSM methods described in the NCHRP 507 report. Additionally, tail fitting was performed similar to that reported in the Wisconsin DOT report. FORM provided higher accuracy since multiple variables were involved and the distribution was not normal; consequently, resistance factors were calculated using FORM. An approach for calibration, similar to that of the previous report, was followed in the second report presented in 2012. In the third report, presented in 2014, FOSM was used to calibrate resistance factors.

### **Database Examination and Quality Metrics**

The International database provided adequate information and an ample number of samples to develop resistance factors for dynamic methods at EOD conditions. The comprehensive database allowed determination of resistance factors for static methods, along with static and dynamic prediction of capacities, but the number of samples was deemed too few. Hence, the database was used to compare trends. The Illinois database did not contain static load tests as such, so it was used to compare predictions from static and dynamic methods, as well as to compare the agreements between them. The database for the second report, ICT 27-69, was specifically developed for Illinois' practice of driven piles and geological conditions. Only one pile was excluded from the static capacity prediction, due to sensor malfunction. The database for the third report, ICT-14-021, contained 111 pile cases, an extension of the 45 piles reported on in 2012. Only one static load test was performed in the Phase II study in 2014.



In the first report, presented in 2009, for the case of comparison of prediction methods, efficiency, instead of the value of the resistance factor, was chosen to designate quality. This is due to the fact that the resistance factor itself is affected by bias. Therefore, efficiency was calculated by normalizing the resistance factor by bias, bias being defined as the ratio of measured capacity to predicted capacity. Additionally, tail fitting was performed similar to that described in the Wisconsin DOT report. Since multiple variables were involved and the distribution was not normal, resistance factors were calculated using FORM, which provides higher accuracy. The corrected K-IDOT method resulted in the best agreement of capacities from dynamic equation and static load tests. The “corrected” term referred to the optimization procedure used to calibrate the K-IDOT method. Similarly FHWA-Gates, GHWA-UI, and WSDOT formulae were established as the most promising dynamic methods in this study. Of those three, the WSDOT formula appeared to be the dynamic formula that exhibited the best overall for predicting capacity with precision. The formulae were further developed by using correction factors; however, due to the simplicity of the WSDOT dynamic formula, the report recommends its use with a resistance factor of 0.55 for target reliability of 2.33 and coefficient of variation of 0.451. Additionally, static capacity predictions were not as precise as the dynamic predictions, but by modifying the IDOT to the K-IDOT formula, it produced the most satisfactory results among other static capacity prediction formulae. The modifications were performed to improve the predictions, as well as to match the predictions with dynamic predictions. The suggested resistance factor for corrected K-IDOT was 0.40, with a target reliability index of 2.33 and coefficient of variation of 0.525. Since IDOT estimated pile lengths based on the static method and the final length of pile was determined by a dynamic equation, a difference between estimated and actual occurred. According to this study, the combination of the IDOT and WSDOT formulae was such that there is a 50% chance that driven lengths will be greater than estimated when the corrected K-IDOT is used for static prediction and WSDOT is used for dynamic prediction.

Similar approaches were taken to ascertain the quality of data in the ICT 27-69 report of 2012. Since the pile data cases collected were restricted to IDOT practice and Illinois soil and geological conditions, the measured and predicted capacity agreed well, providing designers the ability to estimate pile capacity more precisely and increasing the maximum nominal load they can specify. The difference between predicted length and embedment length was reduced by using  $N_{SPT}$  instead of  $(N_1)_{60}$ , modifying the relationship between the capacity predictions by the WSDOT formula and K-IDOT formula. Due to inclusion of pile set -p specific to Illinois soil, the coefficient of variation from the WSDOT method was reduced to 0.252 from the previous value of 0.451 mentioned in ICT R27-24 report of 2009. Additionally, information and control over stress due to driving was monitored by comparing WEAP and CAPWAP results, and the

Simplified Stress Formula was developed that could be used without WEAP analysis. The resistance factor calibrated at 0.55 from the same previous report was increased to 0.62 for the WSDOT method. Due to modifications in the K-IDOT method, the coefficient of variation decreased to 0.492 from 0.525 from the previous report. However, the resistance factor decreased to 0.33 from 0.44 since bias of the method also changed in the new analysis. The efficiency defined as ratio of resistance factor over bias for WSDOT is significantly higher than K-IDOT, ( $\phi/\lambda = 0.68$  and  $0.39$ , respectively), which indicated that pile capacities resulting from WSDOT can provide the same reliability for shorter piles. In order to improve the agreement between the K-IDOT and WSDOT methods for capacity prediction, a relationship was determined to predict WSDOT capacity from K-IDOT capacity, which is shown as  $K-IDOT * 0.87 = WSDOT$ .

As a continued study in Phase II, research efforts were expanded throughout the whole state to 111 cases for H piles and shell piles. The statistical parameter mean was adjusted to achieve the median value of unity. Such treatment resulted in calibration that over-predicted the capacity half the time and under-predicted it the other half of the time. Estimates from WSDOT were improved by prescribing factors dependent on pile type, soil conditions, and driving conditions, such as EOD and BOR, and included pile set-up instead of using the current factor of 0.47 for all steel piles. The correction factors proposed for the BOR condition considered restrike with set-up duration.

The State of Washington uses the following formula (Allen 2005) to determine pile capacity:

$$R_n = 6.6F_{eff}WHln(10N)$$

Where,

$R_n$  = ultimate pile capacity (kips)

$F_{eff}$  = hammer efficiency factor based on hammer and pile type

$W$  = weight of hammer (kips)

$H$  = drop of hammer (ft.)

$N$  = average pile penetration resistance (blows/in)

Currently, the parameter  $F_{eff} = 0.47$  is used for open-ended diesel hammers with steel piles. The WSDOT formula has been utilized by IDOT for EOD capacity verification.

K-IDOT made improvements for predictions for H piles by prescribing new factors to be used for portions of the pile, depending upon whether they are in cohesive or cohesionless soil. H-piles were improved by increasing the estimate by a factor of 1.265. New  $F_s$  and  $F_p$  for H piles in cohesionless soil were 0.19 and 0.38; for H piles in cohesive soil,  $F_s = 0.94$ ,  $F_p = 1.89$ . WSDOT

suggested resistance factors of 0.58 and 0.63 for H piles and shell piles, respectively for EOD condition; whereas, a resistance factor of 0.61 was suggested for both types of piles for BOR condition. Resistance factors for H-piles driven to shale were 0.56 for EOD and BOR. A resistance factor of 0.37 was suggested by K-IDOT for all piles types and all soil types. Separate resistance factors for soil, shale, and rock were applied previously. The coefficient of variation for K-IDOT and WSDOT was reported as 0.55 and 0.3 in the analysis. However, the resistance factors were modified to account for the static load test by relating predicted capacity to that determined from CAPWAP, and then relating the CAPWAP capacity to that expected from the static load test. The intermediate relation to CAPWAP was necessary because only one static load test was performed. Hence, the final recommendations for resistance factors for WSDOT were 0.6 for both types of piles for EOD condition, 0.62 for both types of piles for BOR condition, and 0.6 for H piles in shale for EOD conditions. The factors are only for open-ended diesel hammer. Similarly, a final resistance factor of 0.37 was suggested by K-IDOT for all pile types and soil types with coefficient of variation of 0.62.

#### **Washington DOT(Allen 2005).**

Prior to 1997, WSDOT used the Engineering News Record (ENR) formula for driving piling to the design capacity. The Washington State Department of Transportation (WSDOT) sponsored research published in 1988 had shown that the ENR formula was quite inaccurate and that moving toward the Gates formula would be a substantial improvement (Fragaszy, et al., 1988). Hence, in 1996, an in-house study was initiated to update the driving formula used for pile driving acceptance in the WSDOT Standard Specifications. The study showed that the Gates formula was superior to the ENR formula. Consequently, the Gates formula was further modified to fit the WDOT practice and to develop a WDOT formula to improve its prediction quality.

#### **Database**

The database used in the analysis and calibration was provided by Paikowsky et al. (2004). The database was presented in detail in the report and contains information such as location, pile type, soil type, hammer type, blow count, and much more. Additionally, capacity from load test, CAPWAP, and WSDOT, were included in database. Most of the data was provided for EOD condition, but a limited amount of data was provided for BOR condition. Measured bearing capacity, used to quantify the accuracy of predictive methods, resulted from load tests.

### Calibration Approach

Monte Carlo simulation was used for the reliability analysis and development of resistance factors. The load statistics parameters needed for the reliability analysis were developed and reported by Nowak (1999) and are shown below.

Table 2-22. Load Statistics used for Calibration of Resistance Factors (from Nowak, 1999)

	Bias	COV	Load factor
Live load	$\lambda_{LL}=1.15$	$COV_{LL}=0.18$	$\hat{U}_{LL}=1.75$ ,
Dead load	$\lambda_{DL}=1.05$	$COV_{DL}=0.10$	$\hat{U}_{DL}=1.25$ ,

In this study, dead load and live load were both considered following normal distribution, and the ratios of 2 to 5 (dead load to live load) were investigated.

Table 2-23. Recommended Resistance Factors for Pile Foundations

Pile Resistance Prediction Method	$\beta = 2.3$	$\beta = 3.0$
	Resistance Factor $\phi$	Resistance Factor $\phi$
WSDOT Formula (developed energy)	0.55	0.45
FHWA Modified Gates Formula (estimated developed energy)	0.45	0.40
CAPWAP (EOD with $N < 8$ bpi)	0.75	0.65
CAPWAP (BOR with $N < 8$ bpi)	0.70	0.60

The table above shows that there is a significant difference in resistance factors required for small pile groups (i.e., less than five piles in a group). The resistance factor required for low redundancy piles (when  $\beta$  was given to 3) was approximately 80% of that required for larger pile groups (when  $\beta = 2.3$ ). Since the DL/LL ratio has a minor effect in resistance factor calibration,  $\phi=0.55$  was recommended for the WSDOT Pile Driving Formula for larger pile group. The recommendation for smaller pile groups was  $\phi=0.45$  so that a higher reliability index was achieved. (Higher reliability relates to lower failure probability.) The Table 2-23 provides a summary of resistance factors for reliability indexes of 2.3 and 3.0. In addition to these recommended values, resistance factors for other pile-bearing-resistance-field verification methods are also presented in Table 2-23.

### Database Examination and Quality Metrics

The database did not provide observed stroke for single-acting and double-acting hammer. In such cases, use of rated energy would result in higher driving resistance and would eventually affect the calibration of resistance factor for the WSDOT formula. Hence, GRLWEAP was used to estimate the observed stroke for the types of the hammers mentioned above.

Similar to the Illinois DOT and the Oregon DOT, tail fitting was performed in the calibration process. The DL/LL ratio did not show a major effect on the resistance factor. Additionally, the CAPWAP analysis was performed for blow counts of less than 8 blows per inch at BOR condition to avoid overly conservative estimates.

### **Iowa DOT** (Ng et al. 2011; Smith et al. 2011)

The FHWA mandated using the LRFD approach for all new bridges in the United States after October, 2007. As a result, there was an increased use of LRFD design practices among states' DOTs, and the Iowa Highway Research Board (IHRB) sponsored three projects. In 2010, the Iowa DOT prepared an electronic database, PILOT, for driven piles, with an objective of facilitating calibration of the LRFD resistance factor regionally. Many DOTs across the U.S. prepared for migrating toward LRFD calibration of resistance factors. However, most of the databases used by such DOTs, as with the FHWA, included piles driven across the U.S. Such geographical diversity entailed varied soil and site conditions and pile driving practices, and the developed resistance factors performed poorly in terms of being conservative and demanding increased capacity in design. To overcome such drawbacks, the Iowa DOT assembled piles cases inside Iowa to perform LRFD analysis with resistance factors developed for the region, providing optimum designs. Additionally, the electronic management of the database made queries and analysis easy, along with easy graphical user interface. However, the database did not include all soil profiles in Iowa, and thus provided only a limited number of reliable data. PDA driving data were not included; therefore, the development of resistance factors for PDA and CAPWAP could not be conducted. Hence, ten full-scale pile tests were performed, and the results were presented in a report in 2011 as Volume II. Detailed soil investigations were carried out for the 10 full-scale tests with H piles at EOD conditions; and at BOR conditions, PDA data was collected for performing CAPWAP analysis. An increase in pile capacity, as a function of time, was investigated using dynamic analysis methods during re-strikes and measured using SLTs. Volume III described the development of regional LRFD resistance factors, following the incorporation of construction control aspects and soil set-up into pile design. Resistance factors were calibrated for different static methods, dynamic formulas, and dynamic methods.

### **Database**

The Pile Load Test (PILOT) database initially contained 274 piles of various types in various soils, 264 of which had static load test information available. PILOT provided a major pile category database: Steel H-Pile SLTs, Timber Pile SLTs, and Pipe, Monotube, and Concrete Pile SLTs. Under the H-pile category 164 piles were available, 80 of which were usable for investigations dealing with static analysis, while 34 were used to evaluate dynamic methods, as

well as dynamic pile driving formulae. In addition to the H piles, there were 75 timber piles, with 47 out of 75 classified as reliable, and 24 classified as usable-static. Nine of those 24 were labeled as usable-dynamic. Additionally, 16 steel pipe piles, 7 monotube piles, and two prestressed concrete piles were also incorporated into this database. . For each pile in the database, pile capacity was defined by using Davisson's method from static load tests. The ten full-scale load-tested H piles were then added to the PILOT database, increasing data points and covering all five geological regions. The new added cases involved detailed in-situ subsurface investigations, like SPTs, CPTs, as well as laboratory soil consolidation tests. PDA data was recorded for driving and re-strikes conditions for WEAP analysis, static load tests were performed, and pile capacities were determined based on Davisson's method.

### **Calibration Approach**

FOSM was used to assess reliability. Resistance factors at EOD conditions were calibrated. The resistance factor for pile set-up was calculated based on the resistance factor at EOD condition.

### **Database Examination and Quality Metrics**

The database was created for pile cases only in Iowa. Because most of the piles in Iowa are H piles, the majority of the piles in the database were H piles, with a few pipe and monotube piles and very few prestressed concrete piles. The database was based on a well-defined hierarchical classification scheme, which was required to clearly identify the pile load tests containing information for estimation of pile capacity by both static and dynamic methods. Since not every pile load test yielded dependable results, a check in the hierarchical classification scheme of reliability was placed on the pile case to separate reliable pile load tests from the entirety of the PILOT database. Hence, the three tiers were reliable, usable-static, and usable-dynamic. In other words, for the pile data to be reliable, it had to satisfy displacement-based criteria for pile resistance, as defined by Davisson (1972). For a pile to be in the second tier, there had to be enough information for predicting pile resistance using static methods. Similarly, for the pile to be in the third tier, there needed to be enough information for predicting pile resistance using dynamic methods. Quality of the data was maintained by defining soil type. For the soil type to be clay, 70% of the soil along the shaft was required to be clay; likewise for sand. If the criterion was not satisfied, the soil was classified as sand.

Separate resistance factors were calculated for pile resistance at EOD and the resistance factor for pile set-up, as both of the resistance factors were calculated probabilistically, depending upon reliability, and each kind of resistance factor had its own uncertainties. This process ensured that the pile set-up was incorporated into pile resistance, in accordance with the LRFD procedure mandated by FHWA.

Since the comparison of measured pile resistance concluded that pile set-up occurs in cases with clay and mixed soil profiles, the report presented a new calibration procedure for incorporation into the pile set-up in LRFD analysis. In order to validate pile setup, 12 data points in the clay profile were selected from PILOT, along with 5 new added cases. Since no PDA data was recorded in PILOT, for those 12 cases, field tests were used to validate set-up by using a SPT-based set-up equation for pile resistance at EOD. Set-up was defined as the difference between the SLT measured pile resistance and initial pile resistance, using WEAP-IABB. For those 5 new cases, the measured resistance at EOD used the CAPWAP method at EOD, and the measured set-up resulted from the difference between the SLT measured resistance and resistance at EOD, using CAPWAP. Part of the axial loaded piles in Volume I were considered in the Volume II report. For typical value of 1.6 for the ratio of nominal pile resistance to total service load, and typical ratio of dead load to live load of 2.0, resistance factor, 0.66 was suggested for EOD condition when the target reliability index was  $\beta_T = 2.33$  (for non-redundant pile groups), and a resistance factor of 0.21 was suggested for pile set-up for  $\beta_T = 2.33$ . The coefficient of variation for the pile resistance factor at EOD was 0.181 and for the set-up resistance factor was 0.330.

In Volume III, the data from the ten full-scale pile load tests, which was derived from locations spread across the state of Iowa, was used again to examine the preliminary LRFD resistance factors. The nominal, as well as the factored, design capacities were calculated, using dynamic formulas, and were compared to actual capacity of piles measured in the field.

Since ten new pile load tests were added to the PILOT database, the sample size used for calibration was increased, enhancing the accuracy of the final recommendations. For steel H piles, among the five static methods, the in-house Iowa “Blue Book” method, based on Geotechnical Resistance Charts, was recommended for steel H-pile design. It was also indicated that the Blue Book method is the most efficient (based on  $\bar{c}/\lambda$ ). For dynamic methods, comparisons were made for the various ways of entering input for WEAP analysis. For redundant pile groups, it was indicated that WEAP, based on the SA method, had the highest resistance factor in sand soil. IDOT, ST and SA methods performed best in mixed soil. The effect of soil set-up was examined for clay. Similarly, seven dynamic formulas were examined and re-calibrated. The Gates formula rendered the highest resistance factor in sand and clay soil. In addition, it was observed that compared to redundant piles, resistance factors were reduced for non-redundant pile groups by an average of 20%. It was observed that the modified Iowa ENR formula performed best for the construction control of timber piles.

## **Summary**

The calibrated resistance factors reviewed in the above-mentioned nine states are summarized in Table 2-24.



Table 2-24. Recommended Resistance Factors for Pile Foundations

State	Database	Capacity method	Resistance factor $\phi$	Reliability Index $\beta_T$
<sup>1</sup> Oregon (2009,2011)	PDLT 2000; DFLTD FL and FHWA Database	Dynamic (GRLWEAP)	0.55 for EOD condition 0.40 for BOR condition	2.33 2.33
<sup>2</sup> Kansas (2014)	Database from KDOT	Dynamic (KDOT-ENR Formula)	1.45 at EOD for combined PDA/CAPWAP 1.25 at EOD for combined PDA/CAPWAP 1.43 at BOR for combined PDA/CAPWAP 1.24 at BOR for combined PDA/CAPWAP	2.5 3.0 2.5 3.0
<sup>3</sup> Louisiana (2009, 2010, 2013)	Louisiana DOT Database	Static $\alpha$ -Tomlinson and Nordlund method	0.56 (using FOSM) 0.63 (using FORM) 0.63 (using Monte Carlo)	2.33 2.33 2.33
		Schmertman	0.44 (using FOSM) 0.48 (using FORM) 0.49 (using Monte Carlo)	2.33 2.33 2.33
		LCPC/LCP	0.54 (using FOSM) 0.60 (using FORM) 0.59 (using Monte Carlo)	2.33 2.33 2.33
		De Ruyter and Beringen	0.66 (using FOSM) 0.74 (using FORM) 0.73 (using Monte Carlo)	2.33 2.33 2.33
		CPT average	0.55 (using FOSM) 0.61 (using FORM) 0.62 (using Monte Carlo)	2.33 2.33 2.33
		Dynamic (CAPWAP)	1.31 at EOD condition (using FOSM) 1.41 at EOD condition (using FORM) 0.55 at BOR condition (using FOSM) 0.61 at BOR condition (using FORM) 0.62 at BOR condition (using Monte Carlo)	All at reliability index of 2.33
<sup>4</sup> Florida (2000, 2002, 2004, 2012)	PILEUF	Dynamic (FDOT, overall)	0.669 at EOD condition 0.832 at BOR condition	2.5 2.5
Minnesota (2009)	Mn/DOT/LT 2008	Dynamic (MnDOT Formula)	0.25 (current MnDOT formula) 0.45 - Pipe piles (new MnDOT formula) 0.60 - H Piles (new MnDOT formula)	2.33 2.33 2.33
Minnesota (2014)	MnDOT	Dynamic (MPF12—Minnesota Pile Formula 2012)	0.50 - Pipe and concrete piles 0.60 - H piles 0.50 - Non-voided PPC piles , size < 24” 0.80 - Voided PSC piles, 20”<size<54”	All at reliability index of 2.33

State	Database	Capacity method	Resistance factor $\phi$	Reliability Index $\beta_T$
			0.60 – Timber piles All for MPF12 formula	
Wisconsin (2009)	Flaate, 1964 Olson and Flaate, 1967 Fragaszy et. al., 1988,1989 FHWA database Allen, 2005 NCHRP 507 Wisconsin Database	Dynamic (Corrected FHWA-Gates Formula)	0.54 (using FORM) 0.61 (using FORM, fit extremal data)	2.33 2.33
		Dynamic (WSDOT)	0.46 (using FORM) 0.55 (using FORM, fit extremal data)	2.33 2.33
		Dynamic (FHWA- Gates Formula)	0.42 (using FORM) 0.47 (using FORM, fit extremal data)	2.33 2.33
Illinois (2009)	International Database Comprehensive Database IDOT Database	Static (K-IDOT Formula)	0.4 (using FORM)	2.33
		Dynamic (WSDOT)	0.55 (using FORM)	2.33
Illinois (2012)	45 Piles driven only in Illinois	Static (K-IDOT Formula)	0.33 (using FOSM)	2.33
		Dynamic (WSDOT)	0.62 (using FOSM)	2.33
Illinois (2014)	111 Piles driven only in Illinois including previous 45 piles	Static (K-IDOT Formula)	0.37	2.33
		Dynamic (WSDOT)	0.6 – H and shell piles at EOD condition 0.62 - H and shell piles at BOR condition 0.60 – H piles driven to shale at EOD condition	
Iowa (2011)	PILOT	Dynamic (PDA/CAWPAP)	0.66 (Pile resistance at EOD) 0.21 (Pile set up) (For steel H piles)	2.33 2.33

State	Database	Capacity method	Resistance factor $\phi$	Reliability Index $\beta_T$
	PILOT along with 10 new cases	Static (Iowa DOT design charts)	0.61 (using modified FOSM in sand) 0.47 (using modified FOMS in sand) 0.69 (using modified FOSM in clay) 0.52 (using modified FOSM in clay) 0.67 (using modified FOSM in mixed) 0.53 (using modified FOSM in mixed) (For steel H piles)	2.33 3.00 2.33 3.00 2.33 3.00
		Dynamic (Gates and WSDOT)	0.64 (using FOSM in sand) Gates 0.66 (using FOSM in clay) Gates 0.66 (using FOSM in mixed) WSDOT (For steel H piles)	2.33 2.33 2.33
		Dynamic (Gates)	0.64 0.50 (For timber piles)	2.33 3.00
Washington (2005)	Paikowsky et. al., 2004	Dynamic WSDOT Formula	0.55 0.45	2.33 3.00
		CAPWAP (EOD with $N < 8\text{bpi}$ )	0.75 at EOD (PDA/CAPWAP) 0.65 at EOD (PDA/CAPWAP)	2.33 3.00
		CAPWAP (BOR with $N < 8\text{bpi}$ )	0.70 at BOR (PDA/CAPWAP) 0.60 at BOR (PDA/CAPWAP)	2.33 3.00

Note: Resistance factors have been presented in detail in the following tables in the report

1. Table 2-3
2. Table 2-6
3. Table 2-11
4. Table 2-13

## **LRFD Calibration of Drilled Shafts**

The literature review for this study focuses on recent state DOT research efforts and other various research efforts performed on the calibration of LRFD resistance factors for drilled shafts.

### **Florida DOT (McVay et al., 1998; McVay et al., 2003)**

In 1998, the University of Florida was contracted by the Florida Department of Transportation (FDOT) to calibrate resistance factors for the LRFD of deep foundations, shallow foundations, and retaining wall systems. Resistance factors were calibrated by fitting them to ASD and using the reliability theory, then comparing them to those recommended by AASHTO (1994). The drilled shaft load tests used for this study were conventional static load tests, and the results of the study are given in Table 2-25 below. At the time of the study, FDOT was utilizing Statnamic and Osterberg Cell load testing of drilled shafts in addition to the conventional load testing; however, the load tests were very limited, and it would not have been feasible to perform a calibration for these two load test types. It was recommended that the results of the study from the conventional load tests, shown in Table 2-25, also be used for Osterberg Cell load testing and Statnamic load testing.

Table 2-25. Resistance Factors for Drilled Shafts in All Soil Types (McVay et al. 1998)

<b>AASHTO (1994)</b>	<b>Reliability</b>	<b>Fitting</b>
0.45-0.65	0.50-0.65	0.

Over time, there has been an increase in the diameter of drilled shafts and the loads imparted on them. This has resulted in testing problems with conventional load test equipment. In response to this problem, Berminghammer Foundation Equipment developed, in the early 1980s, the Statnamic device, which has a 7500-ton capacity. As previously mentioned, McVay et al. (1998) did not consider the Statnamic load test due to insufficient testing data. As a consequence, the resistance factors produced from the conventional load test database were considered to be equal to those of the Statnamic load test database. In 2003, the University of Florida performed another study, with the goal of establishing a new database for both Statnamic load tests and conventional load tests, and calibrating the new resistance factors. The database consisted of load tests on driven piles and drilled shafts, with the data separated by the type of foundation. Related soil conditions were also included in the database, with the data separated by geologic formations.

### **Database**

Prior to beginning the research, the FDOT already had a database of 13 drilled shaft Statnamic load tests, collected from a few state bridge projects, and 15 pile Statnamic load tests and conventional top-down load tests. Seven of these test piles were in Florida, while the other eight were in Taiwan and Japan. In order to perform a proper study, more drilled shaft and driven pile

load tests were collected from AFT, Birmingham, and the Federal Highway Administration (FHWA), bringing the database to 27 drilled shaft load tests and 34 driven pile load tests. However, only 37 of these 61 load tests achieved the FDOT/Davisson failure criteria for both the Statnamic and the conventional static load tests. A summary of the load testing data is shown in Table 2-26.

### **Calibration Approach**

A statistical analysis was performed for different scenarios to better understand the behavior of Statnamic load testing under various soil and foundation types, as shown in Table 2-27.  $\lambda_R$  represents the bias factor of the resistance,  $R$ ,  $V_R$  represents the coefficient of variation of  $R$ , and  $\sigma_R$  represents the standard deviation of  $R$ . Table 2-28 presents a summary of the statistical parameters of the dead and live loads that were used in the study. The analyses were run both with and without a rate factor,  $RF$ , specific to the soil type. The rate factors were obtained from a report submitted to the National Cooperative Highway Research Program by Dr. Mullins of the University of South Florida (2002). Based on the statistical analysis and the comparison of the static load capacities to the corresponding Statnamic-derived static capacities, the bias factor and coefficients of variation for the ratio of static capacity to Statnamic-derived static capacity were determined. The bias factors of the measured static capacity to the derived Statnamic static capacity ratios, without the rate factors, were generally less than 1.0, indicating that the Statnamic-derived static capacity over predicts the actual static capacity. Applying the rate factors increased the bias factors to an acceptable range. The coefficients of variation were not affected by the rate factors.

A target reliability index,  $\beta_T$ , of 2.5 was chosen for the driven piles, and a reliability index of 3.0 was chosen for the drilled shafts. Because the factor of safety for the Statnamic load test in ASD is unknown, the target reliabilities were taken from the previous LRFD calibration study (McVay et al., 1998). Using these target reliabilities and a known relationship between the probability of failure and the reliability index for a lognormal distribution (Rosenblueth and Esteva, 1972), the resistance factors for the seven different cases, with and without the rate factors, were calculated, as shown in Table 2-29.

Table 2-26. Summary of Load Test Piles (McVay et al., 2003)

Pile Type	Soil Type	Location	SLT Capacity* (kN)	SLD Capacity** (kN)
DS	ROCK	USA	6200	6480
DS	ROCK	USA	5600	4950
Pipe	ROCK	JPN	4380	5087
DP	SAND	USA	3380	5000
DP	SAND	USA	3820	3322
DP	SAND	USA	3500	3957
Pipe	SAND	JPN	1100	1042
Other	SAND	JPN	446	489
DS	SILT	USA	1420	2191
DS	SILT	USA	1700	2450
DS	SILT	USA	2230	3530
DS	SILT	USA	2800	2890
DS	SILT	USA	1013	1730
DS	SILT	USA	2230	2890
DS	SILT	USA	2400	2970
Pipe	SILT	USA	1230	1790
Pipe	SILT	USA	1300	1380
Pipe	SILT	USA	1210	1404
Pipe	SILT	USA	1300	1750
Pipe	SILT	USA	1810	N/F
Pipe	SILT	USA	2380	3850
DP	CLAY	USA	1830	3070
DP	CLAY	USA	2470	N/F
Pipe	CLAY	USA	1668	N/F
Pipe	CLAY	USA	2190	2600
DS	CLAY	USA	1214	1244
DS	CLAY	USA	965	1617
DS	ROCK	CAN	4550	3500
AC	SAND	CAN	1310	1350
Pipe	ROCK	CAN	1560	1800
DP	SILT	USA	2470	2360
Pipe	CLAY	CAN	1040	2550
Pipe	ROCK	CAN	2200	2550
DS	SAND	USA	7130	6370
Pipe	CLAY	USA	1360	892
DP	SAND	JPN	2770	2700
Pipe	SAND	JPN	1890	1490

\*SLT – Static Load Test, \*\*STD – Statnamic Load Test

Table 2-27. Statistical Analysis Summary (McVay et al., 2003)

Case	With Clay						Without Clay					
	With RF			Without RF			With RF			Without RF		
	$\beta_R$	$\alpha_R$	$V_R$	$\beta_R$	$\alpha_R$	$V_R$	$\beta_R$	$\alpha_R$	$V_R$	$\beta_R$	$\alpha_R$	$V_R$
All data	1.11	0.28	0.25	0.88	0.24	0.27	1.10	0.18	0.16	0.89	0.20	0.22
Rock	-	-	-	-	-	-	1.07	0.17	0.16	1.00	0.18	0.18
Sand/ Silt	-	-	-	-	-	-	1.10	0.18	0.16	0.87	0.19	0.22
Clay	1.18	0.52	0.44	0.82	0.40	0.49	-	-	-	-	-	-
Drilled shaft	1.10	0.20	0.18	0.87	0.23	0.26	1.08	0.16	0.15	0.88	0.23	0.26
Driven pile	1.12	0.32	0.29	0.89	0.25	0.28	1.10	0.21	0.19	0.89	0.18	0.20

Note: Rate factor for sands = 0.91 Rate factor for clays = 0.65  
 Rate factor for silts = 0.69 Rate factor for rocks = 0.96

Table 2-28. Dead and Live Load Statistical Parameters (McVay et al., 2003)

$\hat{U}_D$	1.250
$\hat{U}_L$	1.750
$\lambda_{QD}$	1.080
$\lambda_{QL}$	1.150
$COV_{QD}$	0.128
$COV_{QL}$	0.180
$Q_D/Q_L$	2.000

$\hat{U}$  = load factors; D = dead load;  $\lambda$  = bias factors; L = live load, COV = coefficient of variation

The cases with significant clayey soil present were separated from the overall calibration because they were found to have a significant effect on the calculated resistance values. The resistance factors produced from excluding the clay cases are summarized in Table 2-30. Resistance factors of 0.70 and 0.65 can be used for Statnamic load test piles and drilled shafts, respectively, in non-cohesive soils. In soils with significant clayey soil present, it is recommended to reduce the resistance factors to 0.60 for both the driven piles and drilled shafts. However, in predominantly cohesive soils, a resistance factor is not recommended due to insufficient data.

Table 2-29. Summary of Resistance Factors (McVay et al., 2003)

Case	Resistance Factor ( $\phi$ ) $Z/\ddot{u}_T = 2.5$				Resistance Factor ( $\phi$ ) $Z/\ddot{u}_T = 3.0$			
	With Clay		Without Clay		With Clay		Without Clay	
	w/ RF	w/o RF	w/ RF	w/o RF	w/ RF	w/o RF	w/ RF	w/o RF
All data	0.62	0.47	0.72	0.52	0.52	0.40	0.63	0.45
Rock	-	-	0.72	0.52	-	-	0.63	0.44
Sand and silt	-	-	0.71	0.64	-	-	0.62	0.56
Clay	0.43	0.27	-	-	0.34	0.21	-	-
Drilled shaft	0.70	0.47	0.73	0.48	0.61	0.38	0.64	0.41
Driven pile	0.58	0.47	0.69	0.55	0.49	0.40	0.60	0.47

Table 2-30. Recommended Resistance Factors (McVay et al. 2003)

Foundation Type	Rock and Non-cohesive Soils	Clays	Sand-Clay-Rock Mixed Layers
Driven Pile ( $\beta_T = 2.5$ )	0.70	0.45	0.60
Drilled Shaft ( $\beta_T = 3.0$ )	0.65	0.35	0.60

### Iowa DOT (Garder et al., 2012; Ng et al., 2014)

The objective of the study performed by Iowa State University professors was to develop a regional LRFD procedure for drilled shafts in Iowa with preliminary resistance factors, using a probability-based reliability theory. A database, developed in 2012, of local drilled shaft load tests was utilized for these purposes. The scope of the study included, but was not limited to, performing a literature review of the current designs and construction practices of the Iowa DOT and neighboring DOTs, analyzing the Drilled Shaft Foundation Testing (DSHAFT) data, quantifying the measured capacity of each drilled shaft, and developing preliminary regional resistance factors. A majority of the load test results did not pass the displacement requirements.

### Database

The DSHAFT database is a quality-assured, electronic database, developed by Garder, Sritharan, and Roling in 2012, that contains 32 drilled shaft load tests provided by the Iowa, Illinois, Minnesota, and Missouri DOTs and the Nebraska Department of Roads (DOR). One load test was also collected from a drilled shaft load test study performed in Tennessee. Detailed information from each load test was collected and integrated into a comprehensive database, using Microsoft Office Access. Recorded information included location, construction details, subsurface conditions, drilled shaft geometry, load testing methods and results, and concrete quality. Currently, DSHAFT contains 41 drilled shaft load tests from 11 different states, with the majority of the load tests being performed in Iowa, Colorado, and Kansas. Of those 41 tests,



only 28 were usable, i.e., contained the information pertinent to establishing resistance factors, such as structural, subsurface, testing, and construction details. The load tests were categorized in many different ways: construction methods, testing methods, soil type at the shaft base, and soil type along the side of the shaft. The details of each usable drilled shaft load test are summarized in Table 2-31.

Table 2-31. Summary of Usable DSHAFT Data (Garder et al. 2012)

State	D (ft.)	L (ft.)	Concrete f <sub>c</sub> (ksi)	Geomaterials		Construction Method	Testing Method
				Shaft	Base		
IA	3.0	12.7	5.86	Rock	Rock	Wet	Osterberg
IA	4.0	65.8	3.80	Clay+Rock	Rock	Wet	Osterberg
IA	3.5	72.7	3.44	Mixed+IGM	IGM	Casing	Osterberg
IA	4.0	79.3	3.90	Clay+IGM+Rock	Rock	Wet	Osterberg
IA	2.5	64	3.48	Clay	Clay	Casing	Osterberg
IA	3.0	34	4.10	Clay+Rock	Rock	Wet	Osterberg
IA	5.5	105.2	3.80	Mixed+Rock	Rock	Casing	Osterberg
IA	5.0	66.25	5.78	Sand	Sand	Wet	Statnamic
IA	5.0	55.42	5.58	Mixed	Sand	Wet	Statnamic
IA	5.0	54.78	5.77	Mixed	Sand	Wet	Statnamic
KS	6.0	49	6.01	IGM	IGM	Dry	Osterberg
MO	6.0	40.6	6.00	IGM+Rock	IGM	Dry	Osterberg
KS	3.5	19	4.55	IGM	IGM	Wet	Osterberg
KS	6.0	34	5.62	IGM	IGM	Dry	Osterberg
KY	8.0	105.2	N/A	IGM+Rock	Rock	Wet	Osterberg
KS	6.0	26.24	5.42	IGM	IGM	Dry	Osterberg
MN	6.0	55.3	5.90	Sand	Sand	Casing	Osterberg
IL	3.5	37.5	4.10	Clay+IGM	Rock	Dry	Osterberg
IA	5.0	75.17	6.01	Sand	Sand	Wet	Osterberg
IA	5.0	75	5.63	Sand	Sand	Wet	Osterberg
TN	4.0	16	5.77	Rock	Rock	Dry	Osterberg
TN	4.0	23	5.90	Rock	Rock	Dry	Osterberg
CO	3.5	22.6	3.42	IGM	IGM	Dry	Osterberg
CO	3.5	16	3.19	Clay	IGM	Dry	Osterberg
CO	4.0	25.3	3.41	IMG	IGM	Casing	Osterberg
CO	3.5	40.6	3.94	Rock	Rock	Casing	Osterberg
CO	3.0	11.25	4.88	Rock	Rock	Dry	Osterberg
CO	4.0	20	3.54	Rock	Rock	Casing	Osterberg

## Data Quality

Strict acceptance criteria were put into place to ensure the superior quality of DSHAFT. The level of quality of each load test was defined by load test type, the soil and rock classification, cross-hole sonic logging (CSL), and the background on where the information was obtained. Although various load test reports that were collected were incomplete and did not meet the acceptance criteria, they were still put into the database. This allowed for the missing data, should it be obtained, to be added to complete the dataset. To prevent confusion between the complete and incomplete sets, a “Usable Data” category was created, and each dataset was identified as usable by a “yes” or a “no,”

## Calibration Approach

The modified First Order Second Moment (FOSM) method was selected to determine the resistance factors for this study, and the data was verified to fit a lognormal distribution by using a hypothesis test based on the Anderson-Darling (AD) (1952) normality method. This test was chosen over the more common Chi-Square and the Kolmogorov Smirnov tests because the AD method is a better normality test for small sample sizes, such as with the DSHAFT database (Romeu, 2010). If the calculated AD value is smaller than the corresponding critical value (CV), the assumed lognormal distribution characteristic is correct. The equations for the AD and CV value are defined as:

$$AD = \sum_{i=1}^N \frac{1-2i}{N} \{ \ln(F_o[Z_i]) + \ln(1 - F_o[Z_{N+1-i}]) \} - N$$
$$CV = \frac{0.752}{1 + \frac{0.75}{N} + \frac{2.25}{N^2}}$$

Where,

- $F_o[Z_i]$  = cumulative probability density function of  $Z_i = P_r(Z \leq z_i)$
- $P_r( )$  = probability function
- $Z$  = standardized normal distribution of expected resistance bias  $\lambda_R$  or  $\ln(\lambda_R)$
- $z_i$  = standardized normal distribution of estimated resistance bias  $\lambda_R$  or  $\ln(\lambda_R) = \frac{R_i - \mu_R}{\sigma_R}$  or  $\frac{\ln R_i - \mu_{\ln R}}{\sigma_{\ln R}}$
- $\lambda_R$  = resistance bias, a ratio of estimated and measured pile resistances
- $N$  = sample size

To be consistent with the LRFD calibration efforts of driven piles in Iowa, a dead load to live load ratio of 2.0 was considered in the strength limit state, and various reliability indices,  $\beta_T$ , were chosen to cover a wide range of design possibilities. The reliability indices were 2.00, 2.33, 2.50, 3.00, and 3.50. To evaluate the efficiency of the failure criteria compared to the different design methods, the ratios of the resistance factors to the resistance bias were calculated over the given range of the reliability indices. The calibration approach was separated into the individual side and end-bearing resistances of each soil type – clay, sand, rock, and IGM. The various methods utilized in predicting the side and end-bearing resistances of the drilled shafts are summarized in Table 2-32.

Table 2-32. Static Analysis Methods (Ng et al. 2014)

<b>Geomaterial</b>	<b>Unit Side Resistance (<math>q_s</math>)</b>	<b>Unit End Bearing (<math>q_p</math>)</b>
Clay	$\alpha$ -method (O'Neill and Reese, 1999)	Total stress method (O'Neill and Reese, 1999)
Sand	$\beta$ -method (Burland, 1973 & O'Neill and Reese, 1999)	Effective stress method (O'Neill and Reese, 1989)
Cohesive IGM	Eq. 2-11 (O'Neill and Reese, 1999)	Various
Cohesionless IGM	Eq. 2-14 (O'Neill and Reese, 1999)	Eq. 2-22 (O'Neill and Reese, 1999)
Rock	Eq. 2-16 (Horvath and Kenney, 1979)	Various

There are nine analytical methods available for predicting the unit-end bearing resistances in cohesive IGM and rock, and six of those methods were chosen to be used in this study because of the variability of rock mass conditions that could occur beneath a drilled shaft. A combination of these methods was also proposed in this study to simplify the end-bearing prediction. The predicted side resistances in clay, sand, IGM, and rock were compared to three different failure criteria of the measured resistance: the measured resistance obtained directly from the load test report, the measured resistance defined by the one-inch top displacement criterion, and the measured resistance defined by the 5% of shaft diameter for top displacement criterion. An example of this comparison for clay is shown in Figure 2-8. The data sets were found to most closely represent lognormal distributions when based on the AD method.

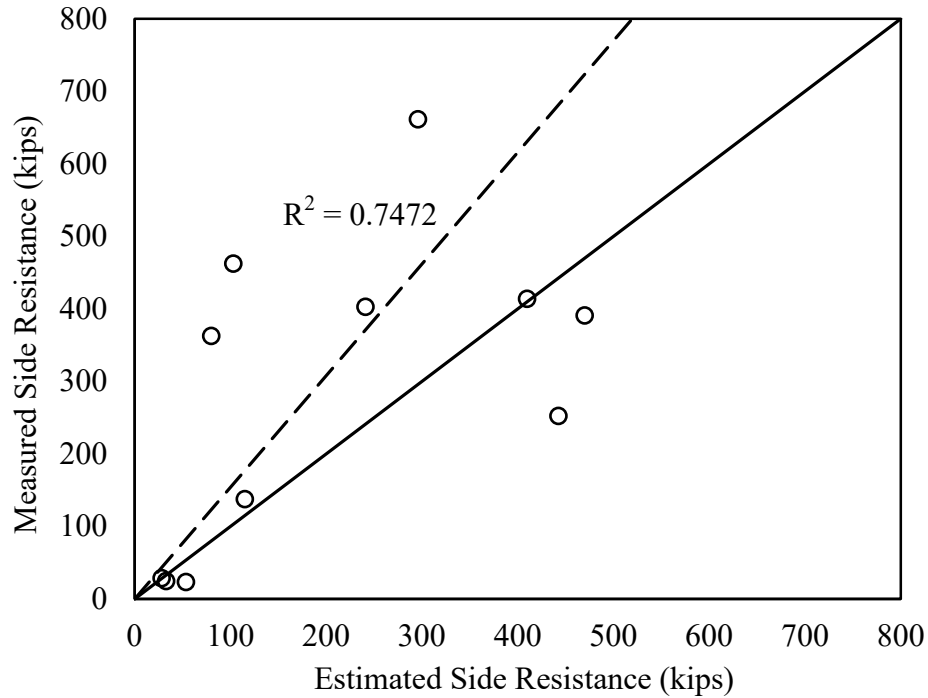


Figure 2-7. Measured (1-in.  $\Delta$ ) Vs. Estimated Side Resistance in Clay (Ng et al. 2014)

Only one usable data point was available for measured end-bearing resistance in clay, so a statistical analysis could not be performed to determine the resistance factor for that category. The predicted end-bearing resistances in sand were compared to the same type of measured resistances as performed for the side resistances; however, the predicted end-bearing resistances for rock and IGM were different. The end-bearing resistances were predicted by using six different analytical methods, and each of these was compared with the three different failure criteria. The majority of this data was also lognormally distributed. The total nominal resistance was also analyzed for the drilled shafts, with 27 data points to compare. After determining all of the resistance factors for side, end bearing, and the total nominal resistance for the various reliability indices, a target reliability index of 3.0 was chosen because a typical drilled shaft cap has four or fewer shafts, which is considered a non-redundant drilled shaft foundation. The total, side, and end-bearing resistance factors, based on this target reliability index, were then compared to the recommended resistance factors by AASHTO (2010), NCHRP (1991, 2004), and FHWA-NHI (2005). Efficiency factors were also generated to compare the three different failure criteria for the drilled shafts. After comparing the various resistance factors and efficiency factors, the one-inch top displacement criterion was selected to have the most efficiency, and the recommended resistance factors for various resistance components are summarized in Table 2-33.

Table 2-33. Recommended Resistance Factors for  $\beta T=3.0$  (Ng et al. 2014)

Resistance Component	Geomaterial	Analytical Method	Resistance Factors
Total Resistance	All	Combination of methods depending on subsurface profile	0.60
Side Resistance	Clay	$\alpha$ -method (O'Neill and Reese, 1999)	0.45
	Sand	$\beta$ -method (Burland, 1973 & O'Neill and Reese, 1999)	0.55
	IGM	Cohesive: Eq. 2-11 (O'Neill and Reese, 1999) and Cohesionless: Eq. 2-14 (O'Neill and Reese, 1999)	0.60
	Rock	Eq. 2-16 (Horvath and Kenney, 1979)	0.55
End Bearing	Clay	Total stress method (O'Neill and Reese, 1999)	0.40
	Sand	Effective stress method (O'Neill and Reese, 1989)	0.50
	IGM	Cohesive: Proposed method and Cohesionless: Eq. 2-22 (O'Neill and Reese, 1999)	0.55
	Rock	Proposed method	0.35
All	All	Static Load Test	0.70

#### New Mexico DOT (Ng & Fazia, 2012)

The New Mexico Department of Transportation (NMDOT) collected field data of drilled shaft load tests performed in cohesionless soils in New Mexico and other states. Field test data from the other states were only selected if the soil strength was equal to or greater than that of New Mexico's soils. An LRFD calibration study was performed, with this drilled shaft data, to adopt a new skin friction resistance factor for drilled shafts in cohesionless soils to replace the generic AASHTO-recommended resistance factor. Three design equations were used to determine the skin frictional resistance, and the resulting resistance factors of each were compared. The three methods used in the study were the O'Neill and Reese method, the method proposed by the FHWA in 2010, and the Unified Design equation.

#### O'Neill and Reese Method (O'Neill and Reese, 1999)

The O'Neill and Reese method uses the beta method to predict the skin friction that will be developed by a drilled shaft in cohesionless soil. This skin friction is calculated as:

$$f_{sz} = \beta \sigma'_z$$

Where,  $\sigma'_z$  is the vertical effective stress in the soil at depth,  $z$ , and  $\beta$  is the side resistance coefficient.  $\beta$  is defined by the following functions:

$$\text{SPT} \geq 15 \text{ blows/1 ft: } \beta = 1.5 - 0.135\sqrt{z} \quad 0.25 \leq \beta \leq 1.20$$

$$\text{SPT} < 15 \text{ blows/1 ft: } \beta = \frac{\text{SPT}}{15} (1.5 - 0.135\sqrt{z}) \quad 0.25 \leq \beta \leq 1.20$$

In very gravelly sands or gravel,  $\beta$  is defined by:

$$\text{SPT} \geq 15 \text{ blows/1 ft: } \beta = 2 - 0.06z^{0.75} \quad 0.25 \leq \beta \leq 1.80$$

For cohesionless soils with SPT values greater than 50, which are defined as cohesionless intermediate geomaterials (IGM), the skin friction is defined by:

$$f_{\text{ult}} = \sigma'_z K_o \tan \phi'$$

Where,  $K_o$  is the at-rest earth pressure coefficient and  $\phi'$  is the friction angle.

### **NHI Method (FHWA 2010)**

A 2010 FHWA publication proposed a new design equation, which is referred to as the NHI Method, for estimating the skin frictional resistance of drilled shafts in cohesionless soils. The skin friction is calculated as:

$$f_{\text{ult}} = \beta \sigma'_z$$

Where,  $\beta$  is defined as:

$$\beta = (1 - \sin \phi) \tan \phi \left( \frac{\sigma'_p}{\sigma'_z} \right)^{\sin \phi} \leq K_p \tan \phi$$

$K_p$  is the Rankine passive earth pressure coefficient, and  $\sigma'_p$  is the preconsolidation pressure.  $\sigma'_p$  is defined as:

$$\sigma'_p = 0.47 \times P_a \text{SPT}^m$$

Where,  $m = 0.6$  for clean quartzite sands and  $m = 0.8$  for silty sands to sandy silts. The angle of internal friction,  $\phi$ , is obtained from the corrected SPT value,  $(N_1)_{60}$ , suggested by Kulhawy and Chen (2007):

$$\phi = 27.5 + 9.2 \log(N_1)_{60}$$

### **The Unified Design Equation (Chua et al. 2000)**

The Unified Design Equation, proposed by Chua et al. (2000), predicts the load-carrying capacity of drilled shafts in both cohesive and cohesionless soils. For the prediction of skin frictional resistance in cohesionless soils, the soil parameters used in the design equation include both the internal friction angle and the unit weight. The unit skin frictional resistance, as with the NHI Method, is calculated as:

$$f_{\text{ult}} = \beta \sigma'_z$$

Where,  $\beta$  is defined as:

$$\beta = (1 - \sin \phi) \tan \phi \left( 1 + \frac{\frac{K_p}{K_o} - 1}{\sqrt{1+z}} \right)$$

And the internal friction angle is defined as:

$$\phi = 30 + 0.15D_R$$

Where,  $D_R$  is the relative density. A correlation exists between relative density and SPT blow counts (Gibbs and Holtz, 1957) at various depths for cohesionless soils. Chua et al. (2000) introduced an equation to quantify this relationship based on regression analysis, given as:

$$D_R = 20.4 \left( \frac{\sigma'_z}{p_a} \right)^{-0.223} \text{SPT}^{0.41}$$

Chua et al. (2000) developed the equation for the internal friction angle based on the relative density; however, DM-7 (U.S. Navy, 1971) developed a correlation between the internal friction angle and the relative density for cohesionless soils based on different soil classifications. This relationship, shown in Figure 2-9, is preferred over the other relationship, since it considers soil classification.

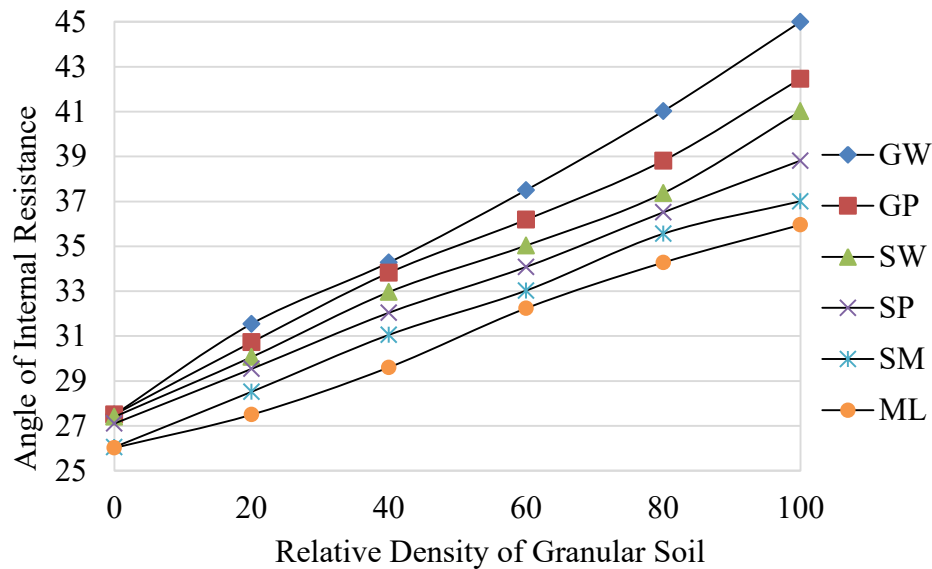


Figure 2-9. Internal Friction Angle (Ng & Fazia, 2012)

### Database

Drilled shaft load testing data was collected from NMDOT and other U.S. states to develop a database of 95 drilled shafts. Only five of the cases were collected from NMDOT, and the rest were from different parts of the U.S. Only 24 of the drilled shaft cases were selected and reported. The skin frictional resistance measured in the field was compared to the estimated skin frictional resistances from the three different methods. Table 2-34 reports these resistances, along with the corresponding drilled shaft information.

Table 2-34. Selected Drilled Shaft Cases (Ng &amp; Fazia, 2012)

<b>Location</b>	<b>Field (ton)</b>	<b>O'Neill &amp; Reese (ton)</b>	<b>Unified (ton)</b>	<b>NHI (ton)</b>	<b>Load Condition</b>	<b>D (ft.)</b>	<b>L (Ft.)</b>
Iowa	83.6	146.4	81.3	81.2	Bottom with O-cell	4.0	59.8
Georgia	152	324.3	337	292.6	Bottom with O-cell	5.5	60
Texas	166	244.3	216.9	274.8	Bottom with O-cell	3.0	34
Florida	445	383.6	480.4	389.4	Bottom with O-cell	4.0	46.8
New Jersey	871	1905.2	1547.9	1767.2	Top load	1.5	68
Georgia	493	287.2	255.9	263.6	Top load	3.0	60
New Mexico	571	627.7	380.3	324	Top load	2.8	30
Alabama	662	625	670.4	664.3	10 ft. from tip with O-cell	4.0	33.2
New Mexico	1620	1429.2	848.6	1079.4	Bottom and middle with O-cell	6.0	81
New Mexico	1800	2559.4	2491.7	2526.1	Bottom and middle with O-cell	4.5	52
Georgia	873.5	1399.7	1115.5	1019.6	Top load	2.6	47
Arizona	2964	1354.5	1662.6	1580.5	42 ft. from tip with O-cell	6.0	62
Arizona	778	730.1	942.5	942.5	42 ft. from tip with O-cell	6.0	53
Arizona	2626.5	2281.4	2608.5	1676.3	22 ft. from tip with O-cell	6.0	90
Arizona	1947	1945	1672.7	1439.6	14 ft. from tip with O-cell	6.0	48
Arizona	1627	1271.9	1308.9	1298.5	24 ft. from tip with O-cell	6.0	77
Arizona	276	352	653.3	527.6	24 ft. from tip with O-cell	6.0	24.3
Arizona	1771	1503.4	1475.1	1152.6	37 ft. from tip with O-cell	7.0	115
New Mexico	705	605.9	613.6	732.3	Bottom with O-cell	4.0	74.6
Japan	2527.7	2048.7	2695	1898.9	No data	3.9	134.5
New Mexico	950	265.7	306.7	240.9	Top load	2.7	40
Florida	456.8	328.3	332	426.6	O-cell	5.0	90
Florida	354.8	661.2	481.7	746.5	O-cell	6.0	90
Florida	404.2	298.2	556.4	503.9	O-cell	5.0	100



### Calibration Approach

A statistical analysis was performed on the bias obtained from the three different design methods. (The bias is the ratio of the measured resistance over the predicted resistance.) The Unified Design Equation produced the smallest coefficient of variation (COV) of 52%. Table 2-35 summarizes the results of this statistical analysis, and Figures 2-10 through 2-12 show the relationships between the measured and predicted skin frictional resistances of each design method.

Table 2-35. Statistical Analysis Summary (Ng & Fazia, 2012)

Design Method	Mean	Standard Deviation	COV
O'Neill & Reese	1.14	0.66	0.58
Unified	1.13	0.59	0.52
NHI	1.21	0.73	0.60

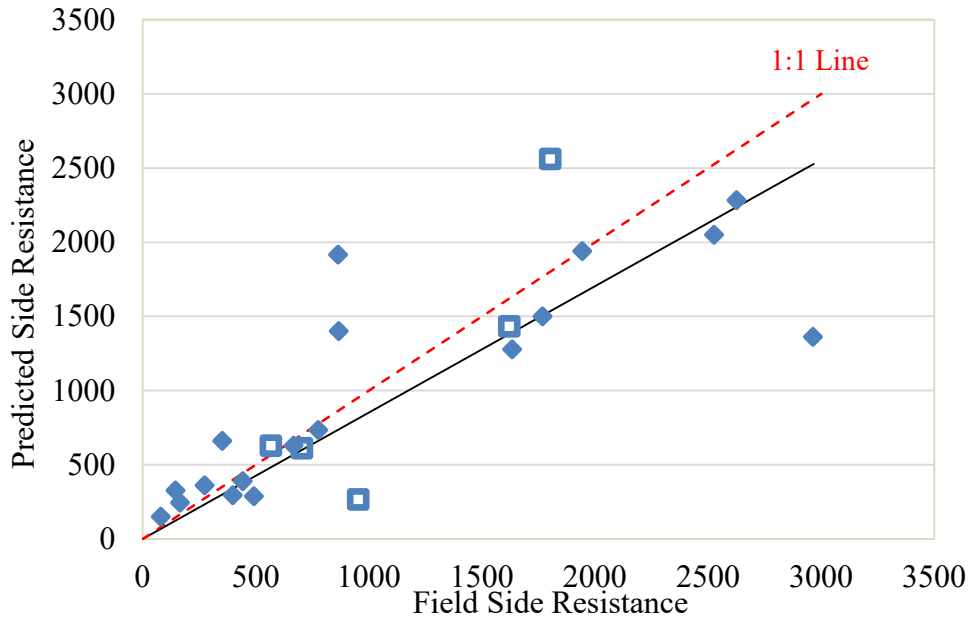


Figure 2-10. O'Neill & Reese Method (Ng & Fazia, 2012)

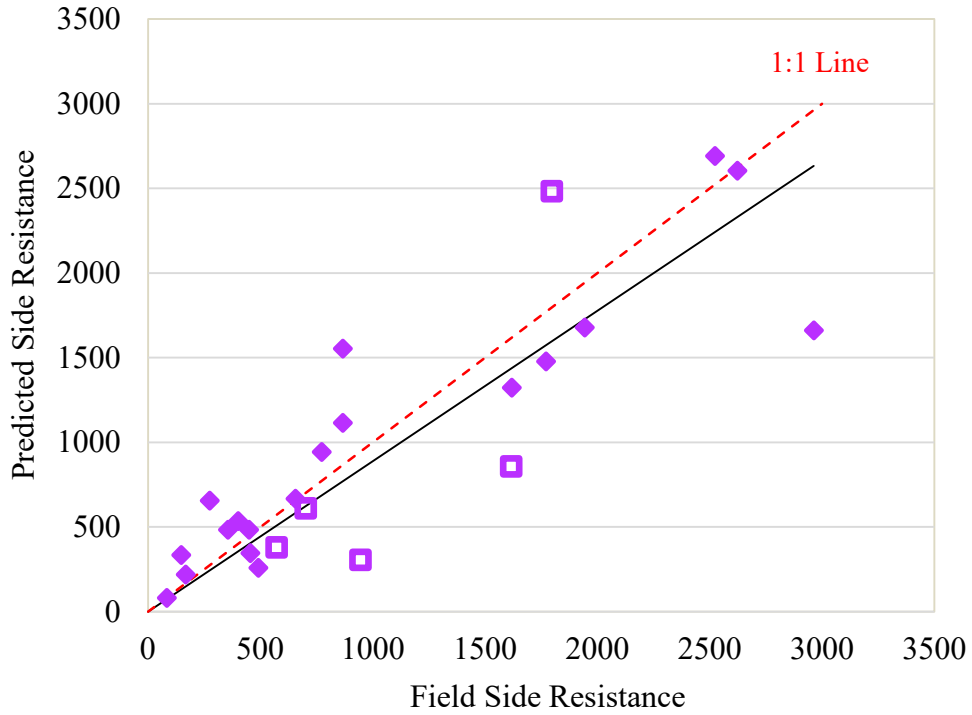


Figure 2-11. Unified Design Method (Ng & Fazia, 2012)

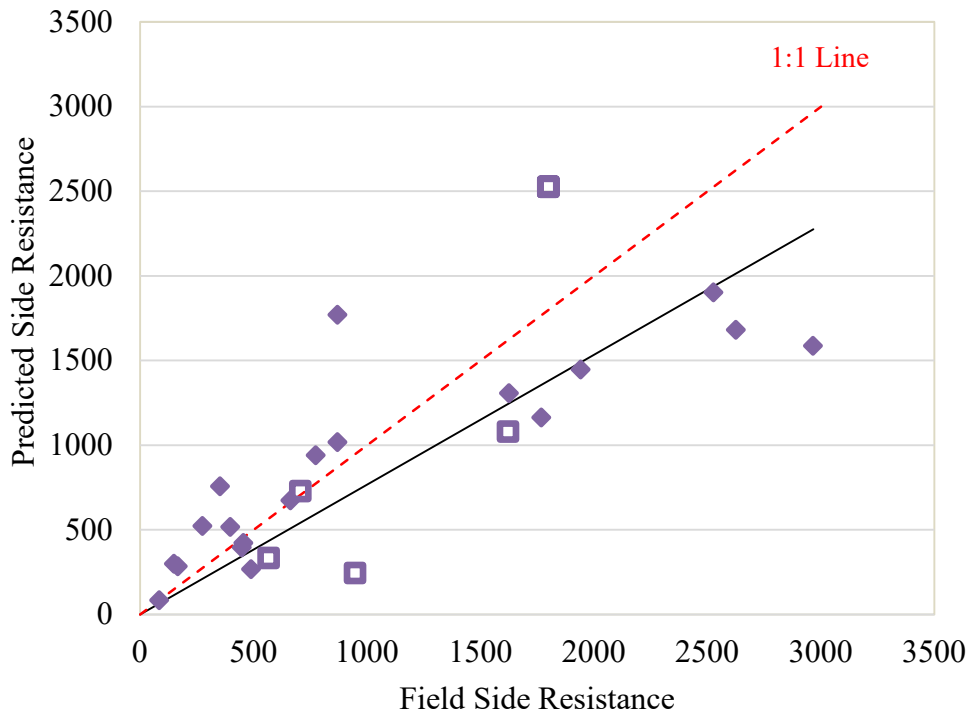


Figure 2-12. NHI Method (Ng & Fazia, 2012)

The resistance biases were assumed to be lognormally distributed, and the method of best-fit-to-tail lognormal distribution (Allen et al., 2005) was used to characterize the data, shown in Table

2-36. These values were selected to be used in the LRFD calibration process instead of the values given in Table 2-35 above.

Table 2-36. Statistical Analysis Summary (Ng & Fazia, 2012)

Design Method	Mean	Standard Deviation	COV
O'Neill & Reese	0.95	0.39	0.41
Unified	1.20	0.68	0.57
NHI	0.88	0.31	0.35

The dead and live loads were also assumed to be lognormally distributed. The selected statistical parameters of each, given below, are the same as those of Paikowsky (2004).

$$\begin{aligned} \gamma_D &= 1.25 & \lambda_D &= 1.05 & \text{COV}_D &= 0.10 \\ \gamma_L &= 1.75 & \lambda_L &= 1.15 & \text{COV}_L &= 0.20 \end{aligned}$$

The resistance biases were also characterized by a curve-fitted polynomial regression model. Both the lognormal and polynomial distribution data were used in the Monte Carlo simulation method to determine the resistance factors for each design method for a probability of failure of 1 in 1000. Table 2-37 summarizes the results of each. The resistance factors produced by using the curve-fitted polynomial regression model were higher than the ones produced by assuming a lognormal distribution, and it was determined that the polynomial model was more rational.

Table 2-37. Monte Carlo Simulation Results (Ng & Fazia, 2012)

Design Method	Lognormal	Polynomial
O'Neill & Reese	0.32	0.45
Unified	0.26	0.49
NHI	0.37	0.47

**Louisiana DOTD** (Abu-Farsakh et al., 2010; Abu-Farsakh et al., 2013)

The Louisiana Transportation and Research Center (LTRC), jointly sponsored by the Louisiana Department of Transportation and Development (LADOTD) and Louisiana State University, has performed multiple LRFD calibration studies over the years, as a continuing effort to implement LRFD methodology for deep foundations in Louisiana. The first study was performed in 2009 for driven piles, and 53 square precast-prestressed-concrete pile load tests that had been performed around the state were collected from LADOTD and used in the calibration. The next study, also conducted in 2009, calibrated resistance factors for axially-loaded drilled shafts. Sixteen drilled shaft load tests were obtained from LADOTD, but because of the limited number of drilled shaft load tests performed in Louisiana, an additional 50 load tests were obtained from the Mississippi Department of Transportation (MSDOT). Once this study was published, the FHWA released the new 2010 LRFD method for predicting the

ultimate resistance of drilled shafts. The LTRC then performed another calibration study to update the previous one. In addition to using the updated design method, 8 more drilled shaft load test cases from Louisiana were added to the database, for a total of 74 cases.

### **Database**

For the first drilled shaft calibration study conducted in 2010, the LTRC was only able to find 16 drilled shaft load tests in LADOTD's archives. Of those 16 cases, only 11 met the FHWA's settlement criterion for determining the nominal resistance. Because of the limited number of cases, the LTRC then obtained 50 drilled shaft load tests from MSDOT. In order to keep the calibration study relevant to the type of soil conditions found in Louisiana, 26 of the 50 cases in Mississippi were selected, based on the similarity of their soil type to that found in Louisiana. Of those 26 cases, only 15 met the FHWA's settlement criterion. Therefore, of the 66 cases available in the database, only 26 cases were used in the calibration study. For the second study conducted in 2013, 8 new drilled shaft load tests from LADOTD were added to the database, for a total of 34 drilled shaft cases. The diameters of the drilled shafts in these cases ranged from 2 to 6 feet, and the lengths ranged from 35.1 to 138.1 feet. Four drilled shafts were tested, using conventional top-down load tests, and the other 22 cases were tested using O-Cells. The majority of the soil types encountered included silty clay, clay, sand, clayey sand, and gravel. Table 2-38 summarizes the locations and characteristics of each drilled shaft used in the study.

### **CALIBRATION APPROACH**

The first drilled shaft calibration study performed by the LTRC used the 1999 FHWA drilled shaft design method to determine the predicted resistances of the drilled shafts. The second study used the 2010 FHWA drilled shaft design method in addition to the 1999 design method. The normalized trend curves given by the two FHWA design methods for determining the load-settlement behavior of drilled shafts in various soil types were used to predict the drilled shafts' resistances at various settlements. The 1999 FHWA design method gives normalized trend curves for side and base load transfer, while the 2010 design method only gives the normalized trend curve for axial compression.

The measured side, end bearing, and total resistances of each of the drilled shaft load tests were determined from the O-Cell load-settlement curves and the equivalent top-down load-settlement curves. The measured nominal resistance of a drilled shaft was selected to be the test load corresponding to settlement at 5% of the shaft diameter or the plunging load, whichever occurs first. The 5%B method, which is recommended by the FHWA, was selected because various statistical studies have shown it to be superior to other methods in producing the closest and most consistent capacities. Figure 2-13 shows the predicted load-settlement curves generated by using the 1999 and 2010 methods and the measured load-settlement curve from the load test of one of the drilled shaft cases.

Table 2-38. Drilled Shaft Summary (Abu-Farsakh et al. 2013)

Location	D (ft.)	L (ft.)	Soil Type	Load Test
Caddo, LA	2.5	53.1	Silty Clay, Sand Base	Top Down
Caddo, LA	2.5	35.1	Clay and Sand, Sand Base	Top Down
E. Baton Rouge, LA	3	54.1	Clayey Silt, Sand Base	O-cell
Ouachita, LA	5.5	76.1	Silty Sand, Sand Base	O-cell
Calcasieu, LA	6	86.9	Stiff Clay, Clay Base	O-cell
Winn, LA	2.5	77.4	Sand Clay, Sand Base	O-cell
Winn, LA	2.5	65	Sand, Clay Base	O-cell
E. Baton Rouge, LA	2.5	49.9	Silt, Clay, Clay Base	O-cell
Beauregard, LA	5.5	40.7	Clay, Silt, Clay Base	O-cell
Caddo, LA	3	44.9	Clay, Silty Clay, Clay Base	Top Down
Caddo, LA	3	62	Clay, Sand Base	Top Down
Union, MS	4.5	49.9	Sand, Sand Base	O-cell
Union, MS	4	73.1	Sand, Clay/Sand Base	O-cell
Washington, MS	4	123	Clay, Sand, Sand Base	O-cell
Washington, MS	4	138.1	Sand, Sand Base	O-cell
Washington, MS	4	119.1	Clay, Sand, Sand Base	O-cell
Washington, MS	5.5	94.1	Sand, Clay, Sand Base	O-cell
Washington, MS	4	96.1	Sand, Sand Base	O-cell
Washington, MS	4	82	Sand, Gravel, Sand Base	O-cell
Washington, MS	4	97.1	Sand, Clay, Sand Base	O-cell
Washington, MS	4	82	Sand, Sand Base	O-cell
Lee, MS	4	89	Clay, Clay Base	O-cell
Forrest, MS	6	47.9	Sand, Sand Base	O-cell
Perry, MS	4.5	64	Sand, Clay, Clay Base	O-cell
Wayne, MS	4	64	Sand, Clay Base	O-cell
Madison, MS	2	40	Clay, Clay Base	O-cell
E. Baton Rouge, LA	4	67.5	Clay, Clay Base	O-cell
E. Baton Rouge, LA	2.5	81.5	Clay, Clay Base	O-cell
E. Baton Rouge, LA	4	77.5	Clay, Clay Base	O-cell
Caddo, LA	6	43	Clay, Sand, Sand Base	O-cell
Caddo, LA	5.5	47.5	Sand, Sand Base	O-cell
Caddo, LA	5.5	48	Sand, Clay, Sand Base	O-cell
Caddo, LA	5.5	53.85	Clay, Sand, Sand Base	O-cell
Caddo, LA	5.5	51.12	Clay, Sand, Sand Base	O-cell

A few drilled shaft load tests did not meet the 5%B settlement criterion, so it was necessary to extrapolate the load-settlement curves to estimate the load corresponding to the needed settlement. The exponential curve-fitting method was chosen, over the hyperbolic, Chin's, cubic spline, and exponential curve fitting methods, as the best method for extrapolating the load-settlement curves. Figure 2-14 compares the extrapolated load-settlement curve to the measured curve to show the accuracy of the method. The extrapolation, however, was only performed on tests that were near the 5%B settlement criterion. Load tests that needed large extrapolations were discarded.

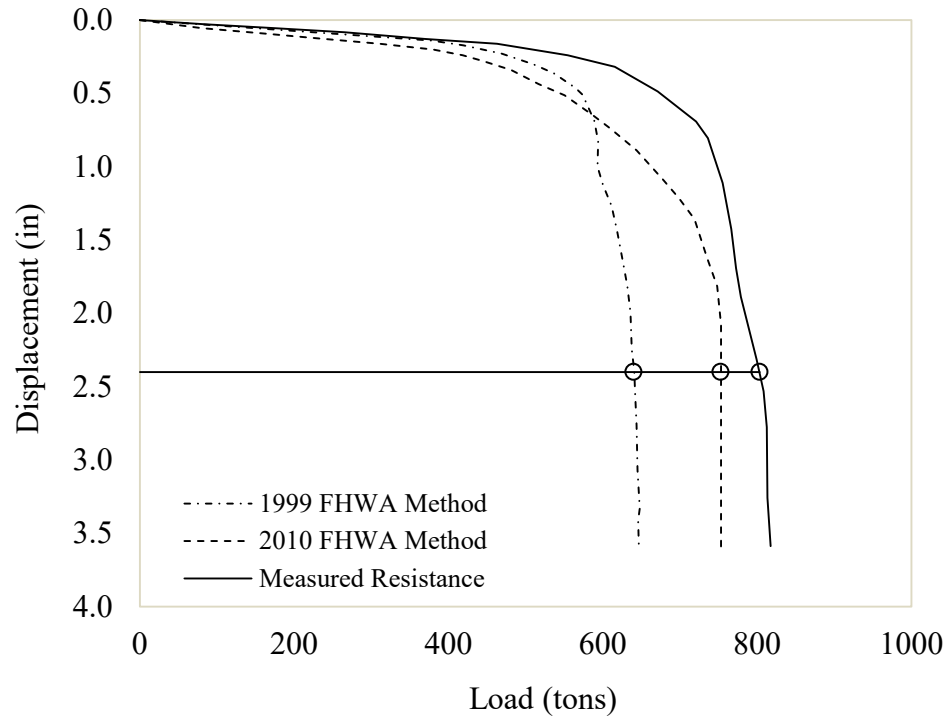


Figure 2-13. Predicted and Measured Load-Settlement Curves (Abu-Farsakh et al., 2013)

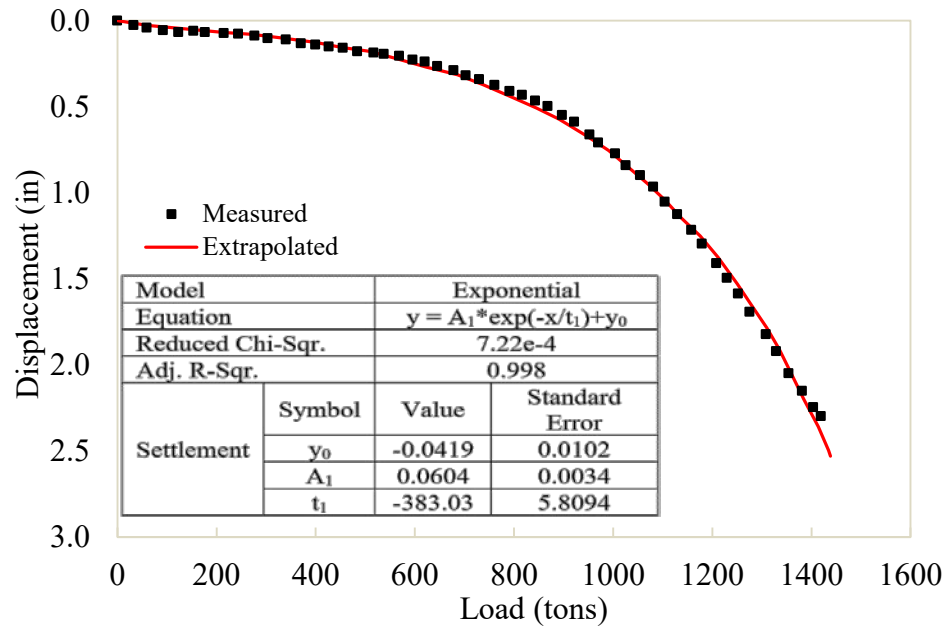


Figure 2-14. Extrapolated Top-Down Load-Settlement Curve (Abu-Farsakh et al., 2013)

The resistance bias factor, which is the measured-to-predicted resistance ratio, was determined for each case, and a statistical analysis was performed to determine the statistical characteristics of each design method, which are summarized in Table 2-39 below. The predicted resistances were plotted against the measured resistances, and a simple regression analysis was performed to determine the line of best fit of the data trend. The regression analysis showed the slope of the best-fit line for the 2010 FHWA design method to be 1.02, which indicated that the method overestimated the drilled shafts' resistances by 2%. On the other hand, the analysis showed that the slope of the best-fit line for the 1999 FHWA design is 0.79, which indicated that the method underestimated the resistances by 21%. The average resistance bias for the 1999 design method decreased from the 1.35 determined in the previous LTRC study; however, the slope of the best-fit line stayed the same.

Table 2-39. Statistical Analysis Summary (Abu-Farsakh et al., 2013)

2010 FHWA Design Method				
Summary Statistics				Best Fit Calculations
$R_m/R_p$			$R_p/R_m$	
Mean	Standard Deviation	COV	Mean	$R_{fit}/R_m$
0.99	0.30	0.30	1.10	1.02
1999 FHWA Design Method				
Summary Statistics				Best Fit Calculations
$R_m/R_p$			$R_p/R_m$	
Mean	Standard Deviation	COV	Mean	$R_{fit}/R_m$
1.27	0.38	0.30	0.87	0.79

The Anderson-Darling goodness of fit test was performed on the resistance biases from the 1999 and 2010 design methods, and it showed that both normal and lognormal distributions fit the data with a significance level of 0.05. Histograms were also generated for the resistance biases, and the lognormal distribution seemed to better fit the data; therefore, the lognormal distribution was chosen to be used in the calibration. The same process was conducted on the side and end-bearing resistance biases, and the lognormal distribution was a better fit for the data.

The Monte Carlo simulation method was used in this study to calibrate the resistance factors. The equation used in the simulation is given as:

$$g(R, Q) = \left( \frac{\gamma_D + \gamma_L \frac{Q_L}{Q_D}}{\phi} \right) \lambda_R - \left( \lambda_D + \lambda_L \frac{Q_L}{Q_D} \right)$$

The statistical characteristics selected for the dead and live loads are the following values:

$$\begin{aligned} \gamma_D &= 1.25 & \lambda_D &= 1.08 & \text{COV}_D &= 0.13 \\ \gamma_L &= 1.75 & \lambda_L &= 1.15 & \text{COV}_L &= 0.18 \end{aligned}$$

A dead-to-live load ratio of 3.0 was also used, and the target reliability index was 3.0. 50,000 simulations were generated, and the total resistance factors for the 2010 and 1999 FHWA design methods were determined to be 0.48 and 0.60, respectively. While the resistance factor for the 2010 design method is much lower than the 1999 method, the 2010 method gives a relatively higher efficiency factor. The simulation was also conducted on the side and end-bearing resistances to determine the resistance factors for each. The side and end-bearing factors, using the 2010 design method, were determined to be 0.26 and 0.53, respectively, and the side and end-bearing resistance factors, using the 1999 design method, were determined to be 0.39 and 0.52, respectively.



## CHAPTER 3 CALTRANS DRIVEN PILE AND DRILLED SHAFT DESIGN PRACTICE

At Caltrans design provisions for driven piles and drilled shafts are specified in AASHTO Articles 10.7 and 10.8, respectively, with corresponding CA Amendments (Caltrans, 2014a). Furthermore, Caltrans Memo to Designers 3-1 (Caltrans, 2014b) provides general guidance for selection and design of the piles or shafts and detailed communication procedures between the Structural Designer (SD) and the Geotechnical Designer (GD).

### Design Practice of Driven Piles

Design Practice of Driven Piles Caltrans foundation design is based on the latest adopted AASHTO LRFD Bridge Design Specifications and the corresponding California Amendments. For small piles (less than 16 inch or 24 inch), the  $\alpha$ -Tomlinson method and Nordlund method are used for static design; For large piles (greater than 16 inch or 24 inch), the API method is used. The following section presents the whole procedures of driven pile design which are including those three methods currently used by Caltrans.

### Design Process

MTD 3-1 (Caltrans, 2014b) lays out the design process for deep foundations. The SD provides factored loads acting on the pile/shaft for different load combinations, and the GD provides tip elevations for compression, tension, and settlement. The settlement tip is calculated based on service-I limit state loads, while compression and tension tips are calculated based on strength and extreme event limit state loads.

The factored weight of the footing (pile cap) and overburden soil should be added to the factored axial force calculated at the base of the column to provide the “gross” factored axial force. The factored weight of the soil from Original Ground (OG) to bottom of the pile cap is subtracted from factored gross axial force to obtain factored “net” axial force. Pile/shaft load calculations are based on net axial force for Service limit state and gross axial force for Strength and Extreme Event limit states.

The lateral tip elevation is provided by SD. The seismic moment and shear are applied at the cut-off point of the pile/shaft, and deflection at the cut-off point is recorded. Then, the length of the pile/shaft is changed, the deflection is recalculated, and the variation of the deflection vs. length of the pile/shaft is drawn. “Critical Depth” of the pile/shaft is the shallowest depth at which any increase in the length of the pile/shaft does not change the cut-off deflection. The

critical length is used to specify “lateral tip” on the plans. A determination of the lateral tip elevation is not necessary for pile/shaft groups in competent soil. For pile/shaft groups in marginal or soft/liquifiable soil it is not necessary to use a factor of safety for determination of the lateral tip elevation.

### **Geomaterial sub-layer investigation**

At each driven pile location, divide the subsurface into a finite number of geomaterial layers (cohesive and cohesionless soil), then assign one of the geomaterial types to each layer. Geomaterial come from an area at which one or more pile foundations will be installed and for which an idealized geomaterial layer profile will be developed. Each layer within the boring log is assigned a layer number  $i$ , thickness ( $\Delta z_i$ ), geomaterial type, and soil strength properties.

### **Limit states and load combination review**

Review the strength and service limit states to be satisfied and the corresponding axial load combinations and load factors for each foundation. The loads and load factors to be used in pile foundation design shall be as specified in chapter 3, AASHTO LRFD Bridge Design Specifications (6<sup>th</sup> Ed.). In addition, the effect of downdrag, uplift due to expansive soils and nearby structures shall be considered at the strength and extreme limit states.

### **Trial driven pile dimension**

For each driven pile, select trial lengths and diameters for initial analyses. Subsurface geotechnical information combined with static analysis methods, preconstruction probe pile programs, and/or pile load tests shall be used to estimate the depth of penetration required to achieve the desired nominal bearing resistance to establish contract pile quantities. If static analysis methods are used, potential bias in the method selected should be considered when estimating the penetration depth required to achieve the desired nominal bearing resistance. Local pile driving experience shall also be considered when making pile quantity estimates.

### **Nominal bearing resistance calculation**

Compute values of nominal unit side resistance for all geo-material layers through which the trial driven pile extends and the nominal unit base resistance at the trial tip elevation. Nominal pile bearing resistance should be field verified during pile installation using static load tests, dynamic tests, wave equation analysis, or dynamic formula. The production piles shall be driven to the minimum blow count determined from the static load test, dynamic test, wave equation, or dynamic formula and, if required, to a minimum penetration needed for uplift, scour, lateral resistance. If it is determined that static load testing is not feasible and dynamic methods are

unsuitable for field verification of nominal bearing resistance, the piles shall be driven to the tip elevation determined from the static analysis.

### Static Load Test

If a static pile load test is used to determine the pile nominal axial resistance, the test shall not be performed prior to completion of the pile set up period as determined by the Engineer. The load test shall follow the procedures specified in ASTM D1143, and the loading procedure should follow the Quick Load Test Procedure. Unless specified otherwise by the Engineer, the nominal bearing resistance shall be determined from the test data as follows:

- For piles 24 in. or less in diameter (length of side for square piles), the Davisson Method;
- For piles larger than 36 in. in diameter (length of side for square piles), at a pile top movement,  $s_f$  (in.), as determined from equation below; and
- For piles greater than 24 in. but less than 36 in. in diameter, criteria to determine the nominal bearing resistance that is linearly interpolated between the criteria determined at diameters of 24 and 36 in.

$$S_f = \frac{QL}{12AE} + \frac{B}{2.5} \quad (3.1)$$

Where:

Q = test load (kips),

L = pile length (ft),

A = pile cross-sectional area (ft<sup>2</sup>),

E = pile modulus (ksi),

B = pile diameter (length of side for square piles) (ft).

### Dynamic Testing

Dynamic testing shall be performed according to the procedures given in ASTM D4945. If possible, the dynamic test should be performed as a restrike test if the Engineer anticipates significant time dependent strength change. Dynamic testing shall not be used without calibrating to static load testing to determine the nominal bearing resistance of piles larger than 36-in. in diameter. The nominal pile bearing resistance shall be determined by a signal matching analysis of the dynamic pile test data if the dynamic test is used to establish the driving criteria. A signal matching analysis (Rausche et al., 1972) of the dynamic test data should always be used to determine bearing resistance if a static load test is not performed. Re-strike testing should be performed if setup or relaxation is anticipated.

### Wave Equation Analysis

If a wave equation analysis is used for the determination of the nominal bearing resistance, then the driving criterion (blow count) may be the value taken either at the end of driving (EOD) or at the beginning of redrive (BOR). The latter should be used where the soils exhibit significant strength changes (setup or relaxation) with time. When restrike (i.e., BOR) blow counts are taken, the hammer shall be warmed up prior to restrike testing and the blow count shall be taken as accurately as possible for the first inch of restrike. Dynamic testing shall not be used without calibrating to static load testing to determine the nominal bearing resistance of piles larger than 36-in. in diameter.

### Dynamic Formula

If a dynamic formula is used to establish the driving criterion, the following modified Gates Formula should be used. The nominal pile resistance as measured during driving using this method shall be taken as:

$$R_{ndr} = 1.83(E_r)^{0.5} \log_{10}(0.83N_b) - 124 \quad (3.2)$$

Where:

$R_{ndr}$  = nominal pile driving resistance measured during pile driving (kips),

$E_r$  = Manufacturer's rating for energy developed by the hammer at the observed field drop height (ft-lb),

$N_b$  = Number of hammer blows in the last foot. (maximum value to be used for N is 96) (blows/ft).

If a dynamic formula other than those provided herein is used, it shall be calibrated based on measured load test results to obtain an appropriate resistance factor. Dynamic formulas should not be used when the required nominal resistance exceeds 600 kips or the pile diameter is greater than or equal to 18-in.

### Static Analysis

The ultimate axial resistance ( $Q_u$ ) of a driven pile consists of the end-bearing resistance ( $Q_b$ ) and the skin frictional resistance ( $Q_s$ ). The ultimate driven pile resistance can then be calculated using the following equation:

$$Q_u = Q_b + Q_s = q_b \cdot A_b + \sum_{i=1}^n f_i A_{si} \quad (3.3)$$

Where,  $q_b$  is the unit tip bearing resistance,  $A_b$  is the cross section area of the pile tip,  $f_i$  is the average unit skin friction of the soil layer  $i$ ,  $A_{si}$  is the area of the pile shaft area interfacing with layer  $i$ , and  $n$  is the number of soil layers along the pile.

The static analysis method should be limited to driven piles 24 in. or less in diameter (length of side for square piles). For steel pipe and cast-in-steel shell (CISS) piles larger than 18 inches in diameter, the static analysis methods from the American Petroleum Institute (API, 2000) publication RP 2A should be used.

For open ended pipe piles, the nominal axial resistances should be calculated for both plugged and unplugged conditions. The lower of the two nominal resistances should be used for design.

#### Side Resistance in Cohesive Soil

##### *$\alpha$ -Tomlinson Method*

For piles in clay, a total stress analysis is often used where ultimate capacity is calculated from the undrained shear strength of the soil. This approach assumes that the shaft resistance is independent of the effective overburden pressure and that the unit shaft resistance can be expressed in terms of an empirical adhesion factor times the undrained shear strength.

The unit shaft resistance,  $f_s$ , is equal to the adhesion,  $C_u$ , which is the shear stress between the pile and soil at failure. This may be expressed in equation form as:

$$f_s = C_u * \alpha \quad (3.4)$$

in which  $\alpha$  is an empirical adhesion factor for reduction of the average undrained shear strength  $C_u$ , of undisturbed clay along the embedded length of the pile. The coefficient  $\alpha$  depends on the nature and strength of the clay, pile dimension, method of pile installation, and time effects. The values of  $\alpha$  vary within wide limits and decrease rapidly with increasing shear strength.

It is recommended that Figure 3-1 generally be used for adhesion calculations, unless one of the special soil stratigraphy cases identified in Figure 3-2 and Figure 3-3 are presented at a site. In cases where either Figure 3-1 or Figure 3-2 could be used, the inexperienced user should select and use the smaller value obtained from either figure. All users should confirm the applicability of a selected design chart in a given soil condition with local correlations between static capacity calculations and static load tests results.

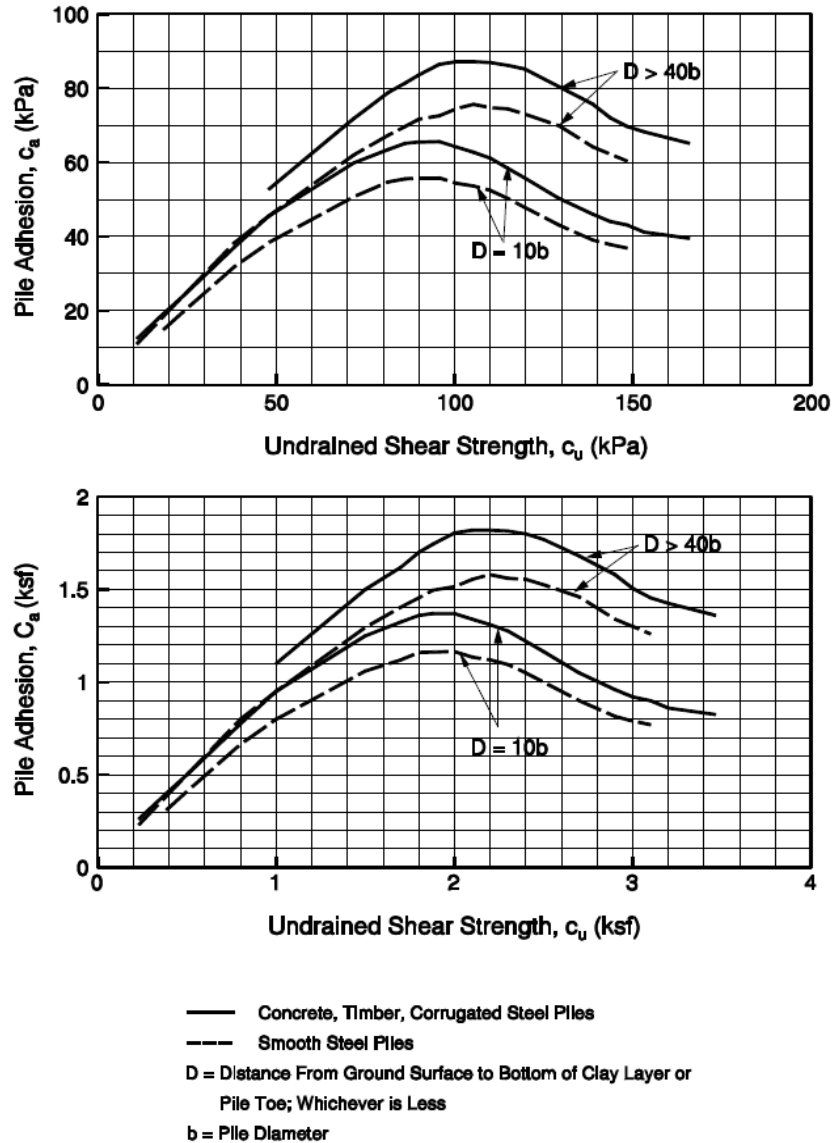


Figure 3-1 Adhesion Values for Piles in Cohesive Soils (after Tomlinson, 1979)

#### STEP BY STEP PROCEDURE FOR - " $\alpha$ -METHOD"

**STEP 1** Delineate the soil profile into layers and determine the adhesion,  $C_a$ , from Figure 3-1 or adhesion factor,  $\alpha$ , from Figure 3-2 or Figure 3-3 for each layer.

Enter appropriate figure with the undrained shear strength of the soil,  $c_u$ , and determine adhesion or adhesion factor based on the embedded pile length in clay,  $D$ , and pile diameter ratio,  $b$ . Use the curve for the appropriate soil and embedment condition.

**STEP 2** For each soil layer, compute the unit shaft resistance,  $f_s$  in kPa (ksf).

$$f_s = C_a = \alpha * c_u \quad (3.5)$$

Where:  $C_a$  = Adhesion.

**STEP 3** Compute the shaft resistance in each soil layer and the ultimate shaft resistance,  $R_s$ , in kN (kips), from the sum of the shaft resistance from each layer.

$$R_s = f_s * A_s \quad (3.6)$$

Where:  $A_s$  = Pile-soil surface area in  $m^2$  ( $ft^2$ ) from (pile perimeter) (length).

**STEP 4** Compute the unit toe resistance,  $q_t$  in kPa (ksf).

$$q_t = 9 * c_u \quad (3.7)$$

Where:

$C_u$  = Undrained shear strength of soil at the pile toe in kPa (ksf).

**STEP 5** Compute the ultimate toe resistance,  $R_t$  in kN (kips).

$$R_t = q_t * A_t \quad (3.8)$$

Where:  $A_t$  = Area of pile toe in  $m^2$  ( $ft^2$ ).

**STEP 6** Compute the ultimate pile capacity,  $Q_u$  in kN (kips).

$$Q_u = R_s + R_t \quad (3.9)$$

**STEP 7** Compute the allowable design load,  $Q_a$  in kN (kips).

$$Q_a = \frac{Q_u}{\text{Factor of safety}} \quad (3.10)$$

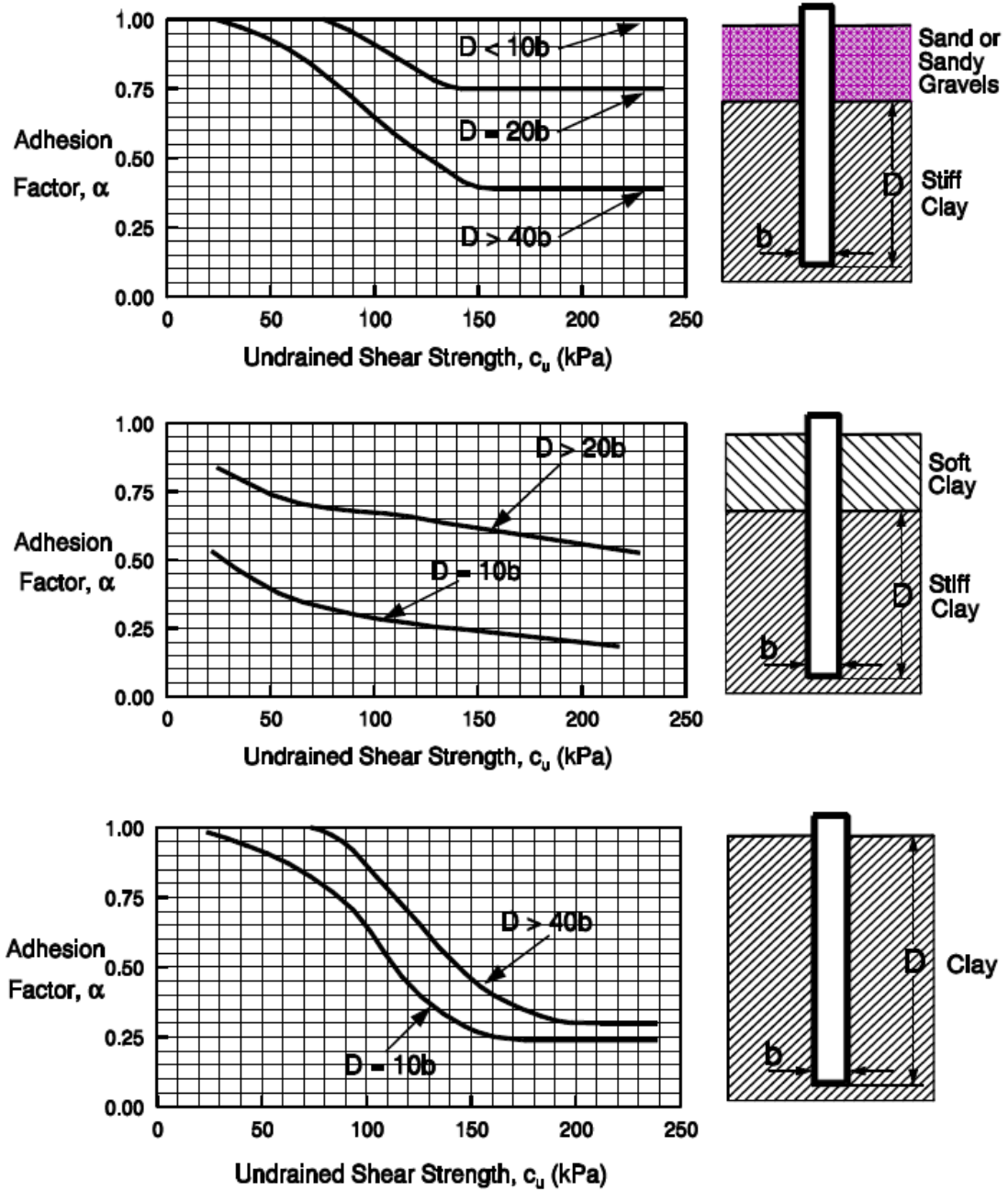


Figure 3-2 Adhesion Factors for Driven Piles in Clay- SI Units (Tomlinson, 1980)



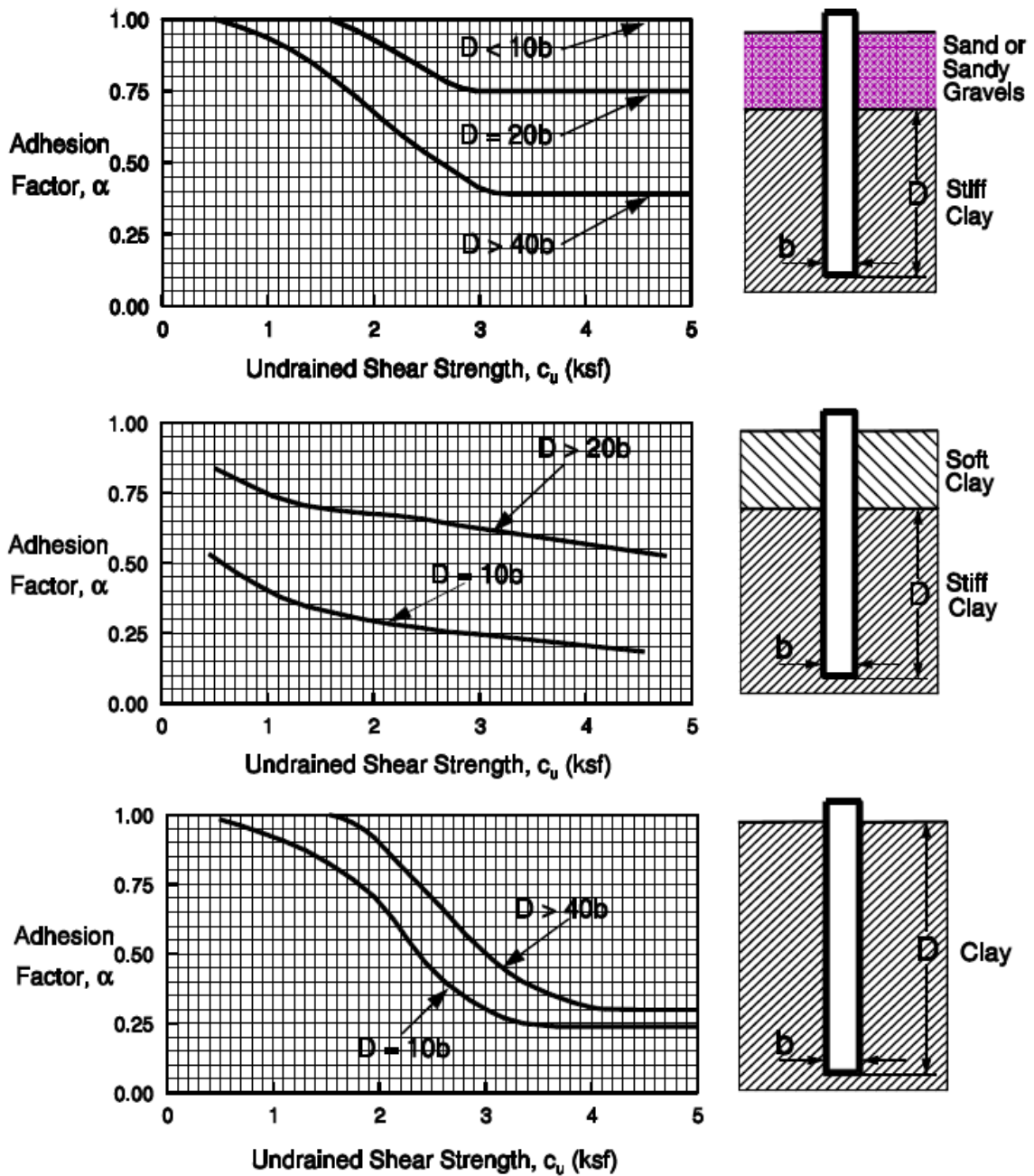


Figure 3-3 Adhesion Factors for Driven Piles in Clay- US Units (Tomlinson, 1980)

### $\beta$ -Method

The  $\beta$ -method, based on effective stress, may be used for predicting side resistance of prismatic piles. The nominal unit skin friction for this method, in ksf, shall be related to the effective stresses in the ground as:

$$f = \beta \sigma'_{vo} \quad (3.11)$$

Where:

$\sigma'_{vo}$  = vertical effective stress (ksf),

$\beta$  = a factor taken from Figure below:

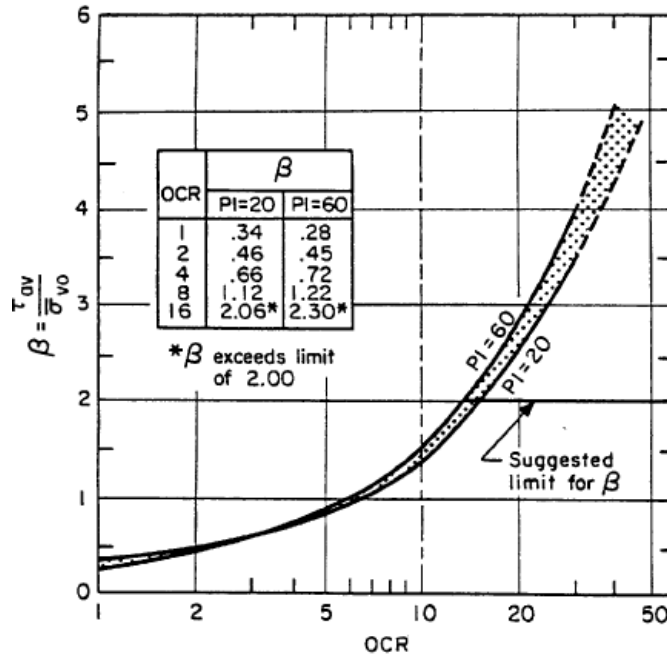


Figure 3-4  $\beta$  Versus OCR for Displacement Piles after Esrig and Kirby (1979)

The  $\beta$ -method has been found to work best for piles in normally consolidated and lightly over-consolidated clays. The method tends to overestimate side resistance of piles in heavily over-consolidated soils.

#### $\lambda$ -Method

The  $\lambda$ -method, based on effective stress (though it does contain a total stress parameter), may be used to relate the unit side resistance, in ksf, to passive earth pressure. For this method, the unit skin friction shall be taken as:

$$f = \lambda (\sigma'_{vo} + 2s_u) \quad (3.12)$$

Where:

$1q_v + 2S$  = passive lateral earth pressure (ksf),

$1q_v$  = the effective vertical stress at midpoint of soil layer under consideration (ksf),

$\lambda$  = an empirical coefficient taken from Figure below.

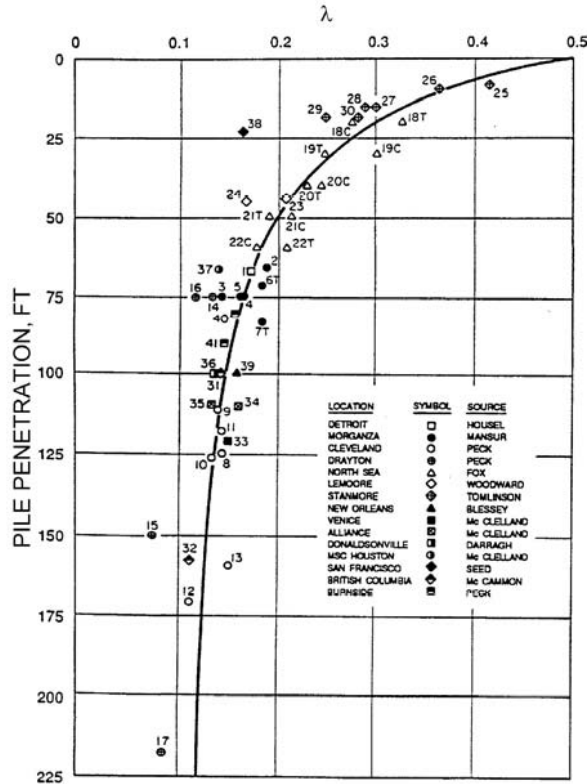


Figure 3-5  $\lambda$  Coefficient for Driven Pipe Piles after Vijayvergiya and Focht (1972)

### Tip Resistance in Cohesive Soils

The nominal unit tip resistance of piles in saturated clay, in ksf, shall be taken as:

$$q_b = 9 s_u \quad (3.13)$$

Where:

$s_u$  = undrained shear strength of the clay near the pile tip (ksf).

### Nordlund/Thurman Method in Cohesionless Soils

The Nordlund Method equation for computing the ultimate capacity of a pile is as follows:

$$Q_u = \sum_{d=0}^{d=D} K_{\delta} C_F p_d \frac{\sin(\delta + \omega)}{\cos \omega} C_d \Delta d + \alpha_t N'_q A_t P_t \quad (3.14)$$

Where:

$d$  = Depth,

$D$  = Embedded pile length,

$K_{\delta}$  = Coefficient of lateral earth pressure at depth  $d$ ,

$C_F$  = Correction factor for  $K_{\delta}$  when  $\delta \neq \phi$ ,

$p_d$  = Effective overburden pressure at the center of depth increment  $d$ ,  
 $\delta$  = Friction angle between pile and soil,  
 $\omega$  = Angle of pile taper from vertical,  
 $\phi$  = Soil friction angle,  
 $C_d$  = Pile perimeter at depth  $d$ ,  
 $\Delta d$  = Length of pile segment,  
 $\alpha_t$  = Dimensionless factor (dependent on pile depth-width relationship),  
 $N'_q$  = Bearing capacity factor,  
 $A_t$  = Pile toe area,  
 $p_t$  = Effective overburden pressure at the pile toe.

For a pile of uniform cross section ( $\omega=0$ ) and embedded length  $D$ , driven in soil layers of the same effective unit weight and friction angle, the Nordlund equation becomes

$$Q_u = (K_\delta C_F p_d \sin \delta C_d D) + (\alpha_t N'_q A_t p_t) \quad (3.15)$$

The soil friction angle  $\phi$  influences most of the calculations in the Nordlund method. In the absence of laboratory test data,  $\phi$  can be estimated from corrected SPT  $N'$  values.

#### STEP BY STEP PROCEDURE FOR USING NORDLUND METHOD

Steps 1 through 6 are for computing the shaft resistance and steps 7 through 9 are for computing the pile toe resistance.

**STEP 1** Delineate the soil profile into layers and determine the  $\phi$  angle for each layer.

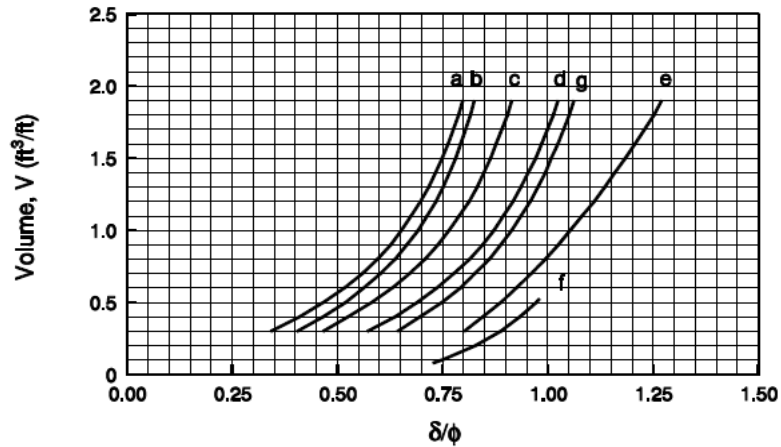
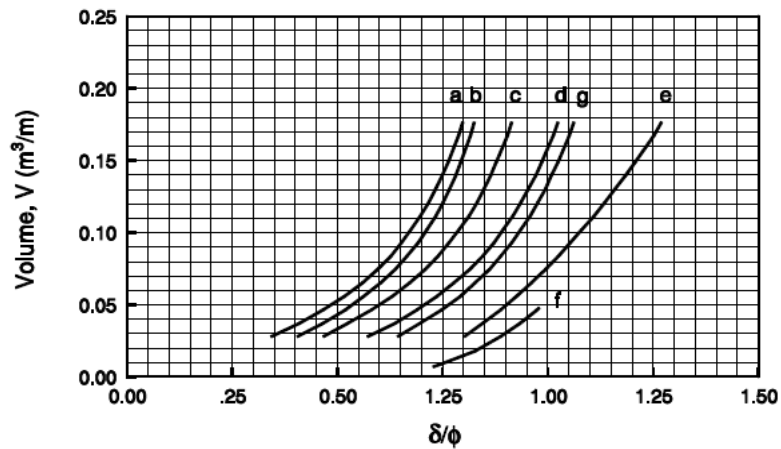
- a. Construct  $p_o$  diagram.
- b. Correct SPT field  $N$  values for overburden pressure using Table 3-1 and obtain corrected SPT  $N'$  values. Delineate soil profile into layers based on corrected SPT  $N'$  values.
- c. Determine  $\phi$  angle for each layer from laboratory tests or in-situ data.
- d. In the absence of laboratory or in-situ test data, determine the average corrected SPT  $N'$  value,  $\bar{N}'$ , for each soil layer and estimate  $\phi$  angle from Table 3-1.

**STEP 2** Determine  $\delta$ , the friction angle between pile and soil based on displaced soil volume,  $V$ , and the soil friction angle,  $\phi$ .

- a. Compute volume of soil displaced per unit length of pile,  $V$ .
- b. Enter Figure 3-6 with  $V$  and determine  $\delta/\phi$  ratio for pile type.
- c. Calculate  $\delta$  from  $\delta/\phi$  ratio.

Table 3-1. Empirical values for  $\phi$ ,  $D_r$ , and unit weight of granular soil based on corrected  $N'$

Description	Very Loose	Loose	Medium	Dense	Very Dense
Relative density $D_r$	0 - 0.15	0.15 - 0.35	0.35 - 0.65	0.65 - 0.85	0.85 - 1.00
Corrected Standard Penetration $N'$ value	0 to 4	4 to 10	10 to 30	30 to 50	50+
Approximate angle of internal friction $\phi^*$	25 - 30°	27 - 32°	30 - 35°	35 - 40°	38 - 43°
Range of approximate moist unit weight, $\gamma$ kN/m <sup>3</sup> (lb/ft <sup>3</sup> )	11.0 - 15.7 (70 - 100)	14.1 - 18.1 (90 - 115)	17.3 - 20.4 (110 - 130)	17.3 - 22.0 (110 - 140)	20.4 - 23.6 (130 - 150)



- a. Closed end pipe and non-tapered portion of monotube piles
- b. Timber piles
- c. Precast concrete piles
- d. Raymond step-taper piles
- e. Raymond uniform taper piles
- f. H-piles
- g. Tapered portion of monotube piles

Figure 3-6 Relationship of  $\delta/\phi$  and Pile Soil Displacement,  $V$ , for Various Types of Piles (after Nordlund, 1979)

**STEP 3** Determine the coefficient of lateral earth pressure,  $K_\delta$ , for each  $\phi$  angle.

- a. Determine  $K_\delta$  for  $\phi$  angle based on displaced volume,  $V$ , and pile taper angle,  $\omega$ , using either Figure 3-7, 3-8, 3-9, or 3-10 and the appropriate procedure described in Step 3b, 3c, 3d, or 3e.
- b. If the displaced volume is 0.0093, 0.093, or 0.930  $\text{m}^3/\text{m}$  (0.1, 1.0 or 10.0  $\text{ft}^3/\text{ft}$ ) which correspond to one of the curves provided in Figure 3-7 through Figure 3-10 and the  $\phi$  angle is one of those provided,  $K_\delta$  can be determined directly from the appropriate figure.
- c. If the displaced volume is 0.0093, 0.093, or 0.930  $\text{m}^3/\text{m}$  (0.1, 1.0 or 10.0  $\text{ft}^3/\text{ft}$ ) which correspond to one of the curves provided in Figure 3-7 through Figure 3-10 but the  $\phi$  angle is different from those provided, use linear interpolation to determine  $K_\delta$  for the required  $\phi$  angle. Table 3-2 and Table 3-3 also provide interpolated  $K_\delta$  values at selected displaced volumes versus  $\phi$  angle for uniform piles ( $\omega=0$ ).
- d. If the displaced volume is other than 0.0093, 0.093, or 0.930  $\text{m}^3/\text{m}$  (0.1, 1.0 or 10.0  $\text{ft}^3/\text{ft}$ ) which correspond to one of the curves provided in Figure 3-7 through Figure 3-10 but the  $\phi$  angle corresponds to one of those provided, use log linear interpolation to determine  $K_\delta$  for the required displaced volume. Table 3-2 and Table 3-3 also provide interpolated  $K_\delta$  values at selected displaced volumes versus  $\phi$  angle for uniform piles ( $\omega=0$ ).
- e. If the displaced volume is other than 0.0093, 0.093, or 0.930  $\text{m}^3/\text{m}$  (0.1, 1.0 or 10.0  $\text{ft}^3/\text{ft}$ ) which correspond to one of the curves provided in Figure 3-7 through Figure 3-10 and the  $\phi$  angle does not correspond to one of those provided, first use linear interpolation to determine  $K_\delta$  for the required  $\phi$  angle at the displaced volume curves provided for 0.0093, 0.093, or 0.930  $\text{m}^3/\text{m}$  (0.1, 1.0 or 10.0  $\text{ft}^3/\text{ft}$ ). Then use log linear interpolation to determine  $K_\delta$  for the required displaced volume. Table 3-2 and Table 3-3 also provide interpolated  $K_\delta$  values at selected displaced volumes versus  $\phi$  angle for uniform piles ( $\omega=0$ ).

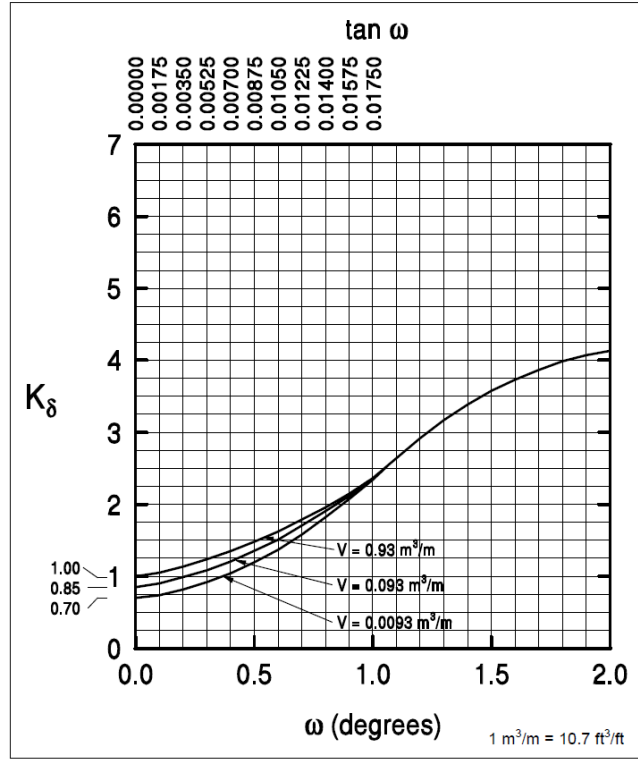


Figure 3-7 Design Curve for Evaluating  $K_\delta$  for Piles when  $\phi = 25^\circ$  (after Nordlund, 1979)

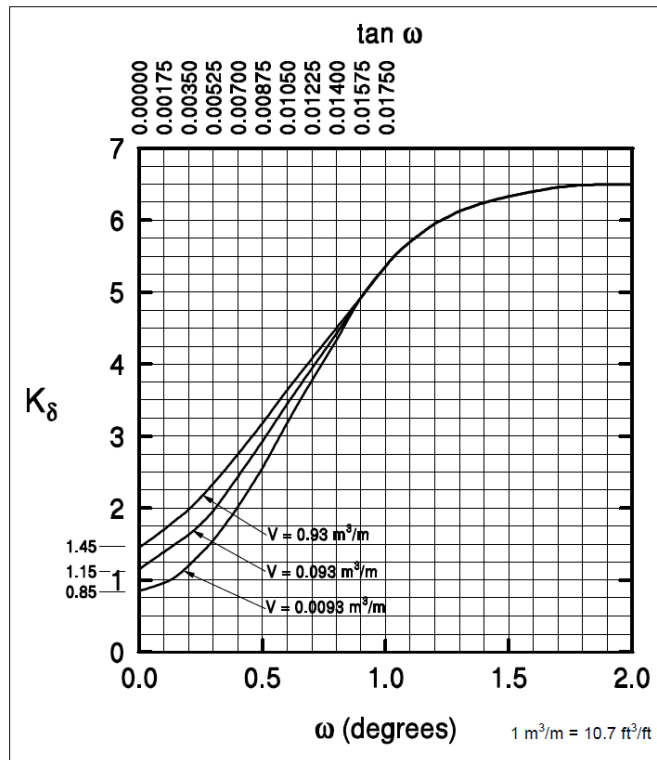


Figure 3-8 Design Curve for Evaluating  $K_\delta$  for Piles when  $\phi = 30^\circ$  (after Nordlund, 1979)

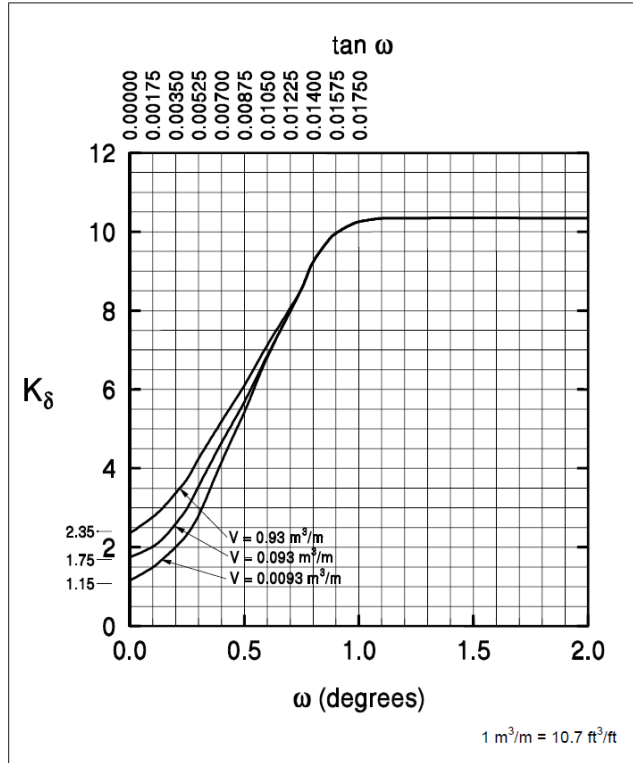


Figure 3-9 Design Curve for Evaluating  $K_\delta$  for Piles when  $\phi = 35^\circ$  (after Nordlund, 1979)

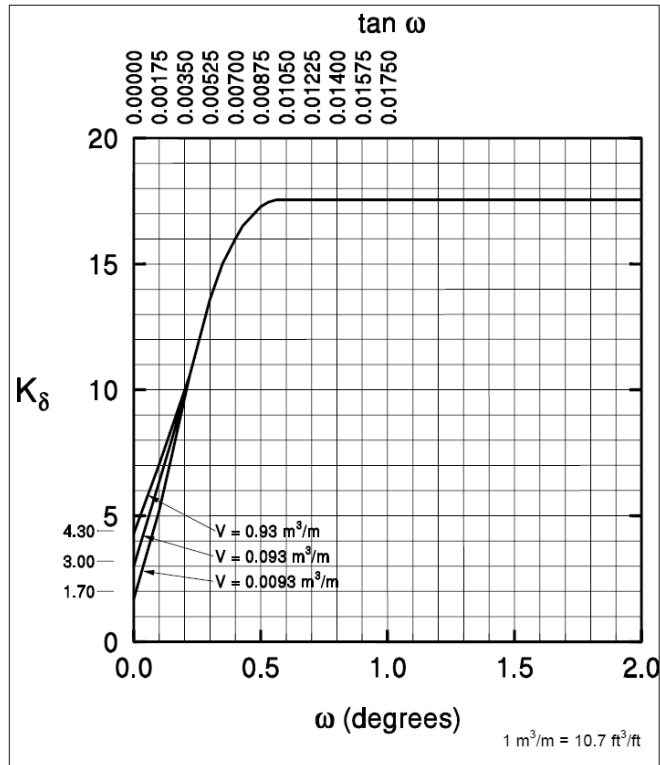


Figure 3-10 Design Curve for Evaluating  $K_\delta$  for Piles when  $\phi = 40^\circ$  (after Nordlund, 1979)



Table 3-2. Design Table for Evaluating  $K_{\delta}$  for Piles when  $\omega = 0^{\circ}$  and  $V = 0.0093$  to  $0.0930 \text{ m}^3/\text{m}$   
( $0.10$  to  $1.00 \text{ ft}^3/\text{ft}$ )

$\phi$	Displaced Volume -V, $\text{m}^3/\text{m}$ , ( $\text{ft}^3/\text{ft}$ )									
	0.0093 (0.10)	0.0186 (0.20)	0.0279 (0.30)	0.0372 (0.40)	0.0465 (0.50)	0.0558 (0.60)	0.0651 (0.70)	0.0744 (0.80)	0.0837 (0.90)	0.0930 (1.00)
25	0.70	0.75	0.77	0.79	0.80	0.82	0.83	0.84	0.84	0.85
26	0.73	0.78	0.82	0.84	0.86	0.87	0.88	0.89	0.90	0.91
27	0.76	0.82	0.86	0.89	0.91	0.92	0.94	0.95	0.96	0.97
28	0.79	0.86	0.90	0.93	0.96	0.98	0.99	1.01	1.02	1.03
29	0.82	0.90	0.95	0.98	1.01	1.03	1.05	1.06	1.08	1.09
30	0.85	0.94	0.99	1.03	1.06	1.08	1.10	1.12	1.14	1.15
31	0.91	1.02	1.08	1.13	1.16	1.19	1.21	1.24	1.25	1.27
32	0.97	1.10	1.17	1.22	1.26	1.30	1.32	1.35	1.37	1.39
33	1.03	1.17	1.26	1.32	1.37	1.40	1.44	1.46	1.49	1.51
34	1.09	1.25	1.35	1.42	1.47	1.51	1.55	1.58	1.61	1.63
35	1.15	1.33	1.44	1.51	1.57	1.62	1.66	1.69	1.72	1.75
36	1.26	1.48	1.61	1.71	1.78	1.84	1.89	1.93	1.97	2.00
37	1.37	1.63	1.79	1.90	1.99	2.05	2.11	2.16	2.21	2.25
38	1.48	1.79	1.97	2.09	2.19	2.27	2.34	2.40	2.45	2.50
39	1.59	1.94	2.14	2.29	2.40	2.49	2.57	2.64	2.70	2.75
40	1.70	2.09	2.32	2.48	2.61	2.71	2.80	2.87	2.94	3.0

Table 3-3. Design Table for Evaluating  $K_\delta$  for Piles when  $\omega = 0^\circ$  and  $V = 0.093$  to  $0.930 \text{ m}^3/\text{m}$  ( $1.0$  to  $10.0 \text{ ft}^3/\text{ft}$ )

$\phi$	Displaced Volume -V, $\text{m}^3/\text{m}$ ( $\text{ft}^3/\text{ft}$ )									
	0.093 (1.0)	0.186 (2.0)	0.279 (3.0)	0.372 (4.0)	0.465 (5.0)	0.558 (6.0)	0.651 (7.0)	0.744 (8.0)	0.837 (9.0)	0.930 (10.0)
25	0.85	0.90	0.92	0.94	0.95	0.97	0.98	0.99	0.99	1.00
26	0.91	0.96	1.00	1.02	1.04	1.05	1.06	1.07	1.08	1.09
27	0.97	1.03	1.07	1.10	1.12	1.13	1.15	1.16	1.17	1.18
28	1.03	1.10	1.14	1.17	1.20	1.22	1.23	1.25	1.26	1.27
29	1.09	1.17	1.22	1.25	1.28	1.30	1.32	1.33	1.35	1.36
30	1.15	1.24	1.29	1.33	1.36	1.38	1.40	1.42	1.44	1.45
31	1.27	1.38	1.44	1.49	1.52	1.55	1.57	1.60	1.61	1.63
32	1.39	1.52	1.59	1.64	1.68	1.72	1.74	1.77	1.79	1.81
33	1.51	1.65	1.74	1.80	1.85	1.88	1.92	1.94	1.97	1.99
34	1.63	1.79	1.89	1.96	2.01	2.05	2.09	2.12	2.15	2.17
35	1.75	1.93	2.04	2.11	2.17	2.22	2.26	2.29	2.32	2.35
36	2.00	2.22	2.35	2.45	2.52	2.58	2.63	2.67	2.71	2.74
37	2.25	2.51	2.67	2.78	2.87	2.93	2.99	3.04	3.09	3.13
38	2.50	2.81	2.99	3.11	3.21	3.29	3.36	3.42	3.47	3.52
39	2.75	3.10	3.30	3.45	3.56	3.65	3.73	3.80	3.86	3.91
40	3.00	3.39	3.62	3.78	3.91	4.01	4.10	4.17	4.24	4.30

**STEP 4** Determine the correction factor,  $C_F$ , to be applied to  $K_\delta$  if  $\delta \neq \phi$ . Use Figure 3-11 to determine the correction factor for each  $K_\delta$ . Enter figure with  $\phi$  angle and  $\delta/\phi$  value to determine  $C_F$ .

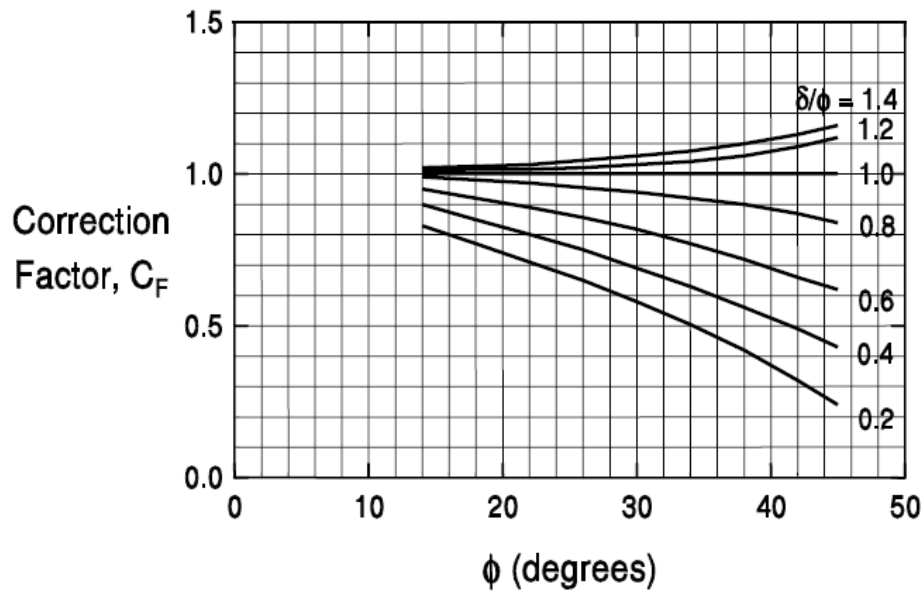


Figure 3-11 Correction Factor for  $K_\delta$  when  $\delta \neq \phi$  (after Nordlund, 1979)

**STEP 5** Compute the average effective overburden pressure at the midpoint of each soil layer,  $p_d$  (kPa).

**STEP 6** Compute the shaft resistance in each soil layer. Sum the shaft resistance from each soil layer to obtain the ultimate shaft resistance,  $R_s$  (kN).

$$R_s = K_\delta C_F p_d \sin \delta C_d D \quad (3.16)$$

(for uniform pile cross section)

**STEP 7** Determine the  $\alpha_t$  coefficient and the bearing capacity factor,  $N'_q$ , from the  $\phi$  angle near the pile toe.

a. Enter Figure 3-12 with  $\phi$  angle near pile toe to determine  $\alpha_t$  coefficient based on pile length to diameter ratio.

b. Enter Figure 3-13 with  $\phi$  angle near pile toe to determine,  $N'_q$ .

c. If  $\phi$  angle is estimated from SPT data, compute the average corrected SPT  $N'$  value over the zone from the pile toe to 3 diameters below the pile toe.

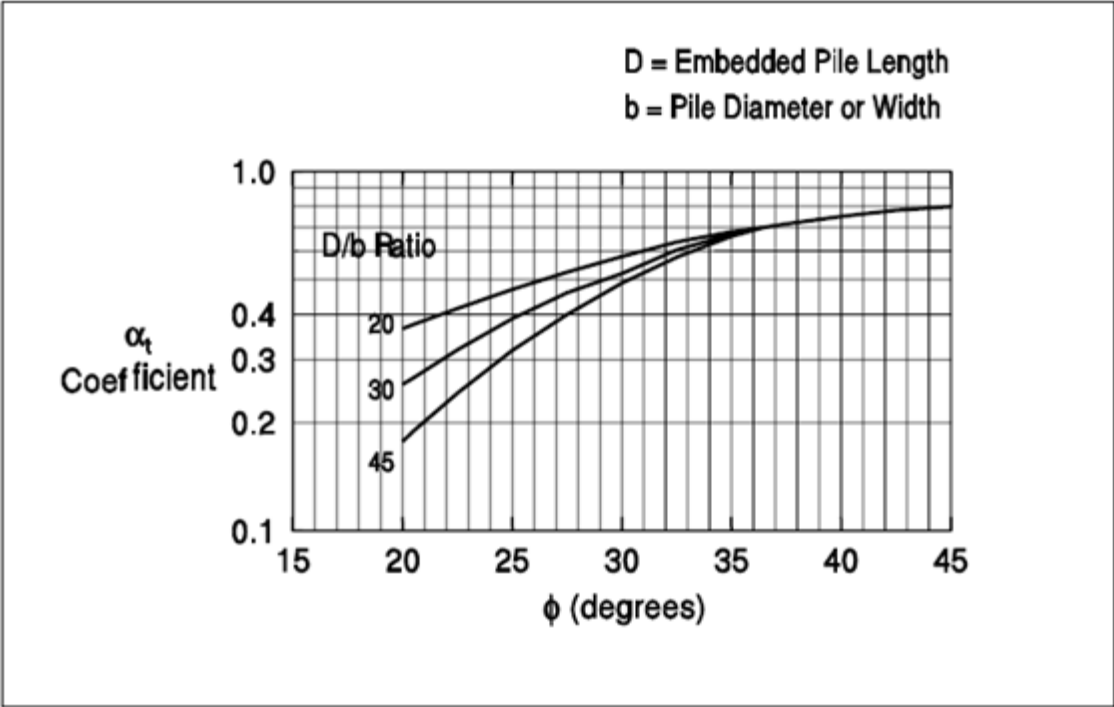


Figure 3-12 Chart for Estimating  $\alpha_t$  Coefficient and Bearing Capacity Factor  $N'_q$  (Chart modified from Bowles, 1977)

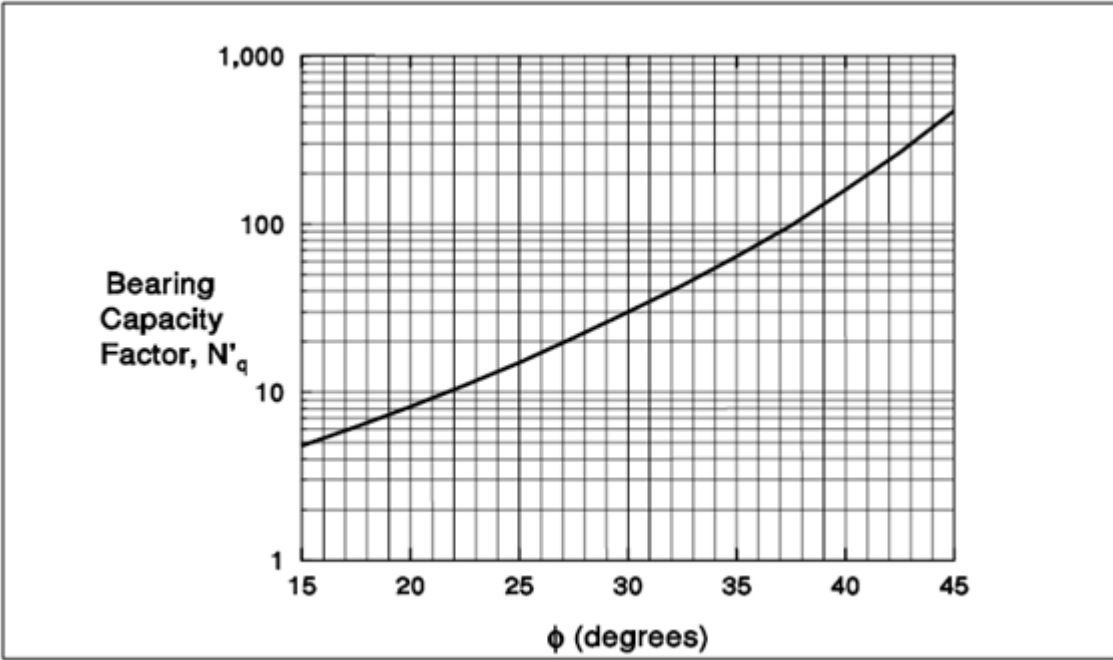


Figure 3-13 Chart for Estimating  $\alpha_t$  Coefficient and Bearing Capacity Factor  $N'_q$  (Chart modified from Bowles, 1977)

**STEP 8** Compute the effective overburden pressure at the pile toe,  $p_t$  (kPa).

**Note:** The limiting value of  $p_t$  is 150 kPa (3 ksf).

**STEP 9** Compute the ultimate toe resistance,  $R_t$  (kN).

$$R_t = \alpha_t N'_q A_t p_t \quad (3.17)$$

$$\text{limiting } R_t = q_L A_t \quad (3.18)$$

$q_L$  value is obtained from:

1. Entering Figure 3-14 with  $\phi$  angle near pile toe determined from laboratory or in-situ test data.
2. Entering Figure 3-14 with  $\phi$  angle near the pile toe estimated from Figure 3-1 Adhesion Values for Piles in Cohesive Soils (after Tomlinson, 1979) and the average corrected SPT  $N'$  near toe as described in Step 7.

c. Use lesser of the two  $R_t$  values obtained in steps a and b.

For steel H and unfilled open end pipe piles, use only steel cross section area at pile toe unless there is reasonable assurance and previous experience that a soil plug will form at the pile toe.

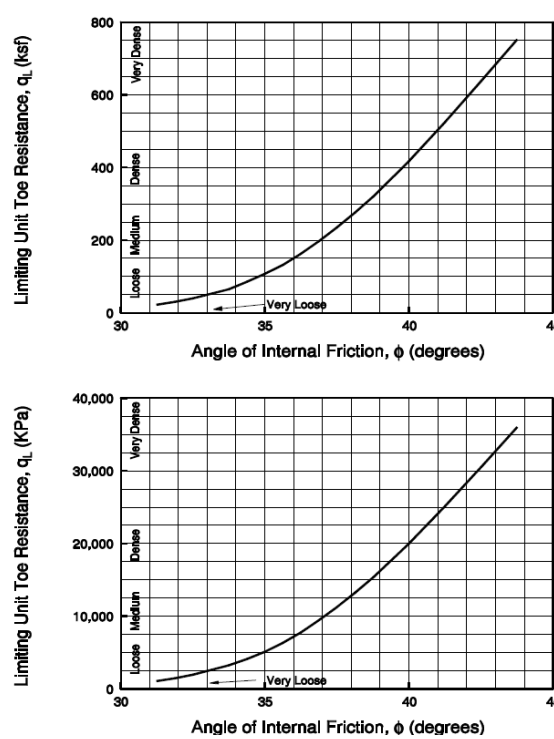


Figure 3-14 Relationship Between Maximum Unit Pile Toe Resistance and Friction Angle for cohesionless soil (after Meyerhof, 1976)

**STEP 10** Compute the ultimate pile capacity,  $Q_u$  (kN) from equation (3.9).

**STEP 11** Compute the allowable design load,  $Q_a$  (kN) from equation (3.10).

The factor of safety used in the calculation should be based upon the construction control method to be specified.

### *API method*

#### Skin Friction and End Bearing in Cohesive Soils

1. For pipe piles in cohesive soils, the shaft friction,  $f$ , in  $\text{lb/ft}^2$  (kPa) at any point along the pile may be calculated by three equations.

$$f = a c \quad (3.19)$$

Where:

$a$  = a dimensionless factor,

$c$  = undrained shear strength of the soil at the point in question.

The factor,  $a$ , can be computed by the equations:

$$\alpha = 0.5 * \varphi^{-0.5} \quad \varphi \leq 1 \quad (3.20)$$

$$\alpha = 0.5 * \varphi^{-0.25} \quad \varphi > 1 \quad (3.21)$$

Where:

$\varphi = c/p'_0$  for the point in question,

$p'_0$  = effective overburden pressure at the point in question  $\text{lb/ft}^2$  (kPa).

2. For piles end bearing in cohesive soils, the unit end bearing  $q$ , in  $\text{lbs/ft}^2$  (kPa), may be computed by the equation

$$q = 9 c \quad (3.22)$$

#### Friction and End Bearing in Cohesionless Soils

1. For pipe piles in cohesionless soils, the shaft friction,  $f$ , in  $\text{lb/ft}^2$  (kPa) may be calculated by the equation

$$f = K p_0 \tan \alpha \quad (3.23)$$

Where:

$K$  = coefficient of lateral earth pressure (ratio of horizontal to vertical normal effective stress),  
 $p_o$  = effective overburden pressure lb/ft<sup>2</sup> (kPa) at the point in question,  
 $\delta$  = friction angle between the soil and pile wall.

For open-ended pipe piles driven unplugged, it is usually appropriate to assume  $K$  as 0.8 for both tension and compression loadings. Values of  $K$  for full displacement piles (plugged or closed end) may be assumed to be 1.0. Table 3-4 may be used for selection of  $\delta$  if other data are not available.

- For piles end bearing in cohesionless soils the unit end bearing  $q$  in lb/ft<sup>2</sup> (kPa) may be computed by the equation:

$$q = p_o N_q \quad (3.24)$$

Where:

$p_o$  = effective overburden pressure lb/ft<sup>2</sup> (kPa) at the pile tip,  
 $N_q$  = dimensionless bearing capacity factor.

Table 3-4. Design Parameters for Cohesionless Siliceous Soil

Density	Soil Description	Soil-Pile Friction Angle, Degrees	Limiting Skin Friction Values kips/ft <sup>2</sup> (kPa)	$N_q$	Limiting Unit End Bearing Values kips/ft <sup>2</sup> (MPa)
Very Loose Loose Medium	Sand Sand-Silt Silt	15	1.0 (47.8)	8	40(1.9)
Loose Medium Dense	Sand Sand-Silt Silt	20	1.4 (67.0)	12	60 (2.9)
Medium Dense	Sand Sand-Silt	25	1.7 (81.3)	20	100 (4.8)
Dense Very Dense	Sand Sand-Silt	30	2.0 (95.7)	40	200 (9.6)
Dense Very Dense	Gravel Sand	35	2.4 (114.8)	50	250 (12.0)

#### *Using SPT in Cohesionless Soils*

These methods shall be applied only to sands and nonplastic silts. The nominal unit tip resistance for the Meyerhof method, in ksf, for piles driven to a depth  $D_b$  into a cohesionless soil stratum shall be taken as:

$$q_b = \frac{0.8(N1_{60})D_b}{D} \leq q_l \quad (3.25)$$

Where:

$N1_{60}$  = representative SPT blow count near the pile tip corrected for overburden pressure as specified in Article 10.4.6.2.4 (blows/ft),

$D$  = pile width or diameter (ft),

$D_b$  = depth of penetration in bearing strata (ft),

$q_l$  = limiting tip resistance taken as eight times the value of  $N1_{60}$  for sands and six times the value of  $N1_{60}$  for nonplastic silt (ksf).

The nominal side resistance of piles in cohesionless soils for the Meyerhof method, in ksf, shall be taken as:

For driven displacement piles:

$$q_s = \frac{\overline{N1_{60}}}{25} \quad (3.26)$$

For non-displacement piles, e.g., steel H-piles:

$$q_s = \frac{\overline{N1_{60}}}{50} \quad (3.27)$$

Where:

$q_s$  = unit side resistance for driven piles (ksf),

$\overline{N1_{60}}$  = average corrected SPT-blow count along the pile side (blows/ft).

Consideration should be given to the potential for change in the nominal axial pile resistance after the end of pile driving. The effect of soil relaxation or setup should be considered in the determination of nominal axial pile resistance for soils that are likely to be subject to phenomena like relaxation, scour and groundwater effects and buoyancy.

### **Strength limit evaluation**

Determination of the nominal bearing (compression) resistance needed to meet strength limit state requirements, using factored loads and factored resistance values. Select appropriate factors, the loads and resistance values are factored as specified in 3.4.1 AASHTO LRFD Bridge Design Specifications (6<sup>th</sup> Ed.) and 10.5.5.2.3-1 California amendment, respectively, for this determination. The summation of factored axial loads may not exceed the summation of factored axial resistances. Iterating from steps necessary, adjust the trial design to satisfy the following LRFD requirement for each strength limit state:



$$\sum \gamma_i Q_{ni} \leq \phi R_n \quad (3.28)$$

Where:

$\gamma_i$  = load factor applicable to a specific load component,

$Q_{ni}$  = a specific nominal load component,

$\sum \gamma_i Q_{ni}$  = the total factored load for the load group applicable to the limit state being considered,

$\phi$  = the resistance factor,

$R_n$  = the nominal resistance.

### **Service limit evaluation**

Conduct load-deformation analysis for each trial design and iterate as necessary to satisfy the LRFD requirement for each service limit state. Service limit state evaluation for axial loading requires analysis of side and bases resistances that are mobilized at axial displacement corresponding to the tolerable deformation established for the structure being designed. Service limit state design of driven pile foundations includes the evaluation of settlement due to static loads, horizontal movements, overall stability, and total scour at the design load.

The step by step procedure presented above is implemented through an iterative process. Trial designs are evaluated for LRFD strength limit states and service limit states. If a trial design fails to satisfy one or more of the required limit states, or if the trial design greatly exceeds all of the required limit states and a more economical design is possible, dimensions of the trial design are modified and re-analyzed. This process is continued until all applicable limit states for axial compression satisfy the LRFD criterion.

### **Measured Pile Resistance from Load Test**

Compression piles tests

In the compression load test, the corresponding load applied on the pile when the deflection equals to 1 inch is considered as measured bearing capacity.

Uplift pile test

$$Q_m = Q_t - W + \text{suction} \quad (3.29)$$

Where:

$Q_t$  = Measured load in the uplift load test when the deflection equals to 1 inch,

$W$  = Pile weight.

## **Design Practice of Drilled Shaft**

A drilled shaft is a deep foundation unit that is entirely or partially embedded in the ground. It's constructed by placing fresh concrete in a drilled hole with or without steel reinforcement. Drilled shaft also known as cast-in-drilled hole (CIDH) can be used in cases where driven piles are not suitable. It can be used when large vertical or lateral resistance is required or to resolve constructability issues.

At the beginning of drilled shaft foundation design, preliminary work for the structures, Preliminary Geotechnical Report (SPGR), and Preliminary Foundation Report (PFR) are performed. Geotechnical Services (GS) of Materials Engineering and Testing Services and Geotechnical Services (METS-GS) provides foundation recommendation based on the factored design loads provided by structure designers (SD). The foundation recommendation includes site seismicity, factored downdrag loads, pile tip elevations, construction recommendations and the log of test borings. SD and Geotechnical Designer (GD) specify pile type, size and construction requirements. SD ensures that the intent of the geotechnical and structural design is preserved in the contract plans and specifications. Any information excluded from the foundation recommendation should be included in the Project Engineer's memo to Specifications Engineer at the submittal of Plans and Quantities (P&Q). When draft specifications are available, review of plans and specifications by GS completes the Plans, Specs and Estimates (PS&E) process, allowing GS to verify concurrence between the plans and Foundation Recommendations (Memo to Designers 3-1, June 2014).

Drilled Shaft design practice of Caltrans is based on the latest adopted AASHTO LRFD Bridge Design Specifications (6<sup>th</sup> Ed.) and the corresponding California Amendments. AASHTO LRFD Design Specifications (6<sup>th</sup> Ed.) mostly follow the design procedure specified in 'Drilled Shafts: Construction procedures and Design Methods (O'Neill and Reese, 1999)'. The SD provides information and controls factored loads for each limit state so that the GD can provide a design to meet or exceed the load demands. The GD also determines the required nominal resistance and resistance factors for the applicable limit states. The drilled shaft design practice is reviewed in the following sections.

### **Subsoil Investigation**

The subsoil investigation at the location of the construction site is crucial for any type of foundation, as the design procedure of drilled shaft is decided based on the type of soil. All relevant data for the investigation shall be collected and provided by Structure Design (SD) or gathered by the geo-professional. SD must provide Draft general plan (GP), Draft foundation plan (FP), and foundation report (FR) request.

A group of borings is acquired to perform different soil tests to determine the subsoil condition such as number of soil layers, bearing capacity, shear strength etc. Number and depth of boring should be sufficient to investigate the geological profile. Borings should coincide with the proposed pile locations.

According to AASHTO LRFD Bridge Design Specifications (2012, 6 ed.), the depth of boring should be extended beyond the depth of drilled shaft by a minimum of 20 ft. or a minimum of two times of maximum pile group dimension, whichever is deeper. For drilled shafts supported on or embedded into rock, a minimum of 10 ft. of rock core, or a length of rock core equal to at least three times the shaft diameter for isolated shafts or two times the maximum shaft group dimension, whichever is greater, shall be extended below the depth of the tip to determine the physical characteristics of rock.

Design of drilled shafts requires the following information:

- Subsurface profile (Soil, ground water etc.)
- Shear strength parameters
- Compressibility parameters
- Chemical composition of soil
- Unit weight
- Permeability of water bearing soils
- Presence of artesian conditions
- Presence of swell soils
- Geologic mapping including orientation and characteristics of rock discontinuities
- Degradation of soft rock in presence of water and air

In situ tests are performed to determine the strength parameters of soil at the location of the foundation. ASTM and AASHTO standards must be followed to perform in situ tests. SPT, CPT, shaft load test, vane shear test, PMT, dilatometer, rock coring etc. can be performed for the field exploration purpose (Draft Deep Foundation Manual).

Performing lab tests is also necessary to classify soil and estimate their engineering properties. Lab tests may include unit weight, particle size analysis, unconfined compression test, resistivity tests, Atterberg limit test, swell potential test, point load strength test, 1-D Oedometer test, triaxial test etc. (Draft Deep Foundation Manual).

For drilled shaft design purpose, soil is classified according to O'Neil and Reese (1999) and Brown et al. (2010). Design approach of drilled shaft varies with each of these soil types.

a) Cohesive Soil: Clay or plastic silt with  $S_u \leq 0.25 \text{ MPa}$  or roughly 2.5 tsf can be termed as cohesive soil (O'Neil and Reese 1999; Brown et al. 2010).

b) Granular Soil: Sand, gravel or non-plastic silt with average  $N \leq 50$  blows/feet within each layer is termed as granular soil as specified in O'Neil and Reese (1999). Brown et al. indicates that all gravels and sand with less than 5 percent fines, gravels and sands with silty fines and non-plastic silts are granular or cohesionless soil.

c) Intermediate Geomaterial (IGM)

Cohesive IGM: In O'Neil and Reese (1999), cohesive IGM is defined as clay with  $0.25 \text{ MPa} \leq S_u \leq 2.5 \text{ MPa}$ . Brown et al. (2010) defines cohesive IGM as materials that exhibit unconfined compressive strengths in the range of 0.48 MPa (10 ksf) to 4.78 MPa (100 ksf).

d) Cohesionless IGM: O'Neil and Reese (1999) define cohesionless IGM as granular soil with average  $N > 50$  blows/feet. In Brown et al. (2010), cohesionless IGMs are grouped under cohesionless soils.

e) Rock: Cemented geomaterial with  $S_u \geq 2.5 \text{ MPa}$  can be termed as rock according to O'Neil and Reese. Brown et al. exhibits that cohesive, cemented geomaterials are identified as rock on the basis of geologic origin.

### **Construction Method**

Drilled shafts can be constructed following two methods. The first is dry method and the second is wet method. Inspection tubes are required in case of construction by wet method. Dry method is followed when there's no standing groundwater in the drilled hole although the bottom of the hole may be damp or wet. This method may still be used if a small amount of groundwater is present in the hole (Draft Deep Foundation Manual).

Wet method is used if standing groundwater is present in the drilled hole. This operation uses drilling slurry to control the groundwater and to maintain the stability of the drilled hole (Draft Deep Foundation Manual). When considering CIDH piles in wet conditions, caution should be exercised in the following cases: 1) lack of redundancy in single column bents; 2) soft cohesive soils, loose sands, or boulders at the support location (constructability); and 3) presence of high ground water pressure that will make it difficult to establish a differential water pressure head for slurry construction. Driven piles should be considered for these situations. If driven piles cannot be used, the designer should anticipate the possibility of defective, non-repairable piles (Memo to Designers 3-1, June 2014).

### **Drilled Shaft Dimension**

A diameter and embedment length of the drilled shaft is estimated based on the soil investigation information as well as the load of the superstructure calculated from the preliminary structural design. The diameter of the drilled shaft also depends on the column size, placement of column and drilled shaft and the availability of diameter sizes.

If groundwater is present at the location of the foundation, Gamma-Gamma Logging (GGL) and Cross Sonic Logging (CSL) tests may be required and PVC inspection tubes have to be installed for that purpose. The diameter of the drilled shaft should be at least 24 inches. The length and diameter of the drilled shaft should have a ratio of 30 or less to ensure quality and constructability (Memo to Designer 3-1).

Caltrans uses two types of drilled shafts based on the diameter.

#### **a) Standard Plan CIDH**

Standard plan piles consist of piles with diameters 16 in and 24 in. These piles are generally designed for 90, 140 and 200 kips of axial load in compression for the service state (Deep Foundation Manual).

#### **b) Non-Standard Plan**

All piles with diameter other than 16 and 24 in are non-standard plan piles. The diameter of non-standard drilled shafts used by Caltrans is 30 to 144 in or larger.

### **Resistance of Drilled Shaft**

The presumed diameter and length of the drilled shaft is assessed based on the nominal axial resistance of the drilled shaft. The nominal axial resistance is comprised of side and tip resistance and both side and tip resistance is determined based on the type of soil layer at the location of the drilled shaft.

Both tip and side resistances for drilled shafts are developed in response to vertical displacement. The maximum or peak resistance values are seldom cumulative because they are not likely to occur at the same displacement. Since side resistance is usually mobilized at small displacement, drilled shafts rely on this component of resistance for most of their capacity, in particular under Service Limit State load. Displacement compatibility must be considered when adding tip resistance and side resistance. GD recommendations may discard or include only a fraction of the tip resistance, especially in wet method construction conditions, unless there is factual evidence that there are no “soft” areas.

### c) Resistance in Cohesive Soil

According to O'Neil and Reese, (1999), cohesive soil can be defined as clay or plastic silt with  $S_u$  value less than 0.25 MPa or roughly 2.5 tsf. Methods to determine side and tip resistance of drilled shaft are discussed in the following section.

#### i. Side Resistance in Cohesive Soil

$\alpha$ -method is used to determine the side resistance for cohesive soil in Caltrans for both standard and non-standard drilled shafts. O'Neil and Reese (1999) and Brown et al. (2010) show the same procedure for measuring the side resistance in cohesive soil. Some sections of the drilled shaft are excluded from the consideration in case of side friction. Such as, at least the top 5 ft of drilled shaft doesn't contribute in the side resistance. According to O'Neil and Reese (1999), A bottom length equal to the shaft diameter is excluded in case of straight shafts. O'Neil and Reese (1999) also indicates that periphery of the belled end as well as a length above the belled end equal to the drilled shaft is kept out of the side resistance calculation.

The unit side resistance for a single drilled shaft in cohesive soil can be calculated as

$$q_s = \alpha S_u \quad (3.30)$$

Where:

$q_s$  = Unit side resistance of drilled shaft,

$S_u$  = Undrained shear strength,

$\alpha$  = A dimensionless correlation coefficient.

$\alpha$  can be determined through the following procedure

$\alpha = 0$ ; Between ground surface and 5 ft. depth.

$$\alpha = 0.55 \text{ for } \frac{S_u}{P_a} \leq 1.5 \quad (3.31)$$

$$\alpha = 0.55 - 0.1 \left( \frac{S_u}{P_a} - 1.5 \right) \text{ for } 1.5 \leq \frac{S_u}{P_a} \leq 2.5 \quad (3.32)$$

#### ii. Tip Resistance in Cohesive Soil

Caltrans doesn't consider the tip resistance of standard drilled shaft for tip in cohesive soil. Tip resistance is used for non-standard drilled shafts if the bottom of the hole is cleaned out.

California Amendment specifies a different approach for tip resistance in cohesive soil than AASHTO LRFD Bridge Design Specifications (6<sup>th</sup> Ed.). According to California Amendment-

If  $Z \geq 3D$ ;

$$q_p = N_c S_u \quad (3.33)$$

If  $Z < 3D$ ;

$$q_p = (2/3)[1 + (1/6)(D/B)]N_c S_u \quad (3.34)$$

$N_c$  can be determined using the following approach-

$$N_c = 9 \text{ for } S_u \geq 2 \text{ ksf} \quad (3.35)$$

$$N_c = (4/3)[\ln(I_r) + 1] \text{ for } S_u < 2 \text{ ksf} \quad (3.36)$$

Where:

$Z$  = Depth of drilled shaft base (ft),

$D$  = Diameter of drilled shaft (ft),

$q_p$  = Nominal unit tip resistance (ksf),

$S_u$  = Undrained shear strength (ksf),

$N_c$  = Bearing capacity factor,

$I_r$  = Rigidity index =  $(E_s/3S_u)$ ,

$E_s$  = Young's modulus of soil for undrained loading (ksf).

For tip resistance in cohesive soil, AASHTO LRFD Bridge Design Specifications follow O'Neil and Reese (1999) which is the same as in Brown et al. (2010).

#### **d) Resistance in Cohesionless or Granular Soil**

Cohesionless soil or granular soil is comprised of sand, gravel or non-plastic silt with  $N$  (average within layer) is less than or equal to  $50B$  or  $0.3$  m (50 blows/ft) according to O'Neil and Reese, (1999). Side and tip resistance of drilled shaft in cohesionless soil determination approach is described in the following section.

##### **i. Side Resistance in Cohesionless Soil**

$\beta$ -method is used to determine the side resistance in cohesionless or granular soil for both standard and non-standard drilled shaft. Nominal unit side resistance of drilled shaft in cohesionless soil can be calculated as:

$$q_s = \beta \sigma'_v \leq 4.0 \text{ for } 0.25 \leq \beta \leq 1.2 \quad (3.37)$$

As specified in O'Neil and Reese (1999),  $\beta$  is different for sandy soil and gravel. For sandy soils,

$$\beta = 1.5 - 0.135\sqrt{z} \text{ for } N_{60} \geq 15 \quad (3.38)$$

$$\beta = \frac{N_{60}}{15} (1.5 - 0.135\sqrt{z}) \text{ for } N_{60} < 15 \quad (3.39)$$

For Gravelly sand and gravel,

$$\beta = 2.0 - 0.06 (z)^{0.75} \quad (3.40)$$

Where:

$q_s$  = Nominal unit side resistance of drilled shaft,

$\beta$  = Side resistance coefficient,

$z$  = Thickness of the soil layer,

$\sigma'_v$  = Vertical effective stress at the middle depth of soil layer.

O'Neill and Reese (1999) recommends allowing  $\beta$  to increase to 1.8 in gravels and gravelly sands, however, it's also recommended to limit the unit side resistance to 4.0 ksf in all soils.

Brown et al. (2010) states a different approach to evaluate  $\beta$ .

$$\beta = (1 - \sin\phi') \left( \frac{\sigma'_p}{\sigma'_v} \right) \tan\phi' \leq K_p \tan\phi' \quad (3.41)$$

$$\phi' = 27.5 + 9.2 \log[(N_1)_{60}] \quad (3.42)$$

$$(N_1)_{60} = N_{60} \left( \frac{P_a}{\sigma'_v} \right)^n \quad (3.43)$$

Where:

$\sigma'_p$  = Effective vertical preconsolidation stress,

$\phi'$  = Effective friction angle,

$N_{60}$  = N value corrected to 60 percent efficiency,

$n$  = Exponent typically equal to 1 in clays and 0.5 in sandy soils.

The value of  $\beta$  at shallow depths should be limited to the value corresponding to a depth of 7.5 ft.

$$\frac{\sigma'_p}{P_a} = 0.47(N_{60})^m \quad (3.44)$$

Where:



$m = 0.6$  for clean quartzitic sands and  $0.8$  for silty sands to sandy silts,  
 $P_a =$  Atmospheric pressure.

In Brown et al.'s method,  $\beta$  accounts for soil strength and in-situ state of stress. In cases where the interface friction angle ( $\delta$ ) between concrete and soil is known, the above equations are changed as follows:

$$f_{sz} = K\sigma'_z \tan\delta \quad (3.45)$$

$$Q_s = \int_0^L K \sigma'_z \tan\delta dA \quad (3.46)$$

Where,  $K$  is the parameter that combines the lateral pressure coefficient and a correlation factor.

## ii. Tip Resistance in Cohesionless Soil

Like cohesive soil, tip resistance is considered only for non-standard drilled shafts. Tip resistance of drilled shaft in cohesionless soil can be calculated as,

$$q_p = 1.2 N_{60} \text{ for } N_{60} \leq 50 \text{ blows/ft} \quad (3.47)$$

Where:

$q_p =$  Nominal unit tip resistance of drilled shaft (ksf),

$N_{60} =$  SPT blow count corrected to 60 percent energy efficiency.

When  $N_{60}$  is greater than 50 blows/ft, the O'Neill and Reese method recommends that the unit base resistance should be calculated using the method for cohesionless intermediate geomaterial (IGM); while in Brown et al.'s method, the unit base resistance in cohesionless soil is limited to the upper-bound value of 30 tsf with N-values exceeding 50.

## e) Resistance in Intermediate Geomaterial

Resistance of drilled shaft in intermediate geomaterial is different for cohesive IGM and cohesionless IGM. Design approach for both cohesive IGM and cohesionless IGM follows O'Neil and Reese (1999), which is going to be discussed here.

### i. Side Resistance in Cohesive IGM

Roughness of the borehole wall plays crucial role in case of side resistance in cohesive IGM. The borehole is considered smooth unless it's roughened artificially. The unit side resistance of drilled shaft in cohesive IGM with smooth borehole wall can be calculated as-

$$q_s = \alpha\phi q_u \quad (3.48)$$

$\alpha$  can be determined from Figure 3-13.

Where:

$E_m$  = Young's Modulus of the IGM mass,

$q_u$  = Unconfined strength of the intact IGM,

$w_t$  = Settlement of the socket at which  $\alpha$  is developed,

$\Phi_{rc}$  = Angle of interface friction.

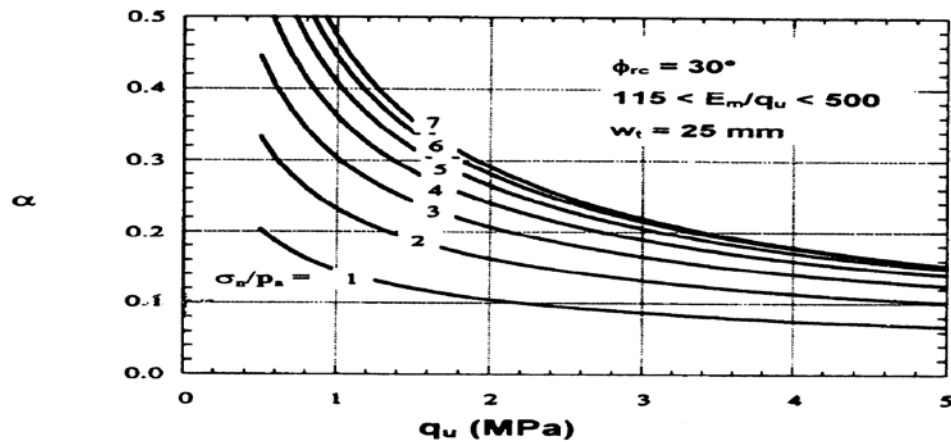


Figure 3-15. Factor  $\alpha$  for cohesive IGM (O'Neil and Reese, 1999)

$\sigma_n$  = Pressure imparted by fluid concrete at the middle of layer =  $0.65\gamma_c z_i$

$\gamma_c$  = Unit weight of concrete at or above 7 in

$z_i$  = Depth below cutoff elevation

If  $\Phi_{rc}$  is different from  $30^\circ$  then it can be calculated using the following equation-

$$\alpha = [\alpha(\text{Figure 3 - 13})] \cdot \left[ \frac{\tan\Phi_{rc}}{\tan 30^\circ} \right] \quad (3.49)$$

$\phi$  is a joint effect factor and it can be determined from Table 3-5.

Table 3-5. Factors  $\phi$  for cohesive IGM's. (O'Neil and Reese, 1999)

RQD (percent)	$\Phi$	
	Closed joints	Open or gouge-filled joints
100	1.00	0.85
70	0.85	0.55
50	0.60	0.55
30	0.50	0.50
20	0.45	0.45

If RQD is less than 20% for a cohesive IGM layer, load test is required to determine unit nominal side resistance.

The unit side resistance of drilled shaft in cohesive IGM with rough borehole wall can be calculated as:

$$q_s = \frac{q_u}{2} \quad (3.50)$$

Generally, the average unconfined strength ( $q_u$ ) within the layer is used to determine the unit side resistance but the median value is used in case of widely varying  $q_u$ .

### ii. Tip Resistance in Cohesive IGM

Tip resistance of drilled shaft in cohesive IGM is similar to tip resistance in rock according to O'Neil and Reese (1999). CALTRAN also follows the same approach to determine the tip resistance.

### iii. Side Resistance in Cohesionless IGM

Unit side resistance of drilled shaft in cohesionless IGM can be determined as specified in O'Neil and Reese as:

$$q_s = \sigma'_{vi} K_{oi} \tan \varphi'_i \quad (3.51)$$

Where:

$\sigma'_{vi}$  = Vertical effective stress at the middle of layer i,

$K_{oi}$  = Design value of earth pressure coefficient at rest in layer i,

$\varphi'_i$  = Design value for angle of friction in layer i.

$K_{oi}$  and  $\varphi'_i$  can be determined through field or laboratory tests or they can be estimated using the following equations.

$$\varphi'_i = \tan^{-1} \left[ \left[ \frac{N_{60}}{12.3 + 20.3 \left( \frac{\sigma'_{vi}}{P_a} \right)} \right]^{0.34} \right] \quad (3.52)$$

$$K_{oi} = (1 - \sin \phi'_i) \left[ \frac{0.2P_a N_{60}}{\sigma'_{vi}} \right]^{\sin \phi_i} \quad (3.53)$$

In this case,  $N_{60}$  should be limited to 100 blows/feet.  $\Delta]_i$  should be limited to 9m (30 ft).

#### iv. Tip Resistance in Cohesionless IGM

If the SPT ( $N_{60}$ ) value is more than 50, then that soil is termed as cohesionless IGM according to O'Neil and Reese (1999). Nominal unit tip resistance of cohesionless IGM can be determined as

$$q_p = 0.59 \left[ N_{60} \left( \frac{P_a}{\sigma'_v} \right) \right] \sigma'_v \quad (3.54)$$

Where:

$P_a$  = Atmospheric Pressure (2.116 ksf),

$\sigma'_v$  = Vertical effective stress at the tip.

#### f) Resistance in Rock

AASHTO LRFD Bridge Design Specifications (2012) is followed to estimate the Side and Tip Resistance of a drilled shaft embedded in rock. These semi-empirical methods are based on load test data and site specific correlation between measured resistance and rock core strength.

##### i. Side Resistance in Rock

AASHTO LRFD Bridge Design Specifications (2012) follows O'Neil and Reese (1999) regarding the evaluation of side resistance in rock. Unit Side Resistance of drilled shaft,  $q_s$  (ksf) in rock, as specified in O'Neil and Reese, can be estimated as –

$$q_s = 0.65 \alpha_E P_a \left( \frac{q_u}{P_a} \right)^{0.5} < 7.8 P_a \left( \frac{f'_c}{P_a} \right)^{0.5} \quad (3.55)$$

Where:

$q_u$  = Uniaxial compressive strength of rock (ksf),

$P_a$  = Atmospheric pressure (2.12 ksf),

$\alpha_E$  = Reduction factor to account for jointing in rock as shown Table 3-7,

$f'_c$  = Compressive strength of concrete (ksi).

Table 3-6. Estimation of  $\alpha_E$  (O’Neil and Reese,1999)

$E_m/E_i$	$\alpha_E$
1.00	1.00
0.50	0.80
0.30	0.70
0.10	0.55
0.05	0.45

The ratio of rock mass modulus to intact rock modulus ( $E_m/E_i$ ) can be estimated from the following table.

Table 3-7. Estimation of  $E_m/E_i$  (O’Neil and Reese,1999)

RQD (Percent)	$E_m/E_i$	
	Closed Joints	Open Joints
100	1.00	0.60
70	0.70	0.10
50	0.15	0.10
20	0.05	0.05

Brown et al. (2010) follows a slightly different approach for measurement of side resistance in rock. It suggests the following equation

$$q_s = C P_a \left( \frac{q_u}{P_a} \right)^{0.5} \quad (3.56)$$

Here, C is a regression coefficient that is used to analyze load test results. Considering the most recent researches on side resistance in rock, Brown et al. recommends a C value of 1.0 for routine rock sockets. For rock that cannot be drilled without some artificial support, the reduction factors given in Table 3-8 are recommended for application to the resistance. As artificial roughening of rock sockets through the use of grooving tools or other measures can increase side resistance, a C value of 1.9 has been suggested.

#### ii. Tip Resistance in Rock

Estimation approach of the tip resistance of drilled shaft in rock is accumulated from O’Neil and Reese (1999). If the rock below the tip of the drilled shaft to a depth of 2B is intact or tightly jointed and the depth of the borehole or socket is more than 1.5B, then unit tip resistance,  $q_p$  (ksf) can be determined from,

$$q_p = 2.5q_u \quad (3.57)$$

If the rock below the tip of the drilled shaft to a depth of 2B is jointed and the joints are randomly oriented, then unit tip resistance  $q_p$  (ksf) can be estimated as –

$$q_p = \left[ \sqrt{s} + \sqrt{(m\sqrt{s} + s)} \right] q_u \quad (3.58)$$

Here,

$q_u$  = Unconfined compressive strength of rock (ksf),

s, m = Fractured rock mass parameters from Table 3-8.

Table 3-8. Approximate relationship between rock-mass quality and material constants used in defining nonlinear strength (AASHTO LRFD Bridge Design Specifications, 6th Ed.)

Rock Quality	Constants	Rock Type				
		A	B	C	D	E
Intact Rock Samples Laboratory size specimens free from discontinuities RMR=100	m	7.00	10.00	15.00	17.00	25.00
	s	1.00	1.00	1.00	1.00	1.00
Very Good Quality Rock Mass Tightly interlocked rock with unweathered joints at 3-10 ft RMR=85	m	2.40	3.43	5.14	5.82	8.567
	s	0.082	0.082	0.082	0.082	0.082
Good Quality Rock Mass Fresh to slightly weathered rock with joints at 3-10 ft RMR=65	m	0.575	0.821	1.231	1.395	2.052
	s	0.00293	0.00293	0.00293	0.00293	0.00293
Fair Quality Rock Mass Several moderately weathered joints at 1-3 ft RMR=44	m	0.128	0.183	0.275	0.311	0.458
	s	0.00009	0.00009	0.00009	0.00009	0.00009
Poor Quality Rock Mass Numerous weathered joints at 2-12 in RMR=23	m	0.029	0.041	0.061	0.069	0.102
	s	$3 \times 10^{-6}$	$3 \times 10^{-6}$	$3 \times 10^{-6}$	$3 \times 10^{-6}$	$3 \times 10^{-6}$
Very Poor Quality Rock Mass Numerous heavily weathered joints in < 2 in RMR =3	m	0.007	0.010	0.015	0.017	0.025
	s	$1 \times 10^{-7}$	$1 \times 10^{-7}$	$1 \times 10^{-7}$	$1 \times 10^{-7}$	$1 \times 10^{-7}$

Different types of rocks used in Table-3-8 is defined below (AASHTO LRFD Bridge Design Specifications, 6<sup>th</sup> ed.).

A = Carbonate rocks with well-developed crystal cleavage— dolomite, limestone and marble.

B = Lithified argillaceous rocks—mudstone, siltstone, shale and slate (normal to cleavage).

C = Arenaceous rocks with strong crystals and poorly developed crystal cleavage sandstone and quartzite.

D = Fine grained polyminerallic igneous crystalline rocks— andesite, dolerite, diabase and rhyolite.

E = Coarse grained polyminerallic igneous & metamorphic crystalline rocks—amphibolite, gabbro gneiss, granite, norite, quartz-diorite.

RMR is Rock Mass Rating which is a geomechanical classification system for rocks. It specifies the quality of rocks. Table 3-10 show variation of rock quality with different RMR values.

Table 3-9. Geomechanics Rock Mass Classes Determined from Total Ratings (AASHTO Bridge Design Specifications, 6th Ed.)

<b>RMR</b>	<b>Rock Quality</b>
100-81	Very Good Rock
80-61	Good Rock
60-41	Fair Rock
40-21	Poor rock
<20	Very Poor Rock

Brown et al. (2010) also contains an approach to evaluate the tip resistance of drilled shaft in rock. According to Brown et al.

$$q_p = N_{cr}^* q_u \quad (3.59)$$

Here,  $N_{cr}^*$  is an empirical bearing capacity for rock. The following can be used in case of availability of data on spacing and condition of discontinuities in rock beneath the tip

$$q_p = 3q_u K_{sp} d \quad (3.60)$$

In which,

$$K_{sp} = \frac{3 + \frac{S_v}{B}}{10 \sqrt{1 + 300 \frac{t_d}{S_v}}} \quad (3.61)$$

$$d = 1 + 0.4 \frac{D_s}{B} \leq 3.4 \quad (3.62)$$

Where:

$q_u$  = Uniaxial compressive strength of the bearing rock,

$S_v$  = Vertical spacing between discontinuities,

$t_d$  = Aperture of discontinuities,

$B$  = Socket diameter,

$D_s$  = Depth of socket embedment.

In this formula, the quantity  $3K_{sp}d$  is equivalent to the base resistance factor  $N_{cr}^*$ . This method is applicable for  $N_{cr}^*$  values between a range of 0.4 and 5.1. Load testing is recommended to verify tip resistance for cases where this criterion does not meet.

### Nominal Axial Resistance

After estimating both side and tip resistance of drilled shaft, the nominal axial bearing resistance can be determined. The factored nominal bearing resistance ( $R_R$ ) can be calculated as (AASHTO LRFD Bridge Design Specifications, 6<sup>th</sup> ED.)

$$R_R = \phi R_n = \phi_{qp} R_p + \phi_{qs} R_s \quad (3.63)$$

$$R_p = q_p A_p \quad (3.64)$$

$$R_s = q_s A_s \quad (3.65)$$

Where:

$R_n$  = Nominal bearing resistance of drilled shaft,

$R_p$  = Drilled shaft tip resistance (kips),

$R_s$  = Drilled shaft side resistance (kips),

$\phi_{qp}$  = Resistance factor for tip resistance of drilled shaft,

$\phi_{qs}$  = Resistance factor for side resistance of drilled shaft,

$q_p$  = Unit tip resistance of drilled shaft (ksf),

$q_s$  = Unit side resistance of drilled shaft (ksf),

$A_p$  = Area of drilled shaft tip (ft<sup>2</sup>),

$A_s$  = Surface area of drilled shaft side (ft<sup>2</sup>).



Caltrans doesn't exactly follow the approach to get the resistance factors specified in AASHTO LRFD Bridge Design Specifications (6<sup>th</sup> Ed.). Caltrans Amendment to AASHTO LRFD Bridge Design Specifications (6<sup>th</sup> Ed.) contains a table for the resistance factors to be used to get Nominal Resistance Factors.

Table 3-10. Geotechnical Resistance Factors for Drilled Shafts (California Amendments to AASHTO LRFD Bridge Design Specifications)

Nominal Resistance	Resistance Determination Methods/Conditions	Resistance Factors	
Axial Compression or Tension or Uplift	All Soils Rock and IGM All Calculation Methods	$\phi_{stat}; \phi_{up}; \phi_{bl};$ $\phi_{ug}; \phi_{load};$ $\phi_{upload}; \phi_{qs}$	0.70
Axial Compression	All Soils Rock and IGM All Calculation Methods	$\phi_{qp}$	0.50
Lateral Geotechnical Resistance	All Soils Rock and IGM All Calculation Methods		1.00

### Pile Load Test

Pile load test is not required for standard drilled shafts. It's also not required for non-standard drilled shafts unless there's unusual site condition. It's also recommended if the diameter is 4 ft or more.

### Settlement of Drilled Shaft

After the assessment of diameter and length of the drilled shaft against axial nominal resistance, it is checked against settlement. In general, the total permissible settlement under the Service-I Limit State should be limited to one inch for multi-span structures with continuous spans or multi-column bents, one inch for single span structures with diaphragm abutments, and two inches for single span structures with seat abutments. Different permissible settlement under service loads may be allowed if a structural analysis verifies that required level of serviceability is met. The SD will provide both total and permanent Service-I Limit State support loads to the GD.

O'Neil and Reese (1999) has provided some curves summarizing the load settlement data for drilled shaft in dimensionless form. These can be used to determine the short term settlement of drilled shaft.

Figure 3-14 shows the settlements at which side resistance is mobilized in cohesive soil. The shaft skin friction is typically fully mobilized at displacement of 0.2 percent to 0.8 percent of the drilled shaft diameter in cohesive soil. Figure 3-15 presents load settlement curves in end bearing in cohesive soil.

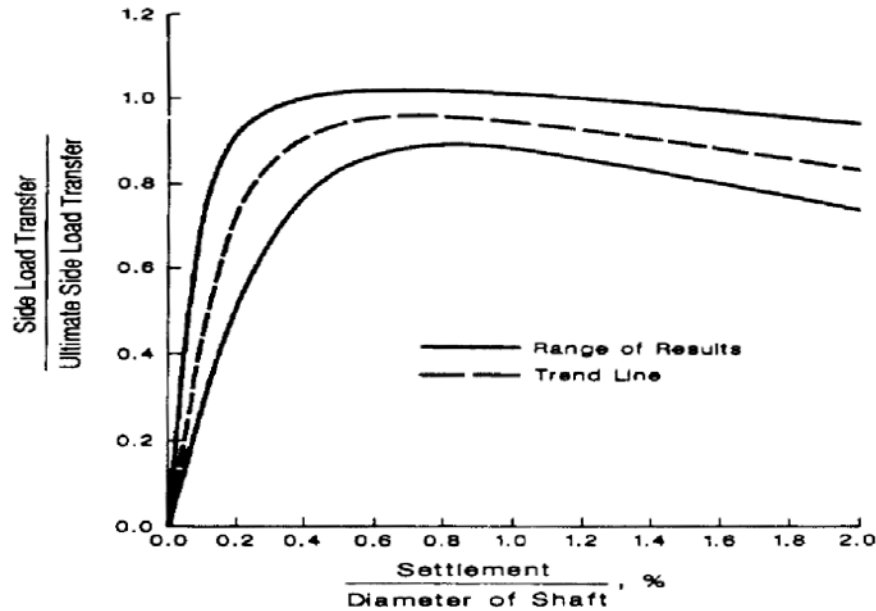


Figure 3-14. Normalized load transfer in side resistance vs settlement in cohesive soil (O'Neil and Reese, 1999)

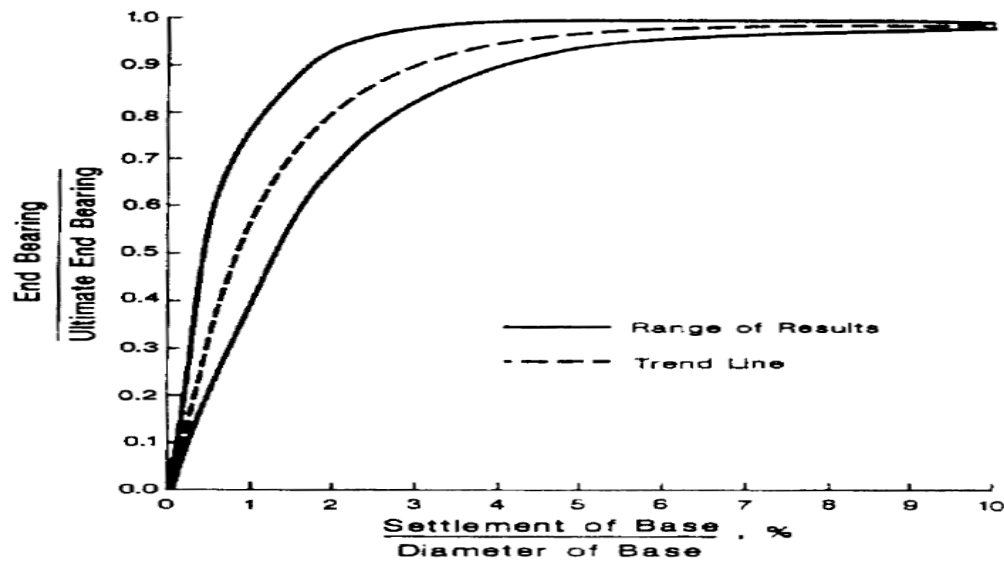


Figure 3-15. Normalized load transfer in end bearing vs settlement in cohesive soil (O'Neil and Reese, 1999)

Figure 3-16 and Figure 3-17 depicts load settlement curves in side bearing and end bearing in cohesionless soil. In cohesionless soil, drilled shaft skin friction is typically fully mobilized at displacement of 0.1 percent to 1.0 percent of the drilled shaft diameter.

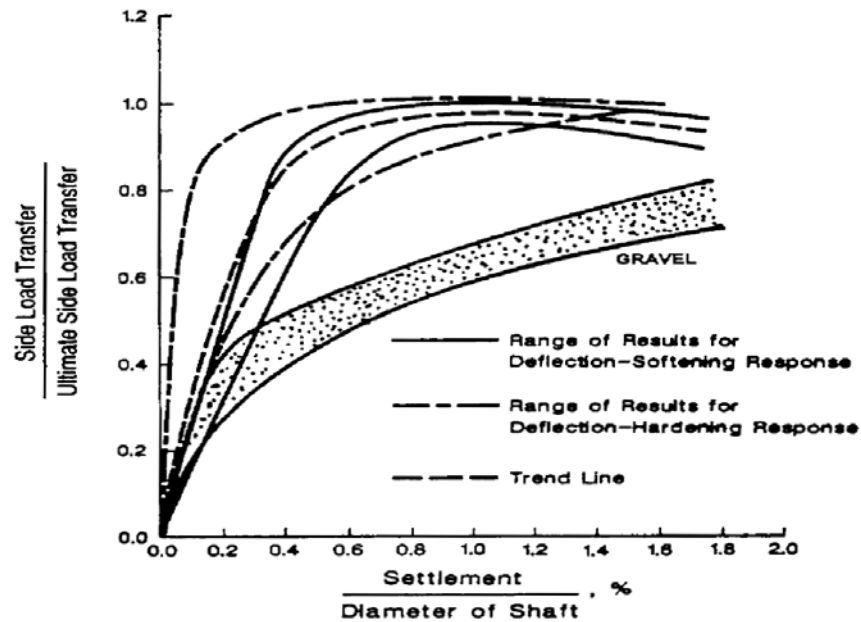


Figure 3-16. Normalized load transfer in side resistance vs settlement in cohesionless soil (O'Neil and Reese, 1999)

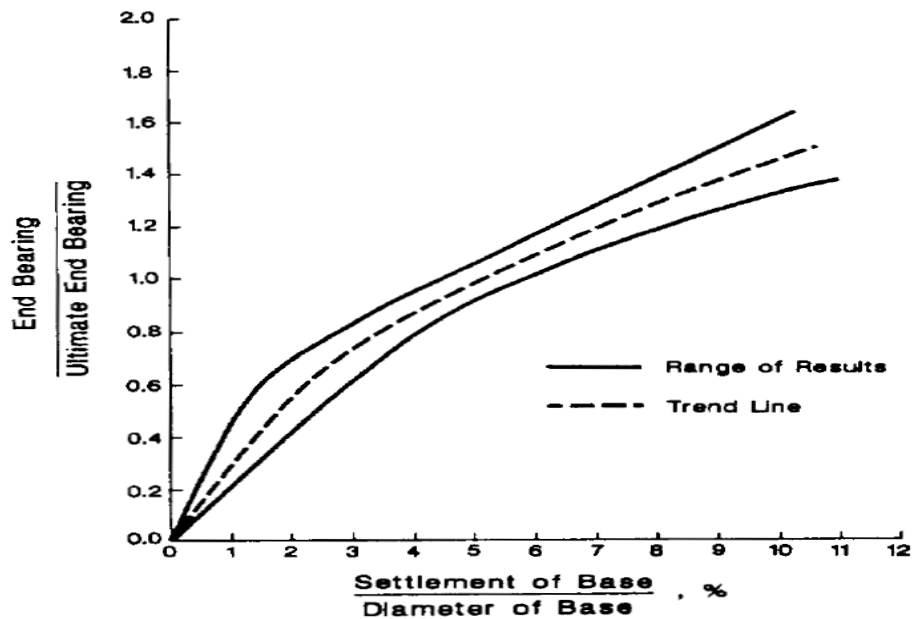


Figure 3-17. Normalized load transfer in end bearing vs settlement in cohesionless soil. (O'Neil and Reese, 1999)

## 4. CHAPTER 4 DEEP FOUNDATION DATABASE AND ANALYSES

As discussed in chapter one, the main objective of this research study is to calibrate the resistance factors for FHWA design methods needed in the LRFD design of driven piles and drilled shafts based on California database and experience. Background information on current driven pile and drilled shaft design methodology is introduced in chapter 3. The collected driven pile and drilled shaft databases are discussed first. Then then the design analyses and load test analyses method are followed.

### Driven Pile Database

Driven pile load tests were collected from Caltrans existing compiled driven pile database as well as some new load tests as the result of this research effort. The final compiled driven pile database includes 127 piles which consist of 23 concrete piles, 90 of pipe piles, 12 H-piles, and 2 CRP piles. Among the 127 piles shown in Table 4-1, 85 piles are tested under compression load and 84 were tested under uplift load. 41 piles were test for both compression and uplift loading. The compiled database includes project background information, soil data, pile materials and properties, and load test data. The methodology of collecting, compiling, and analyzing the driven pile database is presented in this section.

The soil data consist of soil types, depths, water table location, the properties of each layer (unit weight, cohesion, friction angle, etc.). The pile data consist of pile characteristics (pile type and length, stickup, diameter, wall thickness, Young's modulus, sectional area), and pile load test (load test type, applied load, pile failure under testing, etc.). The characteristics of the investigated piles in the database are interpreted based on pile type, load test type, diameter, length, soil classification, and tip soil condition. The summary of these characteristics are shown in Tables 4-1 to 4-6 and Figures 4-1 to Figure 4-7.

Table 4-1 presents the pile type distribution. The major of piles are pipe piles (PP) which includes 23 close-ended and 67 open-ended pipe piles. Eighteen percent of the piles are concrete piles (CP). H-pile (HP) only contributes 9 percent of the total driven pile database.

Table 4-1 Pile type distribution from database

Type		Count	Relative frequency
CP		23	18.11%
PP	Close	23	18.11%
	Open	67	52.76%
HP		12	9.45%
CRP		2	1.57%
<b>Total</b>		<b>127</b>	<b>100%</b>

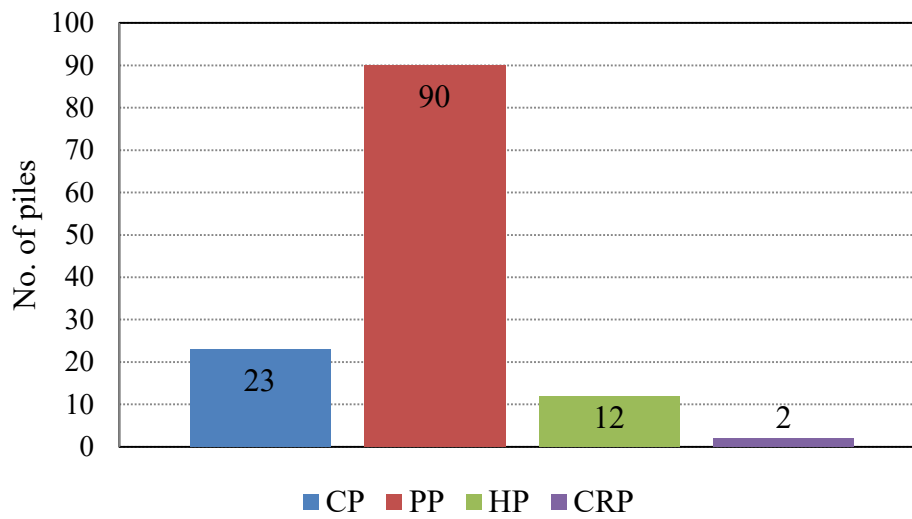


Figure 4-1 Breakdown of pile type and number

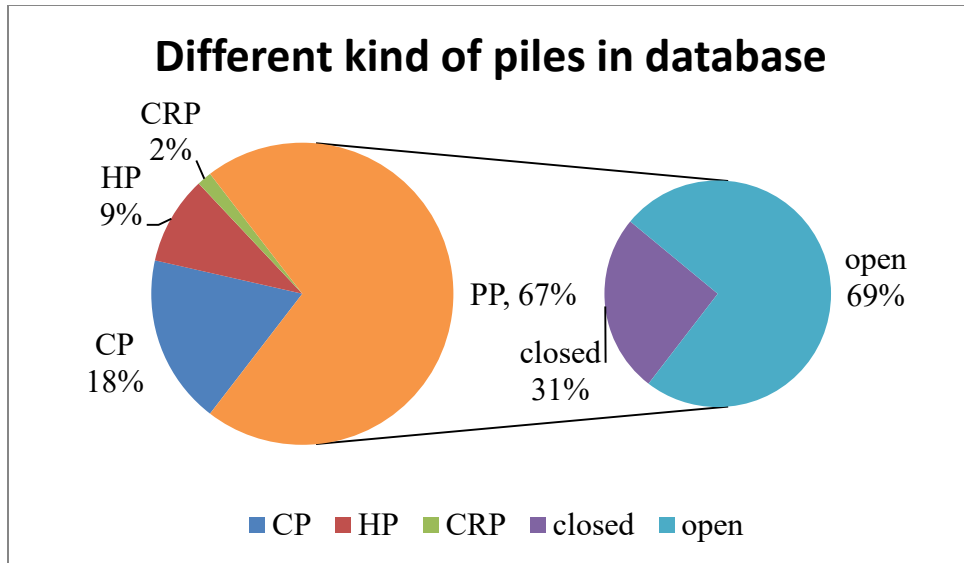


Figure 4-2 Pie chart of pile type distribution

Figure 4-3 presents the loading type of static load tests. There are 72 compression cases and 81 uplift cases in the database. Forty three driven piles were tested for both compression and uplift loading tests. The summary of the load test from the database is present in Figure 4-3 and Table 4-2. Table 4-2 presents the breakdown of loading type for each pile type. It is noticed that concrete pile is less often used in tension as compared with other type of piles.

Table 4-3 and Figure 4-4 present pile diameter distribution. The majority of the piles (88%) have less 30 inch of diameter (width). The average pile diameter is 20 inch. Table 4-4 and Figure 4-5 present pile length distribution. Pile length ranges from 20 ft. to 140 ft. with average length of 66 ft. Sixty four percent of the piles have pile length less than 70 ft. Table 4-5 and Figure 4-6 presents soil type along pile length. 28 cases have sand; 15 cases have clay; 50 cases consist of sand and clay. Table 4-6 and Figure 4-7 presents soil type at pile tip. 69 pies are tipped in clay; 31 piles are tipped in sand. Only 5 piles are tipped in gravel (cobbles).

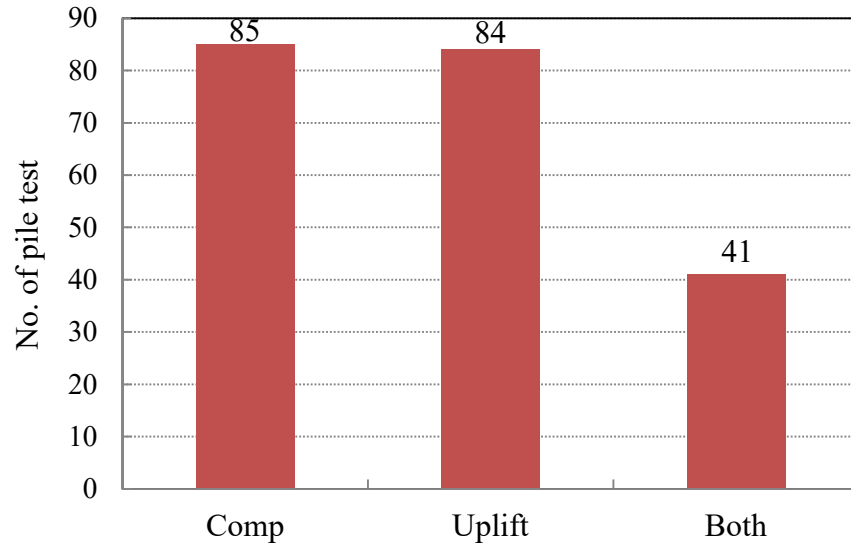


Figure 4-3 Breakdown of total database based on load direction.

Table 4-2 Load test distribution according to pile types

Type	Pile tests			
	Total	Comp	Uplift	Both
CP	23	17	7	1
PP	90	60	67	37
HP	12	6	10	3
CRP	2	2	0	0
<b>Total</b>	<b>127</b>	<b>85</b>	<b>84</b>	<b>41</b>

Table 4-3 Pile diameter distribution in database

Inch	No.	Relative frequency	Density
[0,10]	4	3.15%	0.0031
(10,20]	63	49.61%	0.0496
(20,30]	36	28.35%	0.0283
(30,40]	0	0.0%	0.0000
(40,50]	12	9.45%	0.0094
(50,60]	0	0.0%	0.0000
(60,70]	1	0.79%	0.0008
(70,80]	3	2.36%	0.0024
(80,90]	5	3.94%	0.0039
(90,100]	2	1.57%	0.0016
(100,110]	1	0.79%	0.0008

Total	127	100.0%	0.1000
Mean	26.19		
Standard Deviation	21.50		

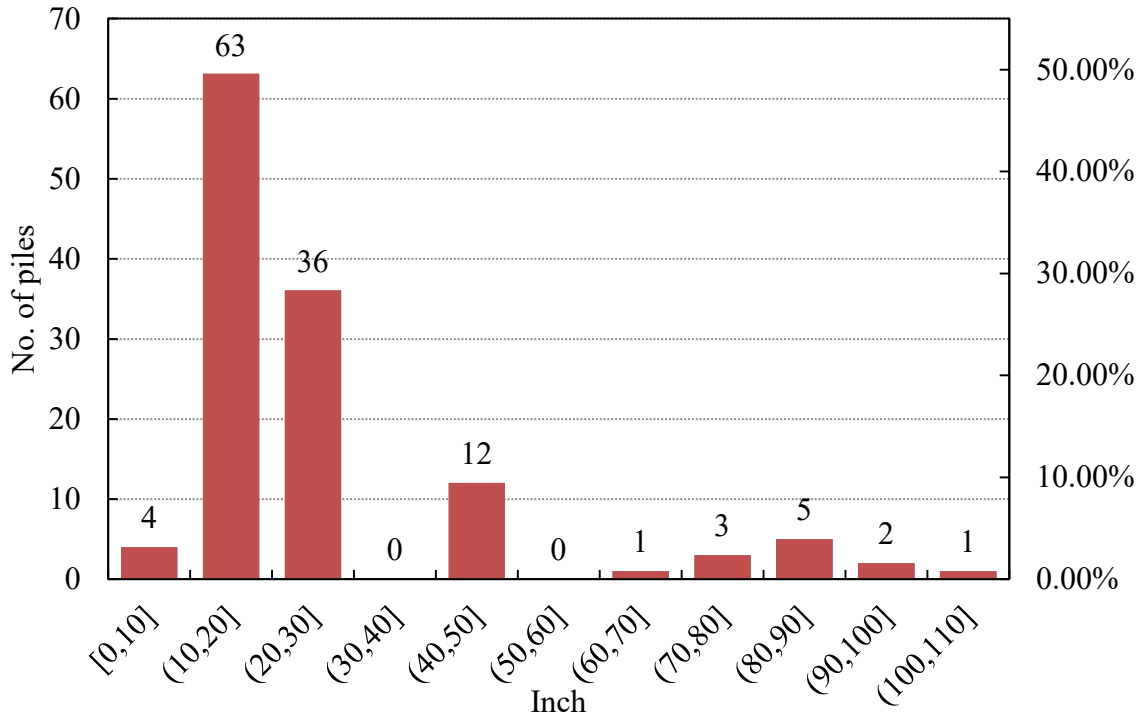


Figure 4-4 Diameter of piles distribution from database

Table 4-4 Pile length distribution

Ft	No.	Relative frequency	Density
[20,30]	3	2.36 %	0.002
(30,40]	12	9.45%	0.009
(40,50]	24	18.90%	0.019
(50,60]	15	11.81%	0.012
(60,70]	21	16.54%	0.017
(70,80]	6	4.72%	0.005
(80,90]	6	4.72%	0.005
(90,100]	10	7.87%	0.008
(100,110]	10	7.87%	0.008
(110,120]	7	5.51%	0.006
(120,130]	3	2.36%	0.002



(130,140]	5	3.94%	0.004
(140,150]	1	0.79%	0.001
(150,160]	0	0.00%	0.000
(160,170]	0	0.00%	0.000
(170,180]	2	1.57%	0.002
(180,190]	1	0.79%	0.001
(190,200]	0	0.00%	0.000
(200,210]	1	0.79%	0.001
Total	127	100.0%	0.100
Mean	74.26		
Standard Deviation	35.41		

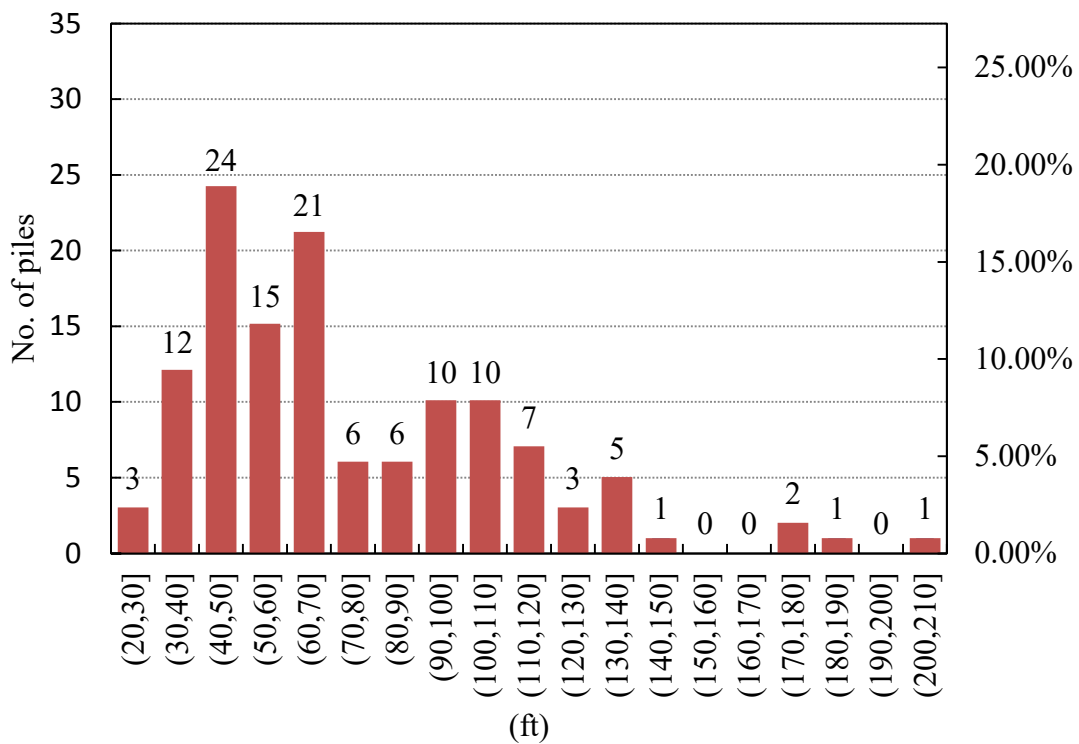


Figure 4-5 Length of piles distribution

Table 4-5 Soil profile distribution from the database

sand	clay	Sand & clay	Sand & clay & gravel (cobble)	Sand & gravel (cobble)	cobbles	other	Total
29	15	56	6	8	2	11	127
22.83 %	11.81%	44.09%	4.72%	6.30%	1.57%	8.66%	100%

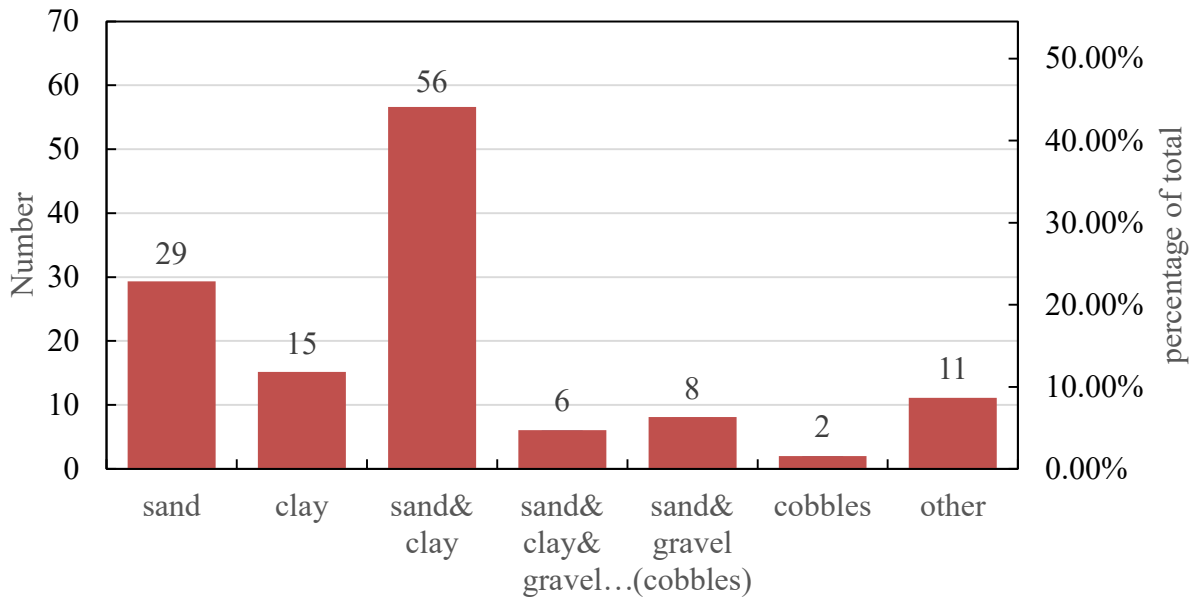


Figure 4-6 Soil profile distribution from database

Table 4-6 Tip soil conditions from database

clay	sand	gravel (cobble)	silt	other	total
72	42	7	2	4	127
56.69%	33.07%	5.51%	1.57%	3.15%	100.00%

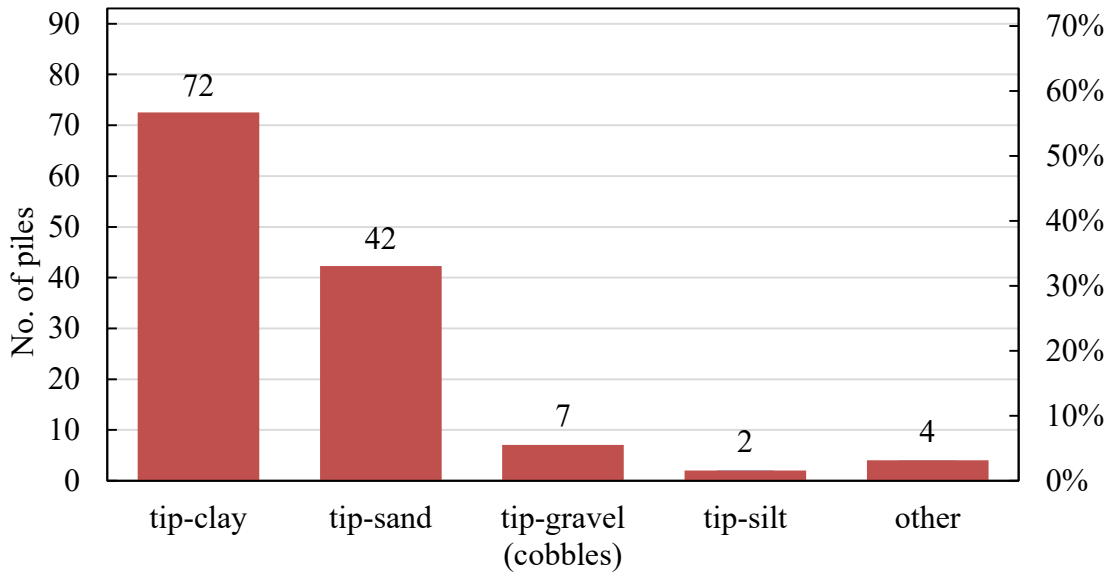


Figure 4-7 Soil type at pile tip

## Analyses of Driven Pile Database

### Data quality factor

In order to quantify the data quality of each collected load test data, a load quality factor scheme shown below is used. The factor considers proximity of boring, elevation control, site variability, driving record, cone data, ground water, sand and clay properties, tip properties, and load test data. The number in parenthesis indicates the score of the factor where 5 is the highest and 1 is the lowest quality. For example, proximity of boring is used to evaluate the distance between the test pile and the nearest boring used for pile analysis. If the distance is less than 30 ft., the data quality factor for proximity of boring is 5. Overall data quality factor (1-5) is decided by reviewing the data quality for each factor and by personal engineering judgement.

**Proximity** of boring: < 30' (5), 30' to 50' (4), 50' to 100' (3), 100' to 200' (2), >200' (1);

**Elevation Control:** boring surveyed, strata lined up (3), boring not surveyed, strata lined up-good to fair confidence(2), boring not surveyed, strata lined up-poor confidence (1);

**Site Variability:** Multiple borings or CPT agree (3), disagree on some small strata (2), disagree on large or key strata (1);

**Driving Record:** Consistent with profile (5), close, but some uncertainty (4), no record available (0).

**Cone data available:** Cone < 50', full depth, data used to verify profile (3), Cone > 50', full depth, data used to verify profile (2), Cone partial depth, data used to partly verify profile (1), cone data not used (0);

**Ground water:** measured (3), guessed with confidence (2), guessed with little confidence (1);

**Sand properties:** SPT energy calibrated with autohammer-all strata have good data (4), based on CPT (2.5-3), energy guessed-safety hammer,-some strata missed (2), hammer type unknown-many strata missed (1);

**Clay properties:**3-inch or larger thin walled sampler-UU test confidence high (multiple tests)-all strata have good data (4), <3-inch thin walled sampler-UU test confidence moderate to high-some strata missed (3), Su/P or CPT based (2.5), UU-test confidence moderate to low-many strata missed (2), pocket penetrometer/minitorvane-estimated (1);

**Tip properties:** tip layer and properties known with confidence (5), guessed but in the ballpark (from nearby borings, CPT, adjacent strata, or driving records)(3), no confidence in assumed properties (0).

Approximate **percentage** capacity due to **sand**; (run analysis below).

**Load test:** No problems, calibrated cell (3), Minor problem, calibrated cell (2), Major problem (1), Unusable (0);

**Failure:** Well defined failure reached (3), Near failure, but not reached (2), extrapolations more than 20% larger than the largest measured load-but beyond elastic (1), still elastic (0);

### **Static Capacity Analysis**

Design Practice of Driven Piles Caltrans foundation design is based on the latest adopted AASHTO LRFD Bridge Design Specifications and the corresponding California Amendments. For small piles (less than or equal to 16 inch),  $\alpha$  - Tomlinson method (clay) and Nordlund method (sand) are used for static design; For large piles (greater than 16 inch), the API method (both sand and clay) is used. Each design method is presented in detail in chapter 3. The nominal resistance is determined as the value determined from the static capacity analysis following the Caltrans design practice.

### **Measured Capacity**

Load settlement curve is available for each collected load test case. Measured capacity was determined from measurement load-settlement curve at 1 inch settlement failure criteria.

### **Drilled Shaft Database**

There are only a few drilled shaft load test data available from Caltrans. Therefore, the research team expanded the drilled shaft data collection to other regions. As results, drilled shaft load test data from Mississippi and Louisiana were selected due to their complete load test and soil data. The Louisiana drilled shaft load tests are obtained from the results of a series of research efforts conducted at Louisiana Transportation Research Center (LTRC) over the past few years (Abu-Farsakh et al. 2010; Abu-Farsakh et al. 2013). The Mississippi drilled shaft data consists of 41 drilled shaft load tests. Efforts were made through Caltrans research office to reach out Caltrans bridge foundation engineers and FHWA offices to collect drilled shaft load tests completed in bridge projects completely recently. Total 30 load tests reports of drilled shafts from LA, and 8 cases from Western states were included in the final drilled shaft load test database. Several drilled shafts were not included because of incomplete soil data (cases) or load tests not performed to 1 inch settlement.

A total of 79 drilled shaft load test cases and their corresponding soil conditions were identified and collected from test shaft reports and corresponding geotechnical site reports. Most drilled shaft cases were collect from Mississippi and Louisiana states, the rest several cases were from Arizona, California and Washington states, which can be summarized as cases from “Western states”. All of the drilled shafts in this study were tested using O-cell except a four cases in LA. Most of the drilled shafts tested with O-cell provide top and bottom O-cell settlement curves in their load test reports. The collected drilled shafts load test data and soil properties were compiled and analyzed. The information and data regarding soil stratification and properties, shaft characteristics, load test data, SPT profiles, etc. were processed and transferred from each load test report. The methodology of collecting, compiling, and analyzing the drilled shaft database is presented in this section.

Figure 4-8 presents the locations of each test shaft on google map. Due to the similarity in soil condition, construction method and shaft size, 8 cases located in Mississippi had been combined to 1 case for reliability analysis. This will avoid sample location bias. As the result, the shaft number in Mississippi has been reduced to 34, and the total number of selected shaft cases is reduced to 72. A schematic drawing of the drilled shaft construction and boring location is shown in Figure 4-9. The construction table for original 79 cases is summarized in Table 4-8. Figure and table below presents locations of Mississippi, Louisiana, Western states of the selected test shaft that were investigated in this research.

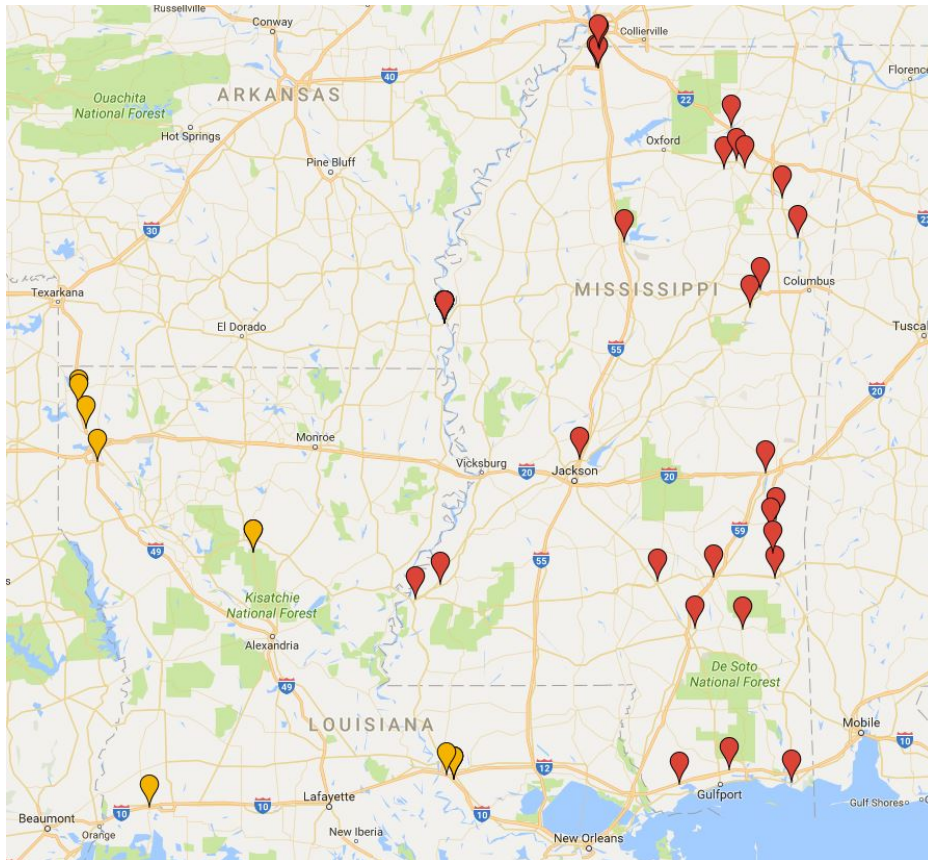
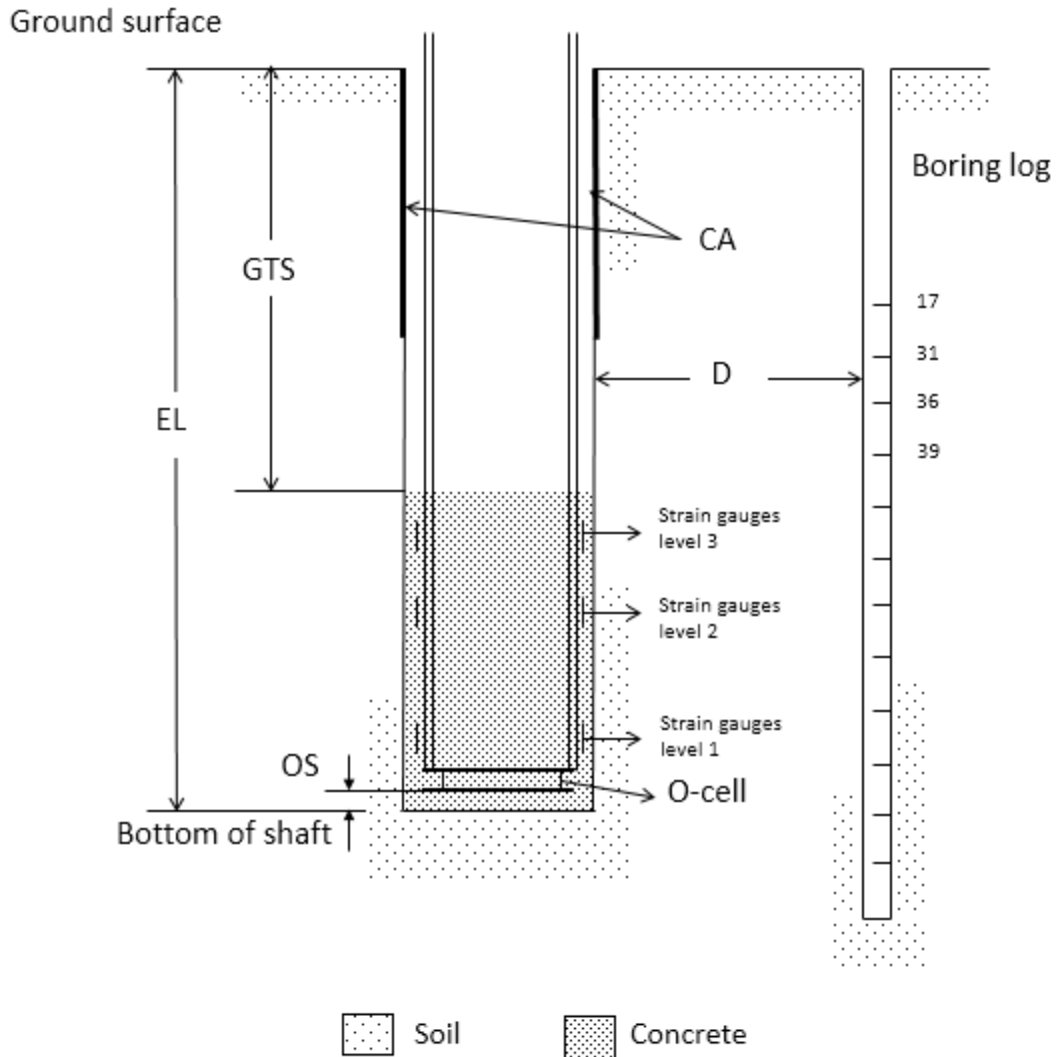


Figure 4-8 Approximate locations of test shafts in Mississippi and Louisiana

Table 4-7 Location of test shaft cases in Western states

Test Shaft	Location
FHWA/CA/TL-94-02 (B-E)	Century Freeway, CA
FHWA/CA/TL-94-02 (B-F)	Century Freeway, CA
NH 10-4(151)/LT-8595	West of I10, Tucson, AZ
LT-9611	San Carlos River, Peridot, AZ
LT-9258	Dixileta Drive - Phoenix, AZ
LT-9604-02	I-5 Columbia River Bridge, WA
LT-9604-03	I-5 Columbia River Bridge, WA
LT-9604-01	I-5 Columbia River Bridge, WA



EL =Excavation length, CA: Casing condition,  
 GTS =Distance between ground surface and top of shaft,  
 D =Distance between boring log and shaft,  
 OS = Distance between bottom of O-cell and bottom of shaft

Figure 4-9 Test shaft schematic

Table 4-8 Construction information of selected drilled shaft cases

Project number	Construction	Drilling fluid	EL (ft.)	GTS (ft.)	CA	D (ft.)
LT 8193 (1)	Wet	WATER	74.5	39	30 ft.	16.0
LT 8193 (2)	Wet	WATER	79.2	45.4	29.4 ft.	3.0
LT 8194	Dry		38.3	0	Temp casing from surface to hole bottom, removed after concrete filled	73.0
LT 8212	Wet	WATER	49.3	18	17 ft casing on the top	14.0
LT 8341	Dry		40	22	7 ft casing on the bottom	9.0
LT 8371 (1)	Dry		26.5	0		8.0
LT 8371 (2)	Dry		66.5	30.4		65.0
LT 8373	Dry		29	0		0.0
LT 8461 (1)	NA	stiff clay and silt, GWT unknown	43	0.5		10.0
LT 8461 (2)	NA		49.7	0.5		54.6
LT 8488 (1)	Dry		65.3	23	casing between surface and part of shaft, removed after concrete filled	71.0
LT 8488 (2)	Wet	Water and polymer	64	41	casing between surface and top of shaft	50.0
LT 8578	Wet	Water and bentonite	91.5	0	outer casing 62ft removed prior the load test, inner casing 45 ft removed after load test	within 20
LT 8618	Dry		41.5	24.3	15ft outer 20ft inner temp. casing between surface and top of concrete	16.4
LT 8655	WET	BENTONITE	164.1	72.6	72.3ft temp. casing	85.2
LT 8745	WET	BENTONITE	82.9	49.3	casing between surface and top of concrete	<30
LT 8786	WET	BENTONITE	47.6	0	20ft temp. casing below ground surface	15.0
LT 8788	DRY		45	5		175.0
LT 8800 (1)	WET	BENTONITE	130.4	7.2	12ft temp. casing below ground surface	65.6
LT 8800 (2)	WET	BENTONITE	139.3	6.2	11ft temp. casing below ground surface	< 10



Project number	Construction	Drilling fluid	EL (ft.)	GTS (ft.)	CA	D (ft.)
LT 8800 (3)	WET	BENTONITE	119.1	8.6	11 ft temp. casing start from 2.5 ft above surface	49.2
LT 8800 (4)	WET	BENTONITE	103.4	10		98.4
LT 8800 (5)	WET	BENTONITE	103.7	9	11 ft temp. casing start from 1 ft above surface	49.2
LT 8800 (6)	WET	BENTONITE	94.4	12	11 ft temp. casing start from 2.5 ft above surface	9.8
LT 8800 (7)	WET	BENTONITE	108	11.2	11.2ft temp. casing, start from 2.3 ft above surface	114.8
LT 8800 (8)	WET	BENTONITE	87.3	5.1	12ft temp. casing start from 1.3 ft above surface	within 10
LT 8825	WET	BENTONITE	75.5	0.6	33ft temp. casing from surface, removed after concrete filled	32.8
LT 8829 (1)	WET*	WATER	53.16	3.29	temp. casing go through whole length of shaft, removed during replacing concrete	6.6
LT 8829 (3)	DRY		36	19	temp.casing removed after load test	18.7
LT 8905	DRY		54.9	38.5	kept 40ft temp. casing during curing and load test	35.0
LT 8912 (1)	DRY		41.3	2.4		2.0
LT 8912 (2)	DRY		34.2	0		0.0
LT 8954 (2)	WET*	WATER	73.2	20	Removed the 55ft inner and 27.2ft outer temp. casings as concreting progressed	40.0
LT 8981	WET*	WATER	52	2.5	30ft inner temp. casing removed as concrete progressed, 19.5ft outer casing removed after concreting	15.0
LT 9147	DRY		60.8	21.8	27ft temp. casing was extracted on the morning of load test day	28.7
LT 9191	WET	MINERAL SLURRY	64	0	45ft temp. casing removed immediately after concreting	0.1
LT 9262	WET	WATER	59	24	17ft perm. Casing start from surface	49.3
LT 9263	WET	MINERAL SLURRY	89	0	25ft temp. casing removed after concreting	93.0
LT 9280 (1)	WET	MINERAL SLURRY	75	7.8	partially removed temp. casing above top of	30.0

Project number	Construction	Drilling fluid	EL (ft.)	GTS (ft.)	CA	D (ft.)
					concrete, replaced it with shorter surface casing	
LT 9280 (2)	WET	MINERAL SLURRY	176.1	1.1	25ft temp. casing removed after concreting	74.5
LT 9280 (3)	WET	MINERAL SLURRY	104.5	9.6	19.5ft temp. casing removed after concreting	30.0
LT 9459 (2)	WET	POLYMER SLURRY	67.5	0	10ft temp. casing removed after concreting	
LT 9459 (3)	WET	POLYMER SLURRY	81.5	0	10ft temp. casing removed after concreting	
LT 9459 (4)	WET	POLYMER SLURRY	46.8	0	10ft temp. casing removed after concreting	
LT 9473 (1)	DRY		36.2	3.7	4ft temp. casing above top of concrete	
LT 9473 (2)	DRY		41.1	1.9	4ft temp. casing above top of concrete	
LT 9597 (1)	WET	BENTONITE	48	1.8	9.8ft temp. casing removed after concreting	
LT 9597 (2)	WET	BENTONITE	53.8	0.4	9.9ft temp. casing removed after concreting	
LT 9694 (1)	WET	BENTONITE SLURRY	51.1	1		
LT-8467	NA		62.67	0.5		
LT 9694 (3)	NA		97	0.14		
LT 9694 (4)	NA		47.42	4		
LT-9934 (1)	WET	BENTONITE	47	2		
LT-9934 (3)	NA		57.2	0.3		
LT-9934 (4)	WET	BENTONITE	59.3	3.7		
LT-9934 (5)	WET	BENTONITE	35.3	0.5		
LT-9938 (1)	WET	BENTONITE	35.85	0.5		
LT-9938 (3)	WET	BENTONITE	43.5	1		
LT-9950 (1)	WET	BENTONITE	71	0.86		
LT-9950 (2)	WET	BENTONITE	47.6	0		
455-08-20, #2	NA					
455-08-20, #3	NA					
LT-8412 (2)	NA		55	1		

Project number	Construction	Drilling fluid	EL (ft.)	GTS (ft.)	CA	D (ft.)
LT-8470	NA		79	2.7		
8915	NA					
LT-8961 (1)	WET					
LT-8961 (2)	WET					
LT-8412 (1)	NA		52.7	2.7		
LT-8944	NA					
455-08-47, 2A	WET	WATER	90.8	55.8	103ft perm. Casing, 79ft temp. casing all above top of concrete	
455-08-47,B	WET	POLYMER SLURRY	137.0	6	20ft perm. Casing goes below top of concrete	< 30 ft
FHWA/CA/TL-94-02	DRY		41.0			within 10 ft
FHWA/CA/TL-94-02	WET	WATER,SOIL-CEMENT	51.0			within 10 ft
NH104(151)/LT-8595	WET	SLURRY	117.5	8.5	35ft perm. Casing start from surface, 15.75 temp. casing pulled after concreting	within 30 ft
LT-9611	DRY		135.5	1.5	9ft outer casing was removed after concreting, 14ft perm. Casing start from surface	within 10 ft
LT-9258	WET	POLYMER SLURRY	90.3	24.25	26ft outer casing was removed after concreting, 30ft perm. Casing start from surface	within 30 ft
LT-9604-02	WET	WATER	250.5	10	216.5 ft inner permanent casing	
LT-9604-03	WET	WATER	130.2	10	Temp. casing to bottom	
LT-9604-01	WET	POLYMER	162.9	9.5	14ft perm. Casing starts from surface, temp. casing reaches almost tip	

Note: Original cases LT-8800-1 to LT-8800-8 had been combined as 1 case for further data analysis. Therefore the total shaft number had been reduced from 79 to 72.

## Database Description

The diameter of selected drilled shafts ranges from 2 to 9.8 ft.; Total concrete filled lengths ranges from 16.9 to 240.5 ft. They were constructed using different construction methods and located in different soil types in varied states. The characteristics of the investigated shafts in the database are interpreted based on diameter, length, construction methods, soil classification, and tip soil condition. The summary of these characteristics are listed in Table 4-9 to 4-12 and Figure 4-10 to 4-20.

Table 4-9 Shaft length distribution

Ft	No.	Relative frequency
[0,20)	4	5.56%
[20,40)	18	25.00%
[40,60)	25	34.72%
[60,80)	12	16.67%
[80,100)	7	9.72%
[120,140)	3	4.17%
[140,160)	1	1.39%
[160,180)	1	1.39%
[240,260)	1	1.39%
Total	72	100.00%
Mean	59.65	
Standard Deviation	37.49	

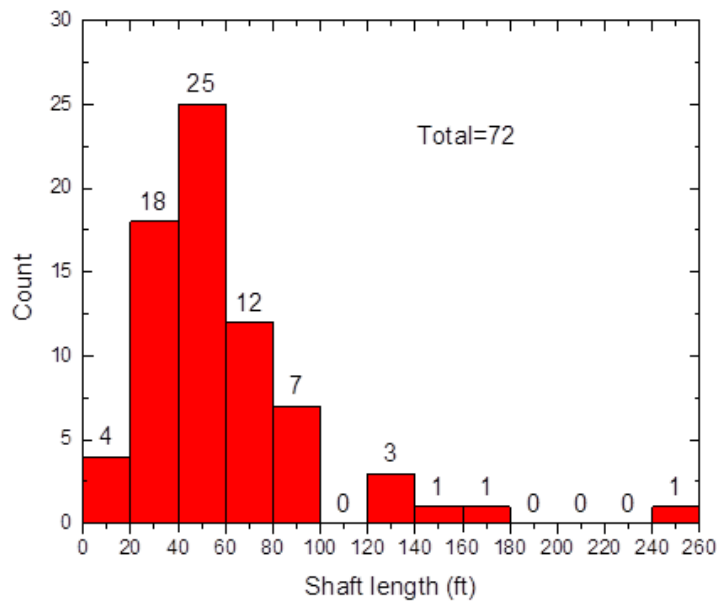


Figure 4-10 Investigated concrete filled length distribution

Table 4-10 Shaft diameter distribution in database

Foot	No.	Relative frequency
[2,3)	7	9.72%
[3,4)	7	9.72%
[4,5)	22	30.56%
[5,6)	21	29.17%
[6,7)	10	13.89%
[7,8)	2	2.78%
[8,9)	2	2.78%
[9,10)	1	1.39%
Total	72	100.00%
Mean	4.79	
Standard Deviation	1.48	

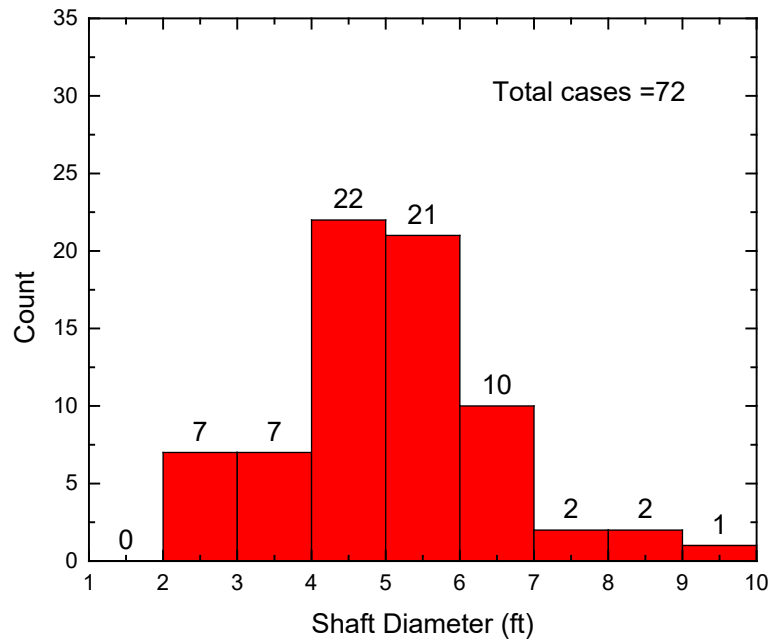


Figure 4-11 Investigated shaft diameter distribution

The methods for construction of drilled shafts can be grouped into three broad categories: dry method, casing method, and wet method. By reviewing the collected load test report, drilled shaft construction methods were identified and listed in Table 4-8. Three construction methods: dry, wet, and NA were identified. NA is used to refer drilled shaft with construction information couldn't be detected from the test shaft report. Figure 4-12 presents the pie chart plot of construction methods for the total drilled shaft database. It can be seen most of selected cases were constructed with wet methods.

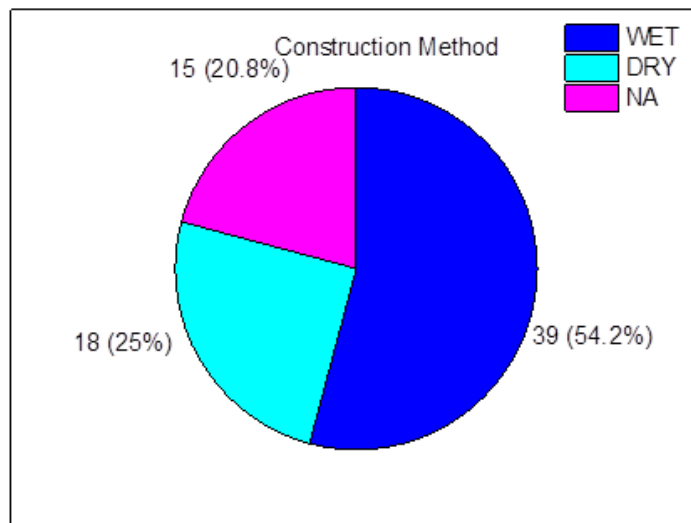


Figure 4-12 Construction method for drilled shaft database

According to FHWA 1999, cohesionless soil materials is divided into cohesionless soil (with  $SPT \leq 50$ ) and cohesionless IGM (with  $SPT > 50$ ) while in FHWA 2010, cohesionless IGM is grouped into cohesionless soil. The soil type along shaft and at tip is identified according to both FHWA 1999 and 2010 methods. The side soil type is classified according to the contribution to the calculated total side resistance. Table 4-11 summarizes the soil type along shaft and Table 4-12 is the soil type at shaft tip.

Table 4-11 Side soil type summary for drilled shaft database

		No. of Cases			
		total	tip-sand	tip-clay	tip-IGM
2010 side	pure sand	17	17	0	--
	80-100% sand	34	31	3	--
	70-100% sand	39	35	4	--
	pure clay	17	1	16	--
	80-100% clay	21	1	20	--
	70-100% clay	24	4	20	--
1999 side	pure sand	3	3	0	0
	80-100% sand	11	9	2	0
	70-100% sand	15	14	0	1
	pure clay	17	1	16	0
	80-100% clay	22	1	21	0
	70-100% clay	24	3	21	0
	pure IGM	4	2	0	2
	80-100% IGM	10	2	0	8
70-100% IGM	12	3	1	8	

Table 4-12 Tip soil conditions for drilled shaft database

Design Method	criteria	Number of cases
2010 tip	sand	46
	clay	26
1999 tip	sand	28
	clay	26
	IGM	18

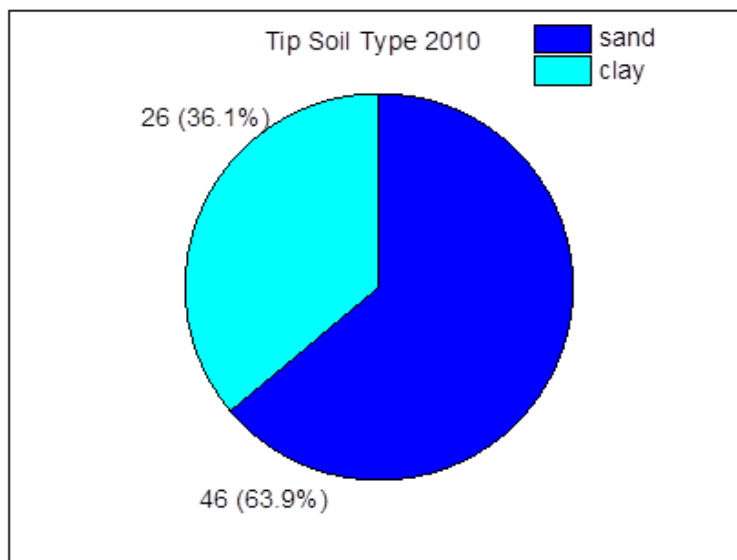


Figure 4-13 Tip soil conditions for drilled shaft database (FHWA 2010)

Measured total resistance was obtained from equivalent top-down curve by O-cell tests. It was defined as the test load corresponding to a settlement of 1 inch or 5% of the test shaft diameter based on different failure criterion. In this research, both 1 inch and 5% of diameter criterion will be verified. Measured resistance of drilled shaft at a settlement of 1 inch or 5% of diameter can be determined by interpreting load-settlement results. Some of measured settlement did not meet 1 inch or 5% of diameter criterions; therefore it was determined by extrapolating load-settlement curves.

Since most selected drilled shaft cases were tested using O-cells, the measured tip and side resistance components could be determined separately for each filled shaft from O-cell results from test shaft reports by using 1 inch and 5% of diameter interpretation

criterion. Since not all the selected cases have those measured curves available, only 56 out of 72 were used to analyze measured tip resistance contribution (ratio of tip resistance over total measured resistance). The results regarding general tip soil resistance contribution and detailed tip-sand, tip-clay resistance contribution are showing below (under both 1 inch and 5% of diameter standards):

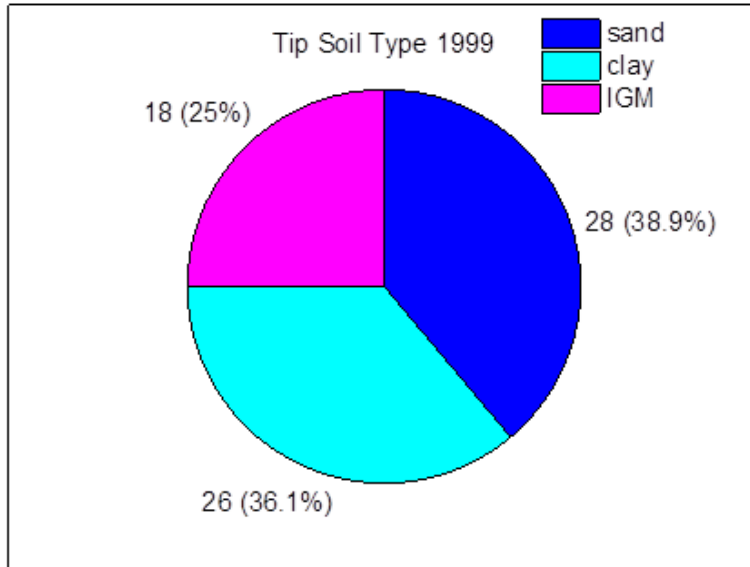


Figure 4-14 Tip soil conditions for drilled shaft database (FHWA 1999)

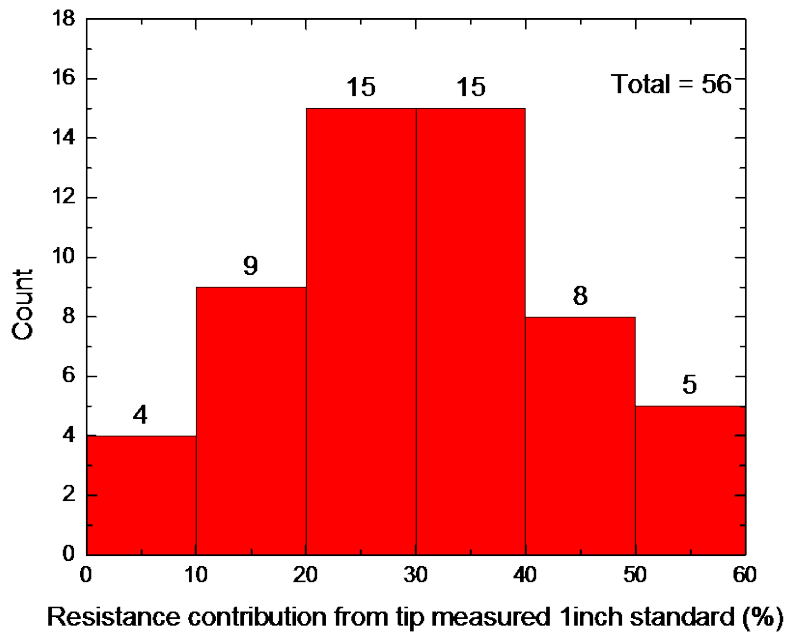


Figure 4-15 Measured resistance contribution from tip 1 inch standard (%)



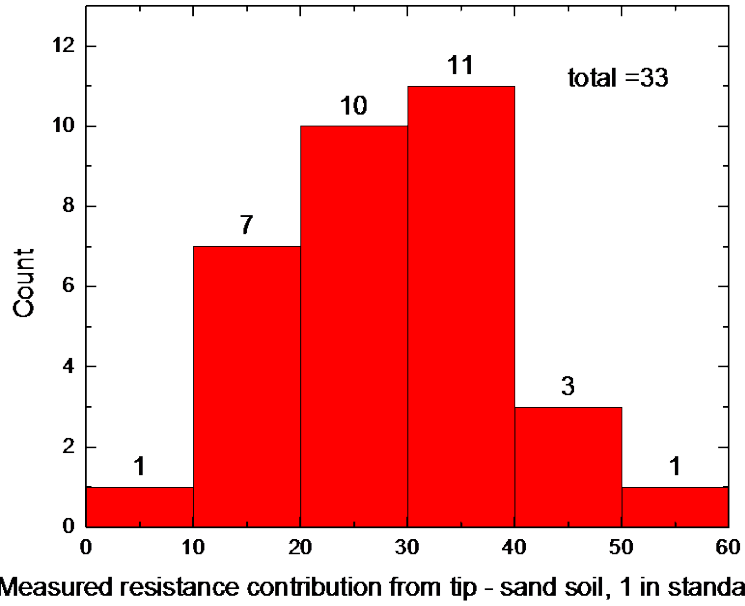


Figure 4-16 Measured resistance contribution from tip - cohesionless soil, 1 inch standard (%)

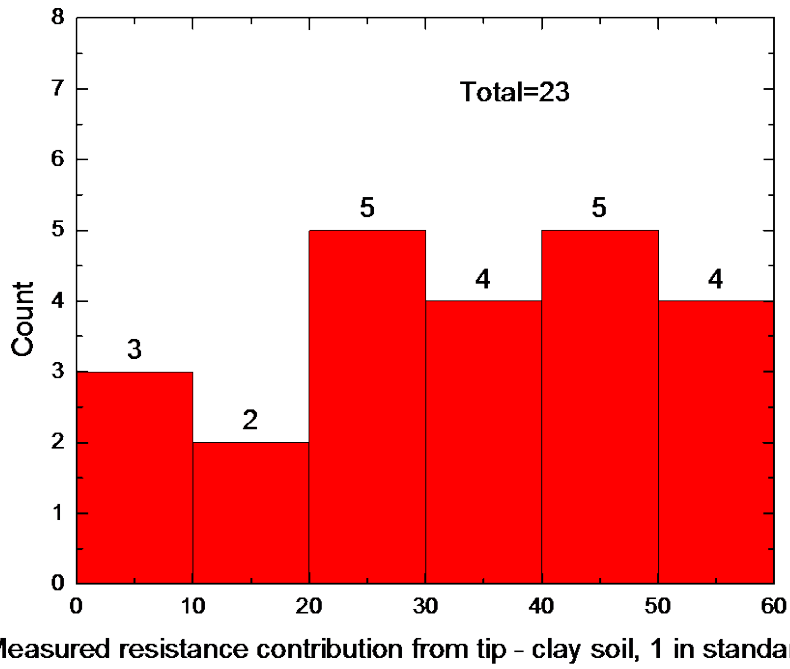


Figure 4-17 Measured resistance contribution from tip - cohesive soil, 1 inch standard (%)

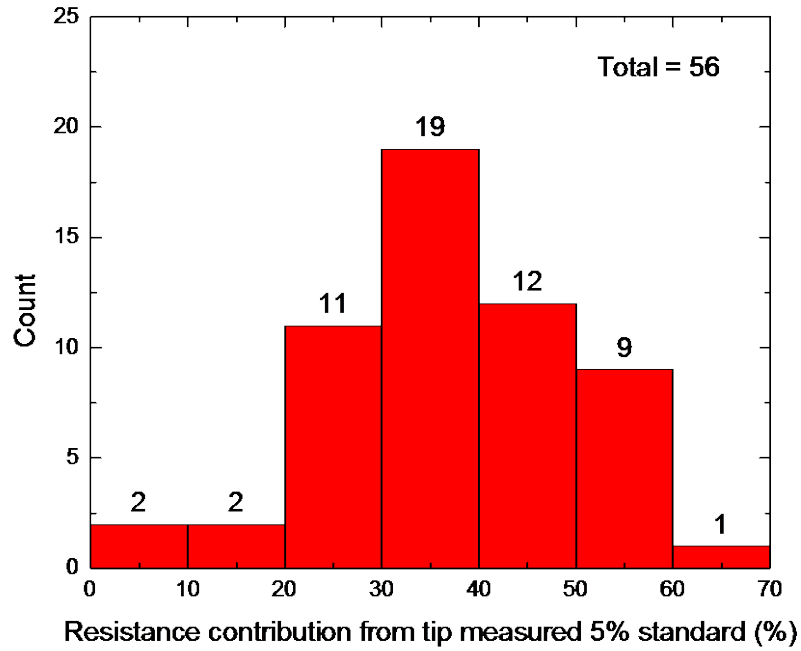


Figure 4-18 Measured resistance contribution from tip 5% diameter standard (%)

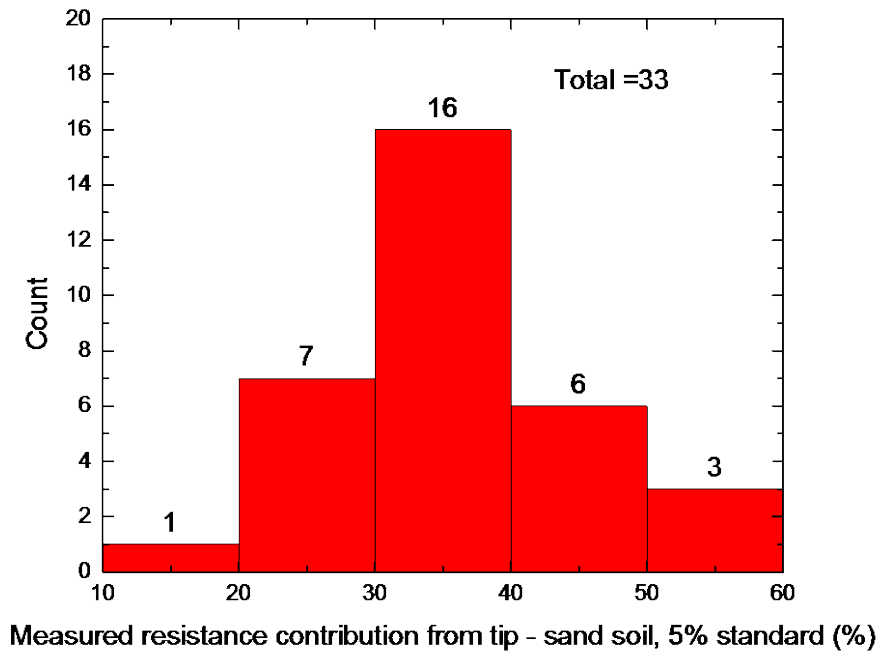


Figure 4-19 Measured resistance contribution from tip - cohesionless soil, 5% diameter standard (%)

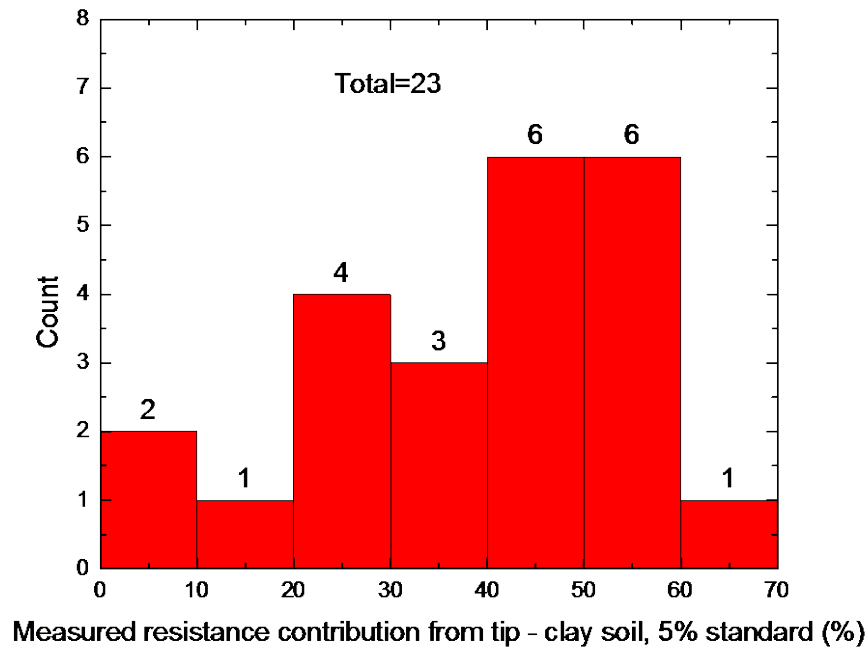


Figure 4-20 Measured resistance contribution from tip - cohesive soil, 5% diameter standard (%)

### Analyses of Drilled Shaft Database

Probabilistic LRFD calibration of resistance factors for a given predictive method requires measured geotechnical drilled shaft resistance (sometimes referred as strength or capacity) from static load test results and predicted drilled shaft resistance from the given predictive method. Prediction of drilled shaft resistance is performed following two design specifications: FHWA 1999 and 2010. Drilled shaft total resistance, including side and tip resistance, is calculated based on the specified predictive method for each soil type. The calculated resistance is the nominal resistance which is defined as ultimate capacity or at chosen failure settlement. Measured drilled shaft resistance is obtained from the load-displacement relations for each drilled shaft from the collected drilled shaft load test database. The measured drilled shaft resistance is not unique and is interpreted from the measured load-settlement curve according to chosen failure criterion and may include judgment. The static load test results depend on the load testing procedures and the applied interpretation method, often being subjective. The following sections present the analyses procedure to determine predicted and measured resistance at chosen failure criteria.

## Drilled Shaft Nominal Resistance

The 1999 and 2010 FHWA drilled shaft design methods described in chapter 3 are used to calculate nominal (ultimate) resistances of the drilled shafts. The ultimate axial resistance,  $Q_u$ , of a drilled shaft consists of end bearing resistance,  $Q_b$ , and skin frictional resistance,  $Q_s$ . The soil subsurface is divided into various layers along the drilled shaft based on the soil type, which are categorized by cohesionless and cohesive soil, rock, and intermediate geomaterial (IGM). Cohesionless IGM soil type is considered in the FHWA 1999; however, it is grouped under cohesionless soil type in FHWA 2010. The ultimate (nominal) axial resistance of the drilled shaft can then be determined from the following equation:

$$Q_u = Q_b + Q_s = q_b A_b + \sum_{i=1}^n f_{si} A_{si}$$

where  $q_b$  is the unit end bearing resistance,  $A_b$  is the cross-sectional area of the base of the drilled shaft,  $f_{si}$  is the average unit skin friction of each individual soil layer,  $A_{si}$  is the area of the drilled shaft interface with each soil layer, and  $n$  is the number of soil layers along the length of the shaft.

## Prediction of Load-Settlement Behavior of Drilled Shaft

The load-settlement behavior of a drilled shaft under short-term compression loading can be calculated using the normalized settlement curves proposed by O'Neill and Reese (1999). The normalized average trend curves for cohesive and cohesionless soils are shown in Figure 4-21. The side friction resistance ( $R_s$ ) developed for each layer  $i$  at a given shaft top settlement ( $w_T$ ) can be calculated using the ratio of the average deflection along the sides of a drilled shaft ( $w_s$ ) to the shaft diameter ( $B$ ). The average deflection along the side of a drilled shaft can be calculated using the following equation:

$$w_s = w_T - \delta_s / 2 \quad (18)$$

where,  $\delta_s$  is the approximate elastic compression of the drilled shaft, and  $w_T$  is the estimated deflection of the head of the drilled shaft.

The developed side friction resistance ( $R_{sd}$ ) can be obtained from the vertical axis of Figure 4-21 (a) and (c) for cohesive soils and cohesionless soils, respectively. The same procedure can be applied to calculate the base resistance developed at the same top settlement ( $w_T$ ). The deflection at the base of a drilled shaft ( $w_b$ ) can be computed using:

$$w_b = w_T - \delta_s \quad (19)$$

Using the ratio of the deflection at the base to the base diameter ( $w_b/B_b$ ), the developed base resistance ( $R_B$ ) can be calculated from the vertical axis of Figure 1 (b) and (d) for cohesive soils and cohesionless soils, respectively.

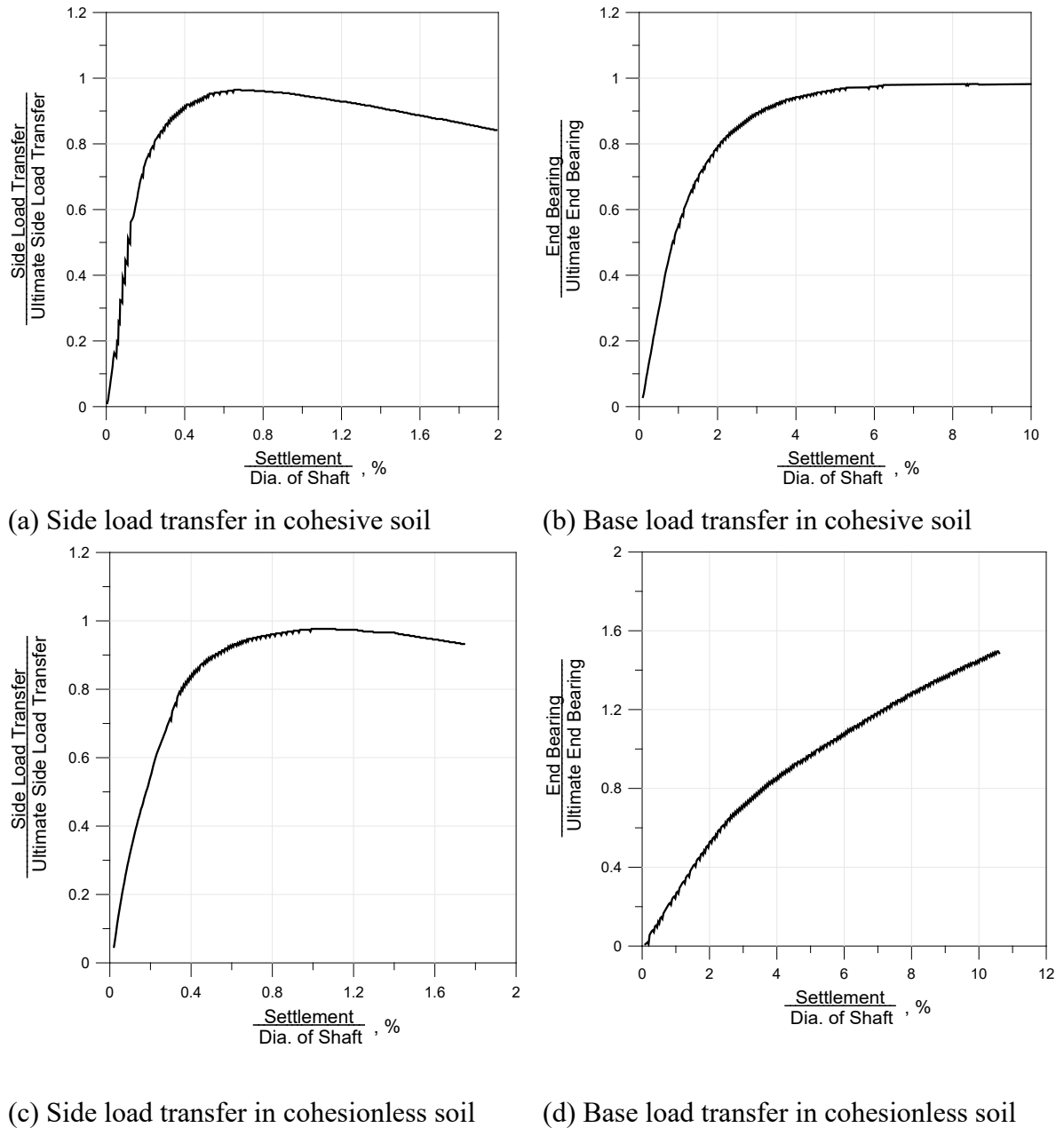


Figure 4-21 Normalized load transfer representing the average trend value for drilled shaft (after O'Neill and Reese 1999)

The developed load ( $Q_T$ ) at the specific settlement ( $w_T$ ) can then be calculated as follows:

$$Q_{Td} = R_{Bd} \text{ (developed)} + R_{sd} \text{ (developed)} \quad (20)$$

In this study, the load-settlement behavior was calculated following the above procedure in EXCEL with rigid shaft assumption which the shaft top and bottom has the same settlement. An example of a predicted load-settlement (LT-8786) curve is shown in Figure 4-22. In the above procedure, predicted side and tip settlement curve can also be obtained.

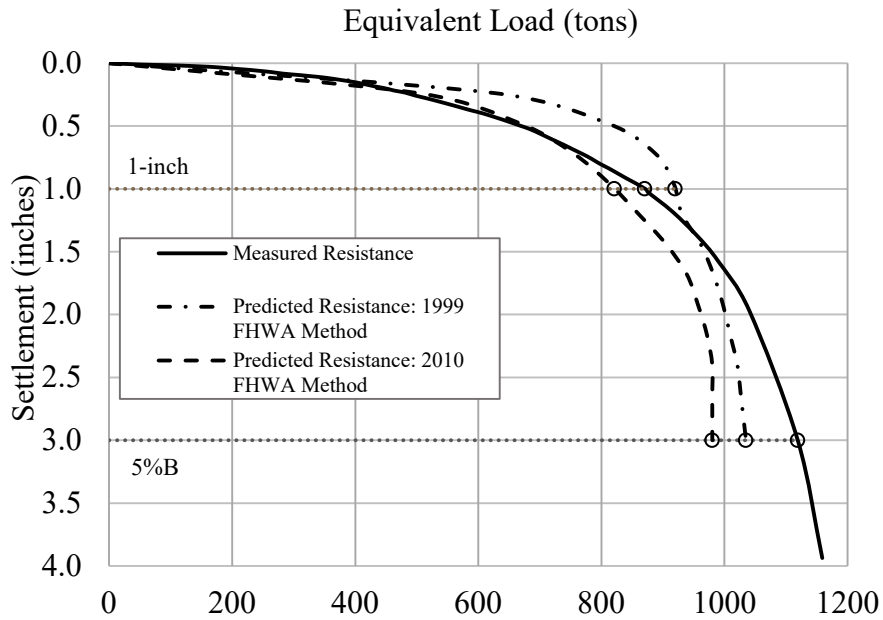


Figure 4-22 An example of a predicted and measured top-down load-settlement curve

### Prediction of Load-Settlement Curves Using FHWA 2010 design method

The load settlement behavior of a drilled shaft under short term compression loading can be estimated using the normalized relations proposed by Chen and Kulhawy [23]. The normalized average trend curves for cohesive and cohesionless soils are shown in Figure 4-23. The failure threshold, which corresponds to the axial force at 4.0% B (B: diameter of the drilled shaft), is computed as the sum of nominal side and base resistance as:

$$Q_{\text{Failure threshold}} = R_{\text{SN}} + \eta R_{\text{BN}}$$

Where  $R_{\text{SN}}$  and  $R_{\text{BN}}$  are nominal side and base resistance, respectively;  $\eta = 1.0$  for cohesive soil and 0.71 for cohesionless soil.

The normalized total axial force at a specific settlement can be obtained from the vertical axis of figure below using the ratio of the average deflection ( $\delta$ ) to the shaft diameter (B). To generate the predicted side resistance and end bearing load settlement curves, the predicted side and end bearing resistances were assumed to be directly proportional to that of the 1999 method.

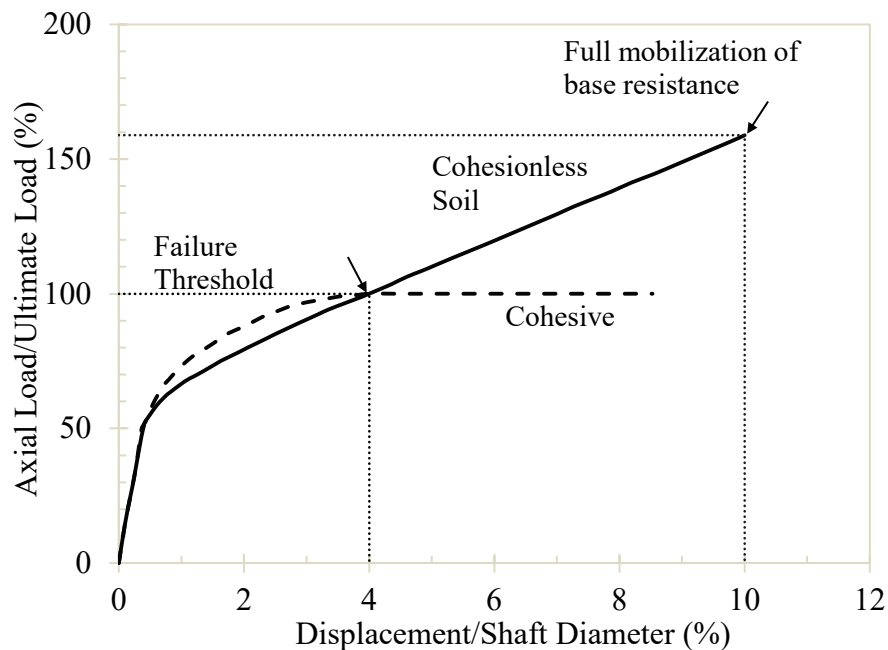


Figure 4-23 2010 Normalized Trend Curves for to total load-settlement (Brown et al. 2010)

## **Measured Load-Settlement Behavior of Drilled Shafts**

O-cell test has been widely used in the United States to determine resistance of drilled shafts. Unlike the conventional top-down load test, the load in an O-cell test is applied at the bottom or near the bottom of drilled shafts via a preinstalled hydraulic cell. During an O-cell load test, the shaft above the cell moves upward, and the shaft below the cell moves downward. As a result, both side friction and end bearing (including side friction between o-cell and shaft tip) can be measured separately from O-cell test as shown in Figure 4-24. The upward load shown in the figure was the net upward load (the O-cell measured upward load minus buoyant weight of the drilled shaft). An equivalent top-down curve can be constructed from the two component curves to investigate the combined total capacity. Construction of the equivalent top-down curve begins by determining the side shear friction at an arbitrary deflection point on the side shear-deflection curve (Figure 4-25). The shaft is assumed as rigid; its top and bottom move together and have the same movement at this load. Then the end bearing at the same movement can be determined from the downward curve. By adding the side shear to the mobilized end bearing at the chosen displacement, one can determine the total load. Thus one point with the total load at the chosen settlement can be determined for the top-down load settlement curve (without elastic compression). The complete curve at different settlement can be obtained by repeating this process. The equivalent top-down load settlement curve with the elastic compression correction is usually available in the collected pdf load test report. Figure 4-25 shows an example of the construction of an equivalent top-loaded settlement curve from O-cell test results.

### Correction of Measured Side Resistance for O-Cell Shaft Tip

O-cell is generally located at certain distance above drilled shaft tip. The location positioned to provide sufficient reaction to mobilize both side and tip resistance. The top and bottom movement curves provided O-cell are the recorded top and bottom reaction forces. The bottom reaction force consists both shaft and tip resistance from the shaft below O-Cell. The shaft side resistance measured from the top and bottom curves does not include the shaft resistance below the O-cell and above the tip. This will result in underestimation of side resistance and over-estimate the tip resistance. A correction is presented by assuming the shaft resistance below O-cell and above O-cell with the unit side friction. This can be achieved using the average net unit side shear values reported in the load test report. It is typically assumed the bottom shaft has the same unit side resistance as the reported average net unit side shear values for the strain gauge level 2 to



O-cell. Thus the side resistance (load) can be estimated by using the side resistance ratio between the bottom shaft and the top shaft.

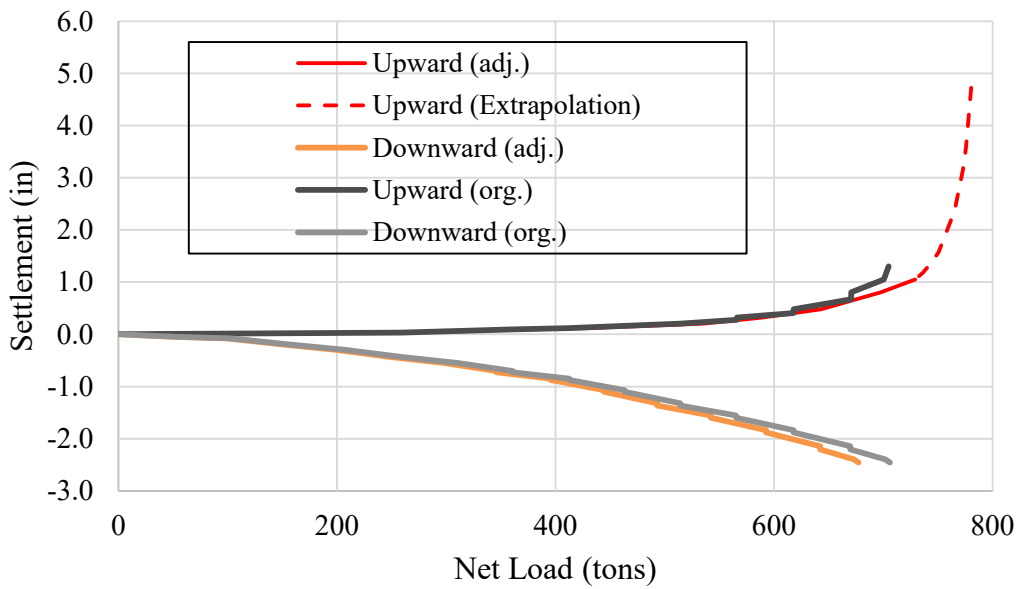


Figure 4-24 Original and adjusted O-Cell Load Displacement Curves

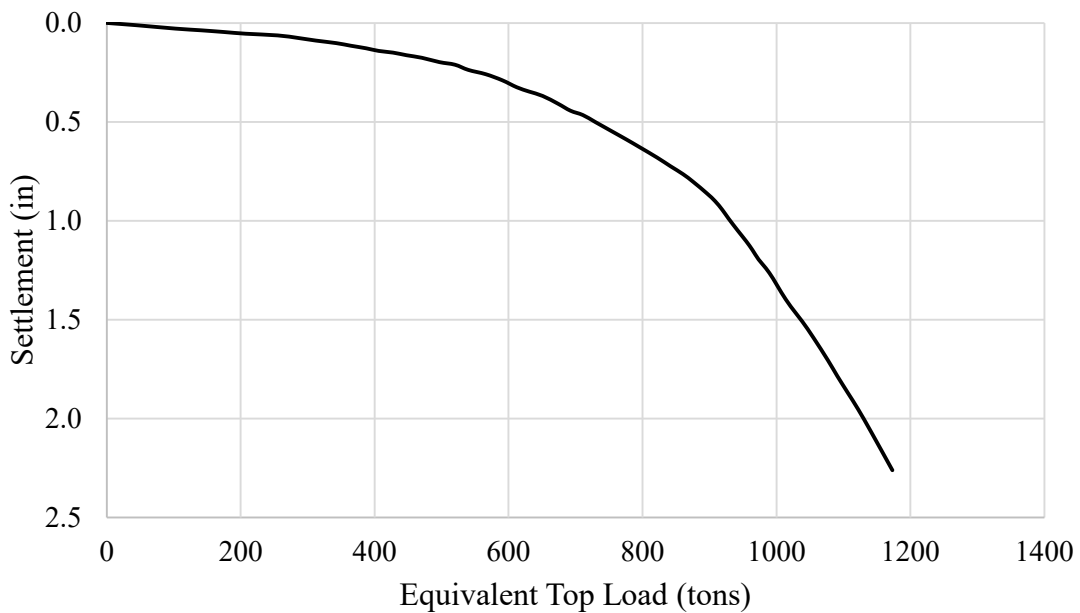


Figure 4-25 Equivalent top-down settlement curve

According to the comparison study available in literature, the O-cell method has a very close result as the traditional top-down method in terms of measurement of equivalent

top-down load-settlement curve (Schmertmann and Hayes 1997). Also the number of drilled shafts tested by top-down load tests in this study is small compared to total drilled shaft tests. Therefore, the difference of load test method has a negligible effect on the calibration of resistance factor for drilled shafts.

### Measured and Predicted Resistance at Different Failure Criteria

The measured nominal resistance of each drilled shaft was determined by the test load corresponding to the settlement at 5%B and one-inch, an example of which is shown in Figure 4-26. Most of the load-settlement curves did not meet the 5%B criterion and required extrapolation to determine an estimate of the measured nominal resistance. A study performed by Abu-Farsakh et al. (2010) in a similar LRFD calibration report showed that exponential curve fitting is the best method for extrapolation over hyperbolic, Chin’s method, and cubic spline. Figure 4-27 illustrates the use of the exponential curve fitting method to extrapolate the measured nominal resistance.

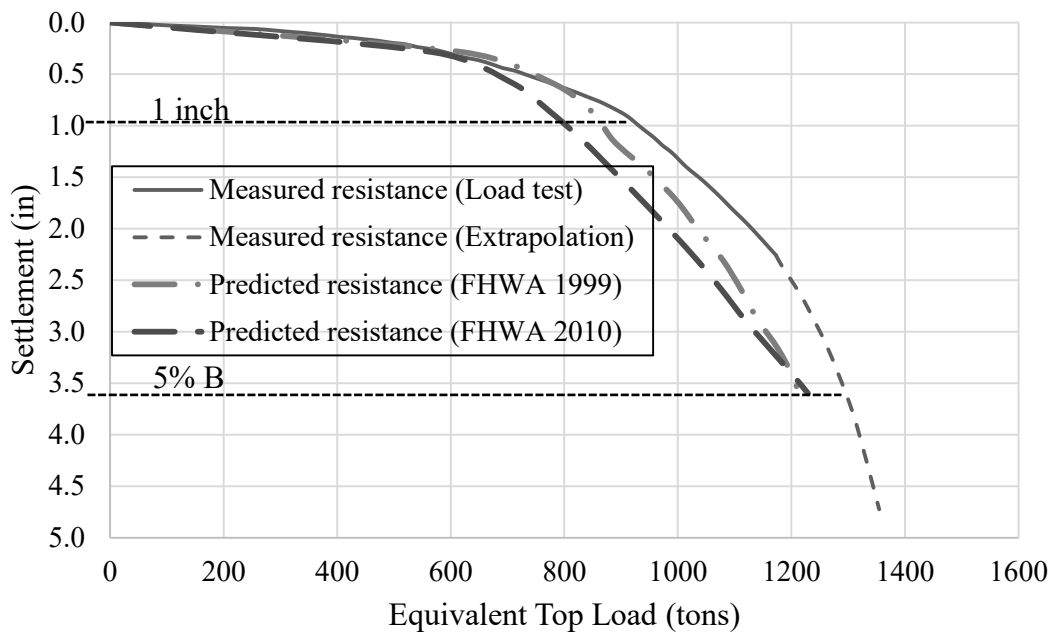


Figure 4-26 Measured Nominal Resistance at 1 inch and 5%B ((LT-8786))

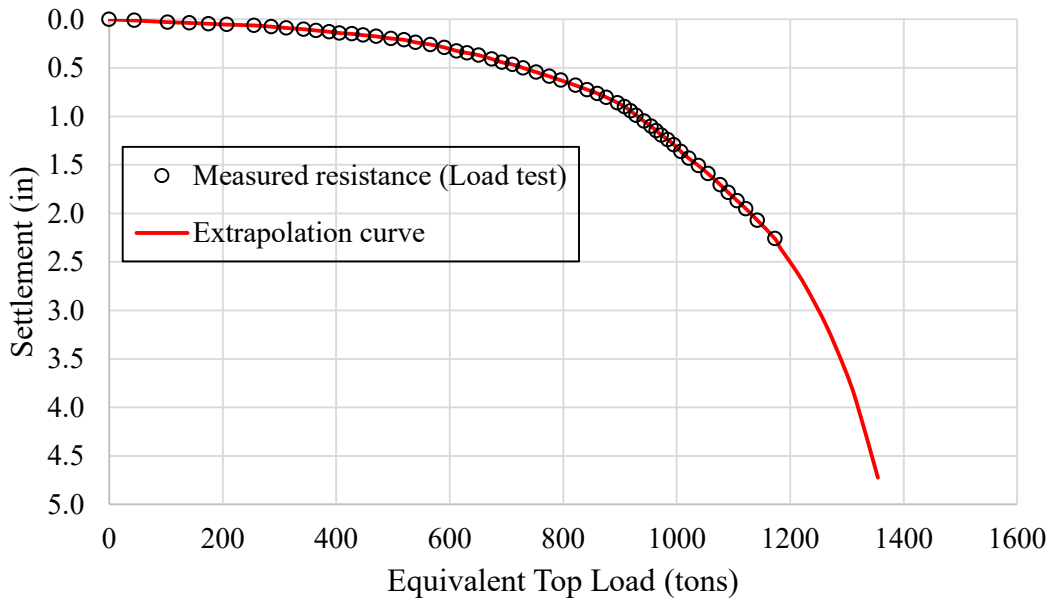


Figure 4-27 Extrapolation of Load-Settlement Curve

The predicted nominal resistances of each drilled shaft at 5%B and one-inch of settlement are determined by the methods outlined in the FHWA design methods. Normalized average trend curves are provided for predicting load-settlement behavior of drilled shafts in cohesionless and cohesive soils. The normalized trend curves given in the 2010 design method are shown in Figure 4-23 (Chen and Kulhawy 2010), and the trend curves given in the 1999 design method are shown in Figure 4-21 (O'Neill and Reese 1999). The resistance developed by each soil layer is calculated using a ratio of the settlement to the diameter of the shaft. Various settlement points are chosen to develop the load-settlement curve. This allows for the predicted nominal resistance to be determined at a given tolerable displacement, 5%B and one-inch in this case.

#### Measured and Predicted Side and Tip Resistance

The measured side and tip resistance at 5%B and 1 inch is determined following similar procedure outlined for total resistance. Predicted side and tip resistance can be determined from predicted side and tip settlement curves. For FHWA 1999 design method, side and tip settlement curves can be directly determined following the above mentioned procedure for settlement prediction. For the 2010 design method, however, the normalized trend curve is only for determining the total nominal resistance. To generate the predicted side resistance and end bearing load settlement curves, the predicted side and end bearing resistances were assumed to be directly proportional to

that of the 1999 method. The measured tip and side resistance can be determined from adjusted O-cell top and bottom load-movement curves as shown in Figure 4-24. To determine measured side and tip resistance, the resistance with greater mobilization was picked first. Then the other resistance, either side or tip, can be determined as the total resistance (as shown in Figure 4-26) minus the first known resistance component. This allows for consistency of total resistance as corrected for elastic compression.

An example results of determined all the resistance component is shown in Table 4-13.

Table 4-13 Summary of total and separated resistance from measured data and predicted methods

<b>Measured Resistance (tons)</b>			
	Equivalent	Side	Tip
1 inch	931.07	722.44	208.63
5% B	1295.96	775.73	520.23
<b>FHWA 1999 (tons)</b>			
	Total	Side	End
1-inch	866.71	642.89	223.82
5%B	1211.51	624.11	587.40
<b>FHWA 2010 (tons)</b>			
	Total	Side	End
1-inch	802.54	594.97	207.57
5%D	1238.08	637.80	600.28

## 5. CHAPTER 5 RESULTS AND ANALYSES

### Driven Pile Results

#### Predicted vs. Measured Driven Pile Resistance

Static pile capacity was calculated following Caltrans design practice. Nordlund and  $\alpha$ -method were used for small piles (diameter less or equal than 16 inch); API method was used for larger piles (diameter greater than 16 inch). Measured pile capacity was interpreted from measured load-settlement curve following several failure criteria which include 1 inch settlement, modified Davisson method, and 5% pile diameter. Comparing the measured pile capacities determined from different failure criteria, little variation was observed. Therefore, the measured pile capacity used in the following data analysis was chosen as larger one of measured capacity interpreted by 5% pile diameter failure criteria and 1 inch failure criteria.

Table 5-1 presents the predicted static driven pile compression capacity and measured pile compression capacity. The static capacity generally under predicts the measured pile capacity. Large variation was observed for the 85 cases as a whole, with standard deviation ( $Q_m/Q_c$ ) greater than 1.7. Table 5-1 presents the predicted static driven pile uplift capacity and measured pile uplift capacity. The uplift results are similar to the compression database. The under estimation of uplift capacity is slight less than the compression pile capacity and the standard deviation ( $Q_m/Q_c$ ) around 1.5. Figure 5-1 and 5-2 presents predicted static capacity vs. measured driven pile capacity for both compression and uplift cases. The data presented in Figure 5-1 and 5-2 were filtered by selected filter criteria.

Table 5-1 Static capacity vs. measured capacity for all 85 compression loaded driven piles

Project No.	Pile Type	Tip Soil	DQF	Set-up days	Diameter (inch)	$Q_c$ (kips)	$Q_m$ (kips)
04-01	CP	tip-clay	3	2	12	399	320
09-03/04	PP (Closed)	tip-sand	3	15	24	713	760
09-05/06	PP (Closed)	tip-clay	4	14	24	710	670
10-01/02	PP (Open)	tip-clay	4	33	42	1206	1245
11-01/02	PP (Closed)	tip-clay	3.5	14	24	589	591
12-01/02	PP (Open)	tip-clay	4.5	31	42	1364	1288
12-03/04	PP (Open)	tip-clay	3	30	42	961	1031

Project No.	Pile Type	Tip Soil	DQF	Set-up days	Diameter (inch)	Q <sub>c</sub> (kips)	Q <sub>m</sub> (kips)
12-05/06	PP (Open)	tip-clay	4	28	42	1415	857
22-03/04	PP (Closed)	tip-sand	2.8	6	14	484	170
29-01/02	PP (Open)	tip-clay	4	30	24	244	363
29-05/06	PP (Open)	tip-clay	4	28	24	273	710
30-01/02	PP (Open)	tip-clay	3	26	42	1264	875
30-03/04	PP (Open)	tip-clay	3	55	42	1257	1209
31-03/04	PP (Closed)	tip-sand	4	42	24	734	1000
31-07/08	PP (Closed)	tip-sand	4	49	24	440	738
31-09/10	PP (Open)	tip-sand	4	38	24	307	781
31-11/12	PP (Closed)	tip-sand	4	41	24	734	922
35-01/02	PP (Open)	tip-sand	3	1	14	76	326
37-01/02	PP (Closed)	tip-rock	2.5	1	14	842	670
40-05	PP (Open)	tip-sand	4.5	76	24	163	1755
40-10/11	PP (Open)	tip-sand	4.5	47	24	169	640
41-01/02	PP (Open)	tip-sand	3	6	16	177	374
41-05/06	PP (Open)	tip-sand	3	6	14	106	318
41-07/08	PP (Open)	tip-sand	3.8	2	16	239	633
41-11/12	PP (Open)	tip-sand	3.8	4	14	158	382
44-01	CP	tip-sand	3	4	14	625	443
60-02	HP	tip-sand	3.5	2	14	476	601
65-01/02	HP	tip-cobbles	3	2	12	575	511
66-01/02	HP	tip-gravel	3	15	12	259	577
77-01	PP (Open)	tip-sand	3	22	24	159	748
77-02	PP (Open)	tip-sand	3	21	24	185	1120
79-07/08	PP (Open)	tip-clay	3.5	168	16	273	300
79-12	CP	tip-clay	3.5	57	14	342	260
79-13	CP	tip-clay	3.5	229	14	342	298
79-15	CP	tip-clay	3.5	67	14	341	272
79-16/17	HP	tip-clay	3.5	186	14	319	291
83-01	PP (Open)	tip-sand	3	67	18	76	789
85-01/02	PP (Open)	tip-sand	3.5	10	24	174	463
86-01/02	PP (Open)	tip-sand	3	25	24	191	620
87-01/02	CP	tip-sand	4	7	14	275	260
87-03	CP	tip-sand	3	7	14	168	236
93-01/02	PP (Open)	tip-sand	3	22	72	2136	1513
95-03/04	PP (Open)	tip-sand	2.8	13	24	437	490
96-01/02	PP (Open)	tip-sand	3	50	16	167	927

Project No.	Pile Type	Tip Soil	DQF	Set-up days	Diameter (inch)	Q <sub>c</sub> (kips)	Q <sub>m</sub> (kips)
96-03/04	PP (Open)	tip-sand	3	50	16	166	608
97-03/04	PP (Open)	tip-sand	2.5	17	24	406	800
98-01/02	PP (Open)	tip-clay	4	35	24	268	214
98-03/04	PP (Open)	tip-clay	4	33	24	265	182
99-01/02	PP (Open)	tip-sand	4.5	30	24	430	902
99-03/04	PP (Open)	tip-sand	4.5	34	24	408	350
100-01/02	PP (Open)	tip-clay	3.5	15	24	258	313
104-01	CP	tip-clay	3.5	unk	12	414	280
109-01	PP (Closed)	tip-sand	3	5	10.75	178	180
111-01	CRP	tip-sand	3	unk	15	361	387
112-01	CRP	tip-sand	3	unk	15	371	455
114-02	PP (Closed)	tip-silt	2.7	7	12	89	122
116-01	CP	tip-sand	2.5	unk	12	277	241
117-01	HP	tip-sand	3	1	10	126	164
118-01	CP	tip-clay	3	4	12	345	281
119-01	CP	tip-sand	2.8	4	12	822	281
121-01	CP	tip-clay	3.5	2	12	351	240
122-01	CP	tip-clay	3	19	12	361	401
124-01	CP	tip-sand	3	5	12	533	281
125-03	HP	tip-sand	2.8	4	14	929	557
127-01	CP	tip-clay	3.5	7	12	435	400
128-01	CP	tip-clay	3	6	12	220	211
129-01	CP	tip-clay	3	8	10	197	158
130-01	PP (Open)	tip-silt	3.3	8	42	1452	1618
133-01	PP (Open)	tip-sand	2.5	29	96	4223	6679
134-01	PP (Open)	tip-clay	2.8	7	48	3869	2363
136-01	PP (Open)	tip-gravel	3	15	87	4648	6494
137-01	PP (Open)	tip-gravel	4	6	66	3612	3200
138-01	PP (Open)	tip-sand	2.5	11	48	3033	3445
139-01	PP (Open)	tip-sand	3	7	74.5	5563	7950
140-01	PP (Open)	tip-rock	2	47	108	5147	7900
141-01	PP (Open)	tip-sand	3	39	90	4358	3805
141-02	PP (Open)	tip-sand	3	39	90	6750	8000
142-01/02	PP (Closed)	tip-sand	4.5	28	24	1512	1140
143-01	PP (Open)	tip-sand	2.5	12	84	1771	1995
143-02	PP (Open)	tip-sand	2.5	12	84	5493	8000
144-01	PP (Open)	tip-sand	2.8	15	72	4624	7211

Project No.	Pile Type	Tip Soil	DQF	Set-up days	Diameter (inch)	Q <sub>c</sub> (kips)	Q <sub>m</sub> (kips)
145-01	PP (Open)	tip-clay	2.8	28	96	7488	7596
146-01/02	PP (Open)	tip-sand	3.3	13	48	1437	2091
147-01	PP (Open)	tip-sand	3	41	48	2069	1724
147-02	PP (Open)	tip-sand	3	30	48	2684	2595

Table 5-2 Static capacity vs. measured capacity for all 83 up lift loaded driven piles

Project No.	Pile Type	Tip Soil	DQF	Set-up days	Diameter (inch)	Q <sub>c</sub> (kips)	Q <sub>m</sub> (kips)
09-03/04	PP (Closed)	tip-sand	3	15	24	366.534	213.731
09-05/06	PP (Closed)	tip-clay	4	14	24	598.023	440.04
10-01/02	PP (Open)	tip-clay	4	33	42	1189.7	886.387
11-01/02	PP (Closed)	tip-clay	3.5	14	24	508.934	399.789
12-01/02	PP (Open)	tip-clay	4.5	31	42	1348.42	868.656
12-03/04	PP (Open)	tip-clay	3	30	42	948.693	814.974
12-05/06	PP (Open)	tip-clay	4	28	42	1314.09	533.072
22-02	PP (Closed)	tip-sand	2.8	1	14	262.308	61.6293
22-03/04	PP (Closed)	tip-sand	2.8	6	14	341.091	106.697
22-06	PP (Closed)	tip-sand	2.5	27	14	286.689	137.113
22-08/09	PP (Closed)	tip-sand	2.5	5	14	289.154	112.441
22-10	PP (Closed)	tip-clay	3	19	14	291.41	199.818
22-11	PP (Closed)	tip-sand	2.5	23	14	314.265	575.61
23-01	PP (Closed)	tip-sand	2.5	13	14	269.495	142.027
23-02	PP (Closed)	tip-clay	3.2	44	14	250.266	167.118
26-01	CP	tip-sand	3.5	4	14	140.667	175.304
29-01/02	PP (Open)	tip-clay	4	30	24	234.135	263.372
29-04	PP (Closed)	tip-clay	4	28	24	291.404	793.633
29-05/06	PP (Open)	tip-clay	4	28	24	262.915	442.749
29-08/09	PP (Closed)	tip-sand	4	16	24	195.818	461.12
29-10	PP (Closed)	tip-clay	4	20	24	250.444	712.135
30-01/02	PP (Open)	tip-clay	3	26	42	1249.3	651.552
30-03/04	PP (Open)	tip-clay	3	55	42	1241.82	854.352
31-01	PP (Open)	tip-sand	4	56	24	271.508	225.986
31-02	PP (Open)	tip-sand	4	62	24	274.172	459.786
31-03/04	PP (Closed)	tip-sand	4	42	24	279.458	522.856
31-05/06	PP (Closed)	tip-sand	4	42	24	330.532	632.355
31-07/08	PP (Closed)	tip-sand	4	49	24	241.795	343.157



Project No.	Pile Type	Tip Soil	DQF	Set-up days	Diameter (inch)	Q <sub>c</sub> (kips)	Q <sub>m</sub> (kips)
31-09/10	PP (Open)	tip-sand	4	38	24	271.508	391.786
31-11/12	PP (Closed)	tip-sand	4	41	24	279.719	311.856
32-01	PP (Open)	tip-sand	3	15	12	152.579	374.747
32-02	PP (Open)	tip-sand	2.5	2	12	37.1263	255.129
35-01/02	PP (Open)	tip-sand	3	1	14	41.0975	150.407
38-01	PP (Open)	tip-sand	3.5	1	16	55.0382	231.462
40-01	PP (Closed)	tip-sand	2.8	17	24	82.6866	689.703
40-02	PP (Open)	tip-sand	2.6	17	24	65.0514	302.607
40-10/11	PP (Open)	tip-sand	4.5	47	24	124.338	254.642
41-01/02	PP (Open)	tip-sand	3	6	16	136.394	224.518
41-03	PP (Open)	tip-sand	3	6	16	194.86	458.3
41-04	PP (Open)	tip-sand	2.8	6	14	140.273	325.466
41-05/06	PP (Open)	tip-sand	3	6	14	90.2014	164.866
41-07/08	PP (Open)	tip-sand	3.8	2	16	191.705	379.603
41-09	PP (Open)	tip-sand	3.5	2	16	269.348	464.903
41-10	PP (Open)	tip-sand	3.8	4	14	199.943	387.842
41-11/12	PP (Open)	tip-sand	3.8	4	14	136.649	206.542
42-04	HP	tip-sand	3.5	18	14	257.546	278.987
42-06	HP	tip-sand	3	17	14	470.638	220.857
50-01	PP (Open)	tip-sand	2.5	13	16	118.006	153.706
56-01	PP (Open)	tip-sand	3	2	14	147.309	331.691
57-01	HP	tip-rock	2.7	25	10	73.6473	298.117
58-02	CP	tip-sand	3	15	12	334.933	256.85
62-01	HP	tip-sand	1	1	10	214.777	78.0905
65-01/02	HP	tip-cobbles	3	2	12	476.403	265.262
66-01/02	HP	tip-gravel	3	15	12	138.376	238.113
79-01	PP (Open)	tip-clay	4	1277	16	274.434	271.626
79-07/08	PP (Open)	tip-clay	3.5	168	16	270.362	302.053
79-18/19	HP	tip-clay	3.5	188	14	322.242	288.118
85-01/02	PP (Open)	tip-sand	3.5	10	24	149.681	222.214
86-01/02	PP (Open)	tip-sand	3	25	24	168.021	292.464
87-01/02	CP	tip-sand	4	7	14	219.399	127.346
88-01	HP	tip-gravel	3.5	1	14	544.994	434.537
93-01/02	PP (Open)	tip-sand	3	22	72	1844.44	1080.71
94-04	PP (Open)	tip-sand	3	33	24	271.616	639.284
94-06	PP (Open)	tip-sand	3	33	24	143.947	581.567
95-02	PP (Open)	tip-sand	2.8	17	24	359.053	719.064

Project No.	Pile Type	Tip Soil	DQF	Set-up days	Diameter (inch)	Q <sub>c</sub> (kips)	Q <sub>m</sub> (kips)
95-03/04	PP (Open)	tip-sand	2.8	13	24	359.053	117.364
96-03/04	PP (Open)	tip-sand	3	50	16	135.891	331.318
97-03/04	PP (Open)		2.5	17	24	399.208	548.084
98-01/02	PP (Open)	tip-clay	4	35	24	265.529	163.156
98-03/04	PP (Open)	tip-clay	4	33	24	261.546	154.364
99-01/02	PP (Open)	tip-sand	4.5	30	24	358.811	359.388
99-03/04	PP (Open)	tip-sand	4.5	34	24	337.907	172.3
100-01/02	PP (Open)	tip-clay	3.5	15	24	254.076	270.72
102-01	CP	tip-sand	2.8	13	12	137.135	193.875
115-02	CP	tip-sand	3	unk	12	163.221	191.075
125-03	HP	tip-sand	2.8	4	14	911.582	267.378
125-05	CP	tip-sand	2.8	4	14	454.764	299.792
131-01	PP (Open)	tip-gravel	3	11	24	424.016	326.139
132-01	PP (Open)	tip-gravel	2.8	7	24	601.716	343.919
135-01	CP	tip-clay	2	unk	14	385.462	180.812
136-01	PP (Open)	tip-gravel	3	15	87	3948.91	3393.89
142-01/02	PP (Closed)	tip-sand	4.5	28	24	1160	799.468
146-01/02	PP (Open)	tip-sand	3.3	13	48	1281.79	1001.65

Qc VS Qm (For Different Types of Piles)

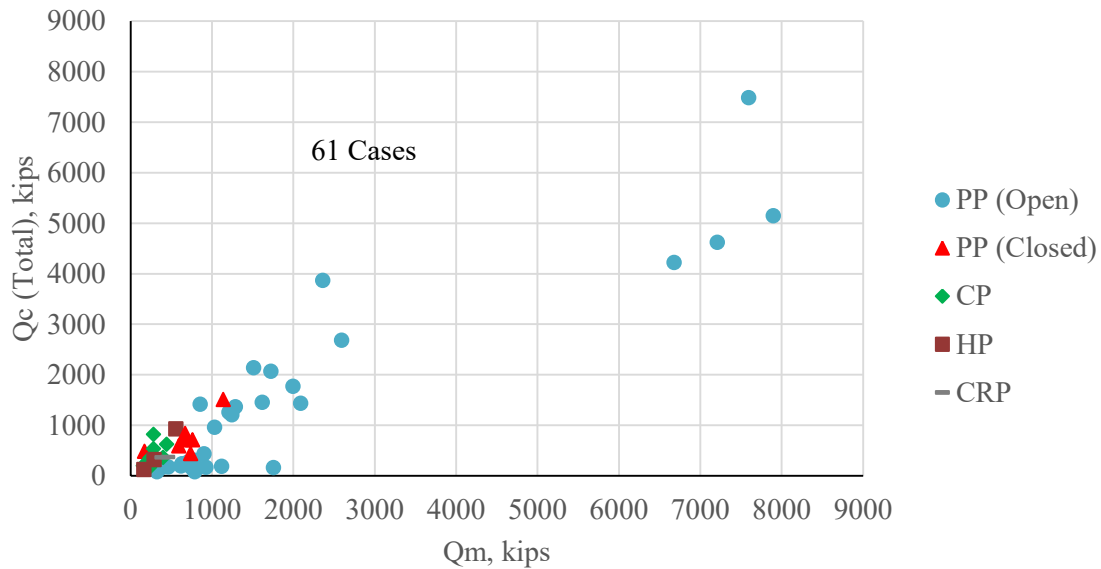


Figure 5-1 Predicted total resistance vs. measured total resistance for compression driven pile load test cases

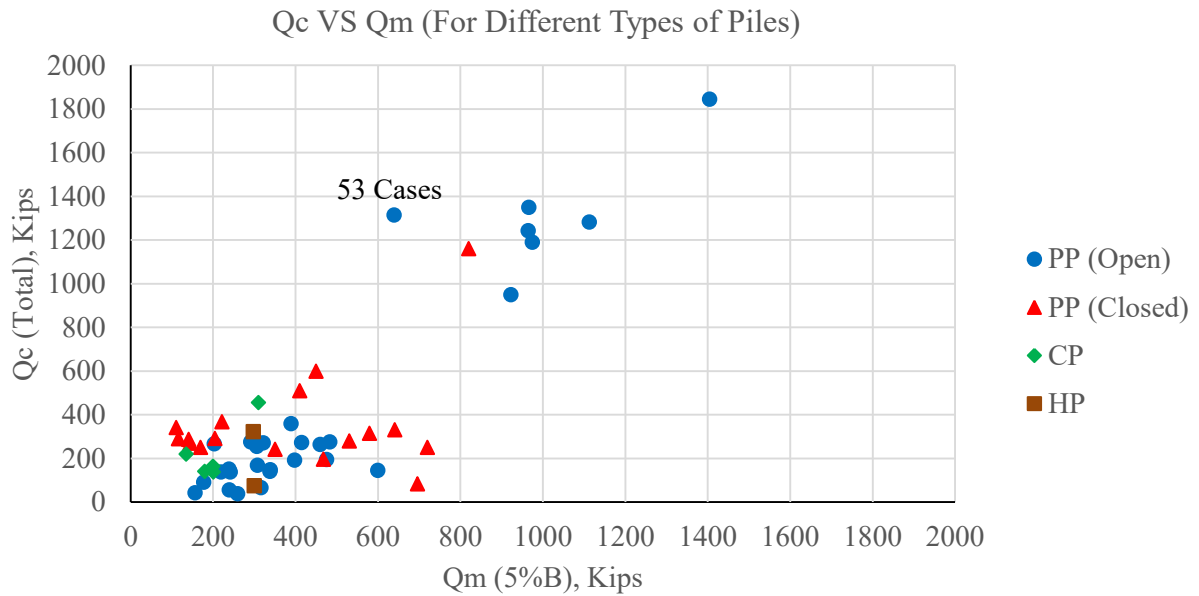


Figure 5-2 Predicted total static resistance vs. measured total resistance for uplift load test cases

### Design Variable Analysis

#### *Residual plots*

Residual is defined as the difference between measured and predicted pile resistance. Ln-residual is defined as the natural log of the residual. Residual plots of various design variables were made to observe their effects on prediction of driven pile static resistance. The design variables presented in the residual plots include predicted static resistance, measured resistance, measured side resistance for sand and clay, measured tip resistance for sand and clay.

The residual plots of measured and predicted static resistance show piles with small resistance (less than 1000 kips for both predicted and measured resistance). Residual plots of predicted side resistance and tip resistance are shown in Figures 5-5 and 5-8. Piles tipped in sand tend to have large uncertainty of the predicted static capacity.

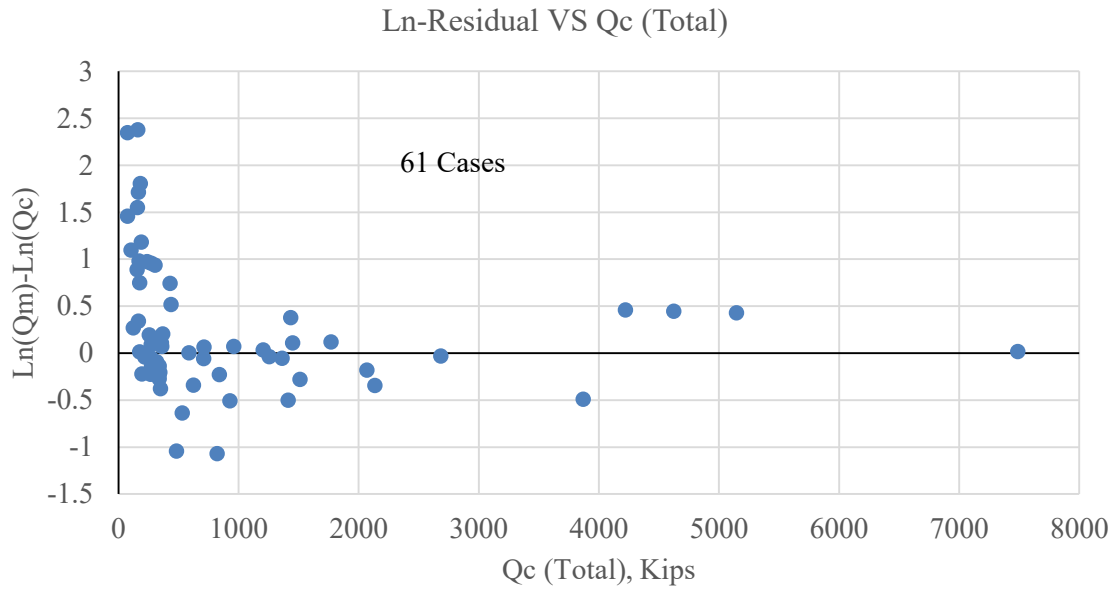


Figure 5-3 Ln-residual at 5% B vs predicted total static resistance for all compression load test cases

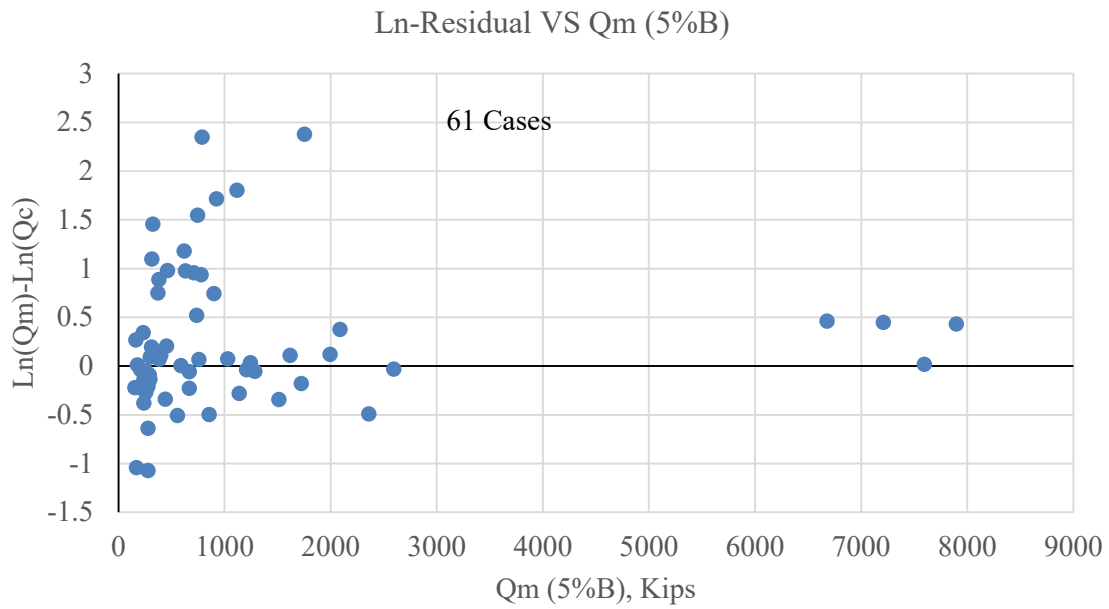


Figure 5-4 Ln-residual at 5% B vs measured total static resistance for all compression load test cases

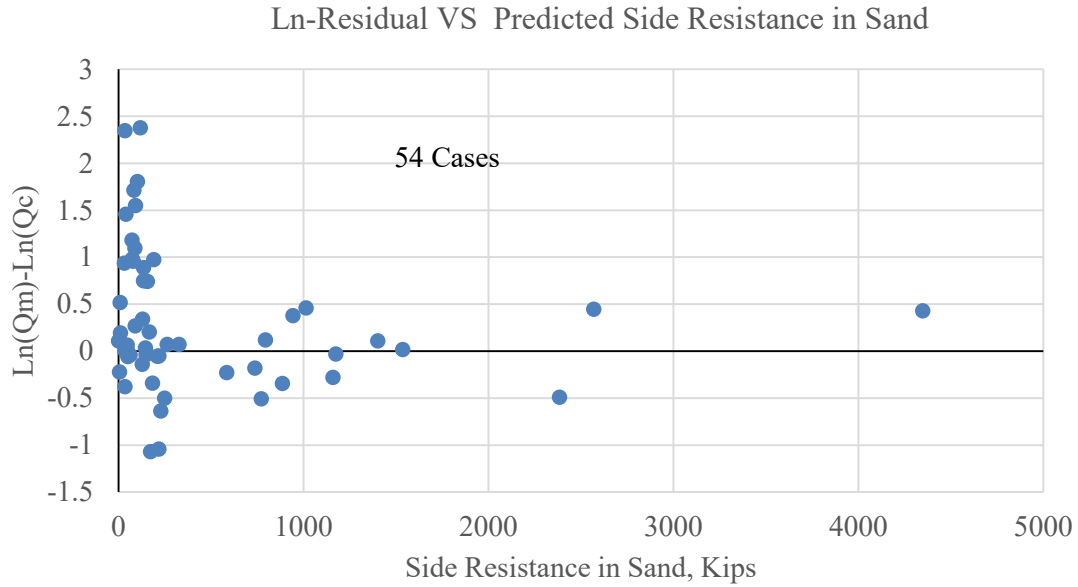


Figure 5-5 Ln-residual at 5% B via FHWA 1999 method vs predicted side resistance in sand for all compression load test cases

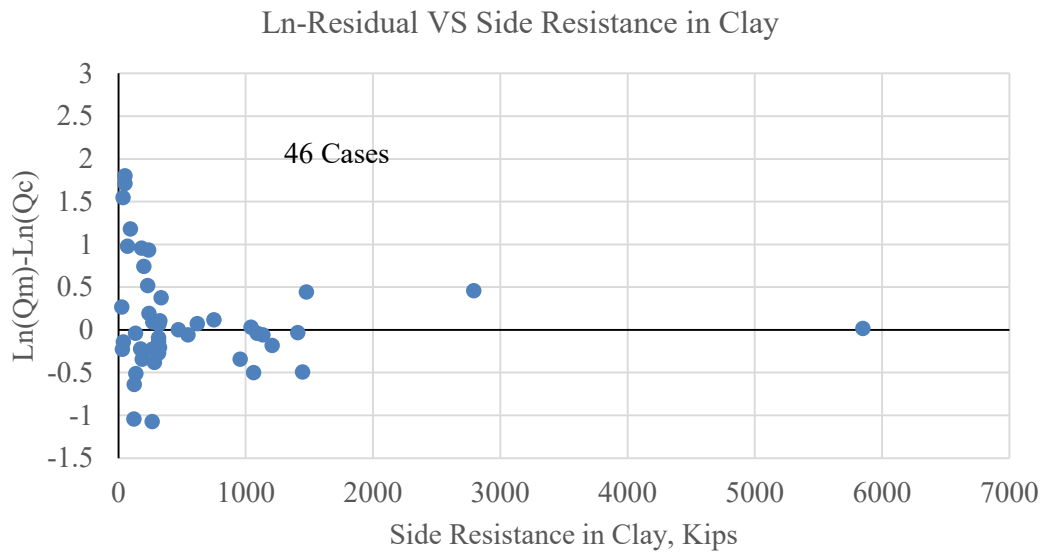


Figure 5-6 Ln-residual at 5% B via FHWA 1999 method vs predicted side resistance in clay for all compression load test cases

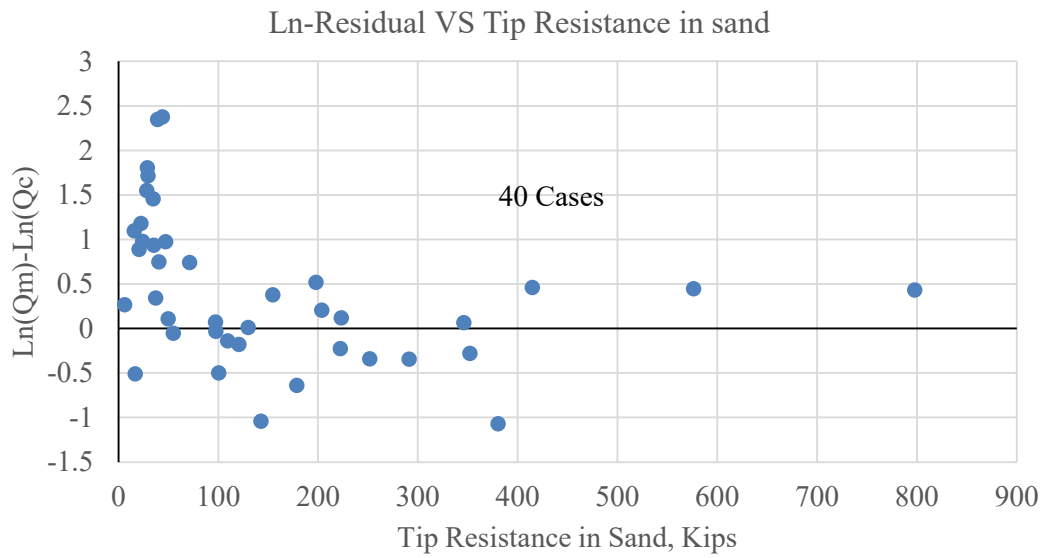


Figure 5-7 Ln-residual at 5% B via FHWA 1999 method vs predicted tip resistance in sand for all compression load test cases

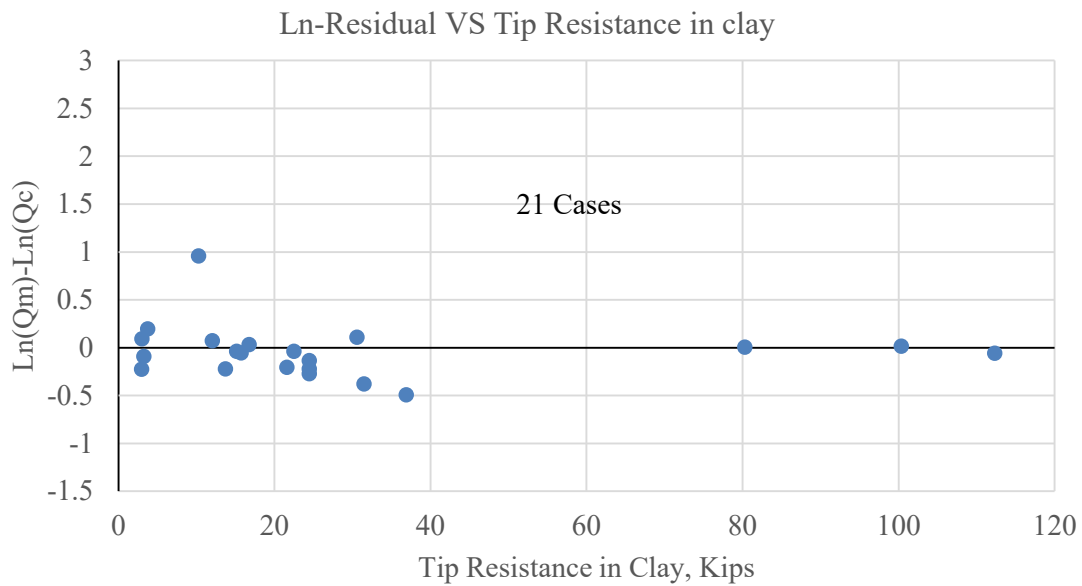


Figure 5-8 Ln-residual at 5% B via FHWA 1999 method vs predicted tip resistance in clay for all compression load test cases

**Breakdown table**

The finalized database listed in Table 5-1 and Table 5-2 (after combination) was broken down to specific sub-datasets according to specified design conditions listed in the Table 5-3 shown below. This breakdown analysis is to group the collected database according to selected design variables. The design variables considered are diameter, pipe type, and soil type along the pile shaft or at the pile tip. For classification of soil type along shaft side, calculated resistance contribution to the total shaft side resistance was used as the classification criteria. Different range (100% and 70%) was chose to determine the dominant soil type. For example, side sand (>70%) filter criteria applies to all piles with more than 70% side resistance calculated from sand regardless of soil type at the tip.

Table 5-3 Filter criteria used for database breakdown analyses of driven pile database

Design variable	criteria	Compression			Uplift		
		Mean	STD.	#	Mean	STD.	#
Diameter	<40"	2.06	2.29	45	1.95	1.67	46
	>40"	1.07	0.32	16	0.77	0.15	7
Pile Type	PP (Open)	2.51	2.48	34	2.00	1.50	29
	PP (Closed)	0.95	0.37	8	1.58	1.92	17
	CP	0.83	0.25	14	1.05	0.38	5
	HP	0.94	0.35	3	2.50	2.23	2
	CRP	1.15	0.11	2			0
Soil Type	Side Sand (100%)	2.98	3.24	15	2.58	2.02	15
	Side Clay (100%)	0.86	0.11	7	0.99	0.18	4
	Side Sand (>70%)	2.51	2.84	22	2.57	1.97	19
	Side Clay (>70%)	1.04	0.42	23	1.07	0.48	21
	Tip-Sand	2.35	2.47	36			NA
	Tip Clay	0.98	0.40	22			NA
	Tip-Silt			1			NA
	Tip-Rock	1.17	0.52	2			NA
<b>ALL</b>	ALL	1.80	2.02	61.00	1.79	1.60	53.00

## Statistical Analysis of Bias

Bias (measured resistance divided by predicted resistance) of the collected driven pile database were plotted in the form of cumulative distribution function (CDF) as shown in Figure 5-9 to Figure 5-12. Two predicted distribution curves: normal distribution and log-normal distribution are shown on the CDF plot. The two predictions were obtained using mean and standard deviation of bias. As shown in the figures, generally the log-normal distribution matches the histogram and CDF better than the normal distribution. In addition, the resistance bias factor ( $\lambda_R = Q_m/Q_c$ ) can range theoretically from 0 to infinity with an optimum value of one; therefore, the distribution of the resistance bias can be assumed to follow a log-normal distribution. In this study, the log-normal distribution was used to evaluate the different methods based on prediction accuracy and to calibrate the resistance factors. The bias distribution for different dataset can also be seen on the histogram plots shown in Figure 5-13 to Figure 5-16. Probability density plot (PDF) of log-normal distribution of the bias is also shown on the same plots. Generally, the log-normal PDF plots match well the well with its histogram plots. Large biases (greater than 3) are observed from the CDF and histogram plots. The calibrated resistance factors are based on the original bias without removing possible outliers (large bias). It is obvious that standard deviation (STD) can be reduced by applying 2STD filter as suggested in NCHR507 report and also commonly seen in other similar resistance factor calibration studies.



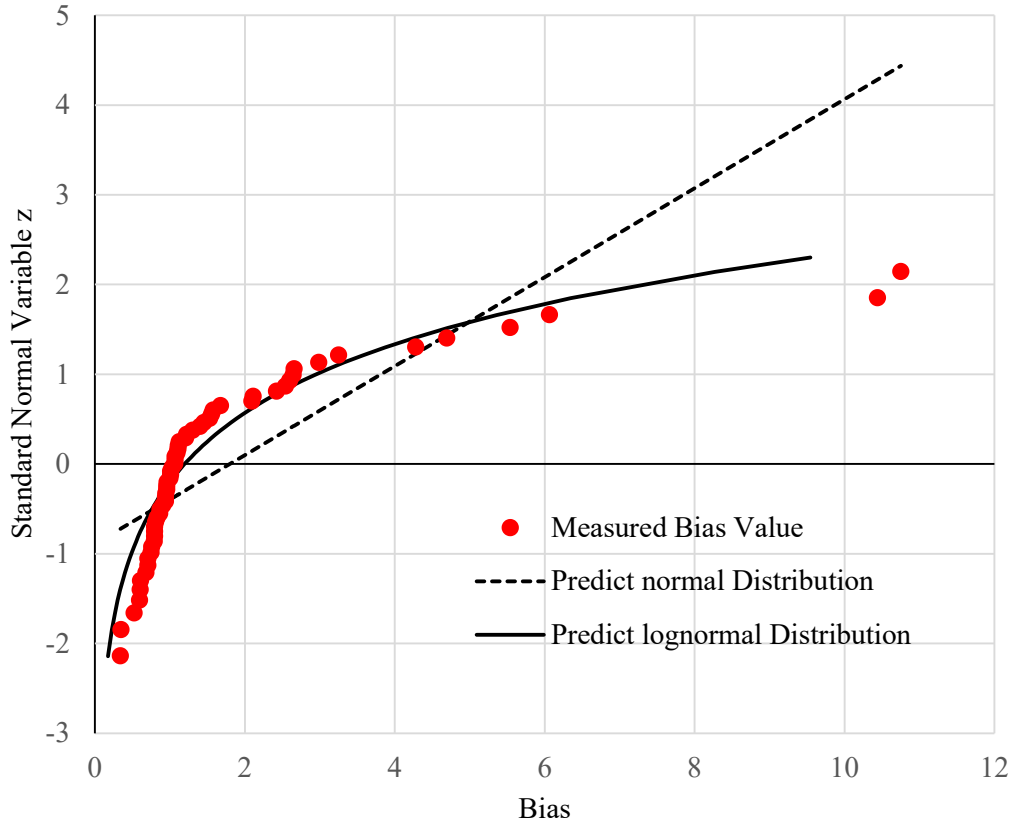


Figure 5-3 CDF curve for 61 compression pile cases

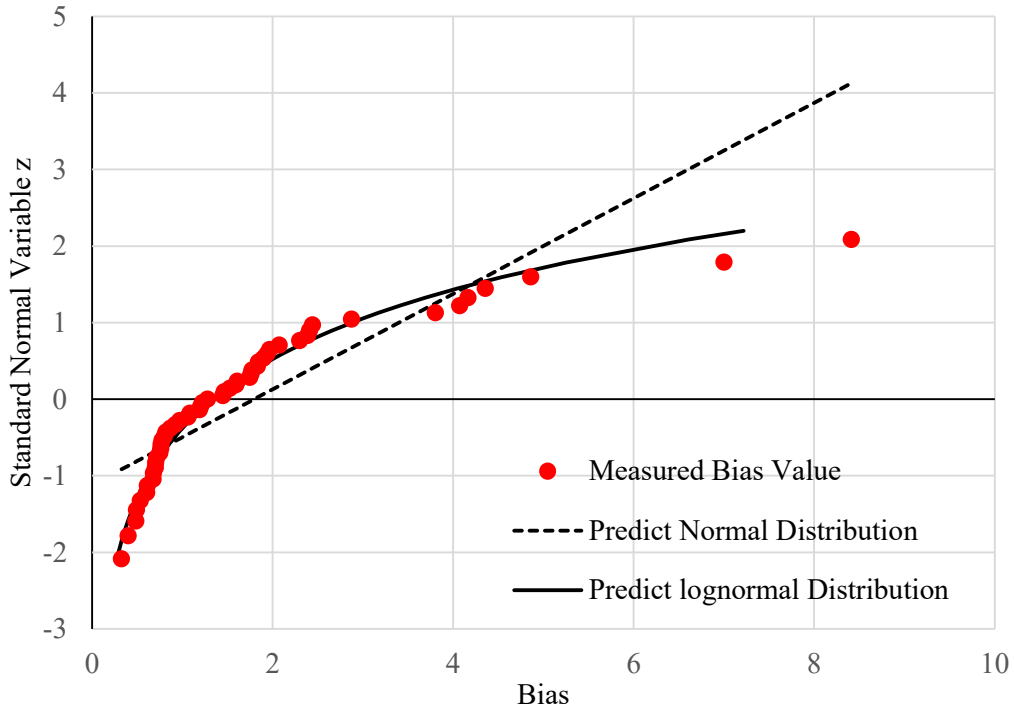


Figure 5-4 CDF curve for 53 uplift pile cases

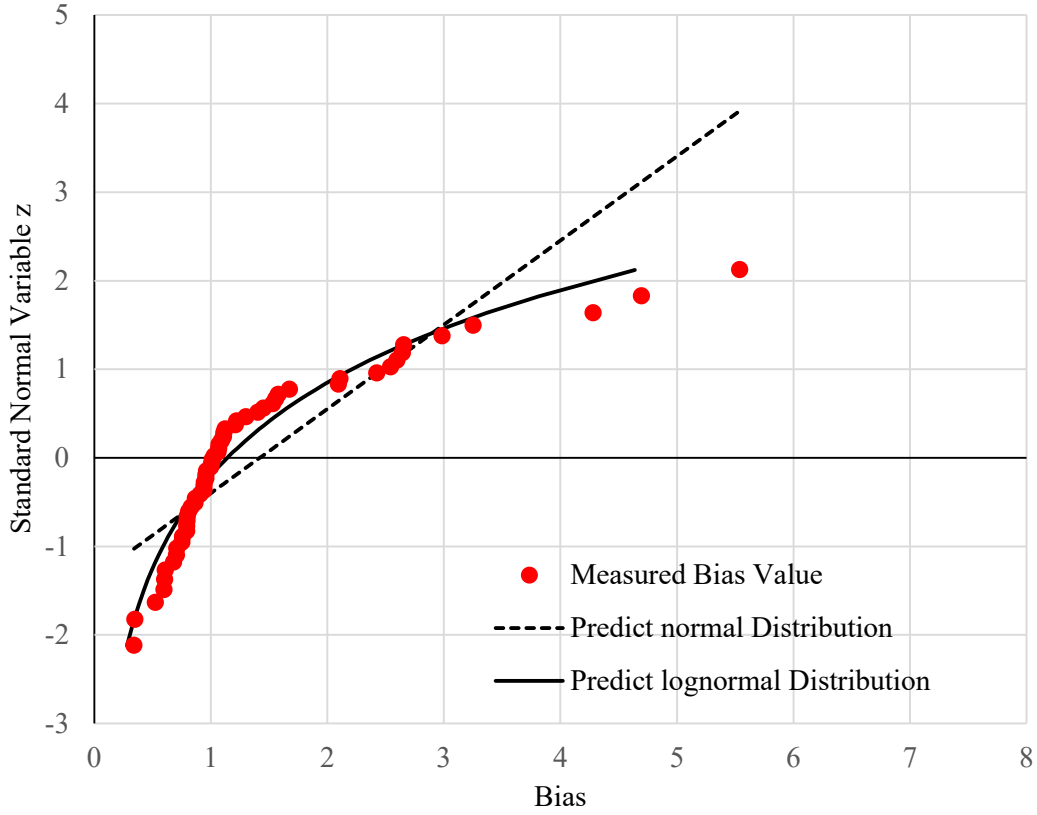


Figure 5-5 CDF curve for 61 compression pile cases filtered with 2STD

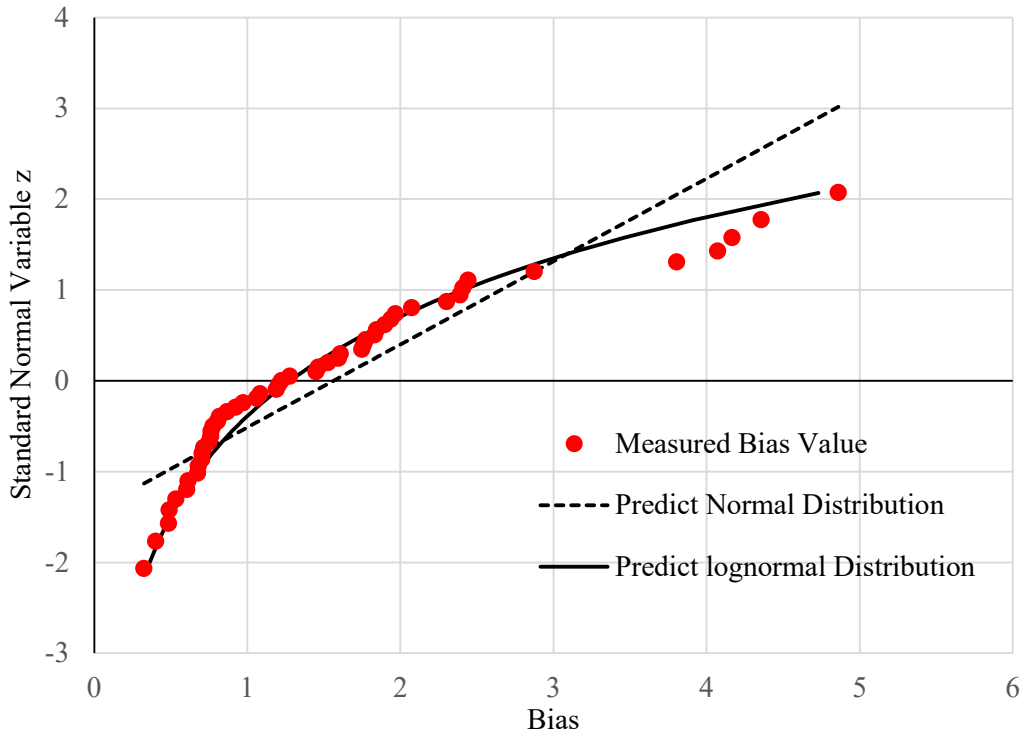


Figure 5-6 CDF curve for 53 uplift cases filtered with 2STD

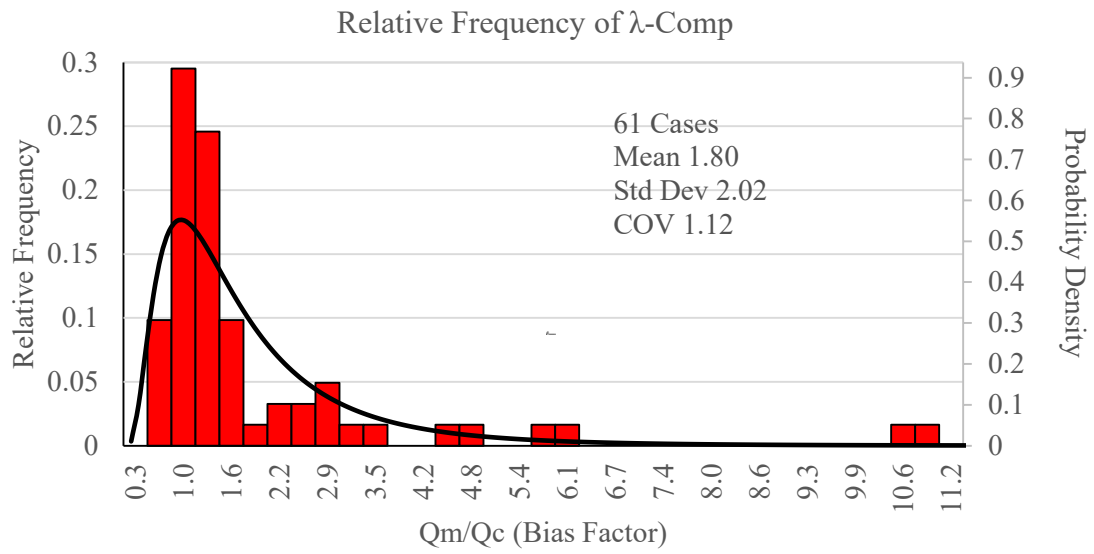


Figure 5-7 PDF and histogram of bias of total for 61compression load test cases

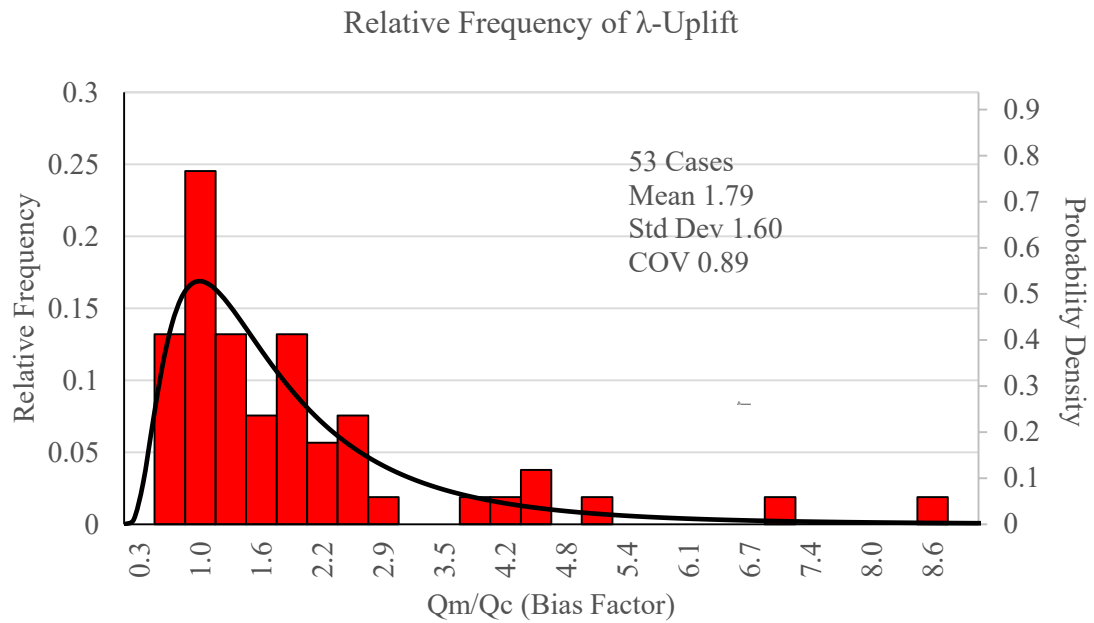


Figure 5-8 PDF and histogram of bias of total resistance for 53 uplift load test cases

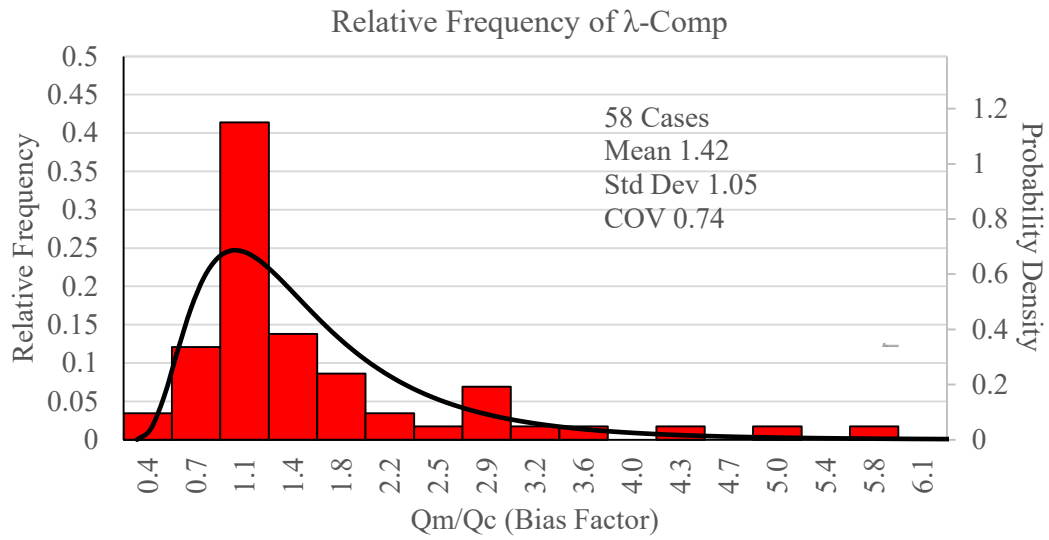


Figure 5-15 PDF and histogram of bias of total for 65 compression load test filtered with 2STD

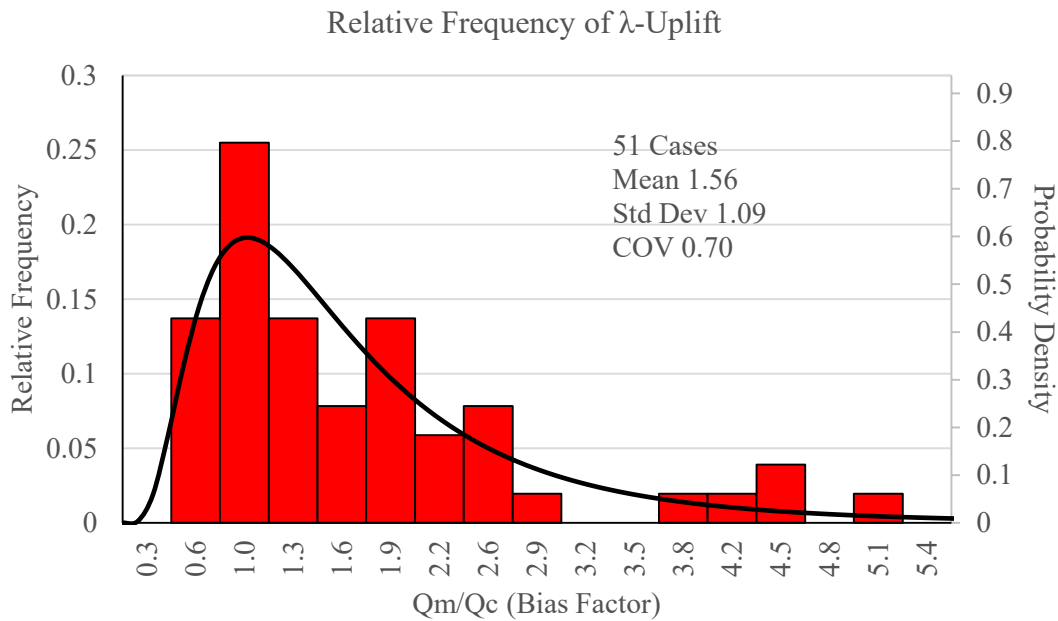


Figure 5-16 PDF and histogram of bias of total resistance for 53uplift load test cases filtered with 2STD

## **Drilled Shaft Results**

### **Predicted vs. Measured Drilled Shaft Resistance**

Nominal drilled shaft resistances were calculated using FHWA 1999 and 2010 design method separately. As Caltrans is still using FHWA 1999 method for drilled shaft design, so both methods are included in the design analyses. 1 inch and 5%B (B: shaft diameter) settlement failure criterion were selected. Predicted resistance ( $R_c$ ) at 1 inch and 5%B settlement criteria were determined. Correspondingly, measured drilled shaft resistances ( $R_m$ ) were also determined at 1 inch and 5%B settlement. The analyses results of all the collected drilled shafts are shown in Table 5-4. The predicted resistance and measured resistance for both 1999 method and 2010 method are plotted in Figure 5-17 to Figure 5-20. Regression analysis was conducted to obtain a line of best fit of the predicted/measured drilled shaft resistances at chosen failure criteria. For 5%B failure criterion, the slope of the best fit line of the 2010 method is 0.80 which is greater than 0.68 of 1999 method. For 1 inch failure criterion, the 1999 method has best fit slope of 0.71 compared with the 0.57 of 2010 method. Through communications with Caltrans bridge foundation engineers, nominal shaft resistance is used as predicted (or calculated) drilled shaft resistance. Therefore, nominal resistance obtained by FHWA 1999 and 2010 method are also compared with measured 1-inch drilled shaft resistance as shown in Figure 5-21 and 5-22. The nominal resistance makes better and more accurate prediction.

### **Data quality check**

Through the data collection effort described in the previous chapter, a list of total 83 drilled shafts was compiled and analyzed among which 45 cases are from Mississippi, 30 cases from Louisiana, and the rest of 8 cases from several western states. The analyses results of these 83 cases were examined through the plots described in the following sections. The plots include predicted vs. measured resistance for different prediction and interpretation methods, residual plots, and histogram and PDF plots of bias. Data quality check was performed through the above plots. Several drilled shaft cases were flagged as possible data outliers that were observed to significantly deviate from the observed trend. The questionable drilled shaft cases were went through thorough quality check for soil profile and load test data. Among these flagged cases, only LT 8487, LT-8829-4 LT-8954-1 and LT-9280-4 were removed from the final database because these cases have very small top shaft movement which is less than 0.01 inch.

Table 5-4 Original results of the analysis conducted on test shafts located in Mississippi, Louisiana, and Western states

Test Shaft	Resistance by 5% B criterion (tons)			Resistance by 1 inch criterion (tons)			Predicted nominal load (tons)	
	Measured (R <sub>m</sub> )	Predicted (R <sub>c</sub> )	Predicted (R <sub>c</sub> )	Measured (R <sub>m</sub> )	Predicted (R <sub>c</sub> )	Predicted (R <sub>c</sub> )	1999	2010
		1999	2010		1999	2010		
LT-8193-1	3133	1965	2023	2659	1661	1387	2088	2010
LT-8193-2	1569	1781	1820	1314	1539	1283	1893	1792
LT-8194	2165	795	902	2013	738	800	889	899
LT-8212	3754	1214	1261	3443	999	889	1287	1285
LT-8341	836	565	624	617	495	510	624	624
LT-8371-1	1551	597	746	1469	540	661	653	746
LT-8371-2	2581	1764	1945	2296	1520	1553	1945	1945
LT-8373	864	920	1005	805	845	926	1005	1005
LT-8461-1	2473	2004	2275	2363	1887	2019	2275	2275
LT-8461-2	1437	796	791	1304	768	702	1004	878
LT-8488-1	1315	341	389	990	323	345	389	389
LT-8488-2	444	453	505	355	415	448	505	505
LT-8578	3115	3276	3335	1928	2449	2059	3490	3415
LT-8618	725	306	339	710	278	301	339	339
LT-8655	4592	2579	3301	1971	2543	2113	2813	3001
LT-8745	963	1093	1171	796	1025	981	1190	1171
LT-8786	1296	1212	1229	931	867	803	1280	1294
LT-8788	213	243	279	207	242	279	279	279
LT-8800-1	1546	2291	1840	1061	2158	1342	2442	1778
LT-8800-2	1440	1846	1480	1096	1711	1313	1995	1589
LT-8800-3	1259	2246	2052	814	2115	1497	2405	1975
LT-8800-4	2180	2577	2204	1463	2222	1473	2744	2206
LT-8800-5	1093	1919	1556	870	1803	1135	2051	1496

LT-8800-6	1261	2197	1666	885	2068	1215	2346	1624
LT-8800-7	1092	797	1185	858	672	864	848	1187
LT-8800-8	847	901	1479	576	782	1079	958	1427
LT-8825	1100	1155	1493	914	899	975	1289	1505
LT-8829-1	1119	987	1016	871	743	851	1195	1186
LT-8829-3	501	549	550	480	454	401	576	565
LT-8905	492	579	635	460	511	546	635	635
LT-8912-1	2675	1048	1169	2446	963	1037	1169	1169
LT-8912-2	3381	1006	1120	3381	922	994	1120	1120
LT-8954-2	1070	1256	1160	781	1187	846	1346	1164
LT-8981	1226	1439	1469	992	1223	1036	1529	1474
LT-9147	1350	466	575	1169	421	460	493	562
LT-9191	3424	1426	1825	2669	1255	1251	1555	1830
LT-9262	4497	1156	1211	3379	939	1014	1273	1382
LT-9263	1431	952	1339	1169	906	977	1024	1299
LT-9280-1	673	693	674	524	589	598	746	784
LT-9280-2	4303	6019	8023	3019	6017	5044	6461	7292
LT-9280-3	2641	2352	2187	1873	1940	1428	2507	2214
LT-9459-2	788	498	669	713	456	593	669	669
LT-9459-3	380	385	430	367	382	422	430	430
LT-9459-4	605	685	750	579	642	665	750	750
LT-9473-1	3008	1677	2203	2456	1378	1438	2139	2248
LT-9473-2	2282	2872	2996	1797	2476	2002	3026	2929
LT-9597-1	786	1118	1258	705	857	841	1238	1417
LT-9597-2	786	1118	1258	705	857	841	1182	1280
LT-9694-1	1115	981	1272	918	981	1272	1213	1363
LT-8467	1583	1577	1926	1298	1207	1287	1715	1957
LT-9694-3	3249	3013	3485	2105	2674	2329	3209	3374

LT-9694-4	2055	1098	1191	1670	980	973	1212	1191	
LT-9934-1	1049	1073	1337	919	768	893	1316	1393	
LT-9934-3	1459	1123	1194	1045	897	842	1188	1224	
LT-9934-4	959	676	881	880	528	588	869	900	
LT-9934-5	968	851	818	787	580	547	894	884	
LT-9938-1	552	617	700	496	443	468	775	748	
LT-9938-3	797	824	893	650	629	630	870	931	
LT-9950-1	2692	1221	2126	2039	865	1421	1493	2139	
LT-9950-2	757	869	864	618	751	577	918	847	
455-08-20, #2	1007	451	572	1007	430	488	500	543	
455-08-20, #3	784	393	444	710	371	378	421	433	
8412, #2	343	231	278	298	226	266	264	278	
8470	1560	1392	1630	1140	1020	1089	1472	1544	
8915	1750	1199	1431	1495	1182	1120	1161	1248	
8961, #1	888	519	706	730	498	602	577	655	
8961, #2	599	388	627	582	386	534	416	576	
8412, #1	283	244	286	271	238	281	273	286	
8944	531	409	571	531	401	460	368	498	
455-08-47, 2A	405	276	351	394	269	332	325	325	
455-08-47, 2B	428	437	498	428	416	472	497	486	
FHWA/CA/TL-94-02	Shaft was not loaded or can't be extrapolated to 5%B settlement.				426	460	563	514	736
FHWA/CA/TL-94-02					655	591	640	663	684
NH10-4(151)/LT-8595					11240	8719	7051	11059	11083
LT-9611					2279	1307	1534	1673	2209
LT-9604-01					11159	11337	8098	13012	12568
LT-9604-02					12946	5235	3947	7587	6848
LT-9604-03	0.4" Max. Sett.				2054	2687	2635	4054	
LT-9258	0.55" Max. Sett.				1618	1362	2349	2424	



Note: Original cases LT-8800-1 to LT-8800-8 had been combined into 1 case shown in the last row of the table below. Therefore the total shaft number had been reduced from 79 to 72.

Table 5-5 Original 8 cases and combined new shaft case

Test Shaft	Resistance by 5%B criterion (tons)			Resistance by 1 inch criterion (tons)			Predicted Nominal load (tons)	
	Measured (R <sub>m</sub> )	Predicted (R <sub>c</sub> )	Predicted (R <sub>c</sub> )	Measured (R <sub>m</sub> )	Predicted (R <sub>c</sub> )	Predicted (R <sub>c</sub> )		
		1999	2010		1999	2010	1999	2010
LT-8800-1	1546	2291	1840	1061	2158	1342	2442	1778
LT-8800-2	1440	1846	1480	1096	1711	1313	1995	1589
LT-8800-3	1259	2246	2052	814	2115	1497	2405	1975
LT-8800-4	2180	2577	2204	1463	2222	1473	2744	2206
LT-8800-5	1093	1919	1556	870	1803	1135	2051	1496
LT-8800-6	1261	2197	1666	885	2068	1215	2346	1624
LT-8800-7	1092	797	1185	858	672	864	848	1187
LT-8800-8	847	901	1479	576	782	1079	958	1427
New LT-8800 (combined)	1340	1847	1683	953	1691	1240	1974	1660

Besides, eight drilled shaft cases LT-8800-1 to LT-8800-8 from one bridge project in Mississippi were combined to one case with the average results of the eight cases. These eight cases have similar drilled shaft diameter of 4.5 ft. and 100 ft. of length, with mostly sand and gravel soils along the side and cohesion less IGM at the tip. These eight cases were constructed with wet method using casing. The resulted bias is very close for each case and all less than 1. To eliminate its single source effect, the eight cases were combined to one case. By comparing the calibration results with 8 cases and one combined cases, a resistance factor increase of around 0.03 is observed. Therefore, the shaft number in Mississippi has reduced to 34, and total number of selected shaft cases has decreased to 72. Among the 72 cases, there are two cases (LT-9604-03, WA; LT-9258, AZ) that have top shaft settlement much less than 1 inch, 0.4 inch for LT-9604-03, and 0.55 inch for LT-9258. All the calibration results are based on the finalized database.

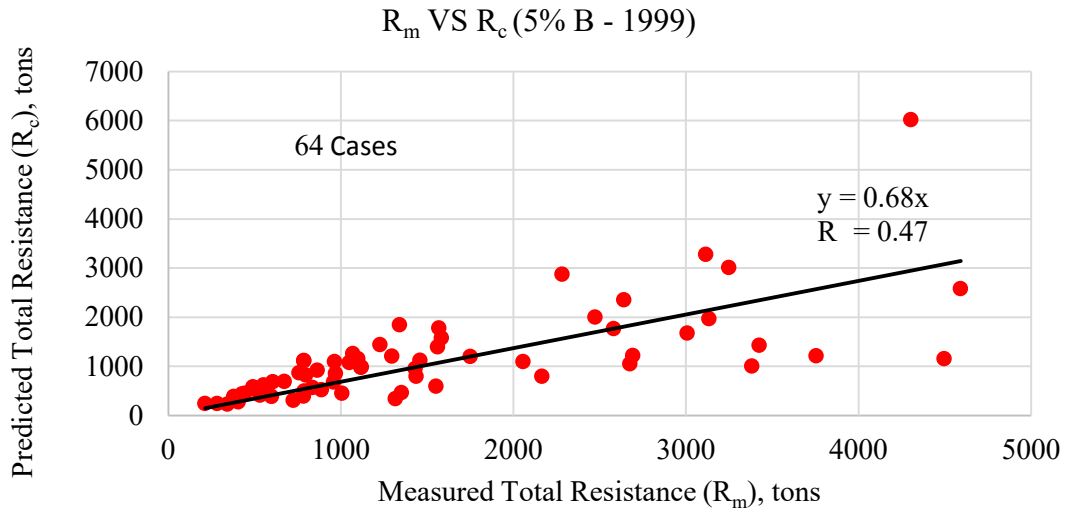


Figure 5-97 FHWA 1999 predicted total resistance vs. measured total resistance at 5% B

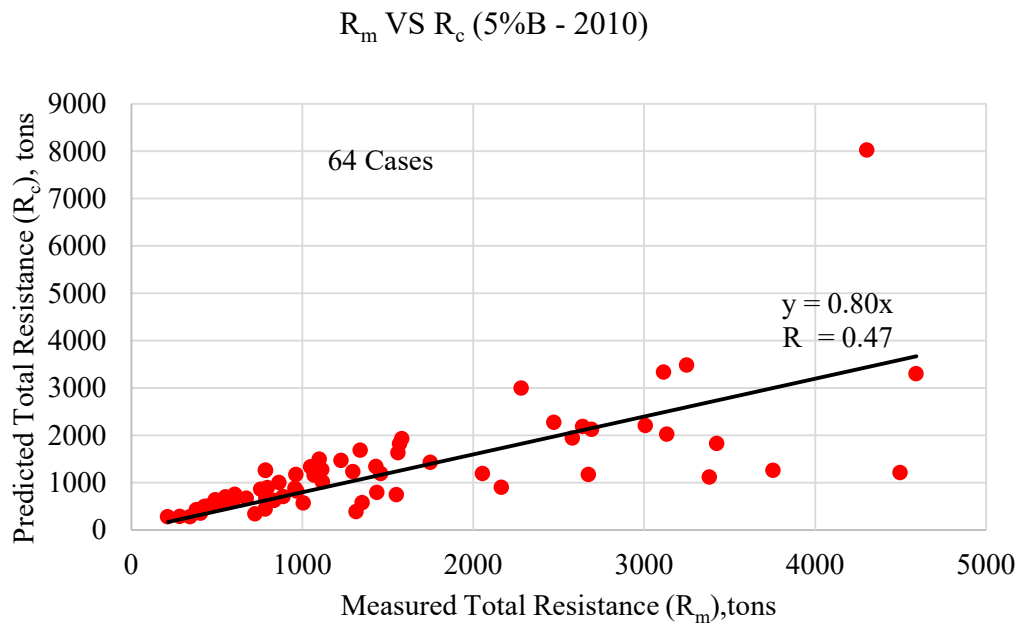


Figure 5-18 FHWA 2010 predicted total resistance vs. measured total resistance at 5% B

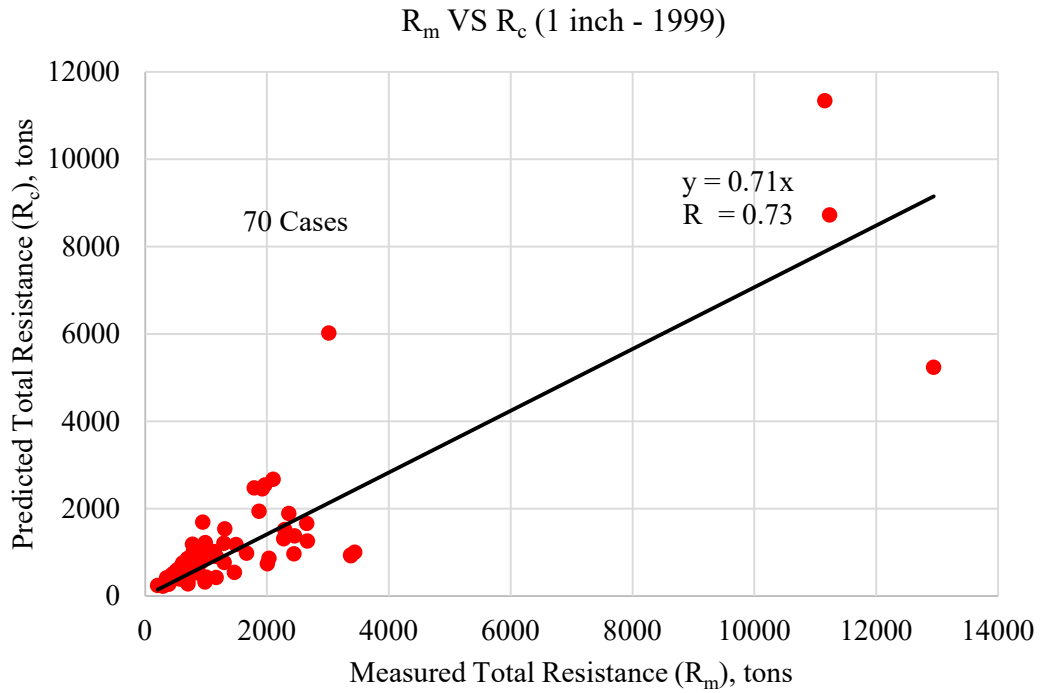


Figure 5-19 FHWA 1999 predicted total resistance vs. measured total resistance at 1 inch

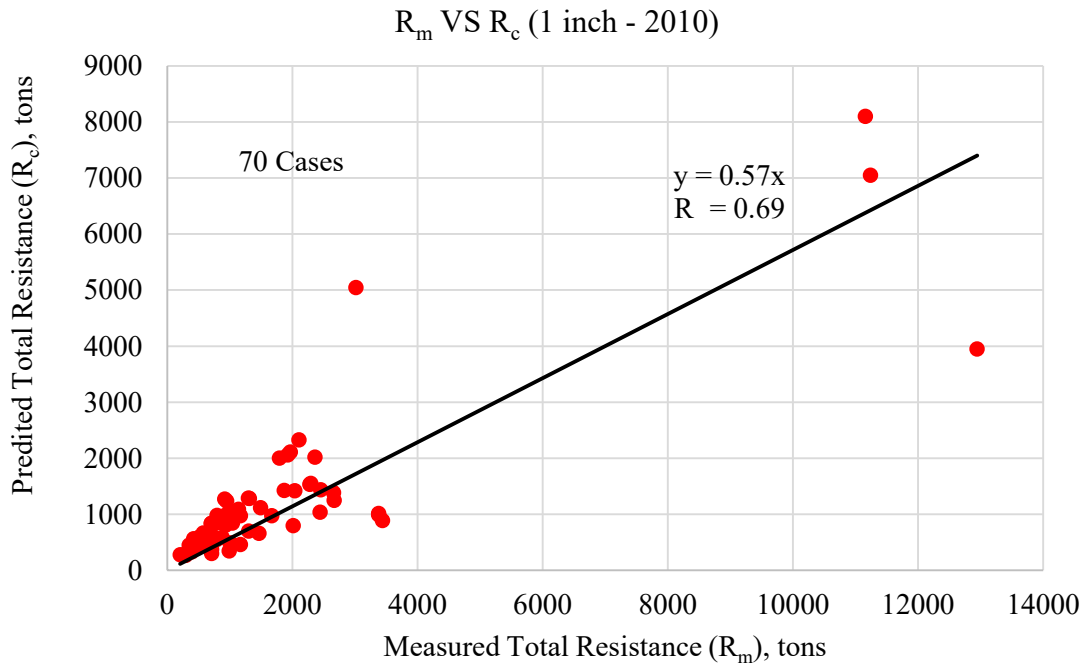


Figure 5-20 FHWA 2010 predicted total resistance vs. measured total resistance at 1 inch

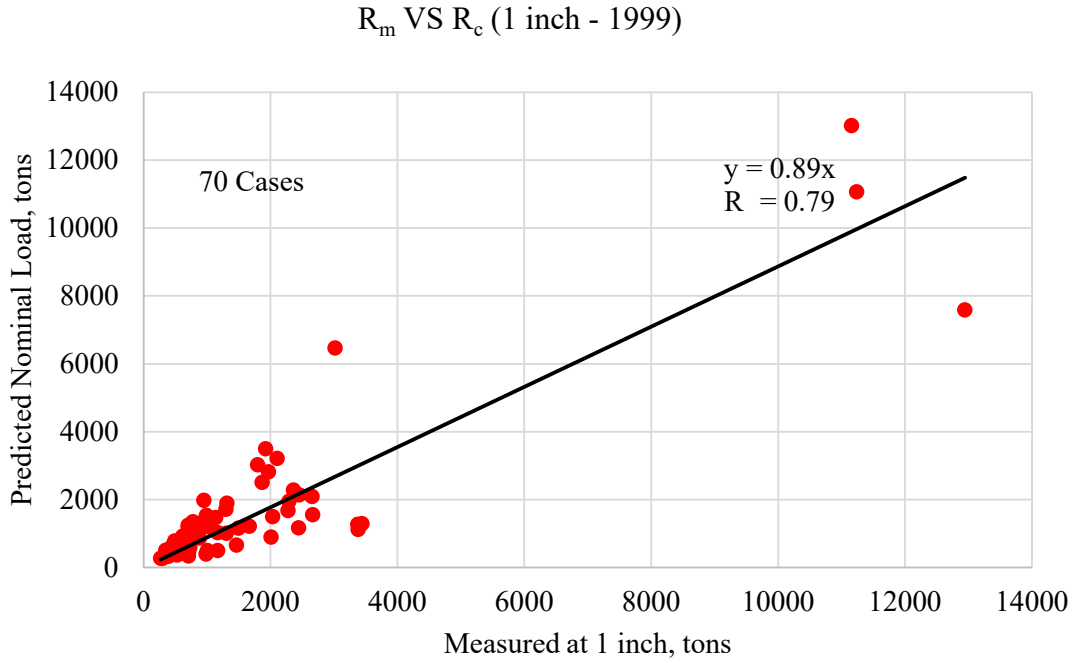


Figure 5-21 FHWA 1999 predicted nominal resistance vs. measured resistance at 1 inch

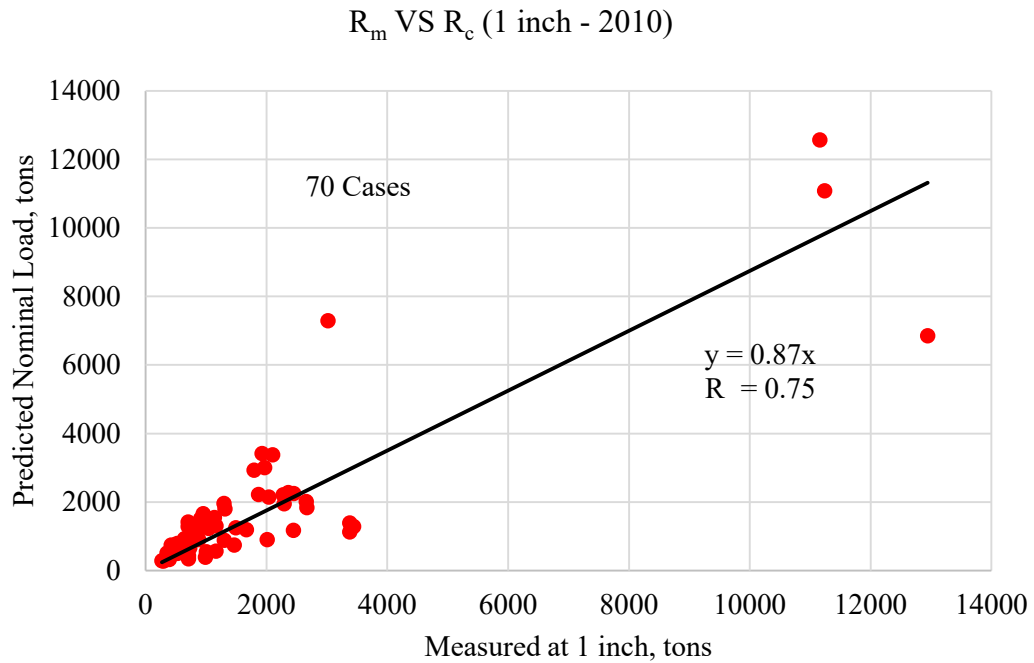


Figure 5-22 FHWA 2010 predicted nominal resistance vs. measured resistance at 1 inch

## Statistical Analyses of Total Resistance

From the results of Table 5-4 and Table 5-5, a statistical analysis was first conducted on the final database of 72 drilled shaft cases to evaluate the statistical characteristics of the total drilled shaft resistance at chosen design/failure criterion. The corresponding resistance bias factor ( $\lambda_R$ ), which is the mean ratio between the measured resistance and the predicted resistance ( $R_m/R_c$ ), was determined. The standard deviation ( $\sigma$ ) and the coefficient of variation (COV) of the bias ( $\lambda_R=R_m/R_c$ ) were also calculated and summarized in Table 5-6. In the bias analysis, measured resistance was interpreted according to both 1 inch and %5 B (diameter of shaft failure criteria. Calculated resistance (or predicted resistance) was determined at the same failure criterion. Predicted resistance was also chosen as nominal resistance by the prediction method. Comparing the statistical analyses results between 1999 method and 2010 method for various biases, 2010 method has slightly less mean values and standard deviation while the COVs for the two methods are approximately the same.

Table 5-6 Statistical summary of biases

Bias	$R_m/R_c$			#
	mean	std	COV	
$R_m$ (5% B)/ $R_c$ (5% B) -1999	1.49	0.77	0.52	64
$R_m$ (5% B)/ $R_c$ (5% B) -2010	1.29	0.68	0.53	64
$R_m$ (1")/ $R_c$ (1") -1999	1.44	0.75	0.52	70
$R_m$ (1")/ $R_c$ (1") -2010	1.40	0.72	0.51	70
$R_m$ (1")/ $R_c$ (nominal) -1999	1.14	0.60	0.53	70
$R_m$ (1")/ $R_c$ (nominal) -2010	1.09	0.58	0.53	70

The COV of  $R_m/R_c$  for different prediction method is around 0.52, which agrees well with the COV for the O'Neill and Reese design method (0.27 - 0.74) as reported by Paikowsky (2005).

Figure 5-23 to Figure 5-28 present the histogram and the lognormal distribution of bias of the drilled shaft ( $R_m/R_c$ ) calculated using different design and failure criteria. As shown in these figures, lognormal distribution matches the histogram of the drilled shaft data; therefore, lognormal distribution was used here in the reliability calibration analysis. The mean and standard deviation of  $\lambda_R$  obtained by statistic calculation shown in Table 5-6 were used in the LRFD calibration process as will be described in the following section.

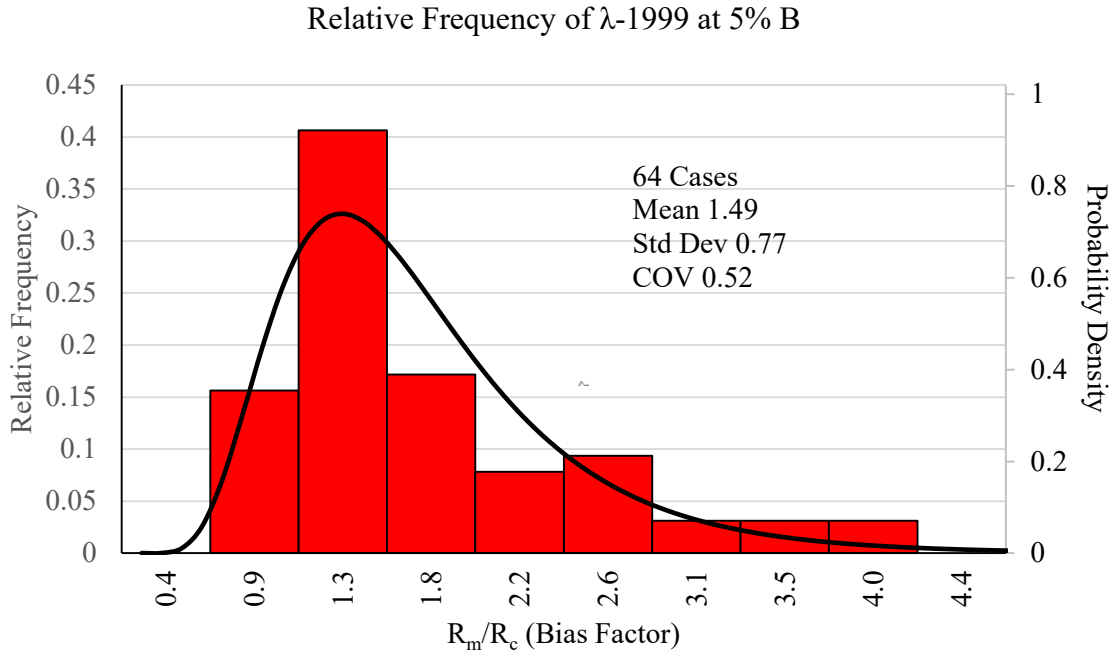


Figure 5-23 PDF and histogram of bias of total resistance at 5% B via FHWA 1999 method

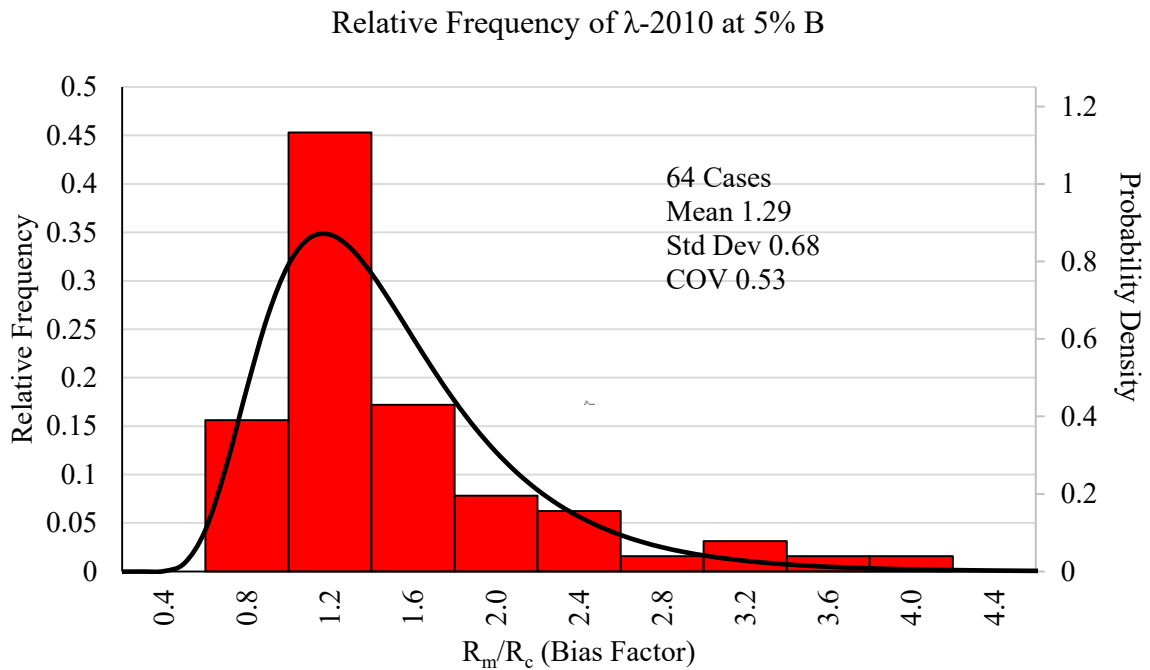


Figure 5-24 PDF and histogram of bias of total resistance at 5% B via FHWA 2010 method

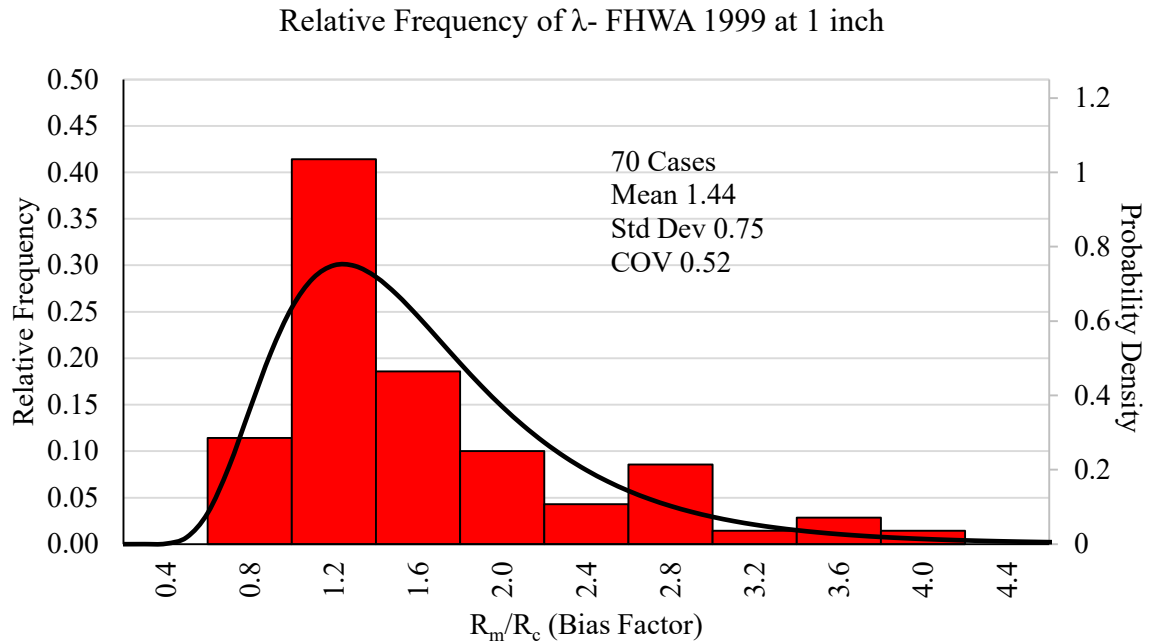


Figure 5-25 PDF and histogram of bias of total resistance at 1 inch via FHWA 1999 method

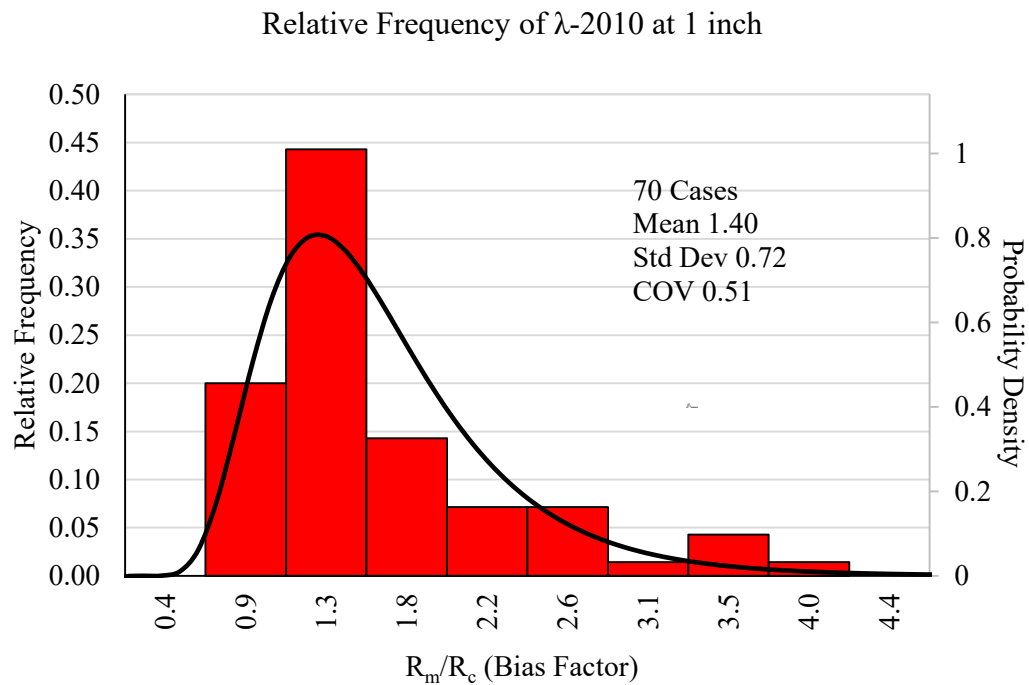


Figure 5-26 PDF and histogram of bias of total resistance at 1 inch via FHWA 2010 method

Relative Frequency of  $\lambda$ -1999 at 1 inch

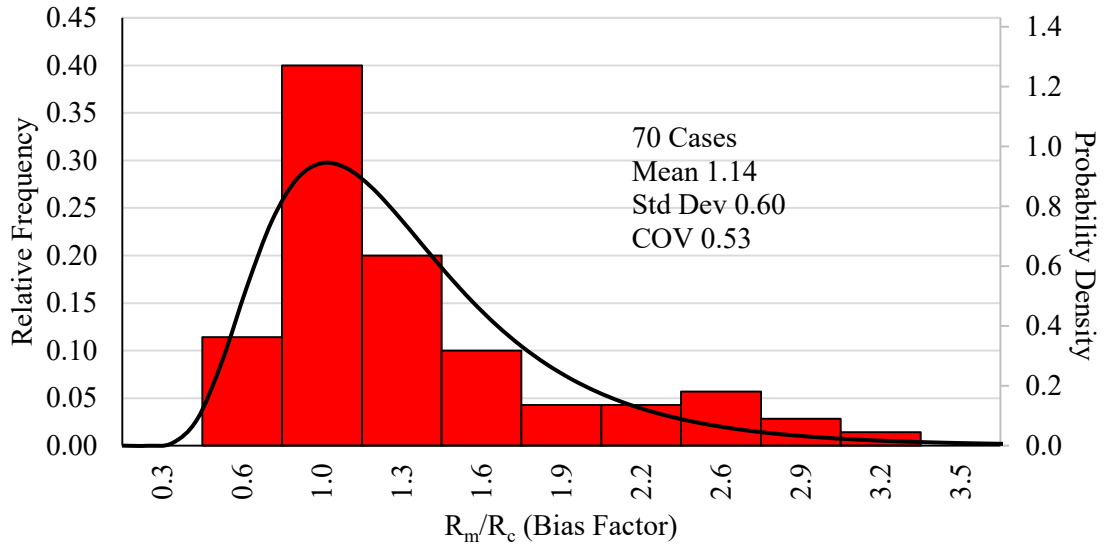


Figure 5-27 PDF and histogram of bias of measured resistance at 1 inch and nominal resistance via FHWA 1999 method

Relative Frequency of  $\lambda$ -2010 at 1 inch

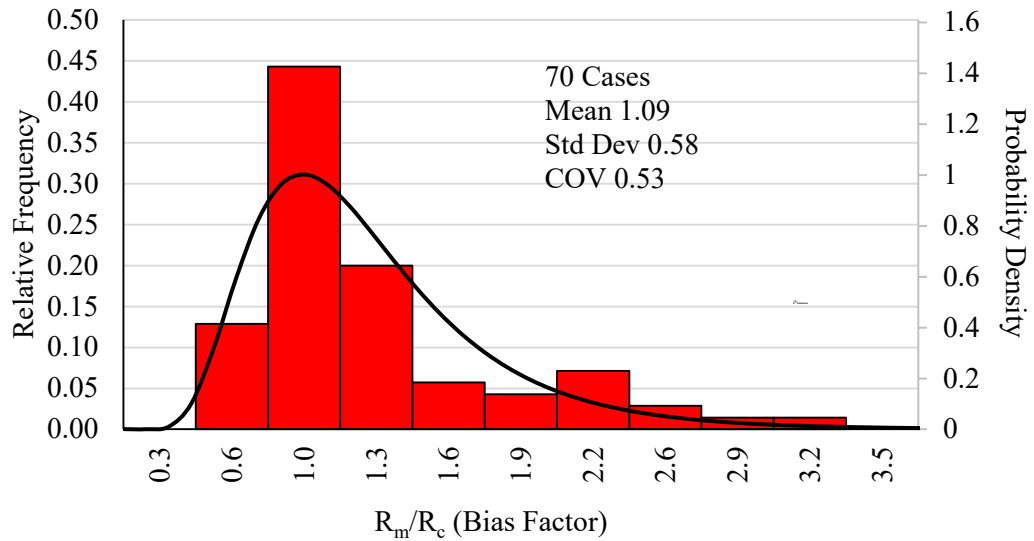


Figure 5-28 PDF and histogram of bias of measured resistance at 1 inch and nominal resistance via FHWA 2010 method



## Design variable analysis

### *Residual plots*

Residual is defined as the difference between measured and predicted drilled shaft resistance. Ln-residual is defined as the natural log of the residual. Residual plots of various design variables were made to observe their effects on prediction method of drilled shaft resistance. The design variables presented in the residual plots include diameter, length, measured resistance, measured side resistance for all soil type and for side in clay only, measured tip resistance for all soil type, clay, sand, and IGM. The residual plots of diameter and length show large diameter (>7 ft.) and long length (>100 ft.) drilled shafts tend to have less conservative prediction of drilled shaft resistance. More data is needed to further verify this observation. Residual plots of measured side resistance as well as predicted side resistance (not shown) are shown in Figures 5-32 and 5-33. It appears that shafts constructed in clay soil along the shaft demonstrate slightly higher bias as compared to the other two soil type (sand and IGM). Residual plots of measured tip resistance as well as predicted tip resistance (not shown) are shown in Figures 5-34 to 5-37. Similar to the soil type along shaft, no obvious effect of tip soil type on the plotted ln-residual is observed. Figure 5-38 shows the ln-residual of construction method. Drilled shafts constructed with wet construction method shows slightly higher variation and tend to have lower bias as compared with dry method. Drilled shafts with no construction methods reported show much less variance.

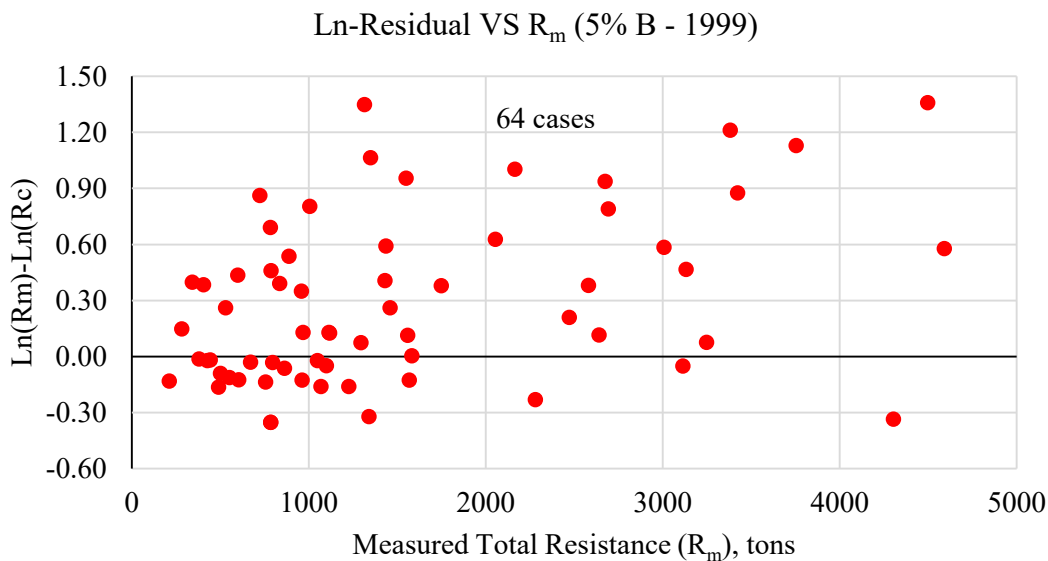


Figure 5-29 Ln-residual at 5% B via FHWA 1999 method vs measured total resistance

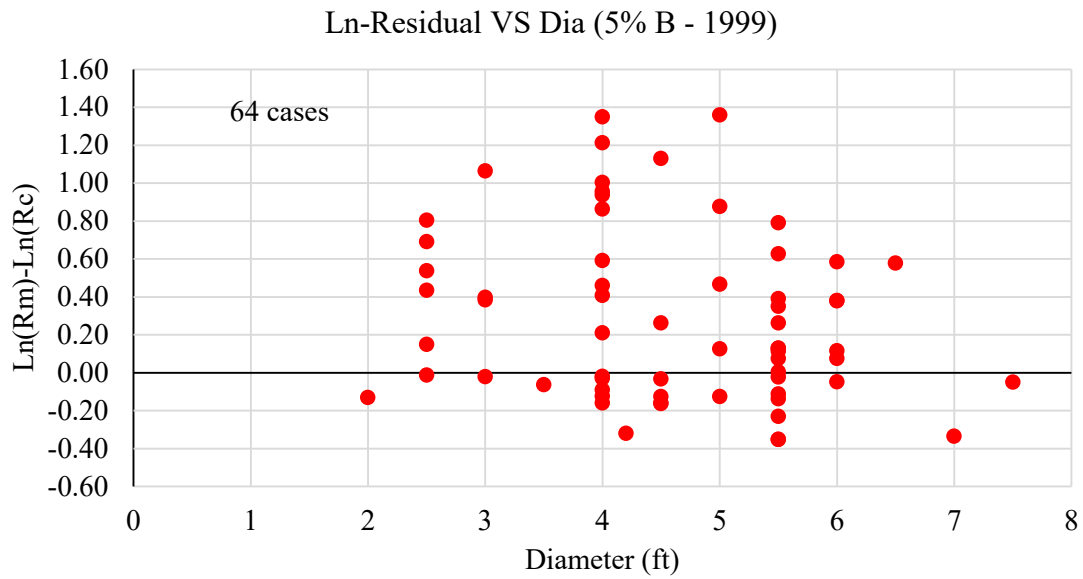


Figure 5-30 Ln-residual at 5% B via FHWA 1999 method vs diameter of shaft

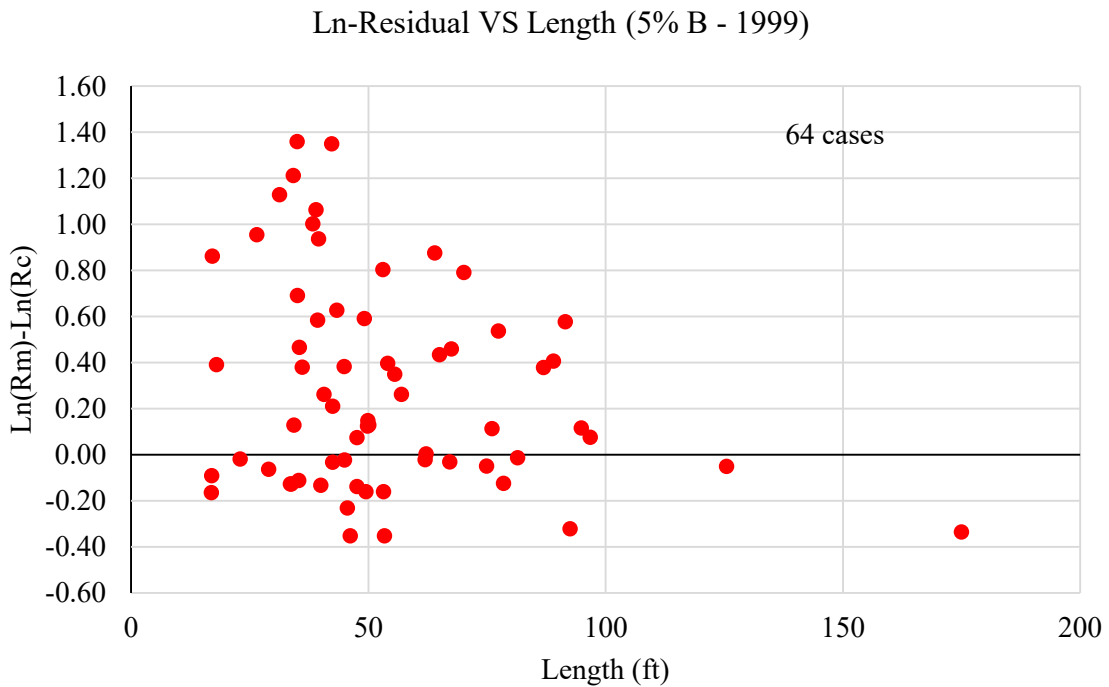


Figure 5-31 Ln-residual at 5% B via FHWA 1999 method vs length of shaft

Ln-Residual VS Measured Side Resistance (5% B - 1999)

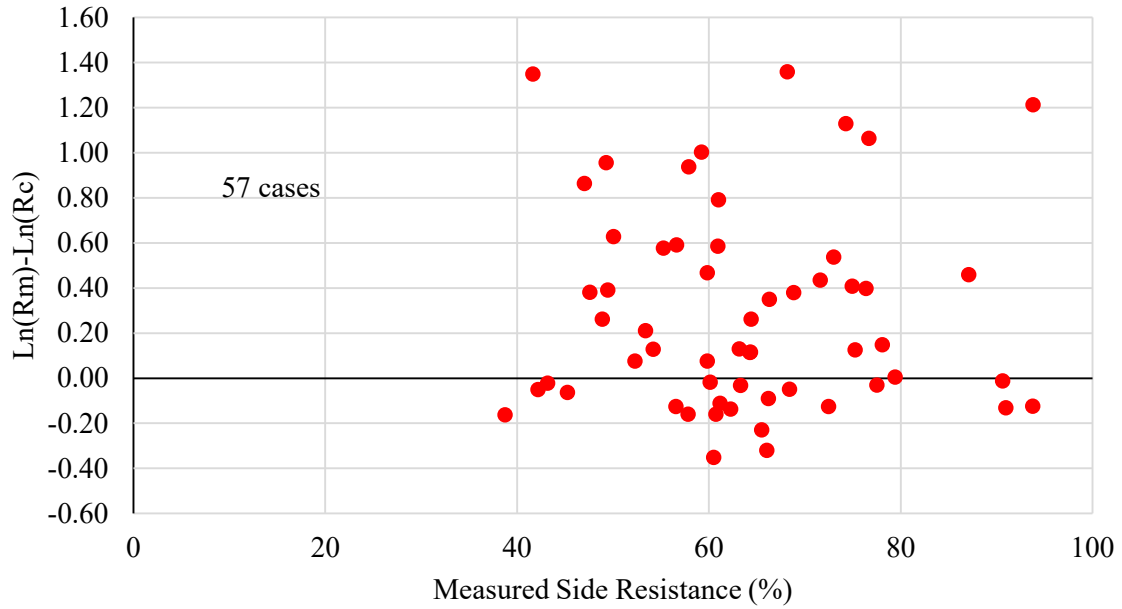


Figure 5-32 Ln-residual via FHWA 1999 method vs measured side resistance at 5% B

Ln-Residual VS Measured Side Resistance-Clay (5% B - 1999)

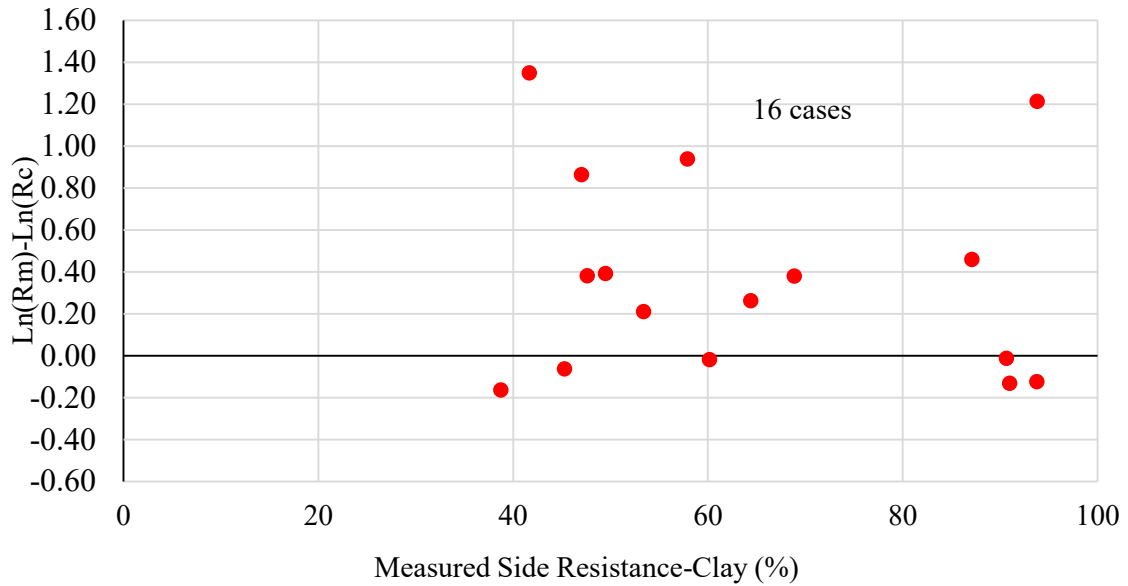


Figure 5-33 Ln-residual via FHWA 1999 method vs measured side resistance in clay at 5% B

Ln-Residual VS Measured Tip Resistance (5% B - 1999)

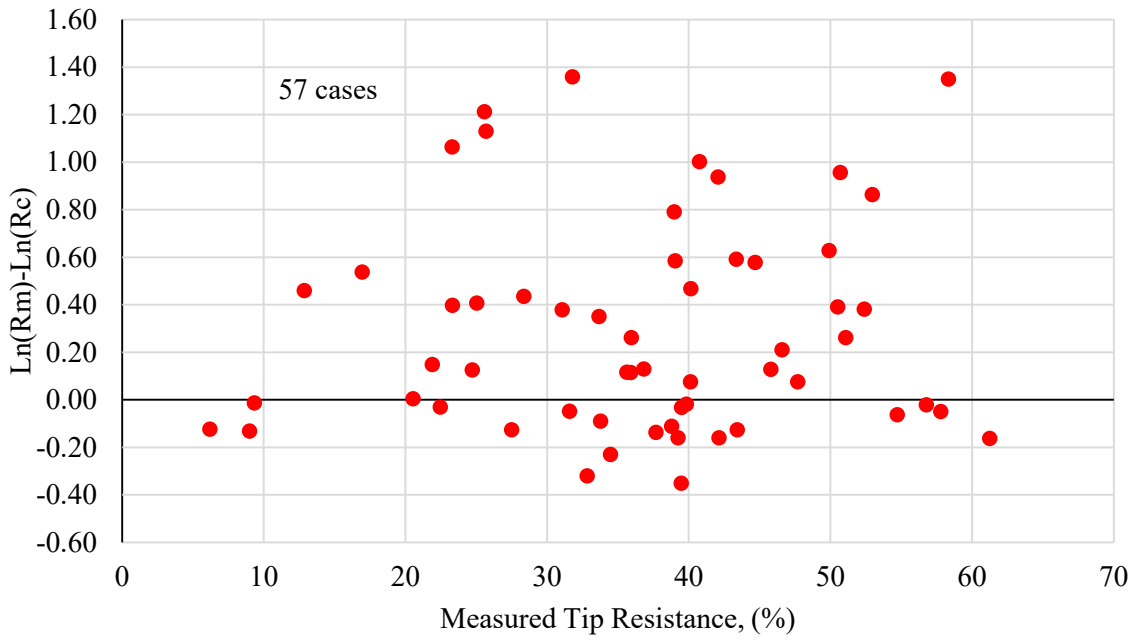


Figure 5-34 Ln-residual via FHWA 1999 method vs measured tip resistance at 5% B

Ln-Residual VS Measured Tip Resistance-sand (5% B - 1999)

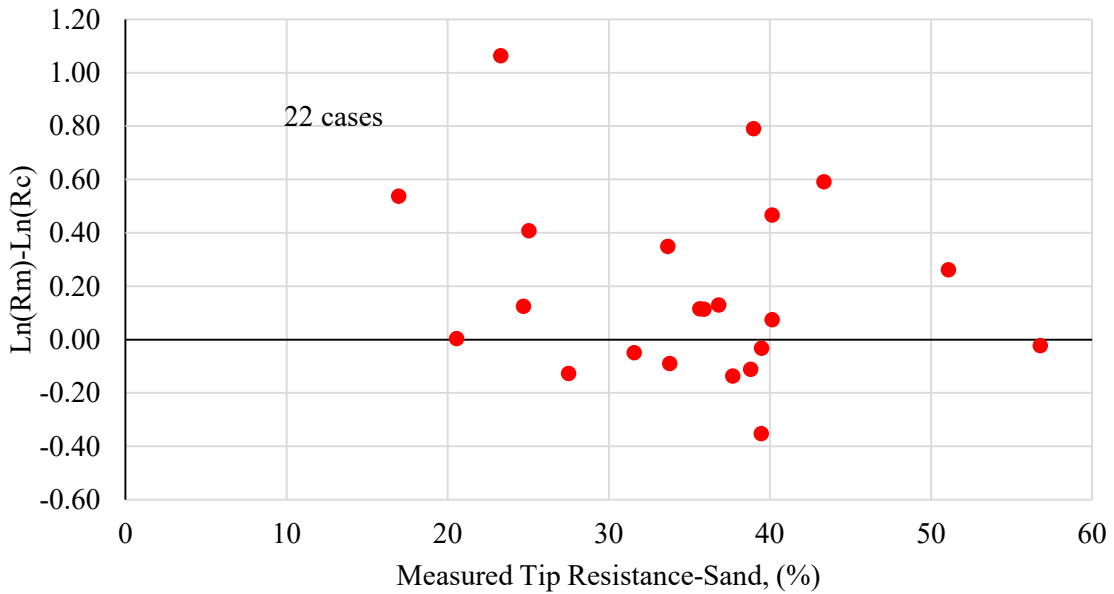


Figure 5-35 Ln-residual via FHWA 1999 method vs measured tip resistance in sand at 5% B

Ln-Residual VS Measured Tip Resistance-Clay (5% B - 1999)

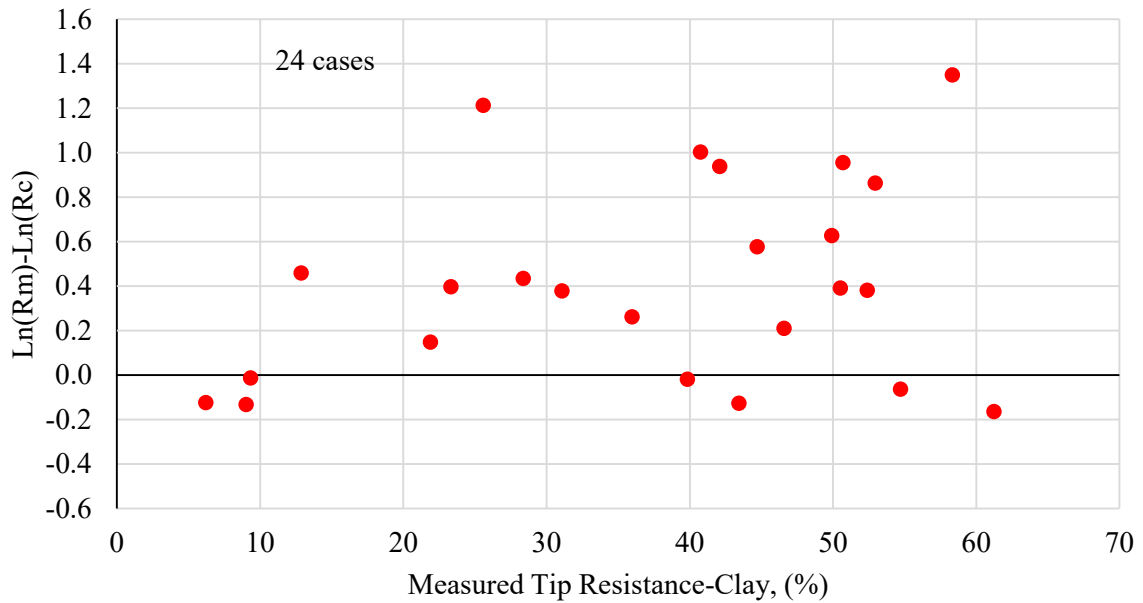


Figure 5-36 Ln-residual via FHWA 1999 method vs measured tip resistance in clay at 5% B

Ln-Residual VS Measured Tip Resistance-IGM (5% B - 1999)

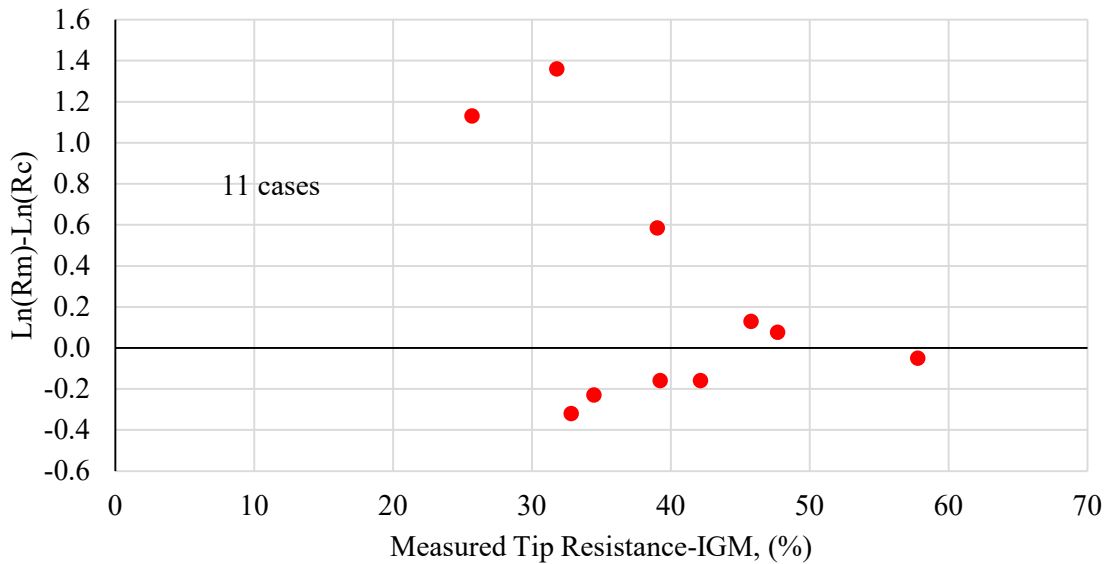


Figure 5-37 Ln-residual via FHWA 1999 method vs measured tip resistance in IGM at 5% B

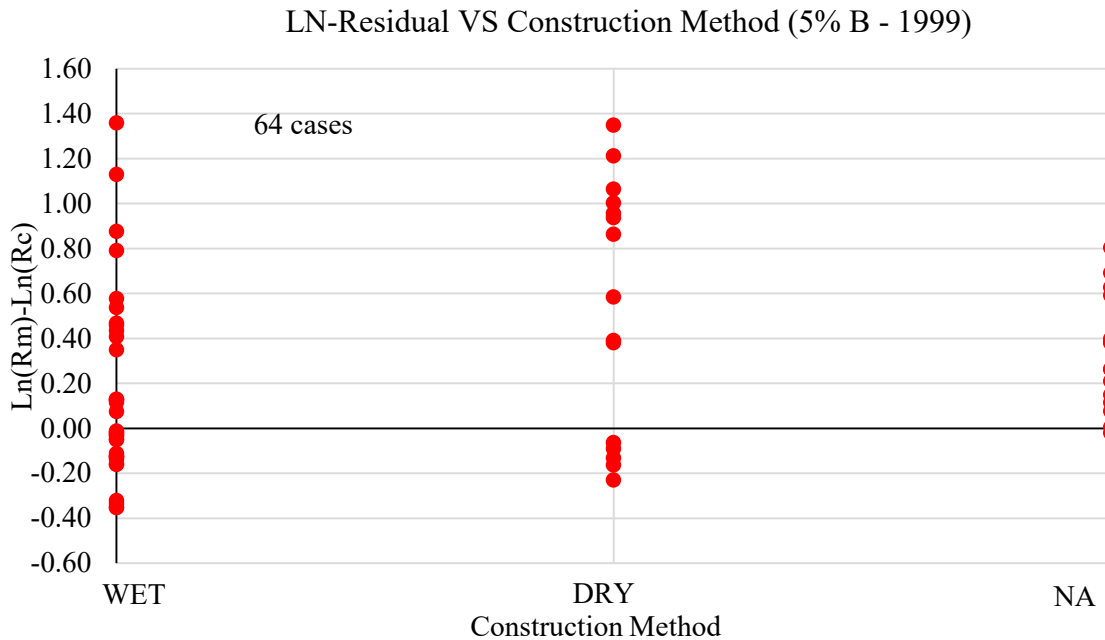


Figure 5-38 Ln-residual via 1999 method at 5% B vs construction method

**Breakdown table**

The finalized database listed in Table 5-4 and Table 5-5 (after combination) was broken down to specific sub-datasets according to specified design conditions listed in the Table 5-7 shown below. This breakdown analysis is to group the collected database according to selected design variables. The design variables considered are construction method, shaft length, region, tip soil type (defined according to both 1999 and 2010 method), and side soil type (defined according to both 1999 and 2010 method). For each side soil type, tip soil type was further specified for complete soil profile including both side and tip soil condition. All soil type at tip includes all cases of a particular soil type along shaft side without specifying soil type at the tip. For classification of soil type along shaft side, calculated resistance contribution to the total shaft side resistance was used as the classification criteria. Different range (100%, 80% - 100%, and 70% - 100%) was chose to determine the dominant soil type.

Table 5-7 Filter criteria used for database breakdown analyses

Design variable	criteria	#case	Design Variable		# of cases (Soil type at Tip)			
			Soil type along shaft side	All	sand	clay	IGM	
Construction	dry	18	2010 side	pure sand	17	17	0	--
	Wet	39		80-100% sand	34	31	3	--
	NA	15		70-100% sand	39	35	4	--
Length	<100 ft	66		pure clay	17	1	16	--
	>100 ft	6		80-100% clay	21	1	20	--
Region	MS	34		70-100% clay	24	4	20	--
	LA	30		Mixed <sup>(1)</sup>	9	7	2	
	Western	8		pure sand	3	3	0	0
2010 tip	sand	46		80-100% sand	11	9	2	0
	clay	26	70-100% sand	15	14	0	1	
2010 side	pure sand	17	pure clay	17	1	16	0	
	pure clay	17	80-100% clay	22	1	21	0	
1999 tip	sand	28	70-100% clay	24	3	21	0	
	clay	26	pure IGM	4	2	0	2	
	IGM	18	80-100% IGM	10	2	0	8	
1999 side	pure sand	3	70-100% IGM	12	3	1	8	
	pure clay	17	Mixed <sup>(2)</sup>	19	8	2	9	
	pure IGM	4						

Mixed <sup>(1)</sup>: Mixed soil type along shaft side for drilled shaft which can't be classified as either 70-100% sand or 70-100% clay.

Mixed <sup>(2)</sup>: Mixed soil type along shaft side for drilled shaft which can't be classified as 70-100% sand, or 70-100% clay, or 70-100% IGM.

Note: only datasets with case number greater or equal than 15 were selected for statistical analyses and phi factor calibration.

### Separate Resistance Analysis

A statistical analysis was conducted on separated resistances to evaluate the statistical characteristics of the nominal drilled shaft side and tip resistances separately. Among the total 72 drilled shaft cases, only 56 drilled shafts can have separated side and tip resistance at chosen failure criterion. As mentioned in the total resistance analysis, the eight western states drilled shaft cases either do not have separated O-cell measurement or were not tested to 1 inch settlement. So these eight cases do not have separated resistance. Four LA drilled shaft load tests, 455-08-20, #2- (LA), 455-08-20, #3-(LA), 455-08-47, 2A, and 455-08-47, 2B, are top-down load tests. Four cases, LT-8788-(MS), LT-9191-(MS), LT-9280-2-(MS), LT-9597-1-(LA), have corrected measured side

resistance exceeds total resistance. So these four cases are not included in the separated resistance analysis. The maximum, minimum, mean ( $\mu$ ), and COV of the bias for side and tip resistances using different analyses methods were calculated and summarized in Table 5-8 and Table 5-9. It can be observed that the separated resistance components have larger variation compared to the total resistance. Prediction of tip resistance is more conservative as the model bias factor is the largest among the three.

Table 5-8 Summary of bias for drilled shaft side resistance

Bias	$R_m/R_c$			#
	mean	std	COV	
$R_m (5\% B)/R_c (5\% B) -1999$	1.61	1.01	0.63	56
$R_m (5\% B)/R_c (5\% B) -2010$	1.40	0.89	0.64	56
$R_m (1'')/R_c (1'') -1999$	1.46	0.94	0.64	56
$R_m (1'')/R_c (1'') -2010$	1.39	0.84	0.60	56

Table 5-9 Summary of bias for drilled shaft tip resistance

Bias	$R_m/R_c$			#
	mean	std	COV	
$R_m (5\% B)/R_c (5\% B) -1999$	1.64	1.38	0.84	56
$R_m (5\% B)/R_c (5\% B) -2010$	1.42	1.09	0.77	56
$R_m (1'')/R_c (1'') -1999$	1.80	1.31	0.73	56
$R_m (1'')/R_c (1'') -2010$	1.76	1.19	0.68	56

Histogram and lognormal distributions of the bias of different resistance components are presented in Figures 5-39 to Figure 5-46. Similar to total resistance condition, the lognormal distribution matches the histogram of bias well; therefore, lognormal distribution was used in reliability calibration analyses. Compared with total resistance histogram plots, the tip and side resistance show larger variation. Much larger biases are observed in tip and side resistance histogram plots.



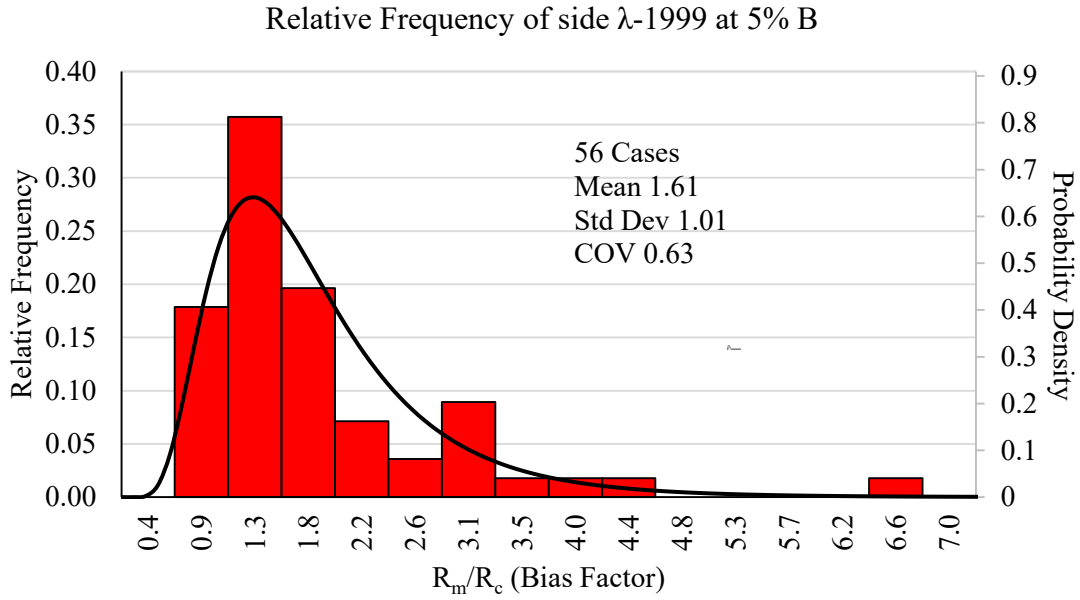


Figure 5-39 PDF and histogram of bias of side resistance at 5% B via FHWA 1999 method

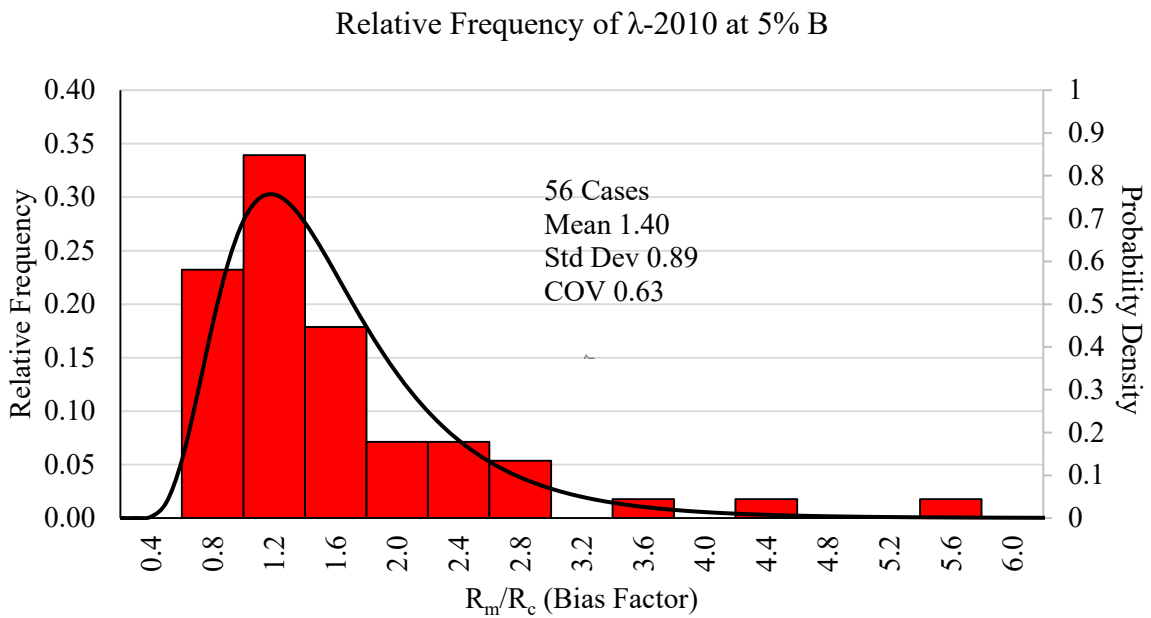


Figure 5-40 PDF and histogram of bias of side resistance at 5% B via FHWA 2010 method

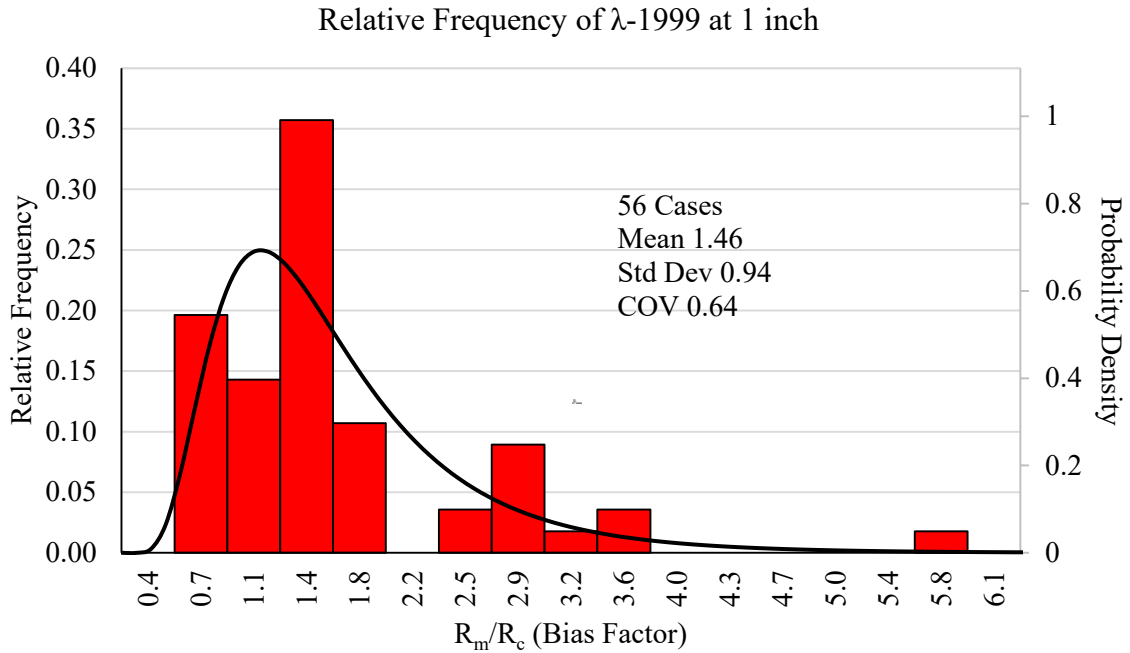


Figure 5-41 PDF and histogram of bias of side resistance at 1 inch via FHWA 1999 method

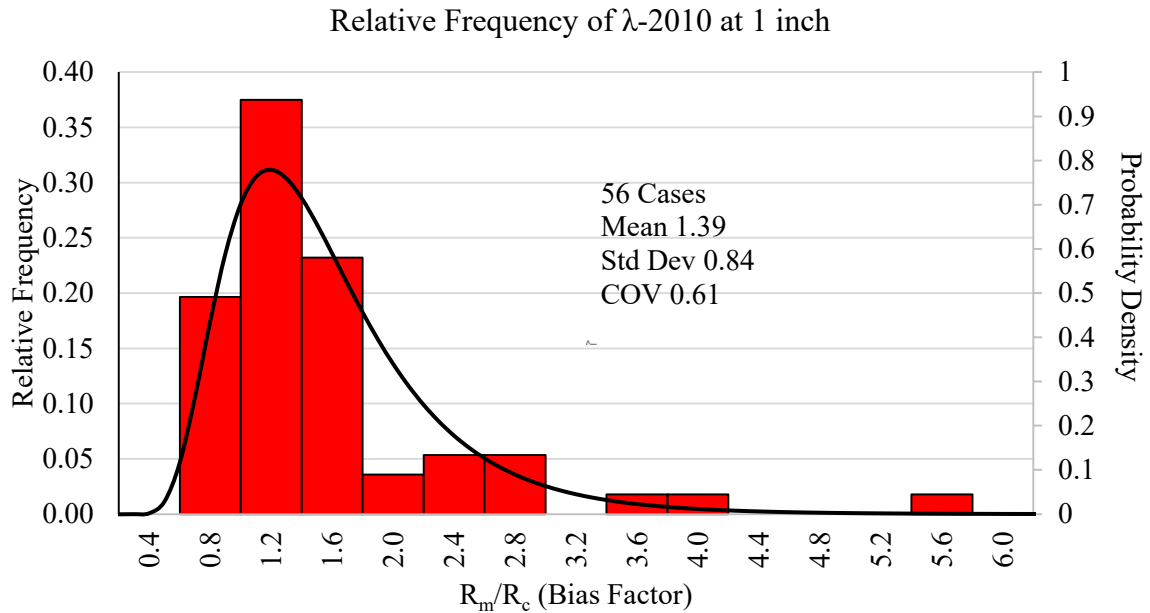


Figure 5-42 PDF and histogram of bias of side resistance at 1 inch via FHWA 2010 method

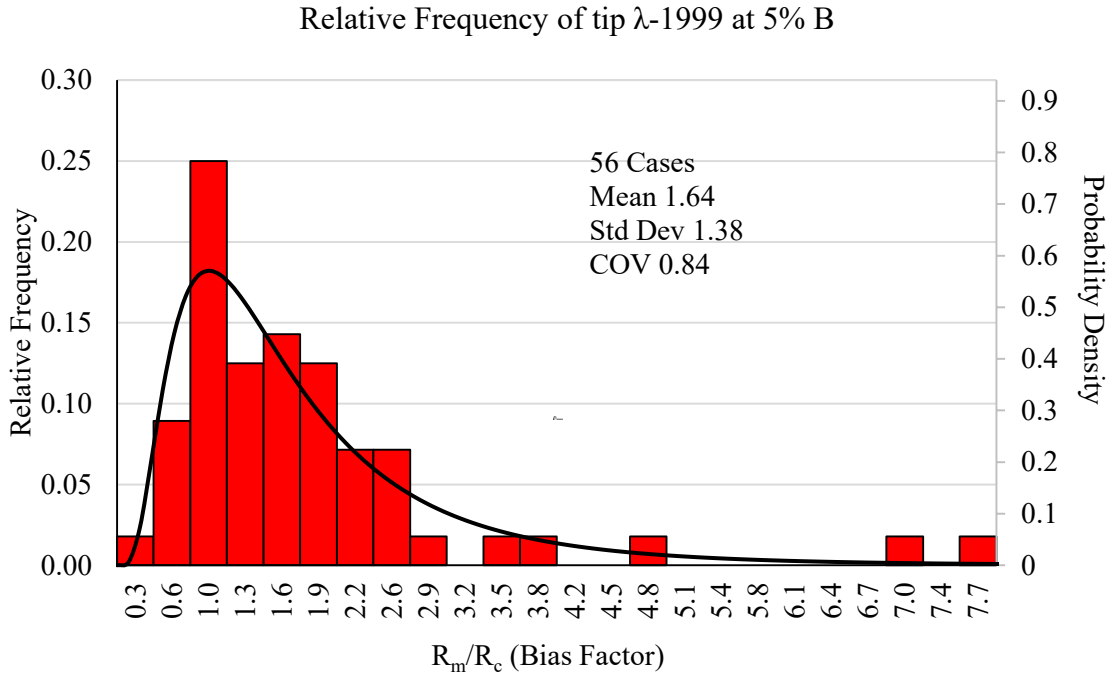


Figure 5-43 PDF and histogram of bias of tip resistance at 5% B via FHWA 1999 method

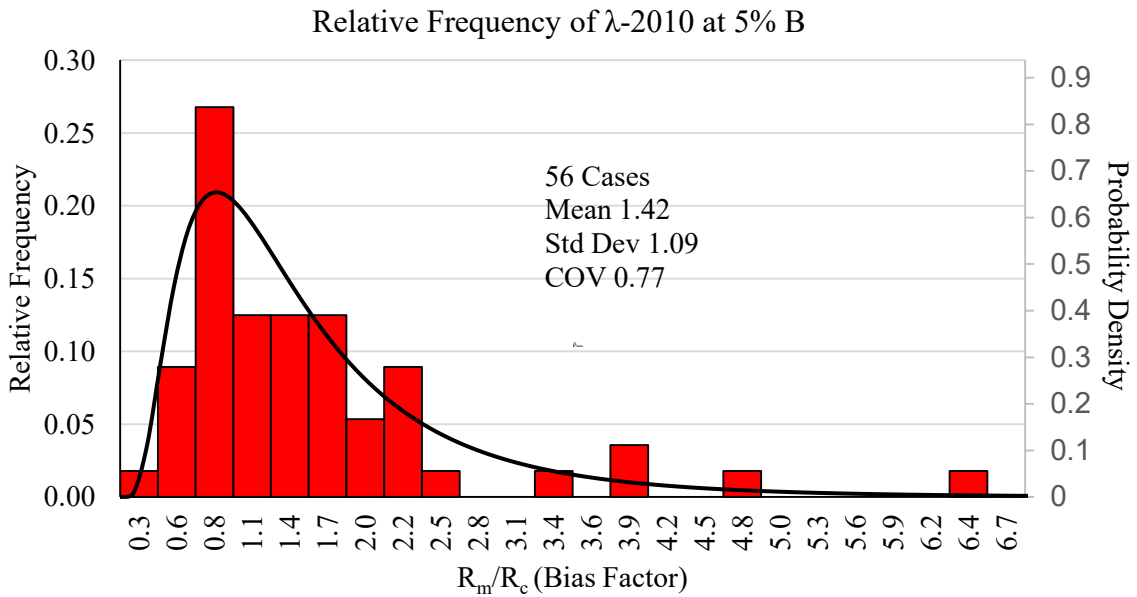


Figure 5-44 PDF and histogram of bias of tip resistance at 5% B via FHWA 2010 method

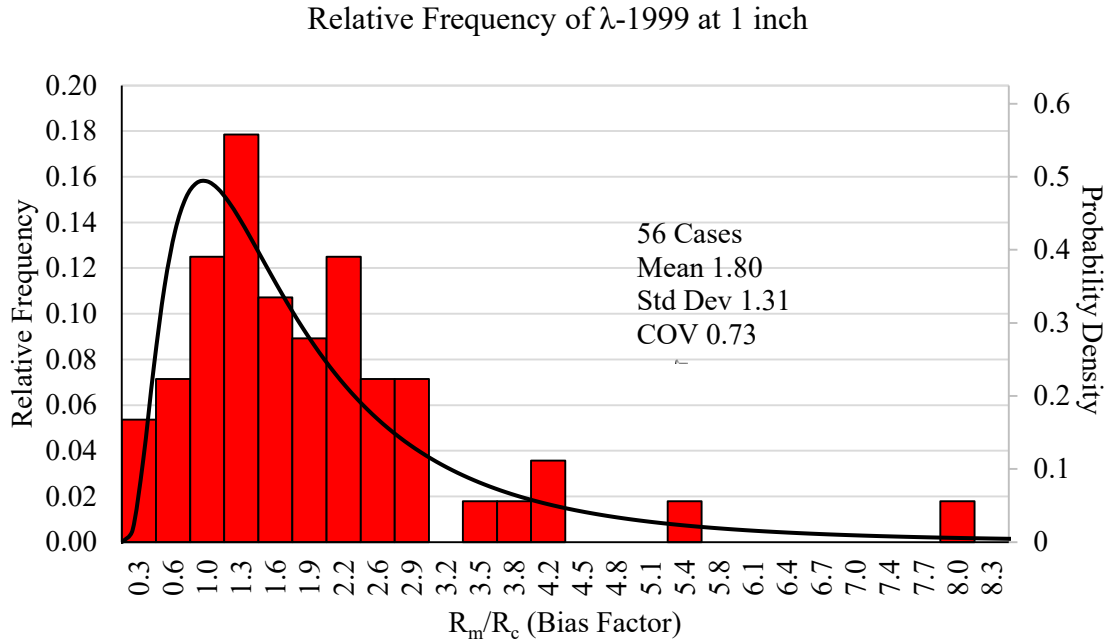


Figure 5-45 PDF and histogram of bias of tip resistance at 1 inch via FHWA 1999 method

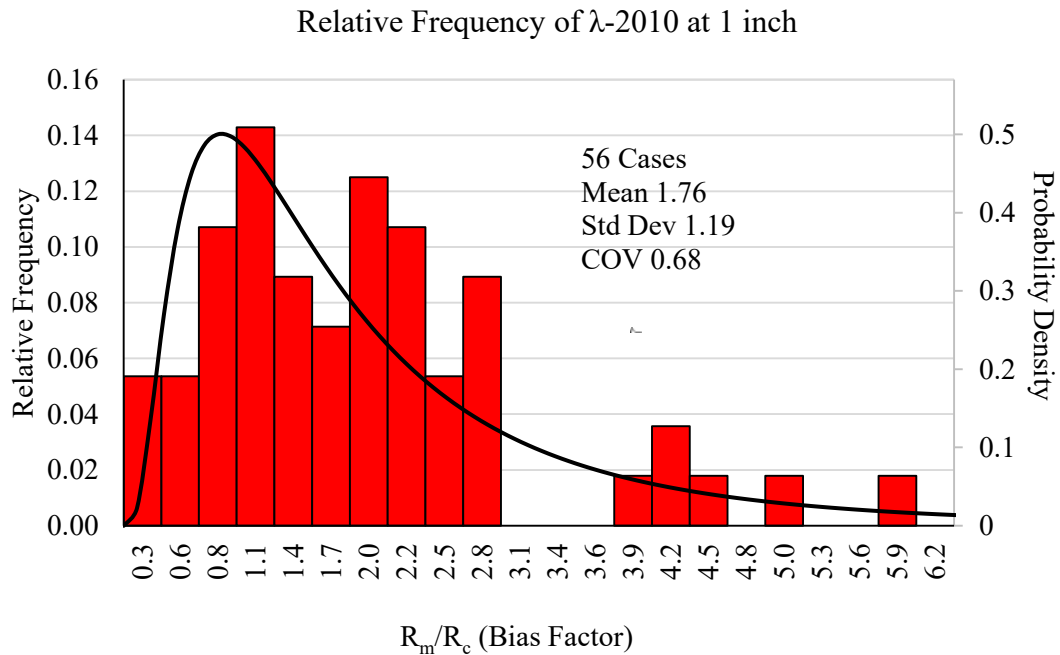


Figure 5-46 PDF and histogram of bias of tip resistance at 1 inch via FHWA 2010 method

## Reliability Theory

There are two limit states that are usually checked in deep foundation design. One is ultimate limit state (ULS), which requires factored resistance should be at least as large as factored loads; the other one is serviceability limit state (SLS), which requires deformation should be less than tolerable deformation. Since deep foundation is primarily controlled by the ultimate limit state, therefore, only ultimate limit state is considered in the following analysis. The ultimate limit state equation can be present as:

$$\sum \gamma_i Q_{ni} \leq \phi R_n$$

Where

$\gamma_i$  = load factor applicable to a specific load component;

$Q_{ni}$  = a specific nominal load component;

$\sum \gamma_i Q_{ni}$  = the total factored load for the load group applicable to the limit state being considered;

$\phi$  = the resistance factor; and

$R_n$  = the nominal resistance.

Load and resistance factors in the Equation below are used to account for material variability, uncertain in magnitude of applied loads, design model prediction uncertainty and other sources of uncertainty (Transportation Research Circular E-C079).

If there is only one load component, equation can be shown as:

$$\phi_R R_n - \gamma_Q Q_n \geq 0$$

Where

$R_n$  = the nominal resistance value;

$Q_n$  = the nominal load value;

$\phi_R$  = a resistance factor; and

$\gamma_Q$  = a load factor.

The limit state equation corresponds to above is:

$$g = R - Q \geq 0$$

Where,

$g$  = a random variable representing safety margin

$R$  = a random variable representing resistance; and

$Q$  = a random variable representing load.

The probability density functions for the load and resistance can be presented by Figure 5-47. Failure can be defined as when applied loading exceeding resistance, which is

shown as the magnitude of red spot larger than that of black spot in load and resistance probability density curves, respectively.

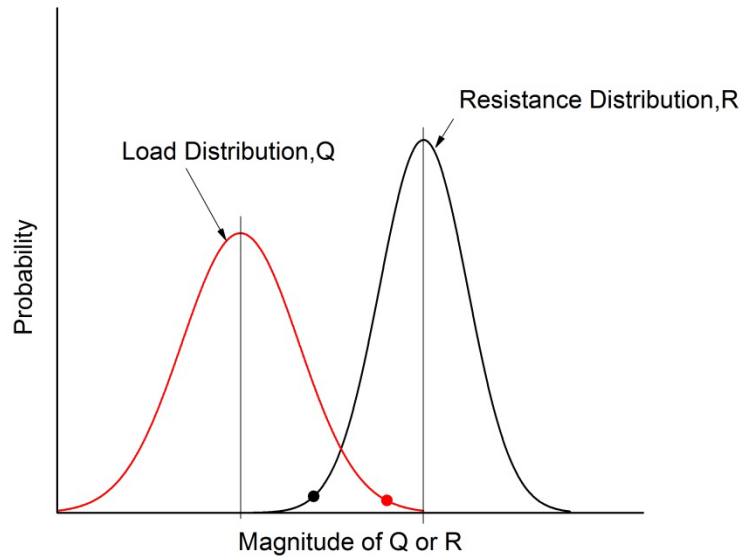


Figure 5-47 Probability density functions for load and resistance

The difference of load distribution curve  $Q$  and resistance distribution curve  $R$  will result in safety margin distribution curve  $g$  as shown in Figure 5-48. Failure can be calculated from the area of shade where  $g = R - Q < 0$ . Parameter  $\beta$  is equal to  $1/\text{COV}$  for the limit state function,  $g = R - Q$ , and is related to the probability of failure.

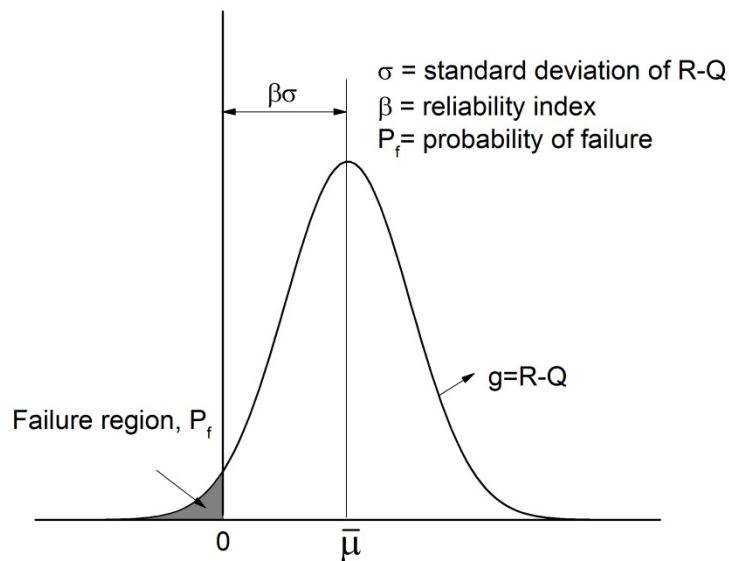


Figure 5-48 Distribution of limit state equation

For the normally distributed function  $g$  showing above, probability of failure will decrease when reliability index  $\beta$  value increases, this relationship can be shown using excel function:

$$\beta = \text{NORMSINV}(P_f)$$

also reliability index  $\beta$  and probability of failure  $P_f$  can be illustrated in Figure 5-49. The relationship showing in Figure 5-49 only applies to normal distribution  $g$ . When the limit state function  $g$  departs from normal distribution, the relationship shown in Figure 5-49 becomes approximate.

The limit state equation in this this study considers both dead load and live load effect, which can be expressed as:

$$\phi R_n = \gamma_{DL} + \gamma_{LL} Q_{LL}$$

Where

$\gamma_{DL}$  = load factor resulting from dead load;

$\gamma_{LL}$  = load factor resulting from live load;

$Q_{DL}$  = the dead load contribution to total load at specified location;

$Q_{LL}$  = the live load contribution to total load at specified location.

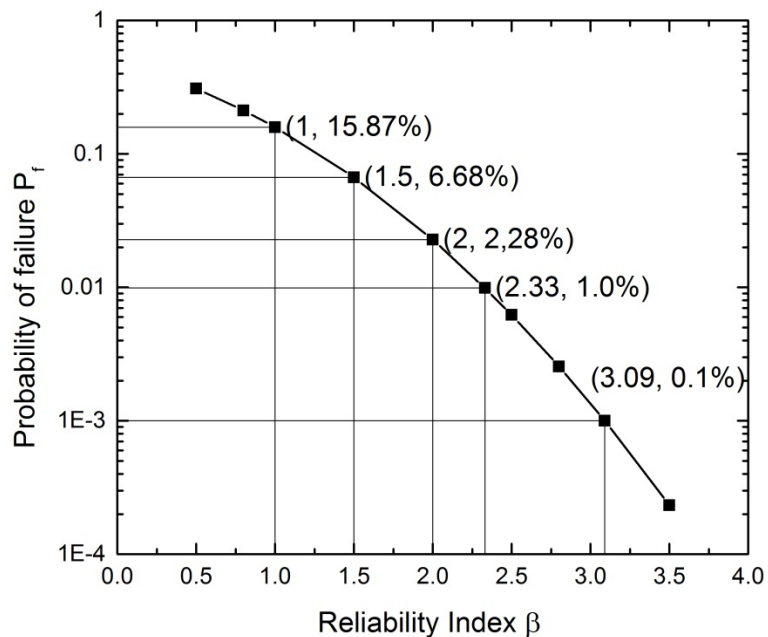


Figure 5-49 Probability of Failure corresponding to varies  $\beta$  values (after Allen et al., 2005)

Load statistics and load factor are selected (AASHTO 2012) as follows:

Table 5-10 Statistical characteristics and load factor

	Bias	COV	Load factor
Live load	$\lambda_{LL} = 1.15$	$COV_{LL} = 0.18$	$\hat{U}_{LL} = 1.75$
Dead load	$\lambda_{DL} = 1.08$	$COV_{DL} = 0.13$	$\hat{U}_{DL} = 1.25$

Where

$\lambda_{LL}$  = Mean value of measured live load over predicted live load;

$\lambda_{DL}$  = Mean value of measured dead load over predicted dead load;

$COV_{LL}$  = Coefficient of variation for live load;

$COV_{DL}$  = Coefficient of variation for dead load;

The ratio of dead load over live load ( $Q_{DL}/Q_{LL}$ ) is a function of a bridge's span length (Allen et al. 2005). Large span length results in larger dead load. In this case, a ratio of DL/LL equals to 3 is selected for calibration, which corresponds to a 50m span length.

In order to perform calibration of resistance factor based on the reliability theory mentioned above, mean value, standard deviation or coefficient of variation, also type of probability distribution must be known for the random variables in the limit state equation. The bias values, defined as the ratio of measured resistance to predicted resistance, are used to generate random resistance variable. Since resistance factor calibration is the primary goal and also load distributions are commonly obtained from current AASHTO code, only bias variable still need to be analyzed. The bias distribution and statistics can be obtained by analyzing the data generated from the ratios of individual measured resistance to predicted resistance for measured drilled shafts.

### **Calibration of Resistance Factors Using Monte Carlo Simulation**

Monte Carlo simulation method is more rigorous when compared to other calibration methods such as FOSM and FORM (Allen et al. 2005). It is a numerical technique which utilizes random number generator to extrapolate the CDF values for random variable in the limit state equation, to randomly generate many more measured load and resistance values than were available from original load test data from local soil. Once load and resistance values have been generated, the random number  $g$  can be calculated as the different of each paired resistance and load values. The failure probability  $P_f$  then can be determined by counting number of pairs with  $g$  less than 0 and dividing it by the total number of pairs. This method for extrapolating CDF curve makes estimate reliability



inde[  $\beta$  possible by increasing Tuantity of measured data, by which statistical analysis could be applied on to reliably predict  $\beta$ .

To generate available measured load and resistance values and obtain resistance factors according to varied reliability index value  $\beta$  using Monte Carlo method, the following steps can be taken:

1. Establish the limit state equation. For this case, since both dead load and live load have been considered, it can be defined as:

$$g = R - Q$$

$$g = \lambda_R \left( \frac{\gamma_{DL} Q_{DL} + \gamma_{LL} Q_{LL}}{\phi} \right) - \left( Q_{DL} \lambda_{DL} + Q_{DL} \frac{Q_{LL}}{Q_{DL}} \lambda_{LL} \right)$$

Assume a nominal value of  $Q_{DL} = 1$  for convenience, since positive or negative of  $g$  value is only thing need to be focused.

2. Select a target value  $\beta = \beta_T$ . In this case, a target value of 3.0 is chosen, which is approximately corresponding to 0.1% failure probability.
3. If load is following lognormal distribution, the generated dead measured load can be defined

$$Q_{DLi} = EXP(\mu_{ln} + \sigma_{ln} z_i)$$

Where

$$\mu_{ln} = LN(\overline{Q_{DL}}) - 0.5\sigma_{ln}^2$$

$$\sigma_{ln} = \{LN[(COV_{DL})^2] + 1\}^{0.5}$$

$Q_{DDi}$  = a randomly generated load value of load using specified set of statistical parameters

$\overline{Q_{DL}}$  = normal mean of load and equal to  $\lambda_{DL} Q_D$ ,  $\lambda_{DL}$  defined previously as mean of bias for dead load;

$COV_{DL}$  = the coefficient of variation of bias for  $Q_{DL}$ ;

$z_i$  =NORMSINV(RAND()), is the random standard normal variable generated using the EXCEL function.

Equation for generating lognormal live load can follow as:

$$Q_{LLi} = EXP(\mu_{ln} + \sigma_{ln} z_i)$$

Where

$$\mu_{ln} = LN(\overline{Q_{LL}}) - 0.5\sigma_{ln}^2$$

$$\sigma_{ln} = \{LN[(COV_{LL})^2] + 1\}^{0.5}$$

$Q_{LLi}$  = a randomly generated load value of load using specified set of statistical parameters

$\overline{Q_{LL}}$  = normal mean of live load and equal to  $\lambda_{LL} Q_L$ ,  $\lambda_{LL}$  defined previously as mean of bias for live load; (Since  $Q_{DL}/Q_{LL} = 3$  has been chosen,  $\overline{Q_{LL}} = \lambda_{LL} Q_{LL} = \lambda_{LL} * \frac{1}{3} * Q_{DL}$ )

$COV_{LL}$  = the coefficient of variation of bias for  $Q_{LL}$ ;

$z_i$  is same as previous.

Similarly, if resistance values are lognormally distributed, generated values of resistance that fit specified distribution characterized by a lognormal mean and lognormal standard deviation can be generated as follows:

$$R_i = EXP(\mu_{ln} + \sigma_{ln} z_i)$$

Where

$$\mu_{ln} = LN(\bar{R}) - 0.5\sigma_{ln}^2$$

$$\sigma_{ln} = \{LN[(COV_R)^2] + 1\}^{0.5}$$

$R_i$  = a randomly generated load value of load using specified set of statistical parameters

$\bar{R}$  = normal mean of resistance and equal to  $\lambda_R R$ ,  $\lambda_R$  defined as mean of bias for resistance; ( $R$  can be calculated as a function of resistance factor and load), then

$$R = \left( \frac{\gamma_{DL} Q_{DL} + \gamma_{LL} Q_{LL}}{\phi} \right) = \left( \frac{\gamma_{DL} * 1 + \gamma_{LL} * \frac{Q_{LL}}{Q_{DL}}}{\phi} \right)$$

$COV_R$  = the coefficient of variation of bias for  $Q_R$ ;

$z_i$  is same as previous defined.

4. Calculate random values of  $g$  using the limit state equation,

$$g_i = R_i - Q_{DD} - Q_{LL}$$

10000 values of  $g$  will be generated.

5. Calculate the probability of failure,  $P_f$ , by taking the number of values of  $g$  calculated that are less than 0 and dividing them by the total 10000 number of  $g$ . Probability index  $\beta$  is related to  $P_f$ , defined as previously.

$$P_f = \frac{\text{count}(g \leq 0)}{N(10000 \text{ cases})}$$

Then the corresponding probability index is calculated as:

$$\beta = NORMSINV(P_f)$$

6. Since statistical characters for load has been specified, (i.e. dead and live load factor, mean of bias, coefficient of variation, and ratio of dead load to live load), also mean of bias and coefficient of variation for resistance can be obtained from local sample data, the only uncertain parameter here is resistance factor. If a trial resistance factor does not result in the desired  $\beta$  values in step 2, change this resistance factor, regenerate random measured load values, count the cases with  $g$  values less than 0 again, until designed  $\beta$  value has achieved.

The load and resistance factors used to get target  $\beta$  value are the ones that can be utilized for the design in the local area to keep this designed failure probability.

## Calibration of Resistance Factors

### Drilled Shafts

#### Calibrated total resistance factor

This study follows the calibration procedure based on the Monte Carlo simulation method recommended in the Transportation Research Circular E-C079 to determine the total, side, and tip resistance factors of drilled shafts (Allen et al. 2005). The required number of Monte Carlo trials is based upon achieving a particular confidence level for a specified number of random variables and is not affected by the variability of the random variables (Allen et al., 2005; Baecher and Christian, 2003; and Harr 1996). Using the procedure described by Harr, the number of Monte Carlo trials required for a confidence level of 90 percent is approximately 9,900 (Harr 1996). For the probabilistic calculations reported in this study, Monte Carlo simulation with 10,000 trials was conducted. The load statistics used for calibration is shown in Table 5-10 with a dead load to live load ratio of 3. For bridge foundation supported by pile or drilled shaft foundation, a target reliability index of 2.33 is suggested for highly redundant pile or shaft group (minimum five), a target reliability index of 3 for pile or shaft group less than five but more than one, and a target reliability index of 3.5 for single pile/shaft foundation. Resistance factors for both reliability index of 2.33 and 3 are provided.

As shown in Table 5-4 and Table 5-5, the finalized drilled database contains 72 drilled shaft load tests. Different design analyses were applied to obtain its corresponding resistance factors. When target reliability index equals to 3.0, total resistance factor ( $\phi$ ) for the 1999 FHWA design method with measured resistance according to 1 inch and 5% of diameter settlement are 0.35 and 0.37, respectively. For the 2010 FHWA method, the calibrated resistance factors ( $\phi$ ) are 0.35 and 0.31 in accordance with measured resistance at 1 inch and 5% of diameter criterion. In addition, resistance factors had also been calibrated for bias values which were calculated from ratio of measured 1 inch resistance to predicted nominal resistance. The total resistance factors for various design analyses at different  $\beta$  values can be summarized below:

Table 5-11 Calibrated total resistance factors for the whole database

Bias	R <sub>m</sub> /R <sub>c</sub>			#	$\phi$ ( $\beta=3.0$ )	$\phi$ ( $\beta=2.33$ )
	mean	std	COV			
R <sub>m</sub> (5% B)/R <sub>c</sub> (5% B) -1999	1.49	0.77	0.52	64	0.37	0.52
R <sub>m</sub> (5% B)/R <sub>c</sub> (5% B) -2010	1.29	0.68	0.53	64	0.31	0.44
R <sub>m</sub> (1")/R <sub>c</sub> (1") -1999	1.44	0.75	0.52	70	0.35	0.50

$R_m(1'')/R_c(1'')$ -2010	1.40	0.72	0.51	70	0.35	0.50
$R_m(1'')/R_c(\text{nominal})$ -1999	1.14	0.60	0.53	70	0.27	0.39
$R_m(1'')/R_c(\text{nominal})$ -2010	1.09	0.58	0.53	70	0.26	0.37

### Calibrated total resistance factor for breakdown table

The total database is grouped into sub datasets to account for the effect of various design considerations. If construction method has been selected, then the total database can be divided into shafts with construction of dry, wet and unknown condition. For example, breakdown summary tables representing construction condition for selected shafts with different prediction methods can be generated accordingly as shown in Table 5-12. As shown in the table, there are 15 drilled shaft cases with no reported construction method. The calibrated resistance factors shown in Table 5-13, 5-14, and 5-15 show that dry method leads to higher bias and data variance as compared with wet construction method. The drilled shafts with unknown construction method yield the best bias statistics with much less data variance.

Table 5-12 Construction condition for drilled shaft database

Construction method	#Cases	Total cases
Dry	18	72
Wet	39	
NA	15	

Table 5-13 Calibrated total resistance factors according to dry construction method

Failure criteria - Prediction method	$R_m/R_c$			#	$\phi$ ( $\beta=3.0$ )	$\phi$ ( $\beta=2.33$ )
	mean	std	COV			
$R_m(5\% B)/R_c(5\% B)$ -1999	1.96	1.01	0.52	15	0.49	0.69
$R_m(5\% B)/R_c(5\% B)$ -2010	1.72	0.87	0.50	15	0.44	0.62
$R_m(1'')/R_c(1'')$ -1999	1.84	0.95	0.51	17	0.46	0.65
$R_m(1'')/R_c(1'')$ -2010	1.74	0.84	0.48	17	0.48	0.66

Table 5-14 Calibrated total resistance factors according to wet construction method

Failure criteria - Prediction method	$R_m/R_c$			#	$\phi$ ( $\beta=3.0$ )	$\phi$ ( $\beta=2.33$ )
	mean	std	COV			
$R_m(5\% B)/R_c(5\% B)$ -1999	1.30	0.70	0.54	34	0.30	0.43
$R_m(5\% B)/R_c(5\% B)$ -2010	1.13	0.63	0.56	34	0.25	0.36
$R_m(1'')/R_c(1'')$ -1999	1.28	0.70	0.55	38	0.29	0.42
$R_m(1'')/R_c(1'')$ -2010	1.29	0.73	0.57	38	0.28	0.40

$R_m(1'')/ \text{nominal 1999 (side)}$	1.50	0.83	0.56	38	0.33	0.48
--	------	------	------	----	------	------

Table 5-15 Calibrated total resistance factors according to unknown construction method

Failure criteria - Prediction method	$R_m/R_c$			#	$\phi$ ( $\beta=3.0$ )	$\phi$ ( $\beta=2.33$ )
	mean	std	COV			
$R_m$ (5% B)/ $R_c$ (5% B) - 1999	1.43	0.38	0.27	15	0.75	0.90
$R_m$ (5% B)/ $R_c$ (5% B) - 2010	1.23	0.36	0.29	15	0.60	0.73
$R_m$ (1'')/ $R_c$ (1'') -1999	1.37	0.40	0.29	15	0.67	0.82
$R_m$ (1'')/ $R_c$ (1'') -2010	1.30	0.38	0.29	15	0.62	0.77

Note: unknown construction method refers to drilled shaft with no reported construction method (either wet or dry).

Statistical characteristics of the bias for various classifications are summarized based on Table 5-10. The final calibrated resistance factors for different classification criterion can be shown in Table 5-16 and Table 5-17, resistance factors were not calculated for a few categories due to small sample size (less than 15). It can be seen that construction method, region, soil type at tip and along the side have noticeable effect on the calibrated resistance factor. For example, drilled shaft in LA has resistance factor of 0.55 for FHWA 1999 design method and 5%B failure criteria while drilled shaft in MS only has resistance factor of 0.35 for the same design analyses method. For 2010 design method tip soil type has negligible effect on the calibrated resistance factors. In contrast, for 1999 design method drilled shafts tipped in IGM has the lowest resistance factors while drilled shafts tipped in sand has the highest resistance factors. For the same dataset, design method and failure criteria have minor effect on the calibrated resistance factors. The variation is generally less than 0.05 with few exceptions for the drilled shaft with dry construction method. Selection of different reliability index (2.33 or 3.0) has noticeable effect on calibrated resistance factor (difference around 0.15).

Table 5-16 Statistical characteristics and calibrated total resistance factors according to different classification ( $\beta=3.0$ )

Design variable	criteria	#case	1"-99				5%B-99				1"-2010				5% B-2010			
			mean	std	#	$\phi$	mean	std	#	$\phi$	mean	std	#	$\phi$	mean	std	#	$\phi$
Construction	Dry	18	1.84	0.95	17	0.46	1.96	1.01	15	0.49	1.74	0.84	17	0.48	1.72	0.87	15	0.44
	Wet	39	1.28	0.70	38	0.29	1.30	0.70	34	0.30	1.29	0.73	38	0.28	1.13	0.63	34	0.25
	NA	15	1.37	0.40	15	0.67	1.43	0.38	15	0.75	1.3	0.38	15	0.62	1.23	0.36	15	0.60
Length	<100 ft	66	1.45	0.75	65	0.36	1.51	0.77	62	0.38	1.39	0.70	65	0.36	1.31	0.68	62	0.32
	>100 ft	6	1.21	0.76	5		0.83	0.17	2		1.56	1.04	5		0.74	0.28	2	
Region	MS	34	1.57	0.96	34	0.3	1.66	0.95	34	0.35	1.56	0.88	34	0.34	1.49	0.84	34	0.32
	LA	30	1.29	0.43	30	0.55	1.29	0.43	30	0.55	1.18	0.33	30	0.59	1.06	0.30	30	0.52
	Western	8	1.42	0.59	6						1.59	0.89	6					
2010 tip	Sand	46	1.37	0.70	44	0.34	1.39	0.72	39	0.34	1.39	0.71	44	0.35	1.22	0.63	39	0.30
	Clay	26	1.55	0.82	26	0.37	1.64	0.83	25	0.41	1.42	0.74	26	0.35	1.40	0.75	25	0.33
2010 side	Pure sand	17	1.27	0.74	15	0.25	1.19	0.67	11	0.25	1.42	0.92	15	0.24	1.11	0.66	11	0.22
	Pure clay	17	1.58	0.85	17	0.37	1.63	0.89	17	0.37	1.45	0.80	17	0.33	1.41	0.80	17	0.30
1999 tip	Sand	28	1.35	0.50	27	0.52	1.34	0.53	26	0.48	1.3	0.41	27	0.58	1.15	0.40	26	0.47
	Clay	26	1.55	0.82	26	0.37	1.64	0.83	25	0.42	1.42	0.74	26	0.35	1.4	0.75	25	0.33
	IGM	18	1.39	0.96	17	0.21	1.49	1.02	13	0.22	1.52	1.02	17	0.24	1.35	0.95	13	0.20
1999 side	Pure sand	3	1.16	0.06	2		1.05	0.10	2		1.04	0.01	2		0.87	0.12	2	
	Pure clay	17	1.58	0.85	17	0.37	1.63	0.89	17	0.37	1.45	0.80	17	0.33	1.41	0.80	17	0.30
	Pure IGM	4	1.66	1.25	4		1.59	1.06	4		1.93	1.37	4		1.54	1.02	4	
Total case	Total resistance	72	1.44	0.75	70	0.35	1.49	0.77	64	0.37	1.40	0.72	70	0.35	1.29	0.68	64	0.31

Table 5-17 Statistical characteristics and calibrated total resistance factors according to different classification ( $\beta=2.33$ )

Design variable	criteria	#case	1"-99				5% B-99				1"-2010				5% B-2010			
			mean	std	#	$\phi$	mean	std	#	$\phi$	mean	std	#	$\phi$	mean	std	#	$\phi$
Construction	Dry	18	1.84	0.95	17	0.65	1.96	1.01	15	0.69	1.74	0.84	17	0.66	1.72	0.87	15	0.62
	Wet	39	1.28	0.70	38	0.42	1.30	0.70	34	0.43	1.29	0.73	38	0.40	1.13	0.63	34	0.36
	NA	15	1.37	0.40	15	0.82	1.43	0.38	15	0.90	1.3	0.38	15	0.77	1.23	0.36	15	0.73
Length	<100 ft	66	1.45	0.75	65	0.51	1.51	0.77	62	0.54	1.39	0.7	65	0.51	1.31	0.68	62	0.46
	>100 ft	6	1.21	0.76	5		0.83	0.17	2		1.56	1.04	5		0.74	0.28	2	
Region	MS	34	1.57	0.96	34	0.44	1.66	0.95	34	0.51	1.56	0.88	34	0.49	1.49	0.84	34	0.47
	LA	30	1.29	0.43	30	0.70	1.29	0.43	30	0.70	1.18	0.33	30	0.72	1.06	0.30	30	0.64
	Western	8	1.42	0.59	6						1.59	0.89	6					
2010 tip	Sand	46	1.37	0.70	44	0.49	1.39	0.72	39	0.49	1.39	0.71	44	0.49	1.22	0.63	39	0.43
	Clay	26	1.55	0.82	26	0.53	1.64	0.83	25	0.59	1.42	0.74	26	0.50	1.40	0.75	25	0.48
2010 side	Pure sand	17	1.27	0.74	15	0.38	1.19	0.67	11	0.37	1.42	0.92	15	0.37	1.11	0.66	11	0.33
	Pure clay	17	1.58	0.85	17	0.53	1.63	0.89	17	0.53	1.45	0.8	17	0.48	1.41	0.80	17	0.44
1999 tip	Sand	28	1.35	0.50	27	0.67	1.34	0.53	26	0.63	1.30	0.41	27	0.73	1.15	0.40	26	0.60
	Clay	26	1.55	0.82	26	0.53	1.64	0.83	25	0.59	1.42	0.74	26	0.50	1.4	0.75	25	0.48
	IGM	18	1.39	0.96	17	0.33	1.49	1.02	13	0.36	1.52	1.02	17	0.38	1.35	0.95	13	0.31
1999 side	Pure sand	3	1.16	0.06	2		1.05	0.10	2		1.04	0.01	2		0.87	0.12	2	
	Pure clay	17	1.58	0.85	17	0.53	1.63	0.89	17	0.53	1.45	0.80	17	0.48	1.41	0.80	17	0.44
	Pure IGM	4	1.66	1.25	4		1.59	1.06	4		1.93	1.37	4		1.54	1.02	4	
Total case	Total resistance	72	1.44	0.75	70	0.50	1.49	0.77	64	0.52	1.40	0.72	70	0.50	1.29	0.68	64	0.44



Table 5-18 Statistical characteristics and calibrated total resistance factors based on detailed soil profile ( $\beta=3.0$ )

Design variable	criteria	#case	1"-99				5% B-99				1"-2010				5% B-2010			
			mean	std	#	$\phi$	mean	std	#	$\phi$	mean	std	#	$\phi$	mean	std	#	$\phi$
2010 side, pure sand	tip-sand	17	1.27	0.74	15	0.25	1.19	0.67	11	0.25	1.42	0.92	15	0.24	1.11	0.66	11	0.22
2010 side, 70-100% sand	tip-sand	35	1.27	0.72	33	0.27	1.28	0.73	28	0.28	1.33	0.75	33	0.29	1.15	0.67	28	0.24
2010 side, pure clay	tip-clay	16	1.59	0.88	16	0.35	1.64	0.92	16	0.35	1.47	0.82	16	0.32	1.43	0.83	16	0.30
2010 side, 70-100% clay	tip-clay	20	1.62	0.83	20	0.40	1.67	0.86	20	0.41	1.49	0.78	20	0.36	1.46	0.78	20	0.35
1999 side, 70-100% sand	tip-sand	14	1.29	0.43	13	0.55	1.30	0.47	12	0.51	1.19	0.27	13	0.70	1.07	0.31	12	0.52
1999 side, pure clay	tip-clay	17	1.59	0.88	16	0.35	1.64	0.92	16	0.35	1.47	0.82	16	0.32	1.43	0.83	16	0.30
1999 side, 70-100% clay	tip-clay	21	1.67	0.85	21	0.42	1.71	0.87	21	0.44	1.53	0.78	21	0.38	1.49	0.77	21	0.37
1999 side, 70-100% IGM	all tip conditions	12	1.51	1.06	11	0.22	1.64	1.13	9	0.25	1.67	1.04	11	0.31	1.51	1.10	9	0.21
1999 side mixed <sup>(1)</sup>	all tip conditions	19	1.23	0.63	19	0.31	1.29	0.60	17	0.37	1.29	0.52	19	0.45	1.15	0.45	17	0.41

1999 side mixed <sup>(1)</sup>: Mixed soil type along the side for drilled shaft which can't be classified as sand (70-100% sand), or clay (70-100% clay), or IGM (70-100%)

Table 5-19 Statistical characteristics and calibrated total resistance factors based on detailed soil profile ( $\beta=2.33$ )

Design variable	criteria	#case	1"-99				5% B-99				1"-2010				5% B-2010			
			mean	std	#	$\phi$	mean	std	#	$\phi$	mean	std	#	$\phi$	mean	std	#	$\phi$
2010 side, pure sand	tip-sand	17	1.27	0.74	15	0.38	1.19	0.67	11	0.38	1.42	0.92	15	0.37	1.11	0.66	11	0.33
2010 side, 70-100% sand	tip-sand	35	1.27	0.72	33	0.40	1.28	0.73	28	0.40	1.33	0.75	33	0.42	1.15	0.67	28	0.35
2010 side, pure clay	tip-clay	16	1.59	0.88	16	0.51	1.64	0.92	16	0.52	1.47	0.82	16	0.47	1.43	0.83	16	0.43
2010 side, 70-100% clay	tip-clay	20	1.62	0.83	20	0.58	1.67	0.86	20	0.59	1.49	0.78	20	0.52	1.46	0.78	20	0.49
1999 side, 70-100% sand	tip-sand	14	1.29	0.43	13	0.70	1.30	0.47	12	0.65	1.19	0.27	13	0.82	1.07	0.31	12	0.64
1999 side, pure clay	tip-clay	17	1.59	0.88	16	0.51	1.64	0.92	16	0.52	1.47	0.82	16	0.47	1.43	0.83	16	0.43
1999 side, 70-100% clay	tip-clay	21	1.67	0.85	21	0.60	1.71	0.87	21	0.61	1.53	0.78	21	0.55	1.49	0.77	21	0.52
1999 side, 70-100% IGM	all tip conditions	12	1.51	1.06	11	0.35	1.64	1.13	9	0.39	1.67	1.04	11	0.46	1.51	1.10	9	0.33
1999 side mixed <sup>(1)</sup>	all tip conditions	19	1.23	0.63	19	0.44	1.29	0.60	17	0.51	1.29	0.52	19	0.59	1.15	0.45	17	0.53

1999 side mixed<sup>(1)</sup>: Mixed soil type along the side for drilled shaft (not belong to sand (70-100% sand), or clay (70-100% clay), or IGM (70-100%))

### Calibrated side and tip resistance factors

The measured side resistance and tip resistances were determined using interpolations from O-cell test data at 1 inch or 5% of shaft diameter settlement. The predicted side and tip resistances were calculated from FHWA 1999 and 2010 methods. The bias of side resistance and tip resistance were considered as independent variables. Therefore, the resistance factor from side and tip were calibrated separately following the same calibration procedure as for the total resistance. The statistical parameters used for the calibration and calibrated resistance factors of separated resistance components are listed in Table 5-20 and Table 5-21.

Table 5-20 Calibrated side resistance factor for the whole database with different design analysis

Bias	R <sub>m</sub> /R <sub>c</sub>			#	φ (β=3.0)	φ (β=2.33)
	mean	std	COV			
R <sub>m</sub> (5% B)/R <sub>c</sub> (5% B) -1999	1.61	1.01	0.63	56	0.29	0.44
R <sub>m</sub> (5% B)/R <sub>c</sub> (5% B) -2010	1.40	0.89	0.64	56	0.25	0.38
R <sub>m</sub> (1")/R <sub>c</sub> (1") -1999	1.46	0.94	0.64	56	0.25	0.38
R <sub>m</sub> (1")/R <sub>c</sub> (1") -2010	1.39	0.84	0.60	56	0.27	0.40

Table 5-21 Calibrated tip resistance factor for the whole database with different design analysis

Bias	R <sub>m</sub> /R <sub>c</sub>			#	φ (β=3.0)	φ (β=2.33)
	mean	std	COV			
R <sub>m</sub> (5% B)/R <sub>c</sub> (5% B) -1999	1.64	1.38	0.84	56	0.16	0.28
R <sub>m</sub> (5% B)/R <sub>c</sub> (5% B) -2010	1.42	1.09	0.77	56	0.17	0.28
R <sub>m</sub> (1")/R <sub>c</sub> (1") -1999	1.80	1.31	0.73	56	0.25	0.39
R <sub>m</sub> (1")/R <sub>c</sub> (1") -2010	1.76	1.19	0.68	56	0.28	0.43

### Calibrated side and tip resistance factors for breakdown table

Statistical characteristics with various classifications had been summarized based on Table 5-10. The final calibrated side and tip resistance factors for different classification criteria can be shown in Table 5-22 to Table 5-29, resistance factors were not calculated for a few categories due to small sample size (less than 15). Both reliability index of 2.33 and 3.0 were used in the calibrated side resistance.

Table 5-22 Statistical characteristics and calibrated side resistance factors according to different classification ( $\beta=3.0$ )

Design variable	criteria	#case	1"-99				5% B-99				1"-2010				5% B-2010			
			mean	std	#	$\phi$	mean	std	#	$\phi$	mean	std	#	$\phi$	mean	std	#	$\phi$
Construction	Dry	18	2.09	1.31	14	0.38	2.23	1.40	14	0.40	1.96	1.17	14	0.38	1.95	1.23	14	0.35
	Wet	39	1.28	0.76	31	0.40	1.45	0.86	31	0.28	1.23	0.69	31	0.26	1.26	0.76	31	0.25
	NA	15	1.16	0.28	11	0.65	1.28	0.29	11	0.74	1.12	0.27	11	0.63	1.10	0.28	11	0.59
Length	<100 ft	66	1.47	0.94	55	0.26	1.63	1.01	55	0.30	1.40	0.84	55	0.27	1.42	0.89	55	0.25
	>100 ft	6			1		0.68		1		0.59		1		0.66		1	
Region	MS	34	1.60	1.17	31	0.22	1.77	1.25	31	0.25	1.58	1.06	31	0.25	1.61	1.11	31	0.24
	LA	30	1.28	0.50	25	0.47	1.41	0.57	25	0.49	1.15	0.32	25	0.57	1.15	0.37	25	0.50
	Western	8			0				0				0				0	
2010 tip	Sand	46	1.29	0.78	33	0.25	1.46	0.88	33	0.28	1.28	0.71	33	0.28	1.29	0.76	33	0.26
	Clay	26	1.69	1.10	23	0.29	1.82	1.16	23	0.32	1.55	1.00	23	0.27	1.56	1.04	23	0.25
2010 side	Pure sand	17	1.16	0.83	10	0.16	1.25	0.86	10	0.19	1.28	0.93	10	0.18	1.19	0.83	10	0.18
	Pure clay	17	1.77	1.25	15	0.26	1.90	1.35	15	0.27	1.63	1.14	15	0.24	1.66	1.21	15	0.23
1999 tip	Sand	28	1.26	0.57	22	0.38	1.42	0.64	22	0.43	1.22	0.42	22	0.50	1.23	0.43	22	0.50
	Clay	26	1.69	1.10	23	0.29	1.82	1.16	23	0.32	1.55	1.00	23	0.27	1.56	1.04	23	0.25
	IGM	18	1.36	1.12	11	0.15	1.54	1.27	11	0.17	1.39	1.10	11	0.16	1.42	1.20	11	0.15
1999 side	Pure sand	3	1.05	0.30	2		1.12	0.26	2		0.95	0.32	2		0.96	0.29	2	
	Pure clay	17	1.77	1.25	15	0.26	1.90	1.35	15	0.27	1.63	1.14	15	0.24	1.66	1.21	15	0.22
	Pure IGM	4	1.52	1.28	4		1.63	1.33	4		1.77	1.40	4		1.59	1.27	4	
Total case	Side resistance	72	1.46	0.94	56	0.25	1.61	1.01	56	0.29	1.39	0.84	56	0.27	1.40	0.89	56	0.25

Table 5-23 Statistical characteristics and calibrated side resistance factors according to different classification ( $\beta=2.33$ )

Design variable	criteria	#case	1"-99				5% B-99				1"-2010				5% B-2010			
			mean	std	#	$\phi$	mean	std	#	$\phi$	mean	std	#	$\phi$	mean	std	#	$\phi$
Construction	Dry	18	2.09	1.31	14	0.57	2.23	1.40	14	0.60	1.96	1.17	14	0.57	1.95	1.23	14	0.53
	Wet	39	1.28	0.76	31	0.61	1.45	0.86	31	0.42	1.23	0.69	31	0.39	1.26	0.76	31	0.37
	NA	15	1.16	0.28	11	0.77	1.28	0.29	11	0.88	1.12	0.27	11	0.75	1.10	0.28	11	0.71
Length	<100 ft	66	1.47	0.94	55	0.40	1.63	1.01	55	0.45	1.40	0.84	55	0.41	1.42	0.89	55	0.38
	>100 ft	6			1		0.68		1		0.59		1		0.66		1	
Region	MS	34	1.60	1.17	31	0.35	1.77	1.25	31	0.41	1.58	1.06	31	0.39	1.61	1.11	31	0.38
	LA	30	1.28	0.50	25	0.61	1.41	0.57	25	0.64	1.15	0.32	25	0.70	1.15	0.37	25	0.63
	Western	8			0				0				0				0	
2010 tip	Sand	46	1.29	0.78	33	0.37	1.46	0.88	33	0.42	1.28	0.71	33	0.41	1.29	0.76	33	0.38
	Clay	26	1.69	1.10	23	0.44	1.82	1.16	23	0.49	1.55	1.00	23	0.41	1.56	1.04	23	0.39
2010 side	Pure sand	17	1.16	0.83	10	0.26	1.25	0.86	10	0.30	1.28	0.93	10	0.28	1.19	0.83	10	0.28
	Pure clay	17	1.77	1.25	15	0.41	1.90	1.35	15	0.43	1.63	1.14	15	0.38	1.66	1.21	15	0.36
1999 tip	Sand	28	1.26	0.57	22	0.52	1.42	0.64	22	0.58	1.22	0.42	22	0.63	1.23	0.43	22	0.63
	Clay	26	1.69	1.10	23	0.44	1.82	1.16	23	0.49	1.55	1.00	23	0.41	1.56	1.04	23	0.39
	IGM	18	1.36	1.12	11	0.24	1.54	1.27	11	0.27	1.39	1.10	11	0.27	1.42	1.20	11	0.24
1999 side	Pure sand	3	1.05	0.30	2		1.12	0.26	2		0.95	0.32	2		0.96	0.29	2	
	Pure clay	17	1.77	1.25	15	0.41	1.90	1.35	15	0.43	1.63	1.14	15	0.38	1.66	1.21	15	0.36
	Pure IGM	4	1.52	1.28	4		1.63	1.33	4		1.77	1.40	4		1.59	1.27	4	
Total case	Side resistance	72	1.46	0.94	56	0.38	1.61	1.01	56	0.44	1.39	0.84	56	0.40	1.40	0.89	56	0.38

Table 5-24 Statistical characteristics and calibrated side resistance factors based on detailed soil profile ( $\beta=3.0$ )

Design variable	criteria	#case	1"-99				5% B-99				1"-2010				5% B-2010			
			mean	std	#	$\phi$	mean	std	#	$\phi$	mean	std	#	$\phi$	mean	std	#	$\phi$
2010 side, pure sand	tip-sand	17	1.16	0.83	10	0.16	1.25	0.86	10	0.19	1.28	0.93	10	0.18	1.19	0.83	10	0.18
2010 side, 70-100% sand	tip-sand	35	1.23	0.78	27	0.21	1.38	0.90	27	0.23	1.23	0.73	27	0.25	1.23	0.79	27	0.21
2010 side, pure clay	tip-clay	16	1.77	1.25	15	0.26	1.90	1.35	15	0.27	1.63	1.14	15	0.24	1.66	1.21	15	0.22
2010 side, 70-100% clay	tip-clay	20	1.77	1.13	19	0.31	1.89	1.21	19	0.33	1.63	1.04	19	0.29	1.65	1.09	19	0.27
1999 side, 70-100% sand	tip-sand	14	1.20	0.54	11	0.36	1.36	0.65	11	0.38	1.10	0.31	11	0.55	1.10	0.35	11	0.49
1999 side, pure clay	tip-clay	17	1.77	1.25	15	0.26	1.90	1.35	15	0.27	1.63	1.14	15	0.24	1.66	1.21	15	0.23
1999 side, 70-100% clay	tip-clay	21	1.83	1.13	20	0.34	1.94	1.20	20	0.36	1.66	1.02	20	0.31	1.68	1.07	20	0.30
1999 side, 70-100% IGM	all tip conditions	12	1.60	1.19	8	0.21	1.64	1.38	8	0.17	1.72	1.17	8	0.27	1.68	1.32	8	0.20
1999 side mixed <sup>(1)</sup>	all tip conditions	19	1.12	0.63	16	0.25	1.30	0.66	16	0.33	1.12	0.50	16	0.33	1.16	0.50	16	0.37

1999 side mixed<sup>(1)</sup>: Mixed soil type along the side (not belong to sand (70-100% sand), or clay (70-100% clay), or IGM (70-100% IGM))

Table 5-25 Statistical characteristics and calibrated side resistance factors based on detailed soil profile ( $\beta=2.33$ )

Design variable	criteria	#case	1"-99				5% B-99				1"-2010				5% B-2010			
			mean	std	#	$\phi$	mean	std	#	$\phi$	mean	std	#	$\phi$	mean	std	#	$\phi$
2010 side, pure sand	tip-sand	17	1.16	0.83	10	0.26	1.25	0.86	10	0.30	1.28	0.93	10	0.28	1.19	0.83	10	0.28
2010 side, 70-100% sand	tip-sand	35	1.23	0.78	27	0.33	1.38	0.90	27	0.36	1.23	0.73	27	0.36	1.23	0.79	27	0.32
2010 side, pure clay	tip-clay	16	1.77	1.25	15	0.41	1.90	1.35	15	0.43	1.63	1.14	15	0.38	1.66	1.21	15	0.36
2010 side, 70-100% clay	tip-clay	20	1.77	1.13	19	0.47	1.89	1.21	19	0.50	1.63	1.04	19	0.43	1.65	1.09	19	0.42
1999 side, 70-100% sand	tip-sand	14	1.20	0.54	11	0.49	1.36	0.65	11	0.52	1.10	0.31	11	0.67	1.10	0.35	11	0.61
1999 side, pure clay	tip-clay	17	1.77	1.25	15	0.41	1.90	1.35	15	0.43	1.63	1.14	15	0.38	1.66	1.21	15	0.36
1999 side, 70-100% clay	tip-clay	21	1.83	1.13	20	0.51	1.94	1.20	20	0.54	1.66	1.02	20	0.47	1.68	1.07	20	0.45
1999 side, 70-100% IGM	all tip conditions	12	1.60	1.19	8	0.34	1.64	1.38	8	0.28	1.72	1.17	8	0.42	1.68	1.32	8	0.33
1999 side mixed <sup>(1)</sup>	all tip conditions	19	1.12	0.63	16	0.36	1.30	0.66	16	0.47	1.12	0.50	16	0.46	1.16	0.50	16	0.50

1999 side mixed<sup>(1)</sup>: Mixed soil type along the side (not belong to sand (70-100% sand), or clay (70-100% clay), or IGM (70-100% IGM))

Table 5-26 Statistical characteristics and calibrated tip resistance factors according to different classification ( $\beta=3.0$ )

Design variable	criteria	#case	1"-99				5% B-99				1"-2010				5% B-2010			
			mean	std	#	$\phi$	mean	std	#	$\phi$	mean	std	#	$\phi$	mean	std	#	$\phi$
Construction	Dry	18	2.07	1.16	14	0.45	2.05	1.57	14	0.25	1.97	1.06	14	0.46	1.80	1.36	14	0.22
	Wet	39	1.67	1.48	31	0.15	1.42	1.42	31	0.10	1.65	1.30	31	0.20	1.21	0.99	31	0.13
	NA	15	1.80	0.97	11	0.42	1.72	0.91	11	0.42	1.80	1.08	11	0.35	1.52	0.92	11	0.29
Length	<100 ft	66	1.79	1.32	55	0.24	1.64	1.39	55	0.17	1.75	1.20	55	0.27	1.42	1.10	55	0.17
	>100 ft	6	2.20		1		1.35		1		2.62		1		1.33		1	
Region	MS	34	1.89	1.22	31	0.32	1.83	1.37	34	0.24	1.94	1.24	31	0.34	1.67	1.20	31	0.23
	LA	30	1.68	1.43	25	0.17	1.40	1.37	25	0.10	1.55	1.12	25	0.22	1.11	0.87	25	0.13
	Western	8			0				0				0				0	
2010 tip	Sand	46	1.71	0.95	33	0.38	1.32	0.76	33	0.27	1.78	1.07	33	0.35	1.20	0.76	33	0.22
	Clay	26	1.91	1.71	23	0.17	2.09	1.88	23	0.19	1.73	1.37	23	0.20	1.73	1.41	23	0.19
2010 side	Pure sand	17	1.84	1.03	10	0.40	1.33	0.64	10	0.37	2.05	1.24	10	0.39	1.23	0.60	10	0.33
	Pure clay	17	1.63	1.34	15	0.17	1.70	1.62	15	0.13	1.53	1.25	15	0.17	1.48	1.43	15	0.11
1999 tip	Sand	28	1.61	0.84	22	0.39	1.21	0.74	22	0.23	1.63	1.00	22	0.31	1.08	0.75	22	0.16
	Clay	26	1.91	1.71	23	0.17	2.09	1.88	23	0.19	1.73	1.37	23	0.19	1.73	0.75	25	0.55
	IGM	18	1.92	1.16	11	0.37	1.55	0.79	11	0.39	2.09	1.18	11	0.45	1.35	0.73	11	0.31
1999 side	Pure sand	3	1.33	0.90	2		0.93	0.11	2		1.17	0.74	2		0.77	0.06	2	
	Pure clay	17	1.63	1.34	15	0.17	1.70	1.62	15	0.13	1.53	1.25	15	0.17	1.48	1.43	15	0.11
	Pure IGM	4	2.45	1.31	4		1.59	0.70	4		1.93	1.56	4		1.50	0.72	4	
Total case	Total resistance	72	1.80	1.31	56	0.25	1.64	1.38	56	0.16	1.76	1.19	56	0.28	1.42	1.09	56	0.17



Table 5-27 Statistical characteristics and calibrated tip resistance factors according to different classification ( $\beta=2.33$ )

Design variable	criteria	#case	1"-99				5% B-99				1"-2010				5% B-2010			
			mean	std	#	$\phi$	mean	std	#	$\phi$	mean	std	#	$\phi$	mean	std	#	$\phi$
Construction	Dry	18	2.07	1.16	14	0.66	2.05	1.57	14	0.41	1.97	1.06	14	0.66	1.80	1.36	14	0.37
	Wet	39	1.67	1.48	31	0.27	1.42	1.42	31	0.18	1.65	1.30	31	0.32	1.21	0.99	31	0.22
	NA	15	1.80	0.97	11	0.60	1.72	0.91	11	0.59	1.80	1.08	11	0.52	1.52	0.92	11	0.44
Length	<100 ft	66	1.79	1.32	55	0.38	1.64	1.39	55	0.28	1.75	1.20	55	0.42	1.42	1.10	55	0.28
	>100 ft	6	2.20		1		1.35		1		2.62		1		1.33		1	
Region	MS	34	1.89	1.22	31	0.50	1.83	1.37	34	0.38	1.94	1.24	31	0.51	1.67	1.20	31	0.37
	LA	30	1.68	1.43	25	0.29	1.40	1.37	25	0.19	1.55	1.12	25	0.34	1.11	0.87	25	0.21
	Western	8			0				0				0				0	
2010 tip	Sand	46	1.71	0.95	33	0.55	1.32	0.76	33	0.40	1.78	1.07	33	0.52	1.20	0.76	33	0.33
	Clay	26	1.91	1.71	23	0.30	2.09	1.88	23	0.32	1.73	1.37	23	0.33	1.73	1.41	23	0.31
2010 side	Pure sand	17	1.84	1.03	10	0.59	1.33	0.64	10	0.51	2.05	1.24	10	0.58	1.23	0.60	10	0.46
	Pure clay	17	1.63	1.34	15	0.30	1.70	1.62	15	0.24	1.53	1.25	15	0.28	1.48	1.43	15	0.20
1999 tip	Sand	28	1.61	0.84	22	0.56	1.21	0.74	22	0.34	1.63	1.00	22	0.46	1.08	0.75	22	0.25
	Clay	26	1.91	1.71	23	0.30	2.09	1.88	23	0.33	1.73	1.37	23	0.33	1.73	0.75	25	0.74
	IGM	18	1.92	1.16	11	0.55	1.55	0.79	11	0.56	2.09	1.18	11	0.65	1.35	0.73	11	0.45
1999 side	Pure sand	3	1.33	0.90	2		0.93	0.11	2		1.17	0.74	2		0.77	0.06	2	
	Pure clay	17	1.63	1.34	15	0.30	1.70	1.62	15	0.24	1.53	1.25	15	0.28	1.48	1.43	15	
	Pure IGM	4	2.45	1.31	4		1.59	0.70	4		1.93	1.56	4		1.50	0.72	4	0.20
Total case	Total resistance	72	1.80	1.31	56	0.39	1.64	1.38	56	0.28	1.76	1.19	56	0.43	1.42	1.09	56	0.28

Table 5-28 Statistical characteristics and calibrated tip resistance factors based on detailed soil profile ( $\beta=3.0$ )

Design variable	criteria	#case	1"-99				5% B-99				1"-2010				5% B-2010			
			mean	std	#	$\phi$	mean	std	#	$\phi$	mean	std	#	$\phi$	mean	std	#	$\phi$
2010 side, pure sand	tip-sand	17	1.84	1.03	10	0.40	1.33	0.64	10	0.37	2.05	1.24	10	0.39	1.23	0.60	10	0.33
2010 side, 70-100% sand	tip-sand	35	1.71	0.92	27	0.40	1.30	0.62	27	0.36	1.80	1.02	27	0.39	1.19	0.60	27	0.30
2010 side, pure clay	tip-clay	16	1.63	1.34	15	0.18	1.70	1.62	15	0.13	1.53	1.25	15	0.16	1.48	1.43	15	0.11
2010 side, 70-100% clay	tip-clay	20	1.63	1.23	19	0.21	1.71	1.47	19	0.17	1.52	1.16	19	0.19	1.49	1.29	19	0.15
1999 side, 70-100% sand	tip-sand	14	1.48	0.52	11	0.61	1.11	0.36	11	0.49	1.41	0.51	11	0.56	0.94	0.33	11	0.38
1999 side, pure clay	tip-clay	17	1.63	1.34	15	0.18	1.70	1.62	15	0.13	1.53	1.25	15	0.16	1.48	1.43	15	0.11
1999 side, 70-100% clay	tip-clay	21	1.68	1.22	20	0.23	1.74	1.44	20	0.19	1.55	1.13	20	0.21	1.52	1.26	20	0.15
1999 side, 70-100% IGM	all tip conditions	12	2.47	1.14	8	0.72	1.81	0.86	8	0.51	2.67	1.21	8	0.79	1.66	0.83	8	0.43
1999 side mixed <sup>(1)</sup>	all tip conditions	19	1.44	0.87	16	0.28	1.42	1.19	16	0.15	1.56	1.02	16	0.27	1.31	1.03	16	0.15

1999 side mixed <sup>(1)</sup>: Mixed soil type along the side (not belong to sand (70-100% sand), or clay (70-100% clay), or IGM (70-100% IGM))

Table 5-29 Statistical characteristics and calibrated tip resistance factors based on detailed soil profile ( $\beta=2.33$ )

Design variable	criteria	#case	1"-99				5% B-99				1"-2010				5% B-2010			
			mean	std	#	$\phi$	mean	std	#	$\phi$	mean	std	#	$\phi$	mean	std	#	$\phi$
2010 side, pure sand	tip-sand	17	1.84	1.03	10	0.59	1.33	0.64	10	0.51	2.05	1.24	10	0.58	1.23	0.60	10	0.46
2010 side, 70-100% sand	tip-sand	35	1.71	0.92	27	0.58	1.30	0.62	27	0.50	1.80	1.02	27	0.56	1.19	0.60	27	0.43
2010 side, pure clay	tip-clay	16	1.63	1.34	15	0.30	1.70	1.62	15	0.24	1.53	1.25	15	0.28	1.48	1.43	15	0.20
2010 side, 70-100% clay	tip-clay	20	1.63	1.23	19	0.34	1.71	1.47	19	0.29	1.52	1.16	19	0.31	1.49	1.29	19	0.25
1999 side, 70-100% sand	tip-sand	14	1.48	0.52	11	0.77	1.11	0.36	11	0.62	1.41	0.51	11	0.71	0.94	0.33	11	0.49
1999 side, pure clay	tip-clay	17	1.63	1.34	15	0.29	1.70	1.62	15	0.24	1.53	1.25	15	0.28	1.48	1.43	15	0.20
1999 side, 70-100% clay	tip-clay	21	1.68	1.22	20	0.37	1.74	1.44	20	0.31	1.55	1.13	20	0.34	1.52	1.26	20	0.27
1999 side, 70-100% IGM	all tip conditions	12	2.47	1.14	8	0.99	1.81	0.86	8	0.70	2.67	1.21	8	1.08	1.66	0.83	8	0.60
1999 side mixed <sup>(1)</sup>	all tip conditions	19	1.44	0.87	16	0.41	1.42	1.19	16	0.25	1.56	1.02	16	0.41	1.31	1.03	16	0.25

1999 side mixed<sup>(1)</sup>: Mixed soil type along the side (not belong to sand (70-100% sand), or clay (70-100% clay), or IGM (70-100% IGM))

## Driven Piles

Resistance factors of driven piles were calibrated using similar procedure as presented for drilled shaft calibration. In the calibration the same statistical parameters of dead and live loads as in drilled shaft application were used. The dead load to live load ratio was chosen as 3, the same as in calibration of resistance factors for drilled shaft. The calibrated resistance factors are presented in the table below. Table 5-30 presents calibration results for a data group of 61 compression driven piles. The 61 compression driven piles were divided into several subgroups using the criteria listed in table 5-31. The number in parenthesis after  $\phi$  is reliability index used for calibration. In general, uplift has higher resistance factors than compression. The calibrated resistance factors are highly varied among different sub groups. For example, compression resistant factor is 0.62 for piles with diameter larger than 40" while the compression resistant factor is 0.21 for piles with diameter less than 40 at target reliability index of 2.33. Among pile type, concrete pile has the highest resistance factors which agree with other calibration study (Abu-Farsakh et al. 2009). Closed ended pipe pile has higher resistance factors.

Resistance factors were also calibrated according to soil type along pile shaft and at pile tip. The soil type along the shaft was determined from calculated shaft resistance. For example, 70% of sand along shaft means that 70% of shaft resistance is from resistance calculated using design method for sand. The calibrated resistance in sand is less than in clay. This may be caused by the uncertainty of strength estimation in gravels and cobbles which are treated as sand.

The 61 compression database and 53 uplift databases were further filtered with 2STD criteria. The purpose of this filter was to remove possible bias outliers outside of the 2 standard deviation range. Data outlier analysis is commonly performed in resistance calibration studies such as NCHRP 507. Table 5-31 presents the counter part of table 2-28 with data filtered with 2STD filter. It is generally observed that resistance factor noticeably increases after the filtering. An increase of 0.1 and 0.2 for some cases are observed. This demonstrates that the resistance factor presented in table 5-31 is conservative.

Table 5-30 Calibrated resistance factor for 65 compression driven pile databases.

Design variable	criteria	Compression					Uplift				
		Mean	STD	#	$\phi$ (3.0)	$\phi$ (2.33)	Mean	STD	#	$\phi$ (3.0)	$\phi$ (2.33)
Diameter	<40"	2.06	2.29	45	0.11	0.21	1.95	1.67	46	0.21	0.33
	>40"	1.07	0.32	16	0.50	0.62	0.77	0.15	7	0.49	0.57
Pile Type	PP (Open)	2.51	2.48	34	0.17	0.32	2.00	1.50	29	0.28	0.42
	PP (Closed)	0.95	0.37	8	0.34	0.44	1.58	1.92	17	0.08	0.14
	CP	0.83	0.25	14	0.38	0.48	1.05	0.38	5	0.42	0.53
	HP	0.94	0.35	3	0.36	0.47	2.50	2.23	2	0.24	0.40
	CRP	1.15	0.11	2	NA	NA					
Soil Type	Side Sand (100%)	2.98	3.24	15	0.19	0.33	2.58	2.02	15	0.33	0.51
	Side Clay (100%)	0.86	0.11	7	0.65	0.73	0.99	0.18	4	0.66	0.76
	Side Sand (>70%)	2.51	2.84	22	0.14	0.25	2.57	1.97	19	0.34	0.53
	Side Clay (>70%)	1.04	0.42	23	0.36	0.47	1.07	0.48	21	0.34	0.44
	Tip-Sand	2.35	2.47	36	0.16	0.27			NA		
	Tip Clay	0.98	0.40	22	0.33	0.44			NA		
	Tip-Silt			1					NA		
	Tip-Rock	1.17	0.52	2	0.37	0.49			NA		
<b>ALL</b>	ALL	1.80	2.02	61.00	0.09	0.18	1.79	1.60	53.00	0.16	0.28

Table 5-31 Calibrated resistance factor for driven pile databases filtered with DQF >2.5 and 2SD (updated with tip-clay, Rakib)

Design variable	criteria	Comp					Uplift				
		mean	std	#	$\phi$ (3.0)	$\phi$ (2.33)	mean	std	#	$\phi$ (3.0)	$\phi$ (2.33)
Diameter	<40"	1.66	1.37	43	0.17	0.29	1.69	1.13	44	0.29	0.42
	>40"	1.07	0.32	16	0.50	0.62	0.77	0.15	7	0.49	0.57
Pile Type	PP (Open)	2.00	1.43	32	0.28	0.44	1.82	1.17	28	0.34	0.48
	PP (Closed)	0.95	0.37	8	0.34	0.44	1.15	0.80	16	0.19	0.27
	CP	0.83	0.25	14	0.38	0.48	1.05	0.38	5	0.42	0.53
	HP	0.94	0.35	3	0.36	0.47	2.50	2.23	2	0.24	0.40
	CRP	1.15	0.11	2	0.94	1.03			0		
Soil Type	Side Sand (100%)	1.81	1.03	13	0.41	0.57	2.17	1.28	14	0.46	0.65
	Side Clay (100%)	0.86	0.11	7	0.65	0.73	0.99	0.18	4	0.66	0.76
	Side Sand (>70%)	1.70	1.17	20	0.28	0.41	2.24	1.40	18	0.43	0.62
	Side Clay (>70%)	0.97	0.27	22	0.48	0.59	1.07	0.48	21	0.34	0.44
	Tip-Sand	1.86	1.45	34	0.24	0.37			NA		
	Tip Clay	0.91	0.16	21	0.61	0.70			NA		
	Tip-Silt			1					NA		
Tip-Rock	1.17	0.52	2	0.37	0.49			NA			
	ALL	1.42	1.05	58.00	0.19	0.30	1.56	1.09	51.00	0.25	0.37

## 6. CHAPTER 6 SUMMARY AND CONCLUSIONS

The design methods calibrated in this study are based on Caltrans design practice for driven piles. For small piles (less than 16 inch or 24 inch), the  $\alpha$ -(Tomlinson) method and Nordlund method are used for static capacity design; For large piles (greater than 16 inch or 24 inch), the API method is used. A pile load test (85 compression load tests and 83 uplift load tests) that was tested to failure was collected from Caltrans and used to calibrate the resistance factors. For each pile load test, the measured ultimate pile resistance was estimated using the Davisson, 1 inch, and 5% failure criteria interpretation method. The failure interpretation criteria for driven piles were not found to have significant effect on calibrated resistance factors.

### Recommended Resistance Factors For Driven Piles

Based on the calibrated resistance factors for static analysis of driven piles presented in chapter 5, the resistance factors listed in Table 6.1 is recommended for static capacity design. The resistance factors were calibrated at two target reliability indexes: one for redundant pile groups and one for non-redundant pile groups. A redundant system refers to a pile group with four or fewer piles. The target probability of failure is  $p_f = 1\%$  for a redundant pile group, corresponding to a reliability index of  $\beta = 2.33$ .

The resistance factors recommended in Table 6.1 were calibrated using load test data without removing possible outliers. For example, 2 times standard deviation filter was applied to the collected load test data when it was used for calibration (NCHRP 507). The recommended resistance factors generally agree well the AASHTO specifications. It can be seen that larger piles (diameter greater than 40") has the highest resistance factors. It should be noticed that only 16 cases were collected for piles with diameter larger than 40". For redundant pile groups, a resistance factor of 0.35 is recommended for pipe piles as well as HP and CRP piles. There are fewer cases of HP and CRP piles in the collected database. When multiple conditions are met, the one with higher resistance factors shall be used.

Table 6.1. Recommended Resistance factors for Static Capacity of Driven Piles

Design Methods	Conditions	Compression		Uplift	
		Redundant $\beta = 2.33$	Non-redundant $\beta = 3.0$	Redundant $\beta = 2.33$	Non-redundant $\beta = 3.0$
Nordlund + $\alpha$ for small piles API for large piles	>40"	0.60	0.5	0.6	0.50
	PP, HP, CRP	0.35	0.25	0.40	0.30
	CP	0.50	0.40	0.50	0.40
	Tip-Sand	0.30	0.20	0.50	0.40
	Tip Clay	0.45	0.35		

This study presented the LRFD calibration of the FHWA (1999 and 2010) method for drilled shaft design based on the 1 inch and 5% B criterion. A drilled shaft load test database of 79 drilled shafts with different sizes and lengths was collected and used to calibrate the total and separated resistance factors. The 79 drilled shafts include 41 cases from Mississippi, 30 cases from Louisiana, 2 cases from California, 2 cases from Arizona, and 3 cases from Washington. Most of the collected drilled shafts were tested using O-cell from which measured total, side, and tip can be determined from O-cell load-settlement curves. For each drilled shaft, the load-settlement behavior was estimated using the FHWA method (1999 and 2010). Tip, side, and total resistance factors ( $\phi$ ) needed in the LRFD design methodology of drilled shafts were determined at reliability indexes ( $\beta$ ) of 2.33 and 3.0.

Statistical analyses comparing the predicted and measured drilled shaft resistances were conducted to evaluate the accuracy of the FHWA design methods in estimating the measured drilled shaft capacity. Results of the analyses showed that the both FHWA 1999 and 2010 methods underestimate the total drilled shaft resistance

### **Recommended Resistance Factors For Drilled Shafts**

The calibrated resistance factors are shown in Table 6.2, 6.3, and 6.4. The total drilled shaft database was grouped according to drilled shaft construction method, drilled shaft location, and soil types. In drilled shaft construction methods, dry and wet construction methods were identified from available drilled shaft load test reports. However, the construction method can't be determined due to the missing original load test report. Therefore, these drilled shafts are listed under the third category "NA" in construction method. Drilled shafts constructed with dry method have much higher resistance factors compared with drilled shaft constructed with wet method. Drilled shaft constructed with wet construction method can be greatly affected by casing, drilling fluid, construction quality control. Therefore large uncertainty is expected for drilled shaft constructed with wet method. Three regions were considered in the region category which includes MS, LA, and the three western states listed in Chapter 4. There are only 7 cases collected from the western states which are not sufficient for statistical analysis. Therefore, resistance factors were not calibrated for the western state cases. Soil type along the shaft and at the tip of drilled shaft is considered in soil type classification. The soil types were classified according to the soil classification in the FHWA design methods. The side – all soils means the soil type along the drilled shaft can be any type of soil or any combination of soil type. The side – sand means that more than 70% of the shaft side resistance was calculated using method for sand.



For drilled shafts in sand (side-sand and tip-sand), the calibrated resistance factor is 0.7 for redundant foundations while 0.55 is recommended in NCHRP 507. It should be noted that only 14 drilled shaft load tests are available for the calibration. For drilled shaft in clay (side-clay and tip-clay), the calibrated resistance factor is 0.6 for redundant foundations while 0.38 is recommended in NCHRP 507. For IGM and mixed soil conditions, the calibrated resistance factors in this study are lower than the values recommend by NCHRP 507.

It should be noted that the resistance factors used in AASHTO were developed using either statistical analysis of drilled shaft load tests combined with reliability theory (Paikowsky et al., 2004), fitting to Allowable Stress Design (ASD), or both. When the two approaches resulted in a significantly different resistance factor, engineering judgment was used to establish the final resistance factor, considering the quality and quantity of the available data used in the calibration.

Table 6.2. Recommended Total Resistance Factors for Drilled shaft ( $\beta=2.33$  and  $3.0$ )

Drilled shaft and Soil Conditions		#case	FHWA 1999 (1-inch)		FHWA (5%D)		NCHRP-507 (%5D) - FHWA	
			$\phi$ - $\beta=2.33$	$\phi$ - $\beta=3.0$	$\phi$ - $\beta=2.33$	$\phi$ - $\beta=3.0$	$\phi$ - $\beta=2.33$	$\phi$ - $\beta=3.0$
Construction – all soils	Dry	18	0.65	0.50	0.70	0.50		
	Wet	39	0.45	0.30	0.45	0.30		
	NA	15	0.80	0.70	0.90	0.75		
Region – all soils	MS	34	0.45	0.30	0.50	0.35		
	LA	30	0.70	0.55	0.70	0.55		
Side-all soils, tip-sand	FHWA 2010	46	0.50	0.35	0.50	0.35		
Side-sand, tip-sand		35	0.40	0.30	0.40	0.30		
Side-all soils, tip-clay		26	0.55	0.40	0.60	0.40		
Side-clay, tip-clay		20	0.6	0.40	0.60	0.40		
Side-all soils, tip-IGM	FHWA 1999	18	0.35	0.25	0.40	0.25		
Side-sand, tip-sand		14	0.70	0.55	0.65	0.51	0.55	0.38
Side-clay, tip-clay		21	0.60	0.45	0.60	0.45	0.38	0.28
Side-IGM, tip-all soils		12	0.35	0.25	0.40	0.25	0.73	0.57
Side-mixed <sup>(1)</sup> , tip-all soils		19	0.45	0.35	0.50	0.40	0.73	0.58

Note: FHWA 1999 and 2010 design methods are used for soil types available in the design methods.

Table 6.3. Recommended Side Resistance Factors for Drilled shaft ( $\beta=2.33$  and 3.0)

Drilled shaft and soil conditions		#case	FHWA 1999 (1-inch)		FHWA (5%D)		NCHRP-507 (%5D) - FHWA	
			$\phi$ - $\beta=2.33$	$\phi$ - $\beta=3.0$	$\phi$ - $\beta=2.33$	$\phi$ - $\beta=3.0$	$\phi$ - $\beta=2.33$	$\phi$ - $\beta=3.0$
Construction – all soils	Dry	18	0.60	0.38	0.60	0.40		
	Wet	39	0.60	0.40	0.42	0.28		
	NA	15	0.75	0.65	0.85	0.75		
Region – all soils	MS	34	0.35	0.25	0.40	0.25		
	LA	30	0.60	0.5	0.65	0.5		
Side-all soils, tip-sand	FHWA 2010	46	0.40	0.25	0.45	0.30		
Side-sand, tip-sand		35	0.35	0.25	0.40	0.25		
Side-all soils, tip-clay		26	0.45	0.30	0.50	0.30		
Side-clay, tip-clay		20	0.50	0.35	0.55	0.35		
Side-all soils, tip-IGM	FHWA 1999	18	0.25	0.15	0.30	0.20		
Side-sand, tip-sand		14	0.50	0.40	0.55	0.40	0.43	0.31
Side-clay, tip-clay		21	0.50	0.40	0.50	0.40	0.46	0.36
Side-IGM, tip-all soils		12	0.35	0.25	0.30	0.20	0.66	0.51
Side-mixed <sup>(1)</sup> , tip-all soils		19	0.40	0.25	0.50	0.35	0.78	0.63

Note: Side resistance factors in NCHRP are based on the shafts for which more than 80% of the total capacity was mobilized in a displacement of less than 2% of the shaft's diameter.

Table 6.4. Recommended Tip Resistance Factors for Drilled shaft ( $\beta=2.33$  and  $3.0$ )

Drilled shaft and soil conditions		#case	FHWA 1999 (1-inch)		FHWA (5%D)		NCHRP-507 (%5D) - FHWA	
			$\phi$ - $\beta=2.33$	$\phi$ - $\beta=3.0$	$\phi$ - $\beta=2.33$	$\phi$ - $\beta=3.0$	$\phi$ - $\beta=2.33$	$\phi$ - $\beta=3.0$
Construction – all soils	Dry	18	0.70	0.45	0.45	0.25	NA	NA
	Wet	39	0.3	0.15	0.20	0.10		
	NA	15	0.60	0.45	0.60	0.45		
Region – all soils	MS	34	0.50	0.35	0.40	0.25		
	LA	30	0.3	0.15	0.20	0.10		
Side-all soils, tip-sand	FHWA 2010	46	0.55	0.40	0.40	0.3		
Side-sand, tip-sand		35	0.60	0.40	0.50	0.40		
Side-all soils, tip-clay		26	0.30	0.20	0.35	0.20		
Side-clay, tip-clay		20	0.35	0.25	0.30	0.20		
Side-all soils, tip-IGM	FHWA 1999	18	0.55	0.40	0.60	0.40		
Side-sand, tip-sand		14	0.70	0.60	0.60	0.30		
Side-clay, tip-clay		21	0.40	0.25	0.35	0.20		
Side-IGM, tip-all soils		12	0.70	0.70	0.70	0.50		
Side-mixed <sup>(1)</sup> , tip-all soils		19	0.45	0.30	0.25	0.15		

## RECOMMENDATIONS

1. More data are needed for open-ended pipe piles, particularly large diameter piles. Soil plugging has significant effect on pile capacity. However, the plugging effect can't be quantified due to lack of plugging measurement
2. It is recommended to select a few on-going bridge projects to evaluate the current design methods. In the analysis of pile capacity, all soil layers along the shaft and at the tip are considered in the capacity analysis regardless of pipe type and construction conditions. In the design practice, weak soils are often ignored.
3. A GIS based deep foundation load test database is recommended.
4. It is recommended to hold a workshop to train Caltrans engineers in the LRFD design of deep foundations.
5. There is only 2 cases of drilled shafts were collected from California. It is recommended to continue collecting drilled shaft test data from new projects, especially for those cases in which the end bearing and side frictional capacities can be separated for possible future re-calibration of resistance factors. A database of a minimum 20 load tests is considered statistically reliable to perform LRFD calibration.
6. It should be noted that performing complete reliability analyses of deep foundations requires the inclusions of all risk factors. Scour is a critical factor in the selection of drilled shaft tip elevations. The risk associated with scour directly impacts the reliability of drilled shaft foundations. This is mainly due to expected changes on the in-situ stress state (overburden and stress history) of the subsurface soil that will affect the laboratory and in-situ test results. However, the scope of this study does not include the evaluation of scour and is recommended to be considered in the future.
7. Global resistance factors are recommended herein for the design of axially loaded pile and drilled shafts in California. However, further research should be conducted to evaluate site variability and in-situ load tests' effect on the selection of resistance factor values.
8. Further research is needed to calibrate resistance factors for deep foundations that are laterally loaded.

## REFERENCES

- AASHTO (2012). "AASHTO LRFD Bridge Design Specifications: Sixth Edition. Parts I and II." 9781560515234, American Association of State Highway and Transportation Officials, Washington, DC.
- Abu-Farsakh, M. Y., Chen, Q., and Haque, M. N. (2013). "Calibration of Resistance Factors for Drilled Shafts for the New FHWA Design Method." 124.
- Abu-Farsakh, M. Y., Yoon, S., and Tsai, C. (2009). "Calibration of Resistance Factors Needed in the LRFD Design of Driven Piles." 120.
- Abu-Farsakh, M. Y., Yu, X., Yoon, S., and Tsai, C. (2010). "Calibration of Resistance Factors Needed in the LRFD Design of Drilled Shafts." 110.
- Allen, T. M. (2005). "Development of the WSDOT Pile Driving Formula and Its Calibration for Load and Resistance Factor Design (LRFD)." 57p.
- Allen, T. M., Nowak, A. S., and Bathurst, R. J. (2005). "*Calibration to Determine Load and Resistance Factors for Geotechnical and Structural Design.*" Publication TRB Circular E-C079, Transportation Research Board.
- Baecher, G. B. and Christian, J. T. *Reliability and Statistics in Geotechnical Engineering*. Wiley, Chichester, England, 2003, 619 pp.
- Bridge Design Practice, February 2015
- Brown, D. A., Turner, J. P., and Castelli, R. J. (2010). "*Drilled shafts: Construction procedures and LRFD design methods.*" US Department of Transportation, Federal Highway Administration.
- Budge, A. S. (2014). "Load and Resistance Factor Design (LRFD) Pile Driving Project - Phase II Study." Minnesota Department of Transportation.
- California Amendments to AASHTO LRFD Bridge Design Specifications-6<sup>th</sup> Edition.
- CALTRANS Deep Foundation Manual.
- Chua, K., Meyers, R., and Samtani, N. "Evolution of a Load Test and Finite Element Analysis of Drilled Shafts in Stiff Soils." ASCE GeoDenver, Denver, CO, 2000.
- Esrig, M. E., and Kirby, R. C. (1979). "Advances in General Effective Stress Method for the Prediction of Axial Capacity for Driven Piles in Clay." Offshore Technology Conference.
- Flaate, K. (1964), "An Investigation of the Validity of Three Pile-Driving Formulae in Cohesionless Material," Publication No.56, Norwegian Geotechnical Inst., Oslo, Norway: 11-22.
- Fragaszy, R. J., D. Argo, and J. D. Higgins (1989), "Comparison of Formula Predictions with Pile Load Test," Transportation Research Board, 22-26 January.

- Fragaszy, R. J., J. D. Higgins, and D. E. Argo (1988), "Comparison of Methods for Estimating Pile Capacity," Washington State Department of Transportation and in cooperation with U.S. Department of Transportation FHWA, August.
- Garder, J. A., Ng, K. W., Sritharan, S., and Roling, M. J. (2012). "Development of a Database for Drilled SHAft Foundation Testing (DSHAFT)."
- Harr, M. E. "*Reliability-Based Design in Civil Engineering*." Dover Publications, Mineola, NY, 1996, 291 pp.
- Long, J., and Anderson, A. (2012). "Improved Design for Driven Piles on a Pile Load Test Program in Illinois."
- Long, J., and Anderson, A. (2014). "Improved Design for Driven Piles on a Pile Load Test Program in Illinois: Phase 2."
- Long, J. H., Hendrix, J., and Baratta, A. (2009). "Evaluation/Modification of IDOT Foundation Piling Design and Construction Policy." University of Illinois, Urbana-Champaign, 213p.
- Long, J. H., Hendrix, J., and Jaromin, D. (2009). "Comparison of Five Different Methods for Determining Pile Bearing Capacities." 176.
- McVay, M. C., Alvarez, V., Zhang, L., Perez, A., and Gibsen, A. (2002). "Estimating Driven Pile Capacities During Construction." 304.
- McVay, M. C., Badri, D., and Hu, Z. (2004). "Determination Of Axial Pile Capacity Of Prestressed Concrete Cylinder Piles." 132 p.
- McVay, M., Ellis, R., Birgisson, B., Consolazio, G., Putcha, S., and Lee, S. M. "Use of LRFD, cost and risk to design a drilled shaft load test program in Florida limestone." *Proc., TRB 2003 Annual Meeting*.
- McVay, M. C., Kuo, C. L., and Singletary, W. A. (1998). "CALIBRATING RESISTANCE FACTORS IN THE LOAD AND RESISTANCE FACTOR DESIGN FOR FLORIDA FOUNDATIONS." 99 p.
- McVay, M. C., Birgisson, B., Zhang, L., Perez, A., and Putcha, S. (2000). "Load and Resistance Factor Design (LRFD) for Driven Piles Using Dynamic Methods—A Florida Perspective." *Geotechnical Testing Journal*, 23(1), 55.
- McVay, M. C., Klammler, H., Faraone, M. A., Dase, K., and Jenneisch, C. (2012). "Development of Variable LRFD  $\Phi$  Factors for Deep Foundation Design Due to Site Variability."
- Memo to Designers 3-1, June 2014
- Michael W. O'Neil and Lymon C. Reese (1999). "Drilled Shaft: Construction Procedures and Design Methods". Report No: FHWA-IF-99-025.

- Ng, K. W., and Sritharan, S. "Verification of LRFD Approach for Piles in Sand and Mixed Soils." *Proc., Transportation Research Board 93rd Annual Meeting*.
- Ng, K. W., Suleiman, M. T., Roling, M., AbdelSalam, S. S., and Sritharan, S. (2011). "Development of LRFD Design Procedures for Bridge Piles in Iowa - Field Testing of Steel H-Piles in Clay, Sand, and Mixed Soils and Data Analysis (Volume II)." Iowa Department of Transportation.
- Ng, Tang-Tat and Fazia, Sadia (2012). "Development and Validation of a Unified Equation for Drilled Shaft Foundation Design in New Mexico."
- Nowak, A. S., 1999, *Calibration of LRFD Bridge Design Code*, NCHRP Report 368, Transportation Research Board, Washington, DC
- Olson, E., and Flaate, Kaare S. (1967). "Pile Driving Formulas for Friction Piles in Sand." *Journal of the Soil Mechanics and Foundations Division. Proceedings of the American Society of Civil Engineers*, 278p.
- Paikowsky, S. G., Birgisson, B., McVay, M., Nguyen, T., Kuo, C., Baecher, G., Ayyub, B., Stenersen, K., O'Malley, K., Chernauskas, L., and O'Neill, M. (2004). "Load And Resistance Factor Design (LRFD) For Deep Foundations." 0309087961, Transportation Research Board, 85.
- Paikowsky, S. G., Marchionda, C. M., O'Hearn, C. M., Canniff, M. C., and Budge, A. S. (2009). "Developing a Resistance Factor for Mn/DOT's Pile Driving Formula." 294.
- Paikowsky, S. G. (2004). "Load and resistance factor design (LRFD) for deep foundations - NCHRP Report 507."
- Penfield, J., Parsons, R., Han, J., and Misra, A. (2014). "Load and Resistance Factor Design Calibration to Determine a Resistance Factor for the Modification of the Kansas Department of Transportation-Engineering News Record Formula." Kansas Department of Transportation.
- Raghavendra, S., C.D. Ealy, A. F. Dimillio, and S.R. Kalaver. User Query Interface for the Deep Foundations Load Test Database. *Transportation Research Record: Journal of the Transportation Research Board*. Transportation Research Board of the National Academies, Washington, DC. Volume 1755. 2001.
- Sharp, M. R., McVay, M. C., Townsend, F. C., and Basnett, C. R. (1998). "Evaluation of Pile Capacity from Insitu Tests." *Proc., Soil Properties Evaluation from Centrifugal Models and Field Performance*, American Society of Civil Engineers.
- Schmertmann, J. H. and Hayes, J. A. "The Osterberg Cell and Bored Pile Testing – A Symbiosis." 3<sup>rd</sup> International Geotechnical Engineering Conference, Cairo, Egypt; 1997, pp. 139-66.



- Smith, T., Banas, A., Gummer, M., and Jin, J. (2011). "Recalibration of the GRLWEAP LRFD Resistance Factor for Oregon DOT." 128p.
- Smith, T. D., and Dusicka, P. (2009). "Application of LRFD Geotechnical Principles for Pile Supported Bridges in Oregon: Phase 1." 67p.
- Thompson, W. R., Axtell, P. J., and Smith, E. M. (2009) "LRFD in Practice - A Case Study for Foundation Designers." *Proc., 41st Annual Southeastern Transportation Geotechnical Engineering Conference.*
- Xinbao Yu and Murad Y. Abu-Farsakh (2015). "Interim Report". Calibration of LRFD Geotechnical Axial (Tension and Compression) Resistance Factors ( $\phi$ ) for California.